SOME CRACK AND INCLUSION PROBLEMS IN ELASTODYNAMICS

Thesis Submitted for the Degree of Doctor of Philosophy (Science)

of

The University of North Bengal

BY

RAMKRISHNA PRAMANIK

MARCH - 2001

ST - VERF

ACKNOWLEDGEMENT

I wish to express my respect and gratitude to my supervisors Professor Mohan Lal Ghosh; D.Sc., Department of Mathematics University of North Bengal and Dr. Subhas Chandra Pal, Lecturer, Department of Computer Science and Applications, University of North Bengal for their valuable guidance and constant encouragement throughout the process of this research work.

I am thankful to the Head and all other members of the Department of Mathematics, University of North Bengal for their co-operation.

I am also thankful to the Head and all other members of the Department of Computer Science and Applications, University of North Bengal for giving facilities required from time to time in connection with this work.

My sincere thanks goes to all members of the CSIR funded project entitled COMPUTER AIDED FRACTURE MECHANICS, Department of Computer Science and Applications, University of North Bengal.

I acknowledge with thanks the valuable help of Dr. R. K. Samanta, Department of Compter Science and Applications, University of North Bengal.

I am greateful to my mother and other family members for their unwavering patience and constant encouragement throughout this work.

Ramkrishna Pramanik

(Ramkrishna Pramanik)

Department of Mathematics
University of North Bengal
Darjeeling - 734430
INDIA.

MARCH - 2001.

C O N T E N T S

CHAPTER - 1

DIFFRACTION OF WAVES

CHAPTER - 2

INCLUSION PROBLEM

CHAPTER - 3

SCATTERING OF WAVES

CHAPTER - 4

ELASTODYNAMIC GREEN'S FUNCTION

I N T R O D U C T I O N

The phenomenon of stress wave propagation in elastic solid offers us a rich variety of waves which was developed a century ago. The first mathematician to describe the vibrations of pendulums, the resonance phenomenon and the vibration of strings was Galileo. The first stage of the investigation on wave propagation associated with the names of Navier, Cauchy, Hooke, Poisson, Stokes, Rayleigh, Kelvin, Green, Lame, Clebsch, Ostrogradsky, Christoffel is characterized by development of the extensive theory of elasticity to the problem of wave propagation and vibrating bodies in the elastic meterial.

In the first three decades of the twentieth century the subject lost much of its glamour and interest to the research workers due to the lack of sophisticated instrument, electronic devices like high speed computer and practical methods for observing the passage of stress wave in elastic solids. But in the later part of the century the interest in the study of elastic waves has been growing rapidly because of the application of the theory in Seismology, Geophysics and in Engineering Science. Since that time, the wave propagation has remained an interesting area in seismology because of the need for detailed information on earthquake phenomena, prospecting techniques and the detection of nuclear exploisions. Bullen [1963], Ewing et al [1957], Cagniard [1962], Pilant [1979] and Aki and Richards [1980] have discussed elaborately about the problems involving seismic waves in their respective books.

Here we point out some of the milestones of progress in elastic waves in chronological order:

1678 : Robert Hooke (England) established the stress-strain relation for elastic bodies.

1760 : John Michell (England) recognized that earthquakes originate within the earth and send out elastic waves through earth's interior.

1821 : Louis Navier (France) derived the differential equations of the theory of elasticity.

1828 : Simeo-Denis Poisson (France) predicted theoretically the existence of longitudinal and transverse elastic waves.

1849 : George Gabriel Stokes (England) conceived the first mathematical model of an earthquake source.

1857 : First systematic attempt to apply physical principles to earthquake effects by Robert Mallet (Ireland).

1885 : C. Somigliana (Italy) produced formal solutions to Navier equations for a wide class of sources and boundary conditions.

1885 : Lord Rayleigh (England) predicted the existence of elastic surface waves.

1899 : C. G. Knott (England) derived the general equations for the reflection and refraction of plane seismic waves at plane boundaries.

1903 : A. E. H. Love (England) developed the fundamental theory of point sources in an infinite elastic space.

1904 : Horace Lamb (England) solved the problem on the propagation of tremors over the surface of an elastic solid.

1907 : Vito Voltera (Italy) published the theory of dislocations based on Somigliana's solution.

1940 : Sir Harold Jeffreys (England) and K. E. Bullen (Australia) published travel time tables for

seismic waves in the earth.

1949 : Lapwood, E. R. First considered the distribution due to a line source in a semi-infinite elastic medium.

1959 : Ari Ben-Menahem (Isreal) discovered that the energy release in earthquakes take place through a propagating rupture over the causative fault.

During the last three decades there has been a remarkable revival of interest in this subject. Most of the experimental works carried out on the wave propagation of elasticity are concerned with studying propagation in specimens of comparatively simple geometrical shape, the results of this experiment could be compared directly with exact or approximate theoratical predictions. With increasing confidence in the experimental techniques and in the interpretation of observations, it is now possible to study more complicated problems of elastodynamics.

All the elastic bodies may be divided roughly into two catagories :

(I) homogeneous and non-homogeneous

(ii) isotropic and anisotropic

A homogeneous body is the body whose elastic properties are the same at different points and a non-homogeneous body has different elastic properties at different points. If the elastic moduli vary from point to point in a continuous manner, the non homogeneity may also be termed continuous. If, however, the elastic moduli undergo discontinuties in passing from point to point, for example change abruptly, the non-homogeneity is said to be discontinuous or discrete.

An isotropic body, with regard to its elastic properties, is one in which these properties are the same for all directions drawm through a given point. An anisotropic body has, in general,

different elastic properties for different directions drawn through a given point. A body may be isotropic or anisotropic and at the same time homogeneous or non-homogeneous depending on its own structure.

However, natural or artificial materials in our surroundings are generally inhomogeneous and anisotropic.

Since 1950 the theory of elasticity for anisotropic bodies has been continually developed and enriched with new investigations of both serious problems as a general nature and individual aspects of these problems. Thus the general theory has been placed on a rigorous scientific basis and a number of laws have been established with the result that this theory, first worked out by B. De Saint Venant and P.V. Bekhterev [1925], has been revived.

Of great importance is the development and construction of many entirely new anisotropic materials which possesses a number of advantages over those previously known (for example, glass-fibre reinforced plastics). Thus, over two or three decades this branch of science has made great progress, both in a theoratical and a purely practical way, i.e. in constructing new anisotropic materials.

Now we recapitulate the fundamental principles of the theory of elasticity and the general equations which will be used in what follows for the construction of solutions to specific problems of the theory of elasticity for anisotropic bodies.

In studying the states of the stress and strain in anisotropic bodies produced by an external load, we make a number of assumptions imposing certain restrictions. The most important of these assumptions reduce to the following :

(I) A body is solid (a continuous medium), the stresses on any plane within the body and

on its surface are forces per unit area,. In other words, the couple stresses are neglected, as is done in the classical theory of elasticity.

(II) The relation between the components of strain and the projections of displacement and their first derivatives with respect to the co-ordinate is linear.

(III) The stress-strain relations are linear i.e. the material follows the generalized Hooke's law, the co-efficients in these linear relations may be either constant (homogeneous body) or variable, i.e. functions of position, continuous or discontinuous (in the case of a non-homogeneous body).

(IV) The initial stresses i.e. those existing without any external load, including the thermal stresses are disgarded; specific problems of dynamics are not considered.

Thus, the theory of anisotropic elastic bodies can be studied from the classical linear theory of homogeneous or non-homogeneous elastic bodies.

In the general case of anisotropy each strain component is a linear function of all six components of stress. For a homogeneous body having anisotropy of the most general kind, the equations expressing the generalized Hooke's law for this system are

$$\epsilon_{ij} = a_{ijkl}\,\sigma_{kl} \qquad (i,j,k,l = 1,2,3). \tag{1}$$

The number of all constants a_{ijkl} with four subscripts is 81, but, when grouped, they reduce to 21 (of these 18 constants are independent) elastic constants.

The generalized Hooke's law equations, solved for the stress components, are of the form

$$\sigma_{ij} = A_{ijkl}\,\epsilon_{kl}\,. \tag{2}$$

The notation for the elastic constant "a" and "A" with four subscripts has been used by Malmeister, Tanuzh and Terters (1972) in their book.

However, if the elastic body is isotropic, then all directions in the body are elastically equivalent and the generalized Hooke's law for an isotropic body reduces to

$$\epsilon_x = \frac{1}{E}\left[\sigma_x - \gamma(\sigma_y + \sigma_z)\right]$$

$$\epsilon_y = \frac{1}{E}\left[\sigma_y - \gamma(\sigma_z + \sigma_x)\right] \qquad (3)$$

$$\epsilon_z = \frac{1}{E}\left[\sigma_z - \gamma(\sigma_x + \sigma_y)\right]$$

$$\gamma_{yz} = \frac{1}{G}\tau_{yz}, \quad \gamma_{xz} = \frac{1}{G}\tau_{xz}, \quad \gamma_{xy} = \frac{1}{G}\tau_{xy}$$

where E, Young's modulous, γ Poisson ratio and G shear modulous.

In recent years, considering the elastic medium to be either isotropic or anisotropic, problems involving diffraction of elastic waves by crack or by inclusions have attracted considerable attention in view of their application in Seismology and Geophysics. Cracks or inclusions are present in essentially all structural materials either as natural defects or as a result of fabrication processes. Moreover, on many cases the cracks or inclusions are sufficiently small so that their pressence does not significantly reduce the strength of the material. In other cases, however, the imperfections are large enough through fatigue, stress corosion cracking etc., so that they must be taken into account in determining the strength. From the stand point of engineering applications it has been the macroscopic theories based on the notions of continuum solid mechanics and classical thermodynamics which have provided the quantitative working tools for dealing with the fracture

of structural materials. In the microscopic continuum approach to fracture it is implicitly assumed that the material contains some macroscopic flaw which may act as fracture nuclei and that the medium is a homogeneous continuum in the sense that the size of the macroscopic flaws is large in comparison with the characteristic microstructural dimension of the material. The problem is then to study the effects of the applied loads, the flaw geometry and the environmental conditions on the fracture process in the solid.

Fracture mechanics is concerned with the analysis of the stability of cracks. A fracture criterion can subsequently be employed to determine the conditions for crack propagation, both stable and unstable, and for crack arrest.

Fracture mechanics problems that have to be treated as dynamic problem may be classified in two types :

(1) Cracked bodies subjected to rapidly varying loads

(2) Bodies containing rapidly propagating cracks.

In both the cases the crack tip is an environment disturbed by wave motions.

Impact and vibration problems fall into the first type of dynamic problems. It is often found that at inhomogeneities in a body the dynamic stresses are higher than the stresses computed from the corresponding problem of static equillibrium in the analysis of this type of problem.

The second type of problem is equally important. There are several kinds of large engineering structures e.g. gas transmission pipelines, ship-hulls, aircraft fuselages and nuclear reactor components, in which rapid crack growth is a definite possibility. The study of earthquake mechanisms is the another area to which the analysis of rapidly propagating cracks is relevant.

Recently, there have been a number of comprehensive articles in the general area of fracture

mechanics. Some references are those of Achenbach [1972, 1976], Freund [1975, 1976, 1990] and Kanninen [1978].

Engineering structures requiring protection against the possibility of large scale catastrophic crack propagation are, however, generally constructed of ductile, tough materials. Current progress in this area, and a starting point for the development of a dynamic plastic propagating crack tip analysis have recently been presented by Achenbach and Kanninen.

A problem of central importance in dynamic fracture mechanics is that of predicting the way in which a crack will grow in a deformable solid, given the geometrical configuration of the solid, a characterization of the material, the applied load distribution and suitable initial conditions. In the interpretation of laboratory data on rapid crack propagation, a problem of equal importance is that of determining the values of fracture characterization parameters from measurements of the crack motion and applied load distribution.

In order to determine an equation of motion for a crack tip, two main ingradients are essential. The first of these is a crack propagation criterion which must be stated as a fundamental physical postulate, distinct from the postulates dealing with bulk material behaviour and momentum balance. Generally these later potulates can be satisfied for any motion of the crack tip. It is the role of the fracture criterion to select the motion of the crack tip from the class of all such dynamically admissible motions.

The only geometrical configuration for which exact solutions of the elastodynamic field equations, valid for non-uniform crack motion, have been found is a semi-infinite crack motion in an otherwise unbounded solid or configurations which can be shown to be equivalent to this by linear superposition arguments. The solution for antiplane deformation was presented by Kostrov [1964.

1966] and Achenbach [1970] and in-plane deformation by Freund [1973], Burridge [1976] and Kostrov [1975]. Although these solutions have been of major importance in addressing certain fundamental questions on rapid crack propagation, they have been found to be inadequate for describing some dynamic fracture processes of practical importance.

The shape of the cracks which have been studied uptil now are as follows :

(I) Semi-infinite plane cracks

(II) Finite Griffith cracks

(III) Penny shaped and annular cracks

(IV) Non-planer cracks.

A transient problem in which a semi-infinite crack appears suddenly in a stretched elastic sheet was solved by Maue [1954] and was also discussed by Ang [1958] in his dissertation. Baker [1962] solved the problem of a semi-infinite crack suddenly appearing and growing at a constant velocity in a stretched body. A steady state problem in which a semi-infinite crack extends at constant speed through an elastic sheet was solved by Craggs [1960]. Using the method of matched asymptotic expansion the problem involving diffraction of plane elastic waves by a semi-infinite boundary of finite width was solved by Viswanathan and Sharma [1978] and by Viswanathan, Sharma and Datta [1982].

The diffraction problem of a semi-infinite crack has been solved by the Wiener-Hopf technique (Noble [1958]).

In 1921 Griffith considered the problem of a fracture of a glass containing crack like defects. Griffith's work presented a theory of fracture. Among other workers investigating crack problems are Orowan [1948], Sack [1946], Irwin [1957] etc.. A number of crack problems in the theory of

classical elasticity can be found in the literature (e.g. Sneddon and Lowengrub [1969], Sih [1972]}).

Yoffe [1951] considered the inplane problem of propagation of a finite Griffith crack of fixed length at a constant speed in an isotropic elastic solid of infinite extend. Other references treating elastodynamic problems involving a single finite Griffith crack are of Sato [1961], Williams [1957, 1961], Karp and Karal [1962], Ang and Knopoff [1964], Loeber and Sih [1968], Sih and Loeber [1968, 1969, 1970], Willis [1967], Atkinson and Eshebly [1968], Mal [1970a, 1970b, 1972], Hilton and Sih [1971], Chang [1971], Thau and Lu [1971], Sih, Embley and Ravera [1972], Kanninen [1974], Chen [1978], Sih and Chen [1980], Takei, Shindo and Atsumi [1982], Ueda, Shindo and Atsumi [1983], Shindo [1985]. Some other references are of Srivastava, Palaiya and Karaulia [1980a, 1980b], Srivastava, Gupta and Palaiya [1981], Erguven [1987].

The problem of diffraction of finite Griffith crack along the interface of two dissimilar elastic media have been solved by Goldshtein [1966, 1967], Brock and Achenbach [1973a, 1973b, 1974], Atkinson [1974], Matczynski [1974], Brock [1975], Srivastava, Gupta and Palaiya [1978], Neerhoff [1979], Srivastava, Palaiya and Karaulia [1980]. Bostrom [1987] solved the two dimensional scalar problem of scattering of elastic waves under antiplane strain from an interface crack between two elastic half-spaces. The problem of interaction of antiplane shear waves by a Griffith crack at the interface of two bonded dissimilar elastic half-spaces was considered by Srivastava, Palaiya and Karaulia [1980].

The transient stress and displacement fields arround an embedded crack in the shape of a circle were first investigated by Embley and Sih [1971] for extensional impact and by Sih and Embley [1971] for torsional impact. Their method of solution involves isolating the singular portion dynamic stresses in the Laplace transform domain such that the dynamic stress intensity factor can

be obtained by direct application of the Laplace inversion theorem. Some other references are Mal [1968, 1970a], Olesiak and Sneddon [1959], Pal and Sridharan [1980a, 1980b], Arwin and Erdogan [1971], Green [1949], Dhawan [1973], Krenk and Schimidt [1982]. Robertson [1967] solved the problem of diffraction of a plane longitudinal wave by penny-shaped crack. Carrier [1946] studied the propagation of waves in orthotropic medium. Achenbach and Bazant [1975] considered the problem of elastodynamic near-tip stress and displacement fields for rapidly propagating cracks in orthotropic materials. Kassir and Tse [1983] also solved the problem of moving a Griffith crack in an orthotropic material.

The study of interfacial cracks between anisotropic media is of great impotance in fracture analysis of composites. For detection and quantitative measurement of interfacial cracks in a fiber reinforced composite solid, one needs to study the crack scattering problem in an anisotropic solid. A typical example of interfacial cracking in anisotropic solids is the delamination of fiber-reinforced composite laminates. The interfacial cracks in composites are introduced by fabrication defects such as incomplete wetting or trapped air bubles between layers, or by debonding of two laminas as a result of high stress concentration at geometric or material discontinuities (c.f. Pipes and Pagano [1970]). Kuo [1984] determined transient stress intensity factors of an interfacial crack between two dissimilar anisotropic half-spaces. To this effect, the mathematical problem has firstly been reduced to three coupled integral equations. Solution of the singular integral equation has been obtained by the use of the Jacobi polynomial and expressions for stress intensity factors at the crack tip of the interfacial crack has been determined. The surface response of a layered half-space, for both isotropic and anisotropic materials, due to a plane SH-wave, incident at an arbitrary angle, has been studied by Karim and Kundu [1988] using the technique of Neerhoff [1979]. The scattering of elastic waves

by a circular crack in an anisotropic solid has also been studied by Kundu and Bostrom [1991].

We now discuss a certain type of mixed boundary value problems which are known as contact problem in the theory of elasticity. The contact problem is formulated as a problem about the influence of a rigid body on an elastic body.

Hertz investigated the punch problem in 1882. In this time many researchers followed his work. Chaplygin [1950] collected a number of punch problems worked out during the 19th century. Many authors such as Glagolev [1942], Mushkelishvilli [1953, 1963], Mossakovski [1958], Ufliand [1956], Spence [1968, 1975] investigated punch problems. In the literature (e.g. Gladwell [1980]) a variety of punch problems can be found.

The problem of diffraction of antiplane shear wave by one or more finite rigid strip at the interface has been treated by Palaiya and Majumder [1981], Singh and Dhaliwal [1984], Tait and Moodie [1981], Mandal and Ghosh [1992a, 1992b]. Palaiya amd Majumder [1981] considered the problem of diffraction of antiplane shear wave by a finite rigid strip at the interface of two bonded dissimilar half-spaces. The problem of diffraction of antiplane shear wave by a pair of parallel rigid strips at the interface of two bonded dissimilar elastic media was solved by Mandal and Ghosh [1992a]. De Sarkar [1985a, 1985b] solved the punch problem on a micropolar elastic solid.

Different techniques have been adopted by many authors to solve these type of crack and inclusion problems. From this standpoint, these problems may be divided into two catagories :

(I) one for low frequency oscillation of the source or long wave scattering or transmission; and

(II) the other for high frequency oscillation or short wave scattering or transmission in the medium.

The term long and short are used in comparison to the region of the source of disturbance or the size of the crack or strip etc. inside the medium to the wave length of disturbance.

Here we briefly discuss **some techniques** which are generally used in crack problems in elastodynamics.

INTEGRAL TRANSFORM TECHNIQUE

As the equations of motion in the theory of elasticity are partial differential equations which may be discussed with reference either to Helmholtz equation or to Laplace's equation, the method of integral transform is one of the most effective methods for solving such equations as application of this method to such equations results in the lowering of the dimension of an equation by one. There are several forms of integral transform and the choice of an integral transform depends on the structure of the equation and the geometry of the domain.

The integral transform $\bar{f}(p)$ of a function f(x) defined on an interval (a, ∞) is an expression of the form

$$\bar{f}(p) = \int_a^\infty f(x)\, K(x,p)\, dx \qquad (4)$$

where 'a' is a real number and p is a complex parameter varying over some region D of the complex plane. K(x,p) is called the kernel of the transformation. The transformation (4) becomes particularly useful if it possesses inverse mapping. In that case one can express f(x) in terms of its integral transform by

$$f(x) = \frac{1}{2\pi i} \int_\Gamma \bar{f}(p)\, M(x,p)\, dp \qquad (5)$$

where M(x,p) is a suitable function defined in $a < x < \infty$ and $p \in D$ and is called the kernel of the

inverse transform, which is defined for all x in the interval (a, ∞). The complex parameter p is in the region D while Γ is a suitable path of integration in D. After reducing the governing partial differential equation, the reduced problem can be solved for $\bar{f}(p)$. The solution of the original equation can be expressed in terms of the inverse integral, which may then be evaluated. The inversion from the transformed space to the space of actual variables usually involves very complicated integrations. In many cases even the numerical integration can not be performed successfully because of the highly oscillatory character of the integrands (cf Eringen and Suhubi [1975]; Chap.7, Achenbach [1975]; Chap.7). In particular, mixed boundary value problems like the dynamic response of a punch on an elastic half-space and the problem involving the presence of a crack or a strip inside an elastic medium may be reduced to Fredholm integral equation of first kind or to dual integral equations.

NOBLE'S METHOD

Suppose that a mixed boundary value problem is formulated by suitable integral transform so as to be governed by a set of dual integral equations of the form

$$\int_0^\infty x^{-1}\left[1 + K(x)\right] S(x)\, J_\nu(rx)\, dx = f(r); \qquad 0 \le r < a \tag{6}$$

$$\int_0^\infty S(x)\, J_\nu(rx)\, dx = g(r); \qquad r > a \tag{7}$$

where the functions K(x), f(r) and g(r) are known.

According to Noble [1963], when $\nu > -1/2$

$$S(x) = \sqrt{\frac{2x}{\pi}} \left\{ \int_0^a \sqrt{t}\,\Theta(t)\, J_{\nu-\frac{1}{2}}(xt)\, dt + \int_a^\infty t^{\nu+\frac{1}{2}}\, G(t)\, J_{\nu-\frac{1}{2}}(xt)\, dt \right\} \tag{8}$$

where $\Theta(t)$ satisfies the Fredholm integral equation

$$\Theta(t) + \frac{1}{\pi}\int_0^a M(\varsigma,t)\,\Theta(\varsigma)\,d\varsigma = t^{-\nu}F(t) - H(t); \qquad 0 \le t < a \tag{9}$$

in which

$$M(\varsigma,t) = \pi\sqrt{\varsigma t}\int_0^\infty xK(x)\,J_{\nu-\frac{1}{2}}(\varsigma x)\,J_{\nu-\frac{1}{2}}(tx)\,dx \tag{10}$$

$$F(t) = \frac{d}{dt}\int_0^t f(r)\,r^{\nu+1}\,(t^2 - r^2)^{-1/2}\,dr \tag{11}$$

$$H(t) = \sqrt{t}\int_0^\infty xK(x)\,J_{\nu-\frac{1}{2}}(xt)\,dx \int_a^\infty \xi^{\nu+\frac{1}{2}}\,G(\xi)\,J_{\nu-\frac{1}{2}}(x\xi)\,d\xi \tag{12}$$

$$G(\xi) = \int_\xi^\infty g(r)\,r^{-\nu+1}\,(r^2 - \xi^2)^{-1/2}\,dr \tag{13}$$

The integral equation (9) can be solved for $\Theta(t)$ iteratively for low frequency and consequently $S(x)$ can be determined.

All the axisymmetrical contact problems may be solved by using Hankel transforms and they then reduce to the solution of a number of sets (or pairs) of dual integral equations. To solve these dual integral equations there are various methods one of which is Tranter's method. We discuss briefly the method of Tranter [1968] in solving axisymmetric problems.

TRANTER'S METHOD

The solution of certain physical problems involving axisymmetric geometry can be reduced to the determination of $F(p)$ from so called dual integral equations of the form

$$\int_0^\infty G(p)\,F(p)\,J_\nu(rp)\,dp = f(r), \qquad 0 < r < 1 \tag{14}$$

$$\int_0^\infty p\,F(p)\,J_\nu(rp)\,dp = 0, \qquad 1<r<\infty \tag{15}$$

where G(p) and f(r) are known functions.

A solution F(p) of the above integral equations as a series of Bessel functions can be found by setting

$$F(p) = p^{-k}\sum_{m=0}^{\infty} a_m J_{\nu+2m+k}(p) \tag{16}$$

where k is at present an arbitrary parameter, and proceeding as follows :

Substituting from (16) in the second equation of (15) and changing the order of integration and summation, one gets

$$\int_0^\infty p\,F(p)J_\nu(rp)\,dp = \sum_{m=0}^{\infty} a_m \int_0^\infty p^{1-k} J_\nu(rp)\,J_{\nu+2m+k}(p)\,dp \tag{17}$$

provided $\nu > -1$ and $k > 0$, the formula

$$I(\nu,\mu,\lambda,a,b) = \int_0^\infty \frac{J_\nu(at)J_\mu(bt)}{t^\lambda}\,dt \tag{18}$$

$$= \frac{b^\mu \Gamma\left(\frac{\nu}{2}+\frac{\mu}{2}-\frac{\lambda}{2}+\frac{1}{2}\right)}{2^\lambda a^{\mu-\lambda+1}\Gamma(\mu+1)\Gamma\left(\frac{\lambda}{2}+\frac{\nu}{2}-\frac{\mu}{2}+\frac{1}{2}\right)}\; F_1\left(\frac{\nu+\mu-\lambda+1}{2}, \frac{\mu-\lambda-\nu+1}{2}; \mu+1; \frac{b^2}{a^2}\right)$$

shows that all the integrals on the right hand side of (17) vanish when r>1 (because of the factor $\Gamma(-m)$ in the denominator of the term multiplying the hypergeometric function) and hence the series in (16) automatically satisfies the second of the dual equations (15). The coefficients a_m have now to be chosen so that the series in (16) satisfies the first of the dual equations (15). For this purpose

we need the result

$$p^{-k} J_{\nu+2n+k}(p) = \frac{\Gamma(\nu+n+1)}{2^{k-1}\Gamma(\nu+1)\Gamma(n+k)} \int_0^1 r^{\nu+1}(1-r^2)^{k-1} F_n(k+\nu, \nu+1, r^2)\, J_\nu(pr)\, dr \qquad (19)$$

where n is a positive integer or zero and

$$F_n(\alpha, \gamma, x) = F_1(-n, \alpha+n; \gamma: x) \qquad (20)$$

is Jacobi's polynomial.

Substituting from (16) in the first of (15), multiplication by

$$r^{\nu+1}(1-r^2)^{k-1} F_n(k+\nu, \nu+1, r^2),$$

integration with respect to r between 0 and 1, interchange of the order of integrations and use of (19) give

$$\sum_{m=0}^{\infty} a_m \int_0^{\infty} G(p) p^{-2k} J_{\nu+2m+k}(p)\, J_{\nu+2n+k}(p)\, dp = E(\nu, n, k) \qquad (21)$$

where

$$E(\nu, n, k) = \frac{\Gamma(\nu+n+1)}{2^{k-1}\Gamma(\nu+1)\Gamma(n+k)} \int_0^1 f(r)\, r^{\nu+1}(1-r^2)^{k-1} F_n(k+\nu, \nu+1, r^2)\, dr. \qquad (22)$$

Equation (12) with n=0, 1, 2, 3, ... gives a set of simultaneous equations for the determination of the coefficients a_m. These simultaneous equations can be rewritten in more convenient form by making use of the formula

$$\int_0^{\infty} G(p) p^{-1} J_{\nu+2m+k}(p)\, J_{\nu+2n+k}(p)\, dp = \begin{cases} 0, & m \neq n \\ (2\nu+4n+2k)^{-1}, & m = n \end{cases} \qquad (23)$$

this being the form taken by equation

$$\int_0^{\infty} \frac{J_\nu(at)\, J_\mu(at)}{t}\, dt = \frac{\Gamma\left(\frac{\nu}{2}+\frac{\mu}{2}\right)}{2\Gamma\left(1+\frac{\nu}{2}-\frac{\mu}{2}\right)\Gamma\left(1+\frac{\nu}{2}+\frac{\mu}{2}\right)\Gamma\left(1-\frac{\nu}{2}+\frac{\mu}{2}\right)} = \frac{2}{\pi}\frac{\sin\frac{1}{2}(\mu-\nu)\pi}{\mu^2-\nu^2} \qquad (24)$$

when μ and ν are replaced respectively by $\nu+2n+k$, $\nu+2m+k$ and when 'at' is replaced by p, we find in this way

$$a_n + \sum_{m=0}^{\infty} L_{m,n}\, a_m = (2\nu+4n+2k)\, E(\nu,n,k) \tag{25}$$

where

$$L_{m,n} = (2\nu+4n+2k) \int_0^{\infty} \left(G(p)p^{1-2k} - 1\right) p^{-1} J_{\nu+2m+k}(p)\, J_{\nu+2n+k}(p)\, dp. \tag{26}$$

The iterative solution of the simultaneous equations (25) is

$$a_n = E_n - E_n' + E_n'' - \ldots\ldots \tag{27}$$

where

$$E_n = (2\nu+4n+2k)\, E(\nu,n,k), \quad E_n' = \sum_{m=0}^{\infty} L_{m,n}\, E_m, \quad E_n'' = \sum_{m=0}^{\infty} L_{m,n}\, E_m' \tag{28}$$

and so on.

Equations (16), (27), (28), (26) and (23) provide a theoratical solution of the dual integral equations. For a practical solution it is necessary to be able to choose the parameter k so that the expression $\left(G(p)p^{1-2k} - 1\right)$, which occurs in the formula (26) for $L_{m,n}$, is fairly small.

Low frequency diffraction due to disc, cone and rigid cylinder have been studied by Asvestas and Kleinman [1970], Senior [1971], Datta [1974], Roy [1982a, 1982b, 1982c], Sleeman [1967], Roy and Sabina [1982], Datta [1970] considered the problem of diffraction of a plane compressional elastic wave by a rigid circular disc.

Singh and Dhaliwal [1984] solved the closed form solutions of dynamic punch problems by integral transform method. The mixed boundary value problem was reduced to a set of dual integral equations with trigonometrical kernals. The solutions were obtained by using Hilbert transform technique (Srivastava and Lowengrub [1968]). We now discuss the Hilbert transform technique as follows :

HILBERT TRANSFORM TECHNIQUE

Using the theorem (Tricomi [1951]) if $p \in L_2(a,b)$, then the equation

$$\frac{1}{\pi}\int_a^b \frac{h(x)}{x-y}dx = p(y); \quad y\in(a,b) \tag{29}$$

has the solution

$$h(x) = -\frac{1}{\pi}\sqrt{\frac{x-a}{b-x}}\int_a^b \sqrt{\frac{b-y}{y-a}}\frac{p(y)}{y-x}dy + \frac{c}{\sqrt{(x-a)(b-y)}} \tag{30}$$

where c is an arbitrary constant and the first term belongs to the class $L_2(a,b)$. Using the above theorem, Srivastava and Lowengrub [1968] found that the solution of the integral equation

$$\frac{1}{\pi}\int_a^b \frac{2th(t^2)}{t^2-y^2}dt = p(y); \quad y\in(a,b) \tag{31}$$

(Provided that p satisfies the conditions of the above theorem) is given by

$$h(t^2) = -\frac{1}{\pi}\sqrt{\frac{t^2-a^2}{b^2-t^2}}\int_a^b \sqrt{\frac{b^2-y^2}{y^2-a^2}}\frac{2yp(y)}{y^2-t^2}dy + \frac{c}{\sqrt{(t^2-a^2)(b^2-t^2)}} \tag{32}$$

where c is an arbitrary constant.

Using Hilbert transform technique problems involving pair of cracks or strips can easily be solved. Using Hilbert transform technique Sarkar, Mandal and Ghosh [1994] solved the elastodynamic problem involving two co-planar Griffith cracks in a orthotropic medium. Using the same technique Das and Ghosh [1992] treated four co-planar Griffith crack problems in an infinite elastic medium. Itou [1978] solved the problem of dynamic stress concentration around two co-planar Griffith cracks in an infinite elastic medium using Schmidt method. Itou [1980a, 1980b] also considered two different problems involving two finite cracks using the same technique. The problem of determining the transient stress distribution in an infinite elastic medium weakened by two coplanar Griffith cracks has been reduced by Itou to the following equation

$$\sum_{n=1}^{\infty} c_n(s)\left[-\frac{4c_1^3}{k^2s^2b}\int_0^{\infty} g(s,\xi)\sin\left(\frac{a+b}{2}\xi-\frac{n\pi}{2}\right)J_n\left(\frac{b-a}{2}\xi\right)\cos(\xi x)d\xi\right] = -pc_L(bs), \quad a<x<b \tag{33}$$

with

$$g(s,\xi) = \frac{\left[\xi^2 + k^2 s^2/(2c_L^2)\right]^2 - \xi^2 \gamma_1 \gamma_2}{\xi \gamma_1} \tag{34}$$

where locations of the cracks are $a \le |x| \le b$, $|y| < \infty$, $z = 0$, $c_L = \sqrt{\frac{\lambda+2\mu}{\rho}}$, $c_T = \sqrt{\frac{\mu}{\rho}}$, $k = c_L / c_T$ and $c_n(s)$ are unknown coefficients.

To determine the coefficients $c_n(s)$ by Schmidt's method [1958] equation (33) can be rewritten as

$$\sum_{n=1}^{\infty} c_n(s)\, E_n(s,x) = -u(s,x), \qquad a<|x|<b \tag{35}$$

where $E_n(s,x)$ and $u(s,x)$ are known functions and the coefficients $c_n(s)$ are unknown.

A set of functions $P_n(s,x)$ which satisfy the orthogonality conditions

$$\int_0^b P_m(s,x)\, P_n(s,x)\, dx = N_n \delta_{mn}, \qquad N_n = \int_0^b P_n^2(s,x)\, dx \tag{36}$$

can be constructed from the function, $E_n(s,x)$, such that

$$P_n(s,x) = \sum_{n=1}^{\infty} \frac{M_{in}}{M_{nn}} E_i(s,x) \tag{37}$$

where M_{in} is the cofactor of the element d_{in} of D_n, which is defined as

$$D_n = \begin{vmatrix} d_{11} & d_{12} & \cdots & \cdots & d_1 n \\ d_{21} & d_{22} & \cdots & \cdots & d_2 n \\ & & \cdot & & \\ & & \cdot & & \\ & & \cdot & & \\ d_{n1} & \cdots & \cdots & \cdots & d_{nn} \end{vmatrix} \tag{38}$$

$$d_{in} = \int_a^b E_i(s,x)\, E_n(s,x)\, dx.$$

Using equations (35) and (36) one can obtain

$$c_n(s) = \sum_{j=n}^{\infty} q_j \frac{M_{nj}}{M_{jj}} \tag{39}$$

with

$$q_j = -\frac{1}{N_j}\int_a^b u(s,x)\,P_j(s,x)\,dx\ . \tag{40}$$

KELLER'S GEOMETRICAL METHOD

Keller's theory of geometrical diffraction applied to elastodynamics states that the two conical surfaces of diffracted rays are generated when an incident ray strikes an edge. The surface of the inner cone consists of rays of longitudinal motion, while the surface of the outer cone is composed of rays of transverse motion. The half-angles of the cones are related by Snell's law. Fig.1 shows the cones generated by an incident longitudinal ray. For this case the diffracted longitudinal rays make the same angle ϕ_L with the tangent to the edge as the incident ray, and the diffracted rays of transverse motion are under an angle ϕ_T with the edge, where $C_L \cos\phi_T = C_T \cos\phi_L$.

For a straight diffracting edge, and an incident longitudinal ray, the diffracted displacement fields are related quantitatively to the incident field by

$$\vec{u}_d^{\,L} = e^{i\omega s_1/c_L}\left[S_1(1+S_1/R_L)\right]^{-1/2} D_L\ \hat{i}_L^{\,d}\ A\, e^{i\omega(S_0/C_L - t)} \tag{41}$$

$$\vec{u}_d^{\,T} = e^{i\omega s_2/c_T}\left[S_2(1+S_2/R_d)\right]^{-1/2} D_T\ \hat{i}_T^{\,d}\ A\, e^{i\omega(S_0/C_L - t)} \tag{42}$$

Here $A\exp[i\omega(S_0 / C_L - t)]$ defines the amplitude and the phase of the incident field at the point of diffraction, and D_L and D_T are diffraction coefficients which relate the diffracted field to the incident field. Also S_1 and S_2 are the smaller of the principal radii of curvature of the diffracted wave front, or equivalently the distances along the diffracted rays from the points of diffraction to the observation point. The unit vectors $\hat{i}_L^{\,d}$ and $\hat{i}_T^{\,d}$ relate the directions of displacement of the diffracted field to the direction of displacement of the incident field. For a straight diffracting edge

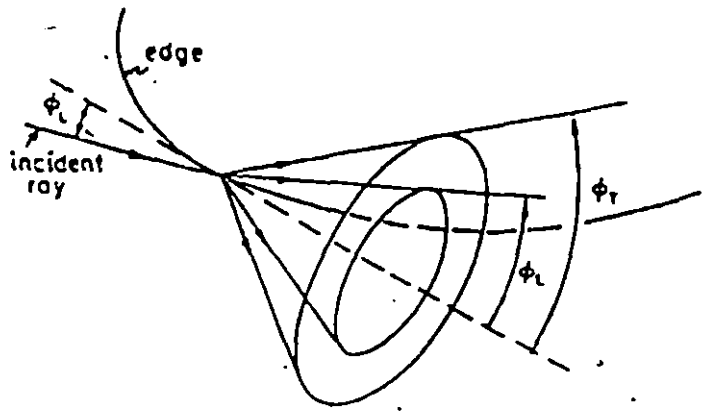

Fig.1. Cones of diffracted longitudinal and trandverse rays for an incident longitudinal ray.

R_L is the radius of curvature at the point of diffraction of the curve formed by the intersection of the incident wave front and the plane which contains the incident ray and the edge, and

$$R_d = R_L \frac{\sin\phi_T}{\sin\phi_L} \frac{\tan\phi_T}{\tan\phi_L}. \tag{43}$$

In case of high frequency oscillation Wiener-Hopf technique (Noble, [1958]) and Keller's [1958] geometrical theory are found to be most suitable. We now briefly discuss this methods.

THE WIENER-HOPF TECHNIQUE

Let a function $\phi(z)$ analytic in the interval $y_- < \mathrm{Im} z < y_+$ be defined in the plane of a complex variable z. It is required to express $\phi(z)$ in the form

$$\phi(z) = \phi_+(z)\,\phi_-(z) \tag{44}$$

where $\phi_+(z)$ and $\phi_-(z)$ are functions analytic in the half-plane $\mathrm{Im} z > y_-$ and the half-plane $\mathrm{Im} z < y_+$ respectively. The problem is called factorization problem. In a more general case, it is required to define two functions $\phi_+(z)$ and $\phi_-(z)$ which are analytic in the same half-planes respectively and which satisfy the following relation in the interval

$$A(z)\,\phi_+(z) + B(z)\,\phi_-(z) + C(z) = 0 \tag{45}$$

where A(z), B(z) and C(z) are given analytic functions in the interval. It is obvious that if C(z)=0, we obtain the representation (44) after the corresponding changes in the notation.

Let us assume that the function $\phi(z)$ which is to be factorised does not have any zeros in the interval $y_- < \mathrm{Im} z < y_+$ and tend to infinity as $x \to \infty$. In this case, neither of the functions $\phi_+(z)$ and $\phi_-(z)$ will have any zero, and we can take the logarithm of both sides of the relation (44)

$$\log\phi(z) = \log\phi_+(z) + \log\phi_-(z). \tag{46}$$

The function $F(z) = \log\phi(z)$ satisfies the condition

$$|F(x+iy)| < C|x|^{-p}; \qquad (p>0 \text{ for } x \to \infty) \tag{47}$$

and hence the relation (46) can always be solved with the help of the transformation

$$F(z) = F_+(z) + F_-(z) . \tag{48}$$

Finally, we get

$$\phi(z) = e^{F_+(z)} . e^{F_-(z)} = \phi_+(z)\,\phi_-(z) . \tag{49}$$

If the function $\phi(z)$ has zeros in the intervals we must consider a new function

$$\phi_1(z) = \frac{(z^2 + b^2)^{N/2}\,\phi(z)}{\prod_{i=1}^{N_1} (z - z_i)^{\alpha_i}} \tag{50}$$

where z_i and α_i are the zeros, their multiplicity in the interval $N_1 \le N$, where N is the total number of zeros, $b > (y_+, y_-)$. The factor in the numerator of (50) ensures that the properties of auxiliary functions are conserved at infinity.

Let us now consider the relation (45) and carry out its factorization into L_+ and $1/L_-$ for the same interval of the ratio A/B. The relation (45) can be represented in the form

$$L_+(z)\,\phi_+(z) + L_-(z)\,\phi_-(z) + L_-(z)\,C(z)/B(z) = 0. \tag{51}$$

The expression $L_-(z)\,C(z)/B(z)$ Can be represented in the following form in accordance with (48)

$$E_+(z) + E_-(z)$$

where $\phi_+(z)$ and $\phi_-(z)$ are functions analytic in the half-plane $y > y_-$ and the half-plane $y < y_+$ respectively. Taking this into account, we get

$$L_+(z)\,\phi_+(z) + E_+(z) = -L_-(z)\,\phi_-(z) - E_-(z). \tag{52}$$

It follows from the generalized Liouville's theorem that the left as well as right hand side of (52) represents the same polynomial $P_n(z)$ of nth degree.

Wiener-Hopf technique and different other techniques for solving partial differential equation

arising in solid mechanics have been elaborately discussed by Duffy [1994] in his book.

BOUNDARY ELEMENT METHOD

The formulation of general wave diffraction problem by a crack in the half-space with the aid of the frequency-domain direct Boundary Element Method (BEM) has been done by Niwa and Hirose [1986] and has also been elaborately decribed in the book Boundary Element Method in Elastodynamics [1988].

Consider the crack $\sum$ with two faces Σ^- and Σ^+ in the half-space V with a free surface S subjected to an oblique harmonic wave that creates a free displacement field $\bar{u}_i^f$.

For this type of geometry one can write the two integral equations

$$-\int_{S+\Gamma} \bar{G}_{ik}\,\bar{t}_k^s\,ds + \int_{S+\Gamma} \bar{F}_{ik}\,\bar{u}_k^s\,ds = \begin{cases} \bar{u}_i^s(x), & x \in V \\ 0, & x \in V^c \end{cases} \tag{53}$$

$$+\int_{\Gamma} \bar{G}_{ik}\,\bar{t}_k^f\,ds - \int_{\Gamma} \bar{F}_{ik}\,\bar{u}_k^f\,ds = \begin{cases} \bar{u}_i^f(x), & x \in \Omega \\ 0, & x \in \Omega^c \end{cases} \tag{54}$$

where Γ represents the surface of a flat cavity Ω that in the limit becomes the crack Σ, superscripts s and f stand for scattered and free fields, respectively and superscript c denotes the complementary domain and G_{ij} is the Green function in infinite medium due to the body force

$$b_j = \delta(\vec{x} - \vec{\xi})\,\delta(t)\,e_j \tag{55}$$

where δ denotes Dirac delta function and e is a constant unit vector and F_{ij} is the corresponding stress

component given by

$$F_{ij} = \left\{\lambda G_{mk,m}\delta_{ij} + \mu(G_{ik,j} + G_{jk,i})\right\} n_j ; \tag{56}$$

n_j being the outward pointing normal vector.

Combination of equations (53) and (54) results in

$$\int_S \bar{F}_{ik}\bar{u}^s_k ds + \int_\Gamma \bar{F}_{ik}\bar{u}_k ds = \begin{cases} \bar{u}^s_i(x), & x\in V \\ -\bar{u}^f_i(x), & x\in\Omega \\ 0, & x\in V^c\cap\Omega^c \end{cases} \tag{57}$$

where the traction free boundary condition on Γ has been taken into account as well as the fact that $\bar{u}_i = \bar{u}^f_i + \bar{u}^s_i$. For crack problems (57) is unsuitable because it leads to an undetermined integral equation. Thus equation (57) is differentiated according to the constitutive law to give

$$\int_S \bar{W}_{ijk}\bar{u}^s_k ds + \int_\Gamma \bar{W}_{ijk}\bar{u}_k ds = \begin{cases} \bar{t}^s_i(x), & x\in V \\ -\bar{t}^f_i(x), & x\in\Omega \\ 0, & x\in V^c\cap\Omega^c \end{cases} \tag{58}$$

where

$$\bar{W}_{ijk} = \lambda \bar{F}_{kj,j} n_j + \mu\left(\bar{F}_{ki,j} + \bar{F}_{kj,i}\right)n_j \tag{59}$$

In the limit as the flat cavity approaches a crack, the above equation becomes

$$\int_S \bar{W}_{ijk}\bar{u}^s_k ds + \int_\Sigma \bar{W}_{ijk}\left[\bar{u}_k\right] ds = \begin{cases} \bar{t}^s_i(x), & x\in V \\ 0, & x\in V^c \end{cases} \tag{60}$$

where the third brackets denote the discontinuity across Σ, i.e.

$$\left[\bar{u}_k\right] = \bar{u}^+_k - \bar{u}^-_k . \tag{61}$$

Taking the limit of equation (60) as the field point x approaches the boundary S or Σ, one

obtains the traction boundary integral equations :

$$\int_S \bar{W}_{ijk}\,\bar{u}^s_k\,ds + \int_\Sigma \bar{W}_{ijk}\left[\bar{u}_k\right]ds = 0\,; \qquad x \text{ on } S \tag{62}$$

$$\int_S \bar{W}_{ijk}\,\bar{u}^s_k\,ds + \int_\Sigma \bar{W}_{ijk}\left[\bar{u}_k\right]ds = -\bar{t}^f_i\,; \qquad x \text{ on } \Sigma \tag{63}$$

where the two parallel line segments on the integral sign signify a finite part integral in the sense of Kutt [1975a-c]. Equations (62) and (63) constitute a system of equations to be solved for the unknowns $\left[\bar{u}_k\right]$ on Σ and $\bar{u}^s_k$ on S following standard direct BEM procedures. The singularities in (62) and (63) are of order r^{-3} and as such stronger than then r^{-2} singularities of (57). They are computed by using the rigid body motion concept and by introducing an auxiliary surface close to the discretized portion of S.

Another special BEM is a direct method which starts with a reciprocity relation that finally yields for the scattered displacement field the integral representation

$$\bar{u}^s_k = \int_\Sigma \bar{F}_{ik}\left[\bar{u}_i\right]ds\,. \tag{64}$$

Equation (64) is then substituted into Hooke's law to derive expressions for the scattered stress tensors in terms of $\left[\bar{u}_i\right]$. Finally, use of the boundary conditions produces a set of singular integral equations for the $\left[\bar{u}_i\right]$. These equations are solved numerically either by employing special quadrature rules or by expanding known and unknown functions in terms of suitable basis functions and then determining the expansion co-efficients of of the $\left[\bar{u}_i\right]$. This method has been succeessfully used by Achenbach et al [1983, 1984], Vander Hijden and Neerhoff [1984a-b] and McMaken [1984] for the solution of wave diffraction problems in the infinite or semi-infinite half-plane containing a crack or in the infinite space containing circular cracks.

The thesis presented here consists of some boundary value problems in elastodynamics involving wave propagation due to some finite source or cracks. The work has been presented in four chapters.

The **first chapter** deals with high frequency diffraction of elastic wave by Griffith cracks which are either stationary or moving in character.

In the **second chapter**, inclusion problem in elastodynamic in infinitely long elastic strip is considered.

The **third chapter** deals with the scattering of elastic waves by vertical crack.

Finally in the **last chapter,** elastodynamic Green's function due to ring source has been treated.

The summary of the thesis is presented here chapterwise .

In the **first problem of chapter-1**, the high frequency elastodynamic problem involving the excitation of an interface crack of finite width lying between two dissimilar anisotropic elastic half planes has been analysed. The crack surface is excited by a pair of time harmonic antiplane line sources situated at the middle of the cracked surface. The problem has first been reduced to one with the interface crack lying between two dissimilar isotropic elastic half planes by a transformation of relevant co-ordinates and parameters. The problem has then been formulated as an extended Wiener-Hpof equation (cf. Noble. 1958) and the asymptotic solution for high frequency has been derived. The expression for the stress intensity factor at the crack tips has been derived and the numerical results for different pairs of materials have been presented graphically.

In the **second problem of this chapter**, the transient elastodynamic problem involving the scattering of elastic waves by a Griffith crack of finite width lying at the interface of two dissimilar

anisotropic half planes has been analysed. The crack faces are subjected to a pair of suddenly applied antiplane line loads situated at the middle of the cracked surface. The problem has first been reduced to one with the interface crack of finite width lying between two dissimilar isotropic elastic half planes by a transformation of relevant co-ordinates and parameters. Spatial and time transforms are the applied to the governing differential equations and to the boundary conditions which yield generalized Wiener-Hopf type equations. The integral equations arising are solved by the standard interation technique. Physically each successive order of iteration correspond to successive scattered or rescattered wave from one crack tip to the other. Finally, expression for the resulting mode III stress intensity factor are determined as a function of time for both symmetric and antisymmetric loadings. Each crack tip stress intensity factor has been plotted versus time for four pairs of different types of materials.

The **third problem** deals with the scattering of horizontally polarised shear wave by a Griffith crack moving with uniform velocity along a bimaterial interface has been investigated. Using Fourier transform technique, the mixed boundary value problem has been reduced to the solution of a pair of dual integral equations. These equations are further reduced to a pair of coupled Fredholm integral equation of the second kind. The singular character of the dynamic stress near the crack tip has been examined and the expression for dynamic stress intensity factor has been derived. The dynamic stress intensity factors for several values of wave number, angle of incidence, crack speed and material constants have been depicted by means of graphs.

In **chapter-2**, we have considered the problem of diffraction of normally incident SH-wave by two co-planar finite rigid strips placed symmetrically in an infinitely long isotropic elastic strip perpendicular to the lateral suface of the elastic strip. The mixed boundary value problem gives rise

to the determination of the solution of the triple integral equations which finally have been reduced to the solution of a Fredholm integral equation of second kind. The equation has been solved numerically for low frequency range. Finally the elastodynamic stress intensity factors are obtained. The variations of the stress intensity factors at the tips of the rigid strips with frequency have been depicted by means of graphs.

The problem of **chapter-3** deals with the scattering of elastic wave by an edge crack. A time harmonic plane longitudinal wave is incident on a half-space containing a vertical edge crack. Both the incident field as well as the scattered field have been decomposed into symmetric and antisymmetric fields with respect to the plane of the crack so that the problem is reduced to the boundary value problem for a 90^0 wedge. In both the symmetric and antisymmetric problem, incident body waves are at first diffracted by the edge of the crack. For high frequency solution, the diffracted body wave being insignificant after a few wave lengths, the significant part of the diffracted wave is the Rayleigh wave which is reflected back from the corner of the wedge giving rise to diffracted Rayleigh wave from the crack tip. This process of reflection of surface wave from the corner of the wedge and subsequent diffraction by the crack tip continues. Considering the contribution from the incident body waves and all the reflected Rayleigh waves, stress intensity factors have been determined and their dependence on the frequency and on the angle of incidence has been depicted by means of graphs.

In the **last chapter** (chapter-4), the elastodynamic Green's functions for time harmonic radial and axial ring sources and for time harmonic torsional ring source as well in a transversely isotropic medium has been derived. The axis of material symmetry and the axis of ring source coincides. Fourier and Hankel transforms have been used to derive the solution in integral form.

Finally, stationary phase method has been used to evaluate the displacement at large distances away from the ring source. For Graphite-epoxy composite material, the displacements have been depicted by means of graphs.

With this much of introduction, we now present the thesis chapterwise. References given in the thesis do not include all the previous workers in this line. But attempt has been made to include most of them.

CHAPTER - 1

DIFFRACTION OF WAVES

[1]HIGH FREQUENCY SCATTERING DUE TO A PAIR OF TIME-HARMONIC ANTIPLANE FORCES ON THE FACES OF A FINITE INTERFACE CRACK BETWEEN DISSIMILAR ANISOTROPIC MATERIALS

1. INTRODUCTION

The extensive use of composite materials in modern technology has created interest among the scientists for carrying on considerable research work in the modeling, testing and analysis of laminated media. The laminated composites which behave as anisotropic material may be weakened by interface flaws which can lead to serious degradation in load carrying capacity.

Neerhoff [1979], therefore, studied the diffraction of Love waves by a crack of finite width at the interface of a layered half-space. Kuo [1992] carried out numerical and analytical studies of transient response of an interfacial crack between two dissimilar orthotropic half-spaces. Kuo and Cheng [1991] studied the elastodynamic responses due to antiplane point impact loading on the faces of a semi-infinite crack lying at the interface of two dissimilar anisotropic elastic materials. The problem of diffraction of normally incident antiplane shear wave by a crack of finite width situated at the interface of two bonded dissimilar isotropic elastic half-spaces has been studied by Pal and Ghosh [1990].

In the present paper we are interested in finding the high-frequency solution of the diffraction of elastic waves by a Griffith crack of finite width excited by a pair of time-harmonic concentrated antiplane line loads situated at the centres of the cracked surfaces. The materials are assumed to possesss certain material symmetry and the crack plane is assumed to coincide with one of the planes

---

[1] **Published in the European Journal of Mechanics A/Solids, V18, 1013-1026, 1999.**

of material symmetry, so that the inplane and the antiplane motion are not coupled.

The high-frequency solution of the diffraction of elastic waves by a crack of finite size is interesting in view of the fact that the transient solution close to the wave front can be represented by an integral of the high-frequency component of the solution. The analysis of the paper is first based on the observation of several researchers, e.g., Achenbach and Kuo [1986], Ma and Hou [1989], Markenscoff and Ni [1984] that antiplane shear deformation in an anisotropic solid can be deduced from the corresponding deformations of an isotropic solid by a transformation of relevant co-ordinates and parameters. Based on this observation, analysis of the interface crack by line loads between two bonded dissimilar anisotropic elastic solids can first be converted to that of a crack between two dissimilar isotropic elastic materials. Later, following the method of Chang [1971], the problem has been formulated as an extended Wiener-Hopf equation. The Wiener-Hopf equation in brief can be found in the book of Achenbach [1973]. The asymptotic solutions for high-frequencies or for wave lengths short compared to the width of the crack have been derived. Expression for the dynamic stress intensity factor near the crack tips has been obtained and the results have been illustrated for different pairs of materials.

2. FORMULATION OF THE PROBLEM

Let (X,Y,Z) be rectangular Cartesian co-ordinates. The X-axis is taken along the interface, Y-axis vertically upwards into the medium and Z-axis is perpendicular to the plane of the paper. Let an open crack of finite width 2L be located at the interface of two bonded dissimilar anisotropic semi-infinite elastic solids lying parallel to X-axis. The anisotropic half-planes are characterized by the elastic moduli $(C_{ik})_j$; (i,k=4,5) and mass density $\bar{\rho}_j$. The subscript j (j=1,2) corresponds to the

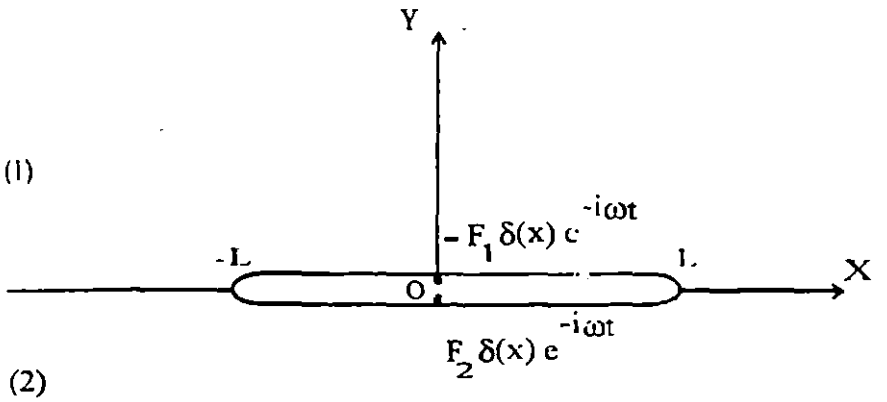

Fig.1. Geometry of the problem.

upper and lower semi-infinite media respectively.

A pair of concentrated time-harmonic antiplane shear forces in the Z-direction of magnitudes F_1 and F_2 act on the crack faces Y=0+ and Y=0- respectively at X=0 as shown in Fig.1. Thus the crack boundary conditions are

$$\sigma_{YZ}(X,Y,t) = \begin{cases} -F_1\delta(X)e^{-i\omega t}; & |X|<L, \quad Y=0+, \\ F_2\delta(X)e^{-i\omega t}; & |X|<L, \quad Y=0-, \end{cases} \tag{1}$$

$$\sigma^{(1)}_{YZ}(X,Y,t) = \sigma^{(2)}_{YZ}(X,Y,t) \quad \text{at } Y=0, \quad |X|>L \tag{2}$$

$$W_1(X,Y,t) = W_2(X,Y,t) \quad \text{at } Y=0, \quad |X|>L, \tag{3}$$

where ω is the circular frequency. Two dimensional antiplane wave motions of homogeneous anisotropic linearly elastic solids are governed by

$$(C_{55})_j \frac{\partial^2 W_j}{\partial X^2} + 2(C_{45})_j \frac{\partial^2 W_j}{\partial X \partial Y} + (C_{44})_j \frac{\partial^2 W_j}{\partial Y^2} = \bar{\rho}_j \frac{\partial^2 W_j}{\partial t^2} \qquad (j=1,2), \tag{4}$$

where W_j (X,Y,t) are the out-of-plane displacements.

The XY-plane has been assumed to coincide with one of the planes of material symmetry such that inplane and anti-plane motions are not coupled.

The relevant stress components are

$$\sigma^{(j)}_{XZ} = (C_{55})_j \frac{\partial W_j}{\partial X} + (C_{45})_j \frac{\partial W_j}{\partial Y}, \tag{5}$$

$$\sigma^{(j)}_{YZ} = (C_{45})_j \frac{\partial W_j}{\partial X} + (C_{44})_j \frac{\partial W_j}{\partial Y}. \tag{6}$$

Following Achenbach and Kuo [1986] and Kuo and Cheng [1991] we introduce a co-ordinate transformation

$$\left.\begin{aligned} x &= X - \frac{(C_{45})_j}{(C_{44})_j} Y, \\ y &= \frac{\mu_j}{(C_{44})_j} Y, \\ z &= Z, \end{aligned}\right\} \qquad (j=1,2) \tag{7}$$

where

$$\mu_j = \sqrt{(C_{44})_j (C_{55})_j - (C_{45})_j^2} \qquad (j = 1, 2). \tag{8}$$

Equation (7) and the chain rule of diffrentiation reduced (4) to the standard wave equation

$$\frac{\partial^2 W_j}{\partial x^2} + \frac{\partial^2 W_j}{\partial y^2} = s_j^2 \frac{\partial^2 W_j}{\partial t^2}, \tag{9}$$

where

$$s_j^2 = \frac{\rho_j}{\mu_j} \quad \text{and} \quad \rho_j = \frac{\bar{\rho}_j (C_{44})_j}{\mu_j}, \tag{10}$$

s_j is the slowness of shear waves. Without loss of generality we assume that

$$s_1 < s_2 . \tag{11}$$

Assume

$$W_j(x,y,t) = w_j(x,y) e^{-i\omega t}, \qquad j = 1,2, \tag{12}$$

so that $w_j(x,y)$ satisfy the following Helmholtz equations

$$\nabla^2 w_j(x,y) + k_j^2 w_j(x,y) = 0, \qquad j = 1,2, \tag{13}$$

with $\nabla^2 = \frac{\partial^2}{\partial x^2} + \frac{\partial^2}{\partial y^2}$ and $k_j = \omega s_j$, $j=1,2$.

It follows from equation (11) that $k_2 > k_1$.

It is easily verified from (4), (5) and (6) that the relevant displacement and the stress component in a physical anisotropic solid are related to those in the corresponding isotropic solid by

$$W_j(X,Y,t) = W_j(x,y,t), \tag{14}$$

$$\sigma_{XZ}^{(j)}(X,Y,t) = \frac{\mu_j}{(C_{44})_j} \sigma_{xz}^{(j)}(x,y,t) + \frac{(C_{45})_j}{(C_{44})_j} \sigma_{yz}^{(j)}(x,y,t), \tag{15}$$

$$\sigma_{YZ}^{(j)}(X,Y,t) = \sigma_{yz}^{(j)}(x,y,t). \tag{16}$$

Further writing

$$\sigma_{yz}^{(j)}(x,y,t) = \tau_{yz}^{(j)}(x,y) e^{-i\omega t}, \qquad j = 1,2, \tag{17}$$

under the changed co-ordinate system the boundary conditions (1), (2) and (3) reduce to

$$\tau_{yz}^{(1)}(x,y) = \mu_1 \frac{\partial w_1}{\partial y} = -F_1\delta(x); \qquad |x|<L, \quad y=0+, \tag{18}$$

$$\tau_{yz}^{(2)}(x,y) = \mu_2 \frac{\partial w_2}{\partial y} = F_2\delta(x); \qquad |x|<L, \quad y=0- \tag{19}$$

and

$$\mu_1 \frac{\partial w_1}{\partial y} = \mu_2 \frac{\partial w_2}{\partial y}, \qquad |x|>L, \quad y=0, \tag{20}$$

$$w_1(x,0+) = w_2(x,0-), \qquad |x|>L. \tag{21}$$

To obtain the solution to the wave equation (13), introduce the Fourier transform defined by

$$\bar{w}(\alpha,y) = \frac{1}{\sqrt{2\pi}} \int_{-\infty}^{\infty} w(x,y) e^{i\alpha x} dx. \tag{22}$$

The transformed wave equations are

$$\frac{d^2\bar{w}_1}{dy^2} - (\alpha^2 - k_1^2)\bar{w}_1(\alpha,y) = 0, \qquad y \geq 0, \tag{23}$$

$$\frac{d^2\bar{w}_2}{dy^2} - (\alpha^2 - k_2^2)\bar{w}_2(\alpha,y) = 0, \qquad y \leq 0. \tag{24}$$

The solutions of (23) and (24) which are bounded as $y \to \infty$ are

$$\bar{w}_1(\alpha,y) = A_1(\alpha) e^{-\gamma_1 y}; \qquad y \geq o, \tag{25}$$

$$\bar{w}_2(\alpha,y) = A_2(\alpha) e^{\gamma_2 y}; \qquad y < o, \tag{26}$$

where

$$\gamma_j = \begin{cases} \sqrt{\alpha^2 - k_j^2}; & |\alpha| > k_j, \\ -i\sqrt{k_j^2 - \alpha^2}; & |\alpha| < k_j. \end{cases} \tag{27}$$

Introduce, for a complex α

$$G_+(\alpha) = \frac{1}{\sqrt{2\pi}} \int_{L}^{\infty} \tau_{yz}^{(1)}(x,0) e^{i\alpha(x-L)} dx, \tag{28}$$

$$G_-(\alpha) = \frac{1}{\sqrt{2\pi}} \int_{-\infty}^{-L} \tau_{yz}^{(1)}(x,0) e^{i\alpha(x+L)} dx, \tag{29}$$

$$G_j(\alpha) = \frac{1}{\sqrt{2\pi}} \int_{-L}^{L} \tau_{yz}^{(j)}(x,0) e^{i\alpha x} dx. \tag{30}$$

The transformed stress at interface y=0 can therefore be written as

$$\bar{\tau}_{yz}^{(j)}(\alpha,0) = G_+(\alpha) e^{i\alpha L} + G_-(\alpha) e^{-i\alpha L} + G_j(\alpha). \tag{31}$$

Using the boundary conditions (18) and (19), we get

$$G_j(\alpha) = (-1)^j \frac{F_j}{\sqrt{2\pi}} \quad (j = 1,2). \tag{32}$$

Now

$$\bar{\tau}_{yz}^{(1)}(\alpha,0+) = \mu_1 \frac{\partial \bar{w}_1(\alpha,0+)}{\partial y} = -\mu_1 \gamma_1 A_1(\alpha), \tag{33}$$

$$\bar{\tau}_{yz}^{(2)}(\alpha,0-) = \mu_2 \frac{\partial \bar{w}_2(\alpha,0-)}{\partial y} = \mu_2 \gamma_2 A_2(\alpha). \tag{34}$$

Using (33) and (34), equation (31) can be written in the form

$$(-1)^j \mu_j \gamma_j A_j(\alpha) = G_+(\alpha) e^{i\alpha L} + G_-(\alpha) e^{-i\alpha L} + (-1)^j \frac{F_j}{\sqrt{2\pi}}.$$

Therefore

$$A_j(\alpha) = \frac{(-1)^j}{\mu_j \gamma_j} \left[G_+(\alpha) e^{i\alpha L} + G_-(\alpha) e^{-i\alpha L} + (-1)^j \frac{F_j}{\sqrt{2\pi}} \right]. \tag{35}$$

Now

$$\bar{w}_1(\alpha,0+) - \bar{w}_2(\alpha,0-) = \frac{1}{\sqrt{2\pi}} \int_{-L}^{L} \left\{ w_1(x,0+) - w_2(x,0-) \right\} e^{i\alpha x} dx = B(\alpha), \text{ say}$$

which is the measure of the displacement discontinuity across the crack surface. Therefore

$$B(\alpha) = A_1(\alpha) - A_2(\alpha). \tag{36}$$

Substituting the values of $A_j(\alpha)$ from (35) in equation (36) one finds an extended Wiener-Hopf equation namely

$$G_+(\alpha) e^{i\alpha L} + G_-(\alpha) e^{-i\alpha L} + B(\alpha) K(\alpha) = \frac{K(\alpha)}{\sqrt{2\pi}} \left\{ \frac{F_1}{\mu_1 \gamma_1} - \frac{F_2}{\mu_2 \gamma_2} \right\}, \tag{37}$$

where

$$K(\alpha) = \frac{\mu_1 \mu_2 \gamma_1 \gamma_2}{\mu_1 \gamma_1 + \mu_2 \gamma_2} = \frac{\mu_1 \mu_2 \sqrt{\alpha^2 - k_1^2}}{\mu_1 + \mu_2} R(\alpha) \tag{38}$$

and

$$R(\alpha) = \frac{(\mu_1+\mu_2)\sqrt{(\alpha_2-k_2^2)}}{\mu_1\sqrt{(\alpha_2-k_1^2)}+\mu_2\sqrt{(\alpha_2-k_2^2)}}. \qquad (39)$$

In order to obtain the high-frequency solution of the Wiener-Hopf equation given by (37) one assumes that the branch points $\alpha=k_1$ and $\alpha=k_2$ of $K(\alpha)$ possess a small imaginary part. Therefore k_1 and k_2 are replaced by k_1+ik_1' and k_2+ik_2' respectively where k_1' and k_2' are infinitesimally small positive quantities which would ultimately be made to tend to zero.

Now $K(\alpha)=K_+(\alpha)\,K_-(\alpha)$ where $K_+(\alpha)$ is analytic in the upper half-plane $\mathrm{Im}\alpha > -k_2'$ whereas $K_-(\alpha)$ is analytic in the lower half-plane $\mathrm{Im}\alpha < k_2'$ are given by (cf. Pal and Ghosh [1990]; Wickham [1980])

$$K_\pm(\alpha) = \sqrt{\frac{\mu_2(\alpha\pm k_1)}{1+m}}\exp\left[\frac{1}{\pi}\int_1^\gamma \frac{\tan^{-1}\left\{\dfrac{\sqrt{(t^2-1)}}{m\sqrt{(\gamma^2-t^2)}}\right\}}{t\pm\dfrac{\alpha}{k_1}}\,dt\right],$$

where $m=\dfrac{\mu_2}{\mu_1}$ and $\gamma=\dfrac{k_2}{k_1}$.

Since $\tau_{yz}(x,0)$ decreases exponentially as $x \to \pm\infty$, $G_+(\alpha)$ and $G_-(\alpha)$ have the common region of regularity as $K_+(\alpha)$ and $K_-(\alpha)$. It may be noted that $B(\alpha)$ is analytic in the whole of α-plane.

Now (37) can easily be expressed as two integral equations relating $G_+(\alpha)$, $G_-(\alpha)$ and $B(\alpha)$ as follows :

$$\frac{G_\pm(\alpha)}{K_\pm(\alpha)} + \frac{1}{2\pi i}\int_{C_\pm}\frac{G_\mp(s)e^{\mp 2isL}}{(s-\alpha)K_\pm(s)}ds - \frac{1}{2\pi i}\int_{C_\pm}\frac{e^{\mp isL}K_\mp(s)}{\sqrt{2\pi}(s-\alpha)}\left\{\frac{F_1}{\mu_1\gamma_1(s)}-\frac{F_2}{\mu_2\gamma_2(s)}\right\}ds$$

$$= -B(\alpha)K_\mp(\alpha)e^{\mp i\alpha L} - \frac{1}{2\pi i}\int_{C_\mp}\frac{G_\mp(s)e^{\mp 2isL}}{(s-\alpha)K_\pm(s)}ds + \frac{1}{2\pi i}\int_{C_\mp}\frac{e^{\mp isL}K_\mp(s)}{\sqrt{2\pi}(s-\alpha)}\left\{\frac{F_1}{\mu_1\gamma_1(s)}-\frac{F_2}{\mu_2\gamma_2(s)}\right\}ds, \qquad (40)$$

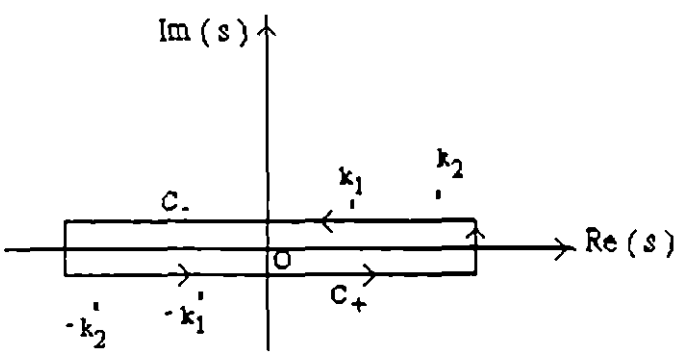

Fig.2. Path of integration in the complex s-plane.

where C_+ and C_- are the straight contours situated within the common region of regularity of $G_+(s)$, $G_-(s)$, $K_+(s)$ and $K_-(s)$ as shown in Fig.2.

In the first equation of (40) (i.e. the equation involving upper subscripts), the left-hand side is analytic in the upperhalf plane whereas the right-hand side is analytic in the lowerhalf plane and both of them are equal in the common region of analyticity of these two functions. So by analytic continuation, both sides of the equation are analytic in the whole of the s-plane. Now, since

$$\tau_{yz} = O(|x \mp L|^{-1/2}) \qquad \text{as} \quad x \to \pm L$$

so $$G_+(\alpha) = O(\alpha^{-1/2}) \qquad \text{as} \quad |\alpha| \to \infty, \quad \mathrm{Im}\alpha > 0$$

and also $$K_\pm(\alpha) = O(\alpha^{1/2}) \qquad \text{as} \quad |\alpha| \to \infty, \quad \mathrm{Im}\alpha \neq 0.$$

So it follows that

$$\frac{G_+(\alpha)}{K_+(\alpha)} = O(\alpha^{-1}) \qquad \text{as} \quad |\alpha| \to \infty, \quad \mathrm{Im}\alpha > 0.$$

Presumably one has $w_1(x,0+) - w_2(x,0-) = O(|x \mp L|^{1/2})$ as $x \to \pm L$.

Then it follows by standard Abelian asymptotics (cf. Noble [1958]; p.36) that

$$B(\alpha) = e^{i\alpha L} O(\alpha^{-3/2}) + e^{-i\alpha L} O(\alpha^{-3/2}) \quad \text{as} |\alpha| \to \infty.$$

Consequently one has

$$B(\alpha) K_-(\alpha) e^{-i\alpha L} = O(\alpha^{-1}) \qquad \text{as} \quad |\alpha| \to \infty, \quad \mathrm{Im}\alpha < 0.$$

Thus both sides of the first equation of (40) are $O(\alpha^{-1})$ as $|\alpha| \to \infty$ in the respective half-planes.

Therefore by Liouville's Theorem, both sides of the first equation of (40) are equal to zero. The second equation of (40) (i.e. the equation involving lower subscripts) can be treated similarly. Therefore from (40) one obtains the system of integral equations given by

$$\frac{G_\pm(\alpha)}{K_\pm(\alpha)} + \frac{1}{2\pi i}\int_{C_\pm} \frac{G_\mp(s) e^{\mp 2isL}}{(s-\alpha)K_\pm(s)} ds - \frac{1}{2\pi i}\int_{C_\pm} \frac{e^{\mp isL} K_\mp(s)}{\sqrt{2\pi}(s-\alpha)} \left\{ \frac{F_1}{\mu_1 \gamma_1(s)} - \frac{F_2}{\mu_2 \gamma_2(s)} \right\} ds = 0. \quad (41)$$

Since $\tau_{yz}^{(1)}(x,0)$ is an even function of x, so from (28) and (29) it can be shown that $G_+(-\alpha) = G_-(\alpha)$ and $K_+(-\alpha) = iK_-(\alpha)$ (cf. Pal and Ghosh [1990]). Using these results and replacing α by $-\alpha$ and s by -s in the first equation of (41) it can easily be shown that both the equations in (41) are identical. So $G_+(\alpha)$ and $G_-(\alpha)$ are to be determined from any one of the integral equations in (41).

3. HIGH FREQUENCY SOLUTION OF THE INTEGRAL EQUATION

To solve the second integral equation of (41) in the case when the normalized wave number $k_1L \gg 1$, the integration along the path C in (41) is replaced by the integration along the contours L_{k_1} and L_{k_2} around the branch cuts through the branch points k_1 and k_2 of the function $K_-(s)$ as shown in Fig.3. Thus the second equation in (41) takes the form

$$G_-(\alpha) = \frac{-K_-(\alpha)}{2\pi i}\int_{L_{k_1}+L_{k_2}} \frac{G_+(s)e^{2isL}}{(s-\alpha)K_-(s)}ds + \frac{K_-(\alpha)}{2\pi i}\int_{L_{k_1}+L_{k_2}} \frac{e^{isL}K_+(s)}{\sqrt{2\pi}(s-\alpha)}\left\{\frac{F_1}{\mu_1\gamma_1(s)} - \frac{F_2}{\mu_2\gamma_2(s)}\right\}ds. \quad (42)$$

For $k_1L \gg 1$, it can be shown that

$$\int_{L_{k_j}} \frac{G_+(s)e^{2isL}}{(s-\alpha)K_-(s)}ds \approx \frac{-1}{\mu_j}\sqrt{\frac{\pi}{k_jL}}\frac{G_+(k_j)K_+(k_j)}{(k_j-\alpha)}e^{i\pi/4}e^{2ik_jL}, \quad j=1,2, \quad (43)$$

and

$$\int_{L_{k_1}+L_{k_2}} \frac{K_+(s)}{\sqrt{2\pi}(s-\alpha)}\left\{\frac{F_1}{\mu_1\sqrt{(s^2-k_1^2)}} - \frac{F_2}{\mu_2\sqrt{(s^2-k_2^2)}}\right\}e^{isL}ds \approx \sum_{j=1}^{2}(-1)^j\frac{F_jK_+(k_j)e^{i(k_jL+\pi/4)}}{\mu_j(k_j-\alpha)\sqrt{k_jL}}. \quad (44)$$

Using the results of (43) and (44) and also the relations $G_+(-\alpha) = G_-(\alpha)$ and $K_-(\alpha) = -iK_+(-\alpha)$ one obtains from (42)

$$F_+(-\alpha) + \sum_{j=1}^{2}\frac{A(k_j)e^{2ik_jL}}{\mu_j(k_j-\alpha)\sqrt{k_jL}}F_+(k_j) = -C(-\alpha), \quad (45)$$

where

$$F_+(\xi) = \frac{G_+(\xi)}{K_-(-\xi)} = \frac{G_-(-\xi)}{K_-(-\xi)}, \quad (46)$$

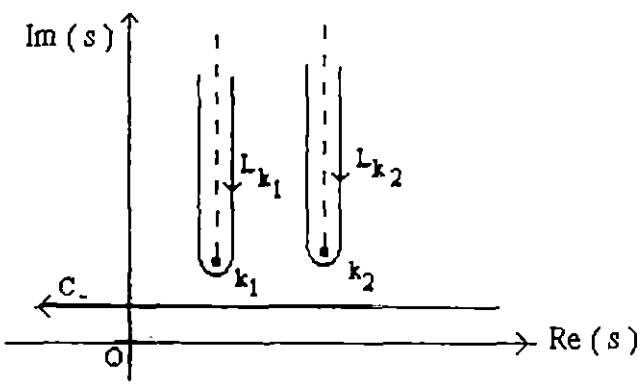

Fig.3. Path of integration C_-, L_{k_1}, L_{k_2}.

$$A(\xi) = \frac{[K_+(\xi)]^2 e^{i\pi/4}}{2\sqrt{\pi}}, \tag{47}$$

$$C(\xi) = \frac{1}{2\pi i}\sum_{j=1}^{2}(-1)^{j+1}\frac{F_j}{\mu_j}\frac{K_+(k_j)}{(k_j+\xi)}\frac{e^{i(k_jL+\pi/4)}}{\sqrt{k_jL}}. \tag{48}$$

Substituting $\alpha=-k_1$ and $\alpha=-k_2$ in (45) one obtains respectively the equations

$$\left[1 + M_1(k_1)e^{2ik_1L}\right]F_+(k_1) + \frac{\mu_1}{\mu_2}M_1(k_2)e^{2ik_2L}F_+(k_2) = -C(k_1) \tag{49}$$

and

$$\frac{\mu_2}{\mu_1}M_2(k_1)e^{2ik_1L}F_+(k_1) + \left[1 + M_2(k_2)e^{2ik_2L}\right]F_+(k_2) = -C(k_2), \tag{50}$$

where

$$M_j(\xi) = \frac{A(\xi)}{\mu_j(k_j+\xi)\sqrt{\xi L}}. \tag{51}$$

Now solution of (49) and (50) gives

$$F_+(k_m) = \left[\frac{\mu_m}{\mu_n}M_m(k_n)C(k_n)e^{2ik_nL} - C(k_m)\left\{1 + M_n(k_n)e^{2ik_nL}\right\}\right]P(k_1,k_2) \tag{52}$$

(for m=1, n=2 and for m=2, n=1)

where

$$P(k_1,k_2) = \left[1 + M_1(k_1)e^{2ik_1L} + M_2(k_2)e^{2ik_2L} + \left(\frac{k_1-k_2}{k_1+k_2}\right)^2 M_1(k_1)M_2(k_2)e^{2i(k_1+k_2)L}\right]^{-1}. \tag{53}$$

For high-frequency, expanding $P(k_1, k_2)$ up to $O(k_jL)^{-1}$ and neglecting the terms involving $(k_jL)^{-2}$ and the higher order terms in $F_+(k_1)$ and $F_+(k_2)$ in (52) respectively, one obtains from equations (45) and (46)

$$G_-(\alpha) = \frac{K_-(\alpha)}{2\pi i}\sum_{j=1}^{2}(-1)^jL(k_j)F_j\left\{\frac{1}{(k_j-\alpha)\mu_j} - \sum_{m=1}^{2}\frac{M_j(k_m)}{\mu_m(k_m-\alpha)}e^{2ik_mL} + \sum_{m=1}^{2}\sum_{n=1}^{2}\frac{M_j(k_m)M_m(k_n)}{\mu_n(k_n-\alpha)}e^{2i(k_m+k_n)L}\right\}, \tag{54}$$

where

$$L(\xi) = \frac{K_+(\xi)e^{i(\xi L+\pi/4)}}{\sqrt{\xi L}}. \tag{55}$$

Replacing α by $-\alpha$ and using the relations $K_-(-\alpha) = -iK_+(\alpha)$ and $G_-(-\alpha) = G_+(\alpha)$ one obtains,

$$G_+(\alpha) = -\frac{K_+(\alpha)}{2\pi}\sum_{j=1}^{2}(-1)^j L(k_j)F_j\left\{\frac{1}{(k_j+\alpha)\mu_j} - \sum_{m=1}^{2}\frac{M_j(k_m)}{\mu_m(k_m+\alpha)}e^{2ik_mL}\right.$$

$$\left. + \sum_{m=1}^{2}\sum_{n=1}^{2}\frac{M_j(k_m)M_m(k_n)}{\mu_n(k_n+\alpha)}e^{2i(k_m+k_n)L}\right\}. \qquad (56)$$

4. STRESS INTENSITY FACTOR NEAR THE CRACK TIPS

For $\alpha \to +\infty$ along the real axis,

$$K_\pm(\alpha) \sim \alpha^{1/2}\sqrt{\frac{\mu_1\mu_2}{\mu_1+\mu_2}}. \qquad (57)$$

From (53) and (56) one obtains,

$$G_+(\alpha) \sim S\,\alpha^{-1/2} \text{ and } G_-(\alpha) \sim -iS\,\alpha^{-1/2}, \qquad (58)$$

where

$$S = -\frac{1}{2\pi}\sqrt{\frac{\mu_1\mu_2}{\mu_1+\mu_2}}\sum_{j=1}^{2}(-1)^j L(k_j)F_j\left\{\frac{1}{\mu_j} - \sum_{m=1}^{2}\frac{M_j(k_m)}{\mu_m}e^{2ik_mL}\right.$$

$$\left. + \sum_{m=1}^{2}\sum_{n=1}^{2}\frac{M_j(k_m)M_m(k_n)}{\mu_n}e^{2i(k_m+k_n)L}\right\}. \qquad (59)$$

Using (57) and (58), equation (37) yields

$$B(\alpha) = \frac{S}{\alpha\sqrt{\alpha}}\left\{ie^{-i\alpha L} - e^{i\alpha L}\right\}\left(\frac{\mu_1+\mu_2}{\mu_1\mu_2}\right) + \frac{1}{\sqrt{2\pi}}\left\{\frac{F_1}{\mu_1} - \frac{F_2}{\mu_2}\right\}\frac{1}{\alpha}. \qquad (60)$$

From equations (18), (19) and (20) one obtains,

$$\tau_{yz}^{(1)}(x,0+) - \tau_{yz}^{(2)}(x,0-) = -(F_1+F_2)\delta(x).$$

Taking Fourier transformation on both sides, we obtain

$$\bar{\tau}_{yz}^{(1)}(\alpha,0+) - \bar{\tau}_{yz}^{(2)}(\alpha,0-) = -\frac{(F_1+F_2)}{\sqrt{2\pi}}$$

or

$$\mu_1\gamma_1 A_1(\alpha) + \mu_2\gamma_2 A_2(\alpha) = \frac{(F_1+F_2)}{\sqrt{2\pi}}. \qquad (61)$$

From equations (60), (61) and (36) one obtains when $\alpha \to +\infty$ along the real axis,

$$A_j(\alpha) = \frac{(-1)^{j+1} S}{\mu_j \alpha \sqrt{\alpha}} \left[i e^{-i\alpha L} - e^{i\alpha L} \right] + \frac{1}{\sqrt{2\pi}} \frac{1}{\alpha} \frac{F_j}{\mu_j}; \quad j=1,2. \tag{62}$$

Now

$$\tau_{yz}^{(j)}(x,y) = \mu_j \frac{\partial w_j(x,y)}{\partial y} = \mu_j \frac{\partial}{\partial y} \left[\frac{1}{\sqrt{2\pi}} \int_{-\infty}^{\infty} A_j(\alpha) e^{-\gamma_j |y| - i\alpha x} d\alpha \right]$$

$$= (-1)^j \frac{\mu_j}{\sqrt{2\pi}} \int_0^{\infty} \gamma_j A_j(\alpha) e^{-\gamma_j |y|} \left[e^{-i\alpha x} + e^{i\alpha x} \right] d\alpha \tag{63}$$

as by equation (35) $A_j(\alpha)$ is an even function of α.

Substituting the values of $A_j(\alpha)$ as $|\alpha| \to \infty$ we can write the stress in the vicinity of the crack tip as

$$\tau_{yz}^{(j)}(x,y) \approx \frac{S}{\sqrt{2\pi}} \int_0^{\infty} \frac{e^{-\alpha|y|}}{\sqrt{\alpha}} \left[e^{i\alpha(x+L)} - ie^{i\alpha(x-L)} - ie^{-i\alpha(x+L)} + e^{-i\alpha(x-L)} \right] d\alpha +$$

$$+ (-1)^j \frac{F_j}{\mu} \int_0^{\infty} e^{-\alpha|y|} \cos x\alpha \, d\alpha$$

$$= \frac{S(1-i)}{\sqrt{2\pi}} \int_0^{\infty} \frac{e^{-\alpha|y|}}{\sqrt{\alpha}} \left[\cos\alpha(x+L) - \sin\alpha(x+L) + \cos\alpha(x-L) + \sin\alpha(x-L) \right] d\alpha +$$

$$+ (-1)^j \frac{F_j}{\mu} \int_0^{\infty} e^{-\alpha|y|} \cos x\alpha \, d\alpha$$

$$= S(1-i) \left[\frac{1}{\sqrt{r_1}} \cos\frac{\theta_1}{2} + \frac{1}{\sqrt{r_2}} \cos\frac{\theta_2}{2} \right] + (-1)^j \frac{F_j}{\pi} \frac{|y|}{x^2+y^2}, \tag{64}$$

where

$$(x-L) + iy = r_1 e^{i\theta_1}, \qquad -(x+L) + iy = r_2 e^{i\theta_2}, \qquad -\pi \le \theta_{1,2} \le \pi. \tag{65}$$

It is to be noted that the final term in equation (64) which can be reduced to $-\frac{F_j}{\pi} \frac{y}{x^2+y^2}$ describes the behaviour of the stress near the source. Therefore at the interface (y=0) we obtain

$$\tau_{yz} \approx \frac{S(1-i)}{\sqrt{(x-L)}} \quad \text{as } x \to L+0, \tag{66}$$

$$\tau_{yz} \approx \frac{S(1-i)}{\sqrt{-(x+L)}} \quad \text{as } x \to -L-0. \tag{67}$$

Now the dimensionless stress intensity factor is defined by,

$$K = \left| \frac{S(1-i)}{F_1\sqrt{k_1}} \right|, \tag{68}$$

where S is given by (59).

5. RESULTS AND DISCUSSIONS

Since from equations (7) and (16) we note that for Y=0, x=X and y=0 and that $\sigma^{(j)}_{YZ}(X,0,t) = \sigma^{(j)}_{yz}(x,0,t)$, therefore, the elastodynamic mode-III stress intensity factor of the interface crack in an anisotropic bimaterials is the same as that of an interface crack of the corresponding isotropic bimaterial given by (68).

Numerical calculations have been carried out for both the cases of antisymmetric ($F_1 = -F_2 = F$) and symmetric ($F_1 = F_2 = F$) antiplane loadings. For numerical evalution of the stress intensity factors, the three material pairs (Nayfen, [1995]), given in Table-1, have been considered.

Table-1. Engineering elastic constants of different materials.

Medium	Name	$\hat{\rho}$(Kg m^{-3})	C_{44} (Gpa)	C_{55} (Gpa)	C_{45} (Gpa)
Type of material pair : I					
1.	Carbon-epoxy	1.57×10^3	3.98	6.4	0
2.	Graphite-epoxy	1.60×10^3	6.55	2.6	0
Type of material pair : II					
1.	Isotropic Chromium	7.20×10^3	115.2	115.2	0
2.	Isotropic Steel	7.90×10^3	81.91	81.91	0
Type of material pair : III					
1.	Graphite	1.79×10^3	5.52	28.3	0
2.	Carbon-epoxy	1.57×10^3	3.98	6.4	0

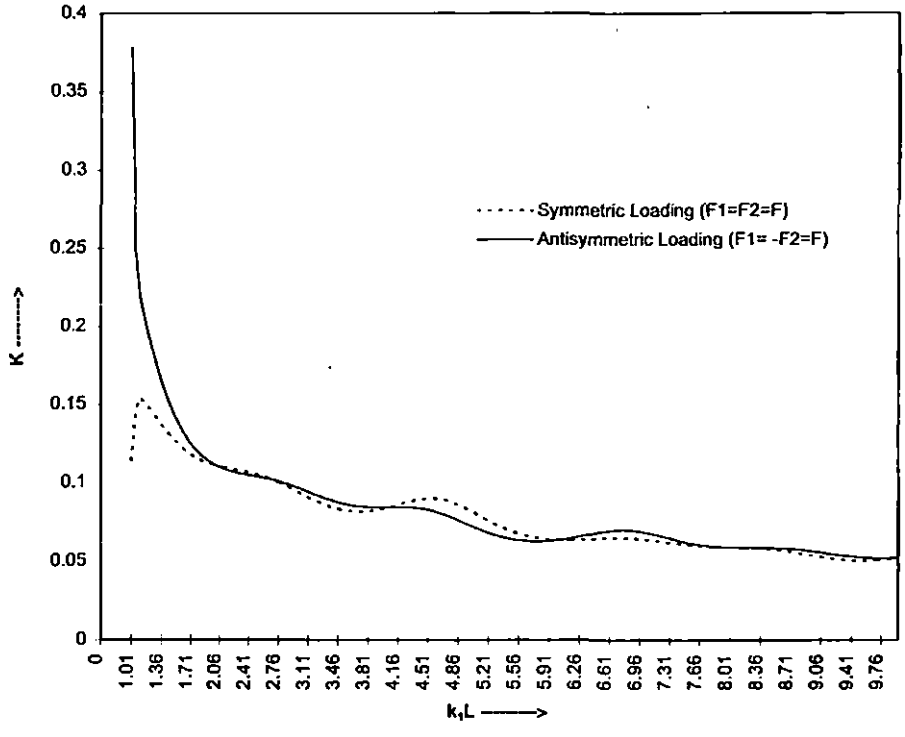

Fig.4. Stress intensity factor K versus dimensionless frequency k_1L for Type-I material pair.

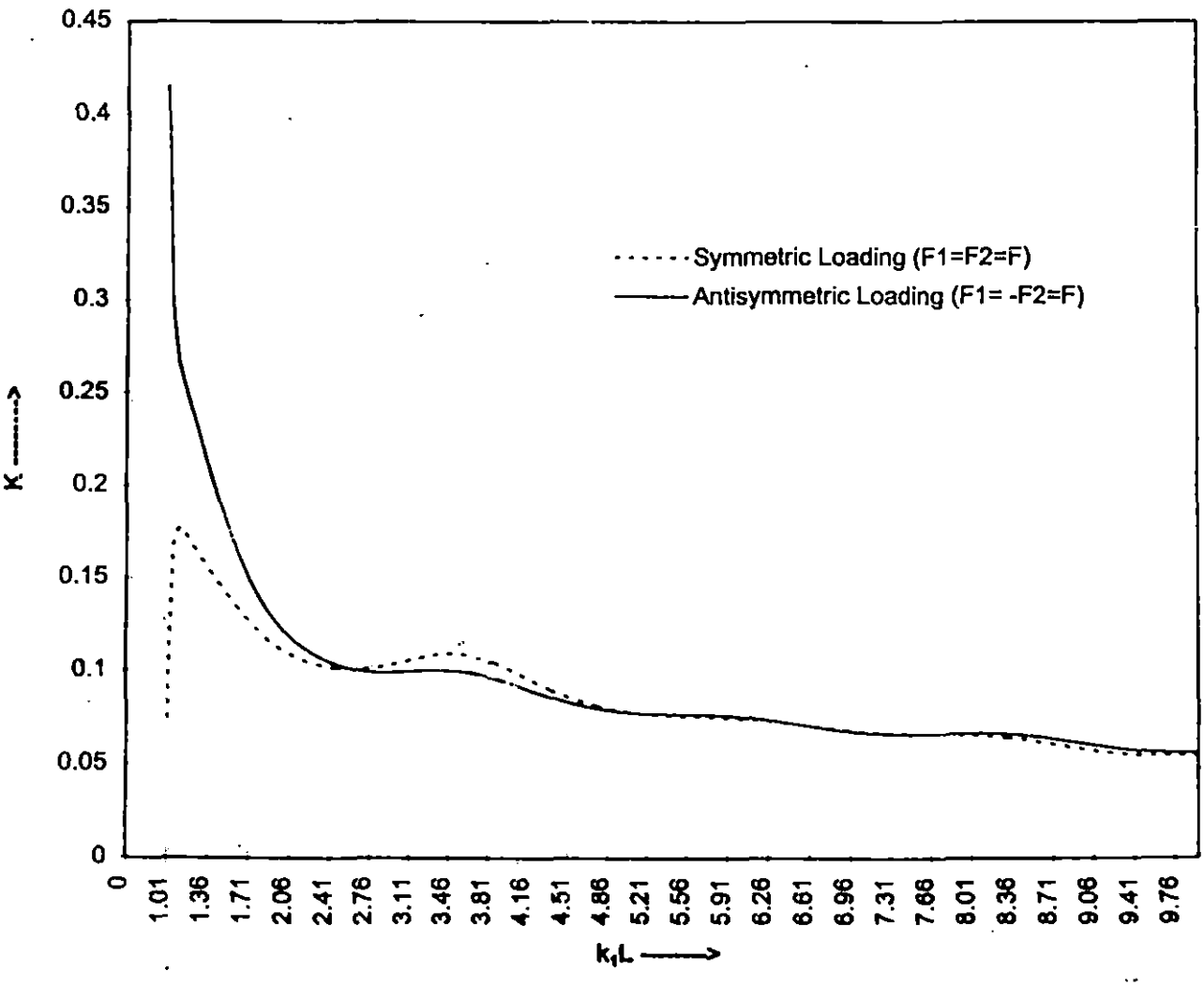

Fig.5. Stress intensity factor K versus dimensionless frequency k_1L for Type-II material pair.

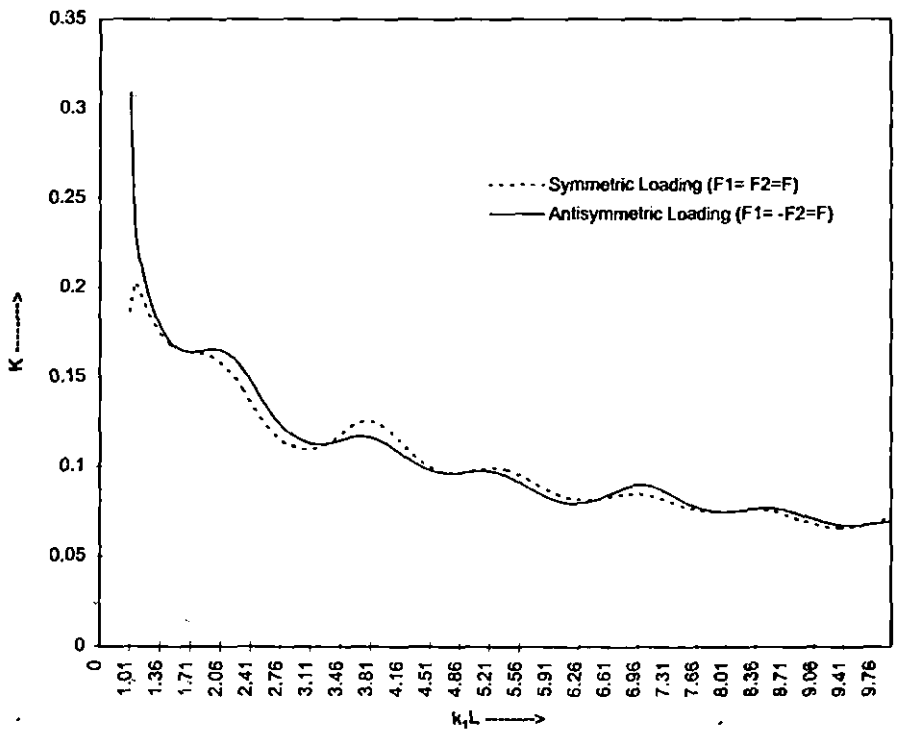

Fig.6. Stress intensity factor K versus dimensionless frequency k_1L for Type-III material pair.

The absolute values of the complex stress intensity factors defined by (68) have been plotted against k_1L in Figs. 4-6, for symmetric as well as for antisymmetric loadings for values of dimensionless frequency k_1L varying from 1.01 to 10.

It is interesting to note that in the case of symmetric loading, the stress intensity factor first increases with the increasing k_1L, attains a maximum and the with further increase of k_1L, decreases gradually with oscillatory behavior. On the other hand in the case of antisymmetric loading, stress intensity factor at first decreases sharply but with the increase of k_1L, it shows almost the same behaviours as the case for symmetric loading. The general oscillatory feature for the curves in Figs. 4-6 are due to the effect of interaction between the waves generated by the two tips of the crack.

----x----

[2]TRANSIENT RESPONSE DUE TO A PAIR OF ANTIPLANE POINT IMPACT LOADING ON THE FACES OF A FINITE GRIFFITH CRACK AT THE BIMATERIAL INTERFACE OF ANISOTROPIC SOLIDS

1. INTRODUCTION

The problem of a crack in an elastic material under the action of impulsive loading has been a subject of considerable interest recently. Sih et al [1972] have considered the problem for an infinite isotropic material and Kassir and Bandyopadhyay [1983] studied infinite orthotropic material. Stephen and Hwel [1970] also investigated the problem of diffraction of transient SH-waves by a crack of finite width and a rigid ribbon, also of finite width.

However in present years the extensive use of composite materials in the modern technology has created interest among scientists for carrying on considerable research work in the modeling, testing and analysis of laminated media. The laminated composites which behave as anisotropic material may be weakened by interface flaws which lead to serious degradation in load carrying capacity.

Kuo [1984] carried out numerical and analytical studies of transient response of an interfacial semi-infinite crack between two dissimilar orthotropic half spaces. The problem of diffraction of transient horizontal shear waves by a finite crack located at the interface of two bonded dissimilar elastic half spaces has been treated by Takei et al [1982].

Neerhoff [1979] studied the diffraction of Love waves by a crack of finite width at the interface of a layered half space. Kuo and Cheng [1991] considered the elastodynamic response due

---

[2] **Published in the Int. J. Engineering Science, V36, 1197-1213, 1998.**

to antiplane point impact loadings on the faces of an interface semi-infinite crack along dissimilar anisotropic materials.

In our present paper, we are interested in the antiplane transient elastodynamic responses and stress intensity factors of a Griffith crack of finite width lying along the interface of two dissimilar anisotropic elastic materials. The crack is subjected to a pair of suddenly applied antiplane concentrated line loading situated at the middle of the cracked surface. The materials are assumed to possess certain material symmetry and the crack plane is assumed to coincide with one of the planes of material symmetry, so that the inplane and the antiplane motion are not coupled.

The analysis of the paper is first based on the observation of several researches, e.g. Markenscoff and Ni [1984], Achenbach and Kuo [1981], that antiplane shear deformation in an anisotropic solid can be deduced from the corresponding deformations of an isotropic solid by a transformation of relevant co-ordinates and parameters. Based on this observation, analysis of the interface crack by transient line loads between two bonded dissimilar anisotropic elastic materials has first been converted to the corresponding problem between two dissimilar isotropic elastic solids. Later following Thau and Lu [1970], spatial and time transform are applied to the governing differential equations and generalized Wiener-Hopf type equations are obtained. The integral equation arising are solved by the standard iteration procedure. Physically, each successive order of iteration corresponds to successive scattered or rescattered wave from one crack tip to other.

Finally results are presented for the stress intensity factor near the crack tips. Each crack tip stress intensity factor is plotted versus time for a pair of different type of anisotropic materials.

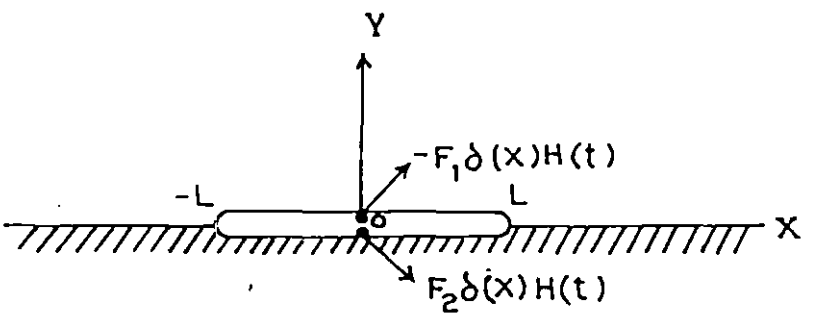

Fig.1. Geometry of the problem.

2. FORMULATION OF THE PROBLEM

Consider antiplane deformation of a Griffith crack of finite width 2L lying between dissimilar anisotropic half planes which are characterized by the elastic moduli $(C_{ik})_j$; (i,k=4,5) and mass density $\hat{\rho}_j$. The subscript j (j=1,2) refers to the upper and lower media respectively. Let (X,Y,Z) be the Cartesian co-ordinates. The X-axis is taken along the interface, Y-axis vertically upwards into the medium and Z-axis is perpendicular to the plane of the paper (Fig.1).

For time $t<0$, the elastic solids are at rest. For time $t\geq 0$, a pair of concentrated antiplane shear forces in the Z-direction of magnitudes F_1 and F_2 act on the crack faces Y=0+ and Y=0- respectively at X=0. Thus the crack boundary conditions are

$$\hat{\sigma}_{YZ}(X,Y,t) = \begin{cases} -F_1\,\delta(X)\,H(t); & |X|<L, \quad Y=0+, \\ F_2\,\delta(X)\,H(t); & |X|<L, \quad Y=0-, \end{cases} \qquad (1)$$

where H() and δ() are the Heaviside step and Dirac delta functions respectively. Ahead of the crack tips, the interface boundary conditions which corresponds to the continuity of the displacement and traction along the welded part of the interface along |X|>L, Y=0 are

$$\hat{\sigma}^{(1)}_{YZ}(X,0,t) = \hat{\sigma}^{(2)}_{YZ}(X,0,t) \qquad (2)$$

$$\hat{W}_1(X,0,t) = \hat{W}_2(X,0,t). \qquad (3)$$

Two dimensional antiplane wave motions of homogeneous anisotropic linearly elastic solids are governed by (Camprin [1981])

$$(C_{55})_j \frac{\partial^2 \hat{W}_j}{\partial X^2} + 2(C_{45})_j \frac{\partial^2 \hat{W}_j}{\partial X \partial Y} + (C_{44})_j \frac{\partial^2 \hat{W}_j}{\partial Y^2} = \hat{\rho}_j \frac{\partial^2 \hat{W}_j}{\partial t^2} \qquad (j=1,2), \qquad (4)$$

where $\hat{W}_j(X,Y,t)$ is the out-of-plane displacement.

The crack plane has been assumed to coincide with one of the planes of material symmetry such that inplane and out-plane motions are not coupled.

The relevant stress components are

$$\hat{\sigma}^{(j)}_{XZ}(X,Y,t) = (C_{55})_j \frac{\partial \hat{W}_j}{\partial X} + (C_{45})_j \frac{\partial \hat{W}_j}{\partial Y} \tag{5}$$

$$\hat{\sigma}^{(j)}_{YZ}(X,Y,t) = (C_{45})_j \frac{\partial \hat{W}_j}{\partial X} + (C_{44})_j \frac{\partial \hat{W}_j}{\partial Y}. \tag{6}$$

Following Achenbach and Kuo [1986] and Ma [1989], we introduce a co-ordinate transformation which has also been used by Kuo and Cheng [1991]

$$\left.\begin{aligned} x &= X - \frac{(C_{45})_j}{(C_{44})_j} Y, \\ y &= \frac{\mu_j}{(C_{44})_j} Y, \\ z &= Z, \end{aligned}\right\} \qquad (j = 1, 2) \tag{7}$$

where

$$\mu_j = \sqrt{(C_{44})_j (C_{55})_j - (C_{45})_j^2} \qquad (j = 1, 2). \tag{8}$$

Transformation given by equation (7) reduce equation (4) to the standard wave equation

$$\frac{\partial^2 \hat{W}_j}{\partial x^2} + \frac{\partial^2 \hat{W}_j}{\partial y^2} = s_j^2 \frac{\partial^2 \hat{W}_j}{\partial t^2}, \tag{9}$$

where

$$s_j^2 = \frac{\rho_j}{\mu_j} \quad \text{and} \quad \rho_j = \frac{\hat{\rho}_j (C_{44})_j}{\mu_j}, \tag{10}$$

s_j is the slowness of shear waves. Without any loss of generality we assume that

$$s_1 < s_2 . \tag{11}$$

It is easily verified from equations (4) - (6) that the relevant displacement and the stress component in the physical anisotropic solid are related to those in the corresponding isotropic solid by

$$\hat{W}_j (X, Y, t) = w_j(x, y, t), \tag{12}$$

$$\hat{\sigma}^{(j)}_{XZ} (X, Y, t) = \frac{\mu_j}{(C_{44})_j} \sigma^{(j)}_{xz}(x, y, t) + \frac{(C_{45})_j}{(C_{44})_j} \sigma^{(j)}_{yz}(x, y, t), \tag{13}$$

$$\hat{\sigma}^{(j)}_{YZ} (X, Y, t) = \sigma^{(j)}_{yz}(x, y, t). \tag{14}$$

From equations (9) and (12), the antiplane wave motions of the corresponding isotropic bimaterial in the transformed co-ordinate are governed by the standard wave equation

$$\frac{\partial^2 w_j}{\partial x^2} + \frac{\partial^2 w_j}{\partial y^2} = s_j^2 \frac{\partial^2 w_j}{\partial t^2}; \qquad (j = 1, 2) \tag{15}$$

and the relevant stress components are

$$\sigma^{(j)}_{yz}(x, y, t) = \mu_j \frac{\partial w_j}{\partial y}. \tag{16}$$

Under the changed co-ordinate system the boundary conditions equations (1) - (3) reduce to

$$\sigma_{yz}(x,y,t) = \begin{cases} -F_1\,\delta(x)\,H(t); & |x|<L, \quad y=0+ \\ F_2\,\delta(x)\,H(t); & |x|<L, \quad Y=0- \end{cases} \tag{17}$$

$$\sigma_{yz}^{(1)}(x,y,t) = \sigma_{yz}^{(2)}(x,y,t); \qquad |x|>L, \quad y=0, \tag{18}$$

$$w_1(x,y,t) = w_2(x,y,t); \qquad |x|>L, \quad y=0. \tag{19}$$

Hence

$$\mu_1 \frac{\partial w_1}{\partial y} = -F_1\,\delta(x)\,H(t); \qquad |x|<L, \quad y=0+ \tag{20}$$

$$\mu_2 \frac{\partial w_2}{\partial y} = F_2\,\delta(x)\,H(t); \qquad |x|<L, \quad y=0- \tag{21}$$

and

$$\mu_1 \frac{\partial w_1}{\partial y} = \mu_2 \frac{\partial w_2}{\partial y}; \qquad |x|>L, \quad y=0 \tag{22}$$

$$w_1(x,0,t) = w_2(x,0,t); \qquad |x|>L, \quad y=0. \tag{23}$$

We begin the analysis by introducing unknown functions w_j and $\partial w_j / \partial y$ along the x-axis over the intervals where the functions are not specified by equations (22) and (23).

Assume that

$$w_j(x,0,t) = g_j(x,0,t); \qquad -L<x<L \tag{24}$$

and

$$\mu_j \frac{\partial w_j}{\partial y} = \begin{cases} \phi(x+L,t); & y=0, \quad x+L<0 \\ \phi(x-L,t); & y=0, \quad x-L>0 \end{cases} . \tag{25}$$

Now we introduce Laplace anf Fourier transforms defined as

$$F(x,y,p) = \int_0^\infty f(x,y,t)\, e^{-pt} dt, \qquad \bar{F}(\zeta,y,p) = \int_{-\infty}^{\infty} F(x,y,p) e^{-i\zeta x} dx \tag{26}$$

so that their inverse transforms are

$$f(x,y,t) = \frac{1}{2\pi i} \int_{BR} F(x,y,p) e^{pt} dp, \qquad F(x,y,p) = \frac{1}{2\pi} \int_{-\infty}^{\infty} \bar{F}(\zeta,y,p)\, e^{i\zeta x} d\zeta . \tag{27}$$

Taking Laplace transform with respect to t of both sides of equation (24) (for $|x| < L$)

$$W_j(x,0,p) = \int_0^\infty w_j(x,0,t) e^{-pt} dt = \int_0^\infty g_j(x,0,t) e^{-pt} dt = G_j(x,0,p); \quad |x|<L. \tag{28}$$

Next taking Laplace and Fourier transform on wave equation (15) one obtains

$$\frac{\partial^2 \bar{w}_1}{dy^2} - (\zeta^2 + k_1^2)\bar{w}_1 = 0; \qquad y>0, \tag{29}$$

$$\frac{\partial^2 \bar{w}_2}{dy^2} - (\zeta^2 + k_2^2)\bar{w}_2 = 0; \qquad y<0, \tag{30}$$

where

$$k_j^2 = s_j^2 p^2; \qquad (j=1,2). \tag{31}$$

The solutions of equations (29) and (30) which are bounded as $|y| \to \infty$ are

$$\bar{w}_1(\zeta,y,p) = A_1(\zeta)e^{-\gamma_1 y}; \qquad y>o, \tag{32}$$

$$\bar{w}_2(\zeta,y,p) = A_2(\zeta)e^{\gamma_2 y}; \qquad y<o, \tag{33}$$

where

$$\gamma_j = \sqrt{(\zeta^2 + k_j^2)}; \qquad (j=1,2). \tag{34}$$

The transformed stress at the interface y=0 can be written as

$$\mu_j \frac{\partial \bar{W}_j(\zeta,0,p)}{\partial y} = e^{i\zeta L}\bar{\Phi}_+(\zeta,p) + \frac{1}{p}\epsilon_j F_j + e^{-i\zeta L}\bar{\Phi}_-(\zeta,p), \quad [j=1,2, \quad \epsilon_j=(-1)^j], \tag{35}$$

where

$$\bar{\Phi}_+(\zeta,p) = \int_{-\infty}^{-L} e^{-i\zeta x}\left[\int_0^{\infty} \phi(x+L,t)e^{-pt}dt\right]dx$$

and

$$\bar{\Phi}_-(\zeta,p) = \int_{L}^{\infty} e^{-i\zeta x}\left[\int_0^{\infty} \phi(x-L,t)e^{-pt}dt\right]dx.$$

$\bar{\Phi}_+$ and $\bar{\Phi}_-$ are analytic in the complex half plane $\mathrm{Im}(\zeta) > -k_1$ and $\mathrm{Im}(\zeta) < k_1$ respectively. So from equations (32) and (33) one obtains

$$\mu_1 \frac{\partial \bar{W}_1(\zeta,0,p)}{\partial y} = -\mu_1\gamma_1 A_1(\zeta), \qquad \mu_2 \frac{\partial \bar{W}_2(\zeta,0,p)}{\partial y} = \mu_2\gamma_2 A_2(\zeta). \tag{36}$$

Equation (35) with aid of equation (36) yields

$$(-1)^j \mu_j\gamma_j A_j(\zeta) = e^{i\zeta L}\bar{\Phi}_+(\zeta,p) + e^{-i\zeta L}\bar{\Phi}_-(\zeta,p) + (-1)^j \frac{F_j}{p}; \quad (j=1,2). \tag{37}$$

Taking aid of equations (19), (28), (32) and (33) one obtains

$$\bar{W}_1(\zeta,0,p) - \bar{W}_2(\zeta,0,p) = \int_{-\infty}^{\infty} \{W_1(x,0,p) - W_2(x,0,p)\} e^{-i\zeta x}\, dx$$

$$= \int_{-L}^{L} \{G_1(x,0,p) - G_2(x,0,p)\} e^{-i\zeta x}\, dx = B(\zeta) \quad \text{(say)}$$

so that

$$A_1(\zeta) - A_2(\zeta) = B(\zeta). \tag{38}$$

By the help of equations (37) and (38) one finds an extended Wiener-Hopf equation namely

$$K(\zeta)B(\zeta) = -\bar{\Phi}_+(\zeta,p)\, e^{i\zeta L} + \bar{\Phi}_-(\zeta,p)\, e^{-i\zeta L} + \frac{K(\zeta)}{p}\left\{\frac{F_1}{\mu_1\gamma_1} - \frac{F_2}{\mu_2\gamma_2}\right\}, \tag{39}$$

where

$$K(\zeta) = \frac{\mu_1\mu_2\gamma_1\gamma_2}{\mu_1\gamma_1 + \mu_2\gamma_2} = \frac{\mu_1\mu_2\sqrt{\zeta^2 + k_1^2}}{\mu_1 + \mu_2} R^1(\zeta) \tag{40}$$

$$= \frac{\mu_1\mu_2\sqrt{\zeta^2 + k_2^2}}{\mu_1 + \mu_2} R^2(\zeta) \tag{41}$$

so that

$$R^{1}(\zeta) = \frac{(\mu_1+\mu_2)\sqrt{(\zeta_2+k_2^2)}}{\mu_1\sqrt{(\zeta_2+k_1^2)}+\mu_2\sqrt{(\zeta_2+k_2^2)}}, \tag{42}$$

$$R^{2}(\zeta) = \frac{(\mu_1+\mu_2)\sqrt{(\zeta_2+k_1^2)}}{\mu_1\sqrt{(\zeta_2+k_1^2)}+\mu_2\sqrt{(\zeta_2+k_2^2)}}. \tag{43}$$

The solution of equation (39) along with two transform inversions completes the problem. Here we shall concentrate on finding and then inverting $\bar{\Phi}_+$ and $\bar{\Phi}_-$ since $\phi(x+L, t)$ and $\phi(x-L,t)$ from equation (25) are equal to the shear stresses directly ahead of the crack tips. Hence they are required for the determination of dynamic stress intensity factors at the crack tips.

In order to solve equation (39), the function $K(\zeta)$ is at first made single valued by drawing branch cuts along the η-axis (recall $\zeta=\xi+i\eta$) from $\eta=k_1$ to ∞ and from $\eta=-k_1$ to $-\infty$. It is then broken up into the product of two functions which are analytic in the overlapping regions $Im(\zeta)>-k_1$ and $Im(\zeta)<k_1$ so that

$$K(\zeta) = K_+(\zeta)\,K_-(\zeta). \tag{44}$$

Next we divide equation (39) by $K_+(\zeta)$ and change ζ to ζ' in it and redivide it by $2\pi i e^{i\zeta' L}(\zeta'-\zeta)$ which yields

$$\frac{e^{-i\zeta' L}K_-(\zeta')B(\zeta')}{2\pi i(\zeta'-\zeta)} = -\frac{\bar{\Phi}_+(\zeta')}{2\pi i K_+(\zeta')(\zeta'-\zeta)} + \frac{\bar{\Phi}_-(\zeta')e^{-2i\zeta' L}}{2\pi i K_+(\zeta')(\zeta'-\zeta)}$$

$$+\frac{K_-(\zeta')e^{-i\zeta' L}}{2\pi i(\zeta'-\zeta)p}\left[\frac{F_1}{\mu_1\sqrt{(\zeta'^2+k_1^2)}}-\frac{F_2}{\mu_2\sqrt{(\zeta'^2+k_2^2)}}\right]. \tag{45}$$

Now with $\zeta'=\xi'+i\eta'$, take a line L_1 in the ζ'-plane lying in the strip $-k_1<\eta'<k_1$; choose

ζ to be a point lying above L_1 (i.e. $\eta>\eta'$) and integrate equation (45) along L_1 from $-\infty<\xi'<\infty$

$$\int_{L_1}\frac{e^{-i\zeta' L}K_-(\zeta')B(\zeta')}{2\pi i(\zeta'-\zeta)}d\zeta' = -\int_{L_1}\frac{\bar{\Phi}_+(\zeta')}{2\pi i K_+(\zeta')(\zeta'-\zeta)}d\zeta' + \int_{L_1}\frac{\bar{\Phi}_-(\zeta')e^{-2i\zeta' L}}{2\pi i K_+(\zeta')(\zeta'-\zeta)}d\zeta'$$

$$+\int_{L_1}\frac{K_-(\zeta')e^{-i\zeta' L}}{2\pi i(\zeta'-\zeta)p}\left[\frac{F_1}{\mu_1\sqrt{(\zeta'^2+k_1^2)}}-\frac{F_2}{\mu_2\sqrt{(\zeta'^2+k_2^2)}}\right]d\zeta'. \qquad (46)$$

Since $B(\zeta')$ is analytic in the entire plane and $K_-(\zeta')e^{-i\zeta' L}$ is analytic in the lower half plane, so considering semicircular contour in the lower half plane the first integral is found to be equal to zero.

Again while evaluating the second integral, a semicircular contour in the upper half plane is considered. Consequently the second integral is found to yield the value $\bar{\Phi}_+(\zeta)/K_+(\zeta)$.

Next for the last two integrals the integration path is deformed to the path round the branch cut through the branch points $\zeta = -ik_1$ and $-ik_2$ as shown in Fig.2 so that finally equation (46) takes the form

$$\bar{\Phi}_+(\zeta) = \frac{iK_+(\zeta)}{\pi\mu_1}\int_0^\infty \frac{\bar{\Phi}_-[-ik_1(1+\lambda)]\,K_-[-ik_1(1+\lambda)]\,e^{-2Lk_1(1+\lambda)}}{[ik_1(1+\lambda)+\zeta]\sqrt{\lambda(\lambda+2)}}d\lambda$$

$$+\frac{iK_+(\zeta)}{\pi\mu_2}\int_0^\infty \frac{\bar{\Phi}_-[-ik_2(1+\lambda)]\,K_-[-ik_2(1+\lambda)]\,e^{-2Lk_2(1+\lambda)}}{[ik_2(1+\lambda)+\zeta]\sqrt{\lambda(\lambda+2)}}d\lambda$$

$$+\frac{iF_1K_+(\zeta)}{\pi\mu_1 p}\int_0^\infty \frac{K_-[-ik_1(1+\lambda)]\,e^{-Lk_1(1+\lambda)}}{[ik_1(1+\lambda)+\zeta]\sqrt{\lambda(\lambda+2)}}d\lambda$$

$$-\frac{iF_2K_+(\zeta)}{\pi\mu_2 p}\int_0^\infty \frac{K_-[-ik_2(1+\lambda)]\,e^{-Lk_2(1+\lambda)}}{[ik_2(1+\lambda)+\zeta]\sqrt{\lambda(\lambda+2)}}d\lambda. \qquad (47)$$

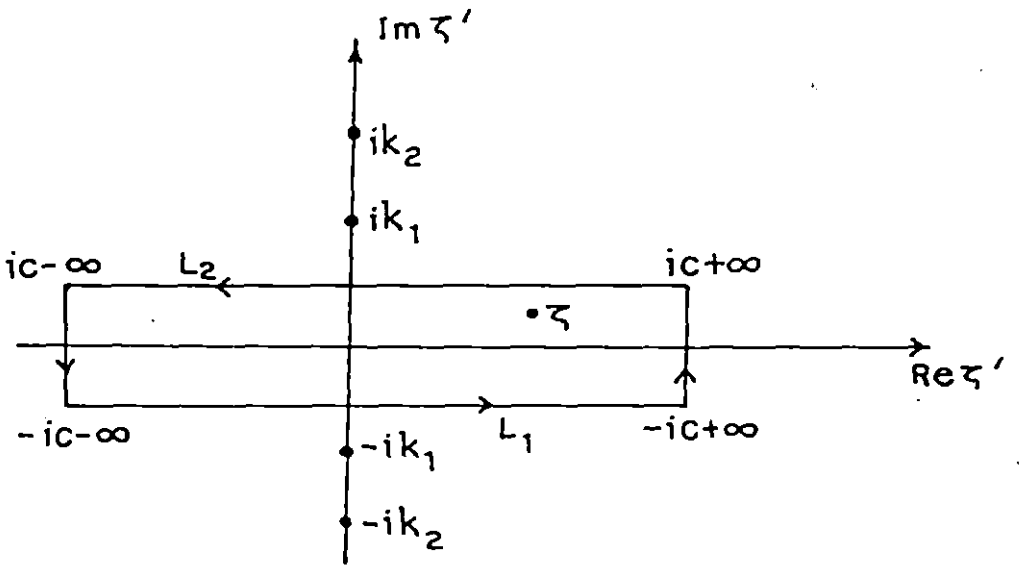

Fig.2. Path of integration.

Similarly we can derive an equation for $\bar{\Phi}_-(\zeta)$ by dividing equation (39) by $2\pi i e^{-2\zeta' L} K_-(\zeta')(\zeta'-\zeta)$ after first changing ζ to ζ' and then choosing a line of integration L_2 in the strip $-k_1<\eta'<k_1$. The point ζ is taken below L_2 and the result analogous to equation (47), then becomes;

$$\bar{\Phi}_-(\zeta) = \frac{iK_-(\zeta)}{\pi\mu_1}\int_0^\infty \frac{\bar{\Phi}_+[ik_1(1+\lambda)]\,K_+[ik_1(1+\lambda)]\,e^{-2Lk_1(1+\lambda)}}{[ik_1(1+\lambda)-\zeta]\sqrt{\lambda(\lambda+2)}}\,d\lambda$$

$$+\frac{iK_-(\zeta)}{\pi\mu_2}\int_0^\infty \frac{\bar{\Phi}_+[ik_2(1+\lambda)]\,K_+[ik_2(1+\lambda)]\,e^{-2Lk_2(1+\lambda)}}{[ik_2(1+\lambda)-\zeta]\sqrt{\lambda(\lambda+2)}}\,d\lambda$$

$$-\frac{iF_1K_-(\zeta)}{\pi\mu_1 p}\int_0^\infty \frac{K_+[ik_1(1+\lambda)]\,e^{-Lk_1(1+\lambda)}}{[ik_1(1+\lambda)-\zeta]\sqrt{\lambda(\lambda+2)}}\,d\lambda$$

$$+\frac{iF_2K_-(\zeta)}{\pi\mu_2 p}\int_0^\infty \frac{K_+[ik_2(1+\lambda)]\,e^{-Lk_2(1+\lambda)}}{[ik_2(1+\lambda)-\zeta]\sqrt{\lambda(\lambda+2)}}\,d\lambda. \qquad (48)$$

The integral equations have been solved by the standard iteration method and it may be noted that each successive order of iteration is a solution of the problem for successively increasing units of time starting from t=0. Since each unit of time here corresponds exactly to the time required for an SH-wave to traverse the crack width, we can interpret physically each order of iteration in terms of the successive scatterings of waves from one crack to other and back again. Now we consider the zeroth order solutions of equations (47) and (48) as

$$\bar{\Phi}_+^{(0)}(\zeta) = \frac{iF_1K_+(\zeta)e^{-Lk_1}}{\pi\mu_1 p}\int_0^\infty \frac{K_-[-ik_1(1+\lambda)]\,e^{-Lk_1\lambda}}{[ik_1(1+\lambda)+\zeta]\sqrt{\lambda(\lambda+2)}}\,d\lambda$$

$$-\frac{iF_2K_+(\zeta)e^{-Lk_2}}{\pi\mu_2 p}\int_0^\infty \frac{K_-[ik_2(1+\lambda)]\,e^{-Lk_2\lambda}}{[ik_2(1+\lambda)+\zeta]\sqrt{\lambda(\lambda+2)}}\,d\lambda \qquad (49)$$

and

$$\bar{\Phi}_-^{(0)}(\zeta) = -\frac{iF_1K_-(\zeta)e^{-Lk_1}}{\pi\mu_1 p}\int_0^\infty \frac{K_+[ik_1(1+\lambda)]\,e^{-Lk_1\lambda}}{[ik_1(1+\lambda)-\zeta]\sqrt{\lambda(\lambda+2)}}\,d\lambda$$

$$+\frac{iF_2K_-(\zeta)e^{-Lk_2}}{\pi\mu_2 p}\int_0^\infty \frac{K_+[ik_2(1+\lambda)]\,e^{-Lk_2\lambda}}{[ik_2(1+\lambda)-\zeta]\sqrt{\lambda(\lambda+2)}}\,d\lambda. \qquad (50)$$

Due to the presence of exponentially decaying terms in the integrands the main contribution to the integrals would be from small values of λ. So approximately evaluating the integrals we obtain finally

$$\bar{\Phi}_+^{(0)}(\zeta) = \frac{F_1K_+(\zeta)K_+(ik_1)e^{-Lk_1}}{\mu_1 p(\zeta+ik_1)\sqrt{2\pi Lk_1}} - \frac{F_2K_+(\zeta)K_+(ik_2)e^{-Lk_2}}{\mu_2 p(\zeta+ik_2)\sqrt{2\pi Lk_2}}, \qquad (51a)$$

$$\bar{\Phi}_-^{(0)}(\zeta) = \frac{iF_1K_-(\zeta)K_+(ik_1)e^{-Lk_1}}{\mu_1 p(\zeta-ik_1)\sqrt{2\pi Lk_1}} - \frac{iF_2K_-(\zeta)K_+(ik_2)e^{-Lk_2}}{\mu_2 p(\zeta-ik_2)\sqrt{2\pi Lk_2}}. \qquad (51b)$$

The expression for $\bar{\Phi}_+^{(0)}(\zeta)$ and $\bar{\Phi}_-^{(0)}(\zeta)$ may be recognised as the solutions corresponding to the separate problems of diffraction of semi-infinite cracks y=0, x>-L and y=0, x<L respectively because until the scattered wave emanating from a given crack tip reaches the opposite crack tip, the semi-infinite crack solution must apply.

The waves originating from concentrated line sources at x=0, y=0+ and x=0, y=0- arrive at the crack edges at $t=s_1L$ and $t=s_2L$ respectively.

The waves arriving at one edge at time $t=s_1L$ and $t=s_2L$ respectively through the upper and lower media reach the opposite edge at times $t=3s_1L$, s_2L+2s_1L through the upper medium and at time $t=s_1L+2s_2L$, $3s_2L$ through the lower medium. So the first order solution $\bar{\Phi}_+^{(1)}(\zeta)$ and $\bar{\Phi}_-^{(1)}(\zeta)$ which we obtain by substituting equations (51a - b) into the integral equations (47) and (48) gives

the effect of these waves and it is valid until $t=5s_1L$ when the second scattered wave from the opposite edge first arrives. So the first order iteration becomes

$$\bar{\Phi}_+^{(1)}(\zeta) = \sum_{r=1}^{2} \frac{K_+(\zeta)\bar{\Phi}_-^{(0)}(-ik_r)K_+(ik_r)e^{-2Lk_r}}{2\mu_r(\zeta+ik_r)\sqrt{\pi Lk_r}} - \sum_{r=1}^{2} \frac{(-1)^r F_r K_+(\zeta)K_+(ik_r)e^{-Lk_r}}{\mu_r p(\zeta+ik_r)\sqrt{2\pi Lk_r}} \quad (52a)$$

and

$$\bar{\Phi}_-^{(1)}(\zeta) = -i\sum_{r=1}^{2} \frac{K_-(\zeta)\bar{\Phi}_+^{(0)}(ik_r)K_+(ik_r)e^{-2Lk_r}}{2\mu_r(\zeta-ik_r)\sqrt{\pi Lk_r}} - i\sum_{r=1}^{2} \frac{(-1)^r F_r K_-(\zeta)K_+(ik_r)e^{-Lk_r}}{\mu_r p(\zeta-ik_r)\sqrt{2\pi Lk_r}}. \quad (52b)$$

For stress intensity factor since we are interested in the singular part of the stress near the crack tip, so making $|\zeta|\to\infty$ and noting that $R_+^{1,2}(\zeta)$ tends to unity as $|\zeta|\to\infty$ we obtain

$$\bar{\Phi}_+^{(1)}(\zeta) = \sqrt{\frac{\mu_1\mu_2}{\mu_1+\mu_2}}\left[\sum_{r=1}^{2} \frac{\bar{\Phi}_-^{(0)}(-ik_r)K_+(ik_r)e^{-2Lk_r}}{2\mu_r\sqrt{(\zeta+ik_r)}\sqrt{\pi Lk_r}} - \sum_{r=1}^{2} \frac{(-1)^r F_r K_+(ik_r)e^{-Lk_r}}{\mu_r p\sqrt{(\zeta+ik_r)}\sqrt{2\pi Lk_r}}\right] \quad (53a)$$

and

$$\bar{\Phi}_-^{(1)}(\zeta) = \sqrt{\frac{\mu_1\mu_2}{\mu_1+\mu_2}}\, i\left[-\sum_{r=1}^{2} \frac{\bar{\Phi}_+^{(0)}(ik_r)K_+(ik_r)e^{-2Lk_r}}{2\mu_r\sqrt{(\zeta-ik_r)}\sqrt{\pi Lk_r}} - \sum_{r=1}^{2} \frac{(-1)^r F_r K_+(ik_r)e^{-Lk_r}}{\mu_r p\sqrt{(\zeta-ik_r)}\sqrt{2\pi Lk_r}}\right]. \quad (53b)$$

Taking inverse Fourier transform we obtain,

$$\Phi_\pm(x\pm L) = \pm\left(\frac{\mu_1\mu_2}{\mu_1+\mu_2}\right)^2 \frac{1}{2\pi\sqrt{(L|x\pm L|)}}\left[-\frac{F_1[R_+^1(ik_1)]^3 e^{s_1 p(\pm x-2L)}}{\mu_1^2\sqrt{\mu s_1 L}\, p^{3/2}}\right.$$

$$\left. + \frac{F_2}{\mu_1\mu_2}\frac{R_+^1(ik_1)R_+^1(ik_2)R_+^2(ik_1)}{\sqrt{\pi s_2 L}}\frac{e^{p(\pm s_1 x - s_1 L - s_2 L)}}{p^{3/2}}\right.$$

$$- \frac{F_1}{\mu_1\mu_2}\frac{R_+^2(ik_2)R_+^2(ik_1)R_+^1(ik_2)}{\sqrt{\pi s_1 L}}\frac{e^{p(\pm s_2 x - s_1 L - s_2 L)}}{P^{3/2}}$$

$$+ \frac{F_2}{\mu_2^2}\frac{[R_+^2(ik_2)]^3}{\sqrt{\pi s_2 L}}\frac{e^{s_2 p(\pm x - 2L)}}{p^{3/2}}\Bigg]$$

$$\pm \frac{1}{\pi}\left(\frac{\mu_1\mu_2}{\mu_1+\mu_2}\right)\frac{1}{\sqrt{(L|x\pm L|)}}\sum_{r=1}^{2}\frac{(-1)^{r+1}F_r R_+^1(ik_r)e^{\pm s_r x p}}{\mu_r p} \quad \text{as } x\to\mp(L+0). \qquad (54)$$

Next from equation (54) the normalized stress intensity factors $K_{\pm L}(t)$ where subscripts -L, +L refer to the corresponding values at the crack tips at x=-L and x=L respectively have been derived.

Noting that $R_+^{1,2}(ik_1)$ and $R_+^{1,2}(ik_2)$ are independent of p and using shifting theorem, the inverse Laplace transform finally gives the normalised dynamic stress intensity factors as

$$|K_{\mp L}(t)| = \left|\frac{1}{F_1}\underset{x\to\mp L}{Lt}\frac{\phi(x\pm L)}{\sqrt{(L|x\pm L|)}}\right| = \left|-\frac{1}{\pi(1+m)}\left[mR_+^1(ik_1)H(\tau-1) - \frac{F_2}{F_1}R_+^2(ik_2)H(\tau-\gamma)\right]\right.$$

$$+ \frac{1}{\pi^2(1+m)^2}\Big[m^2[R_+^1(ik_1)]^3\sqrt{\tau-3}\,H(\tau-3)$$

$$- \frac{F_2}{F_1}mR_+^1(ik_1)R_+^1(ik_2)R_+^2(ik_1)\sqrt{\left(\frac{\tau}{\gamma}-\frac{2}{\gamma}-1\right)}\,H(\tau-2-\gamma)$$

$$+ mR_+^2(ik_2)R_+^2(ik_1)R_+^1(ik_2)\sqrt{(\tau-2\gamma-1)}\,H(\tau-2\gamma-1)$$

$$\left.- \frac{F_2}{F_1}[R_+^2(ik_2)]^3\sqrt{\left(\frac{\tau}{\gamma}-3\right)}\,H(\tau-3\gamma)\Big]\right|, \quad 1<\tau<5, \qquad (55)$$

where

$$m = \frac{\mu_2}{\mu_1}, \quad \gamma = \frac{s_2}{s_1} \quad \text{and} \quad \tau = \frac{t}{s_1 L}.$$

It may be noted that stress intensity factors at the both edges $|K_{+L}(t)|$ and $|K_{-L}(t)|$ are the same which is also obvious from the symmetry of the problem.

3. RESULTS AND DISCUSSIONS

From equations (7) and (14) it is to be noted that Y=0, x=X and y=0 and that $\hat{\sigma}^{(j)}_{YZ}(X,0,t) = \sigma^{j}_{yz}(x,0,t)$.

Therefore, elastodynamic mode III stress intensity factors at the crack tips of the interface crack in an anisotropic bimaterial are the same as that of the interface crack of the corresponding isotropic bimaterial given by equation (55).

While carrying out numerical calculations both the cases of symmetric ($F_1 = F_2 = F$) and antisymmetric ($F_1 = -F_2 = F$) loading have been treated. For numerical evaluation of stress intensity factors at the tips of the cracks of finite width situated at the interface, the four material pairs (Nayfeh [1995]), given in Table-1, have been considered.

The absolute value of the stress intensity factors defined by equation (55) has been plotted against $\tau \left(= \frac{t}{s_1 L} \right)$ for different material pairs in Figs. 3 - 6 for both the symmetric and antisymmetric loading for values of τ varying from 1.0 to 5.0.

It is to be noted that in the case of antisymmetric loading, stress intensity factor increases in two steps, the first step corresponds to the first arrival of the wave at the crack tip moving along the upper face of the crack from the source and the second jump occurring because of the arrival of the wave at the crack tip due to wave moving along the lower face of the crack.

Table-1. Engineering elastic constants of different materials.

Medium	Name	$\hat{\rho}$ (Kg m $^{-3}$)	C_{44} (Gpa)	C_{55} (Gpa)	C_{45} (Gpa)
Type of material pair : I					
1.	Carbon-epoxy	1.57×10^3	3.98	6.4	0
2.	Graphite-epoxy	1.60×10^3	6.55	2.6	0
Type of material pair : II					
1.	Isotropic Chromium	7.20×10^3	115.2	115.2	0
2.	Isotropic Steel	7.90×10^3	81.91	81.91	0
Type of material pair : III					
1.	Isotropic Aluminium	2.70×10^3	26.45	26.45	0
2.	Carbon-epoxy	1.57×10^3	3.98	6.4	0
Type of material pair : IV					
1.	Copper coated Stainless Steel	8.00×10^3	91	135	0
2.	Isotropic Aluminium	2.70×10^3	26.45	26.45	0

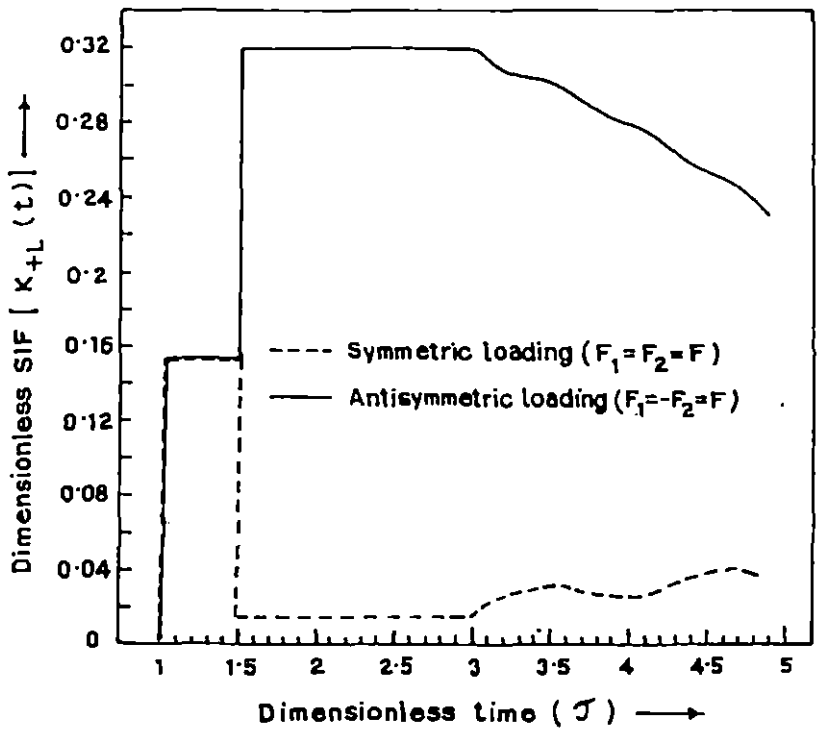

Fig.3. Stress intensity factor versus dimensionless time for Type-I material pair.

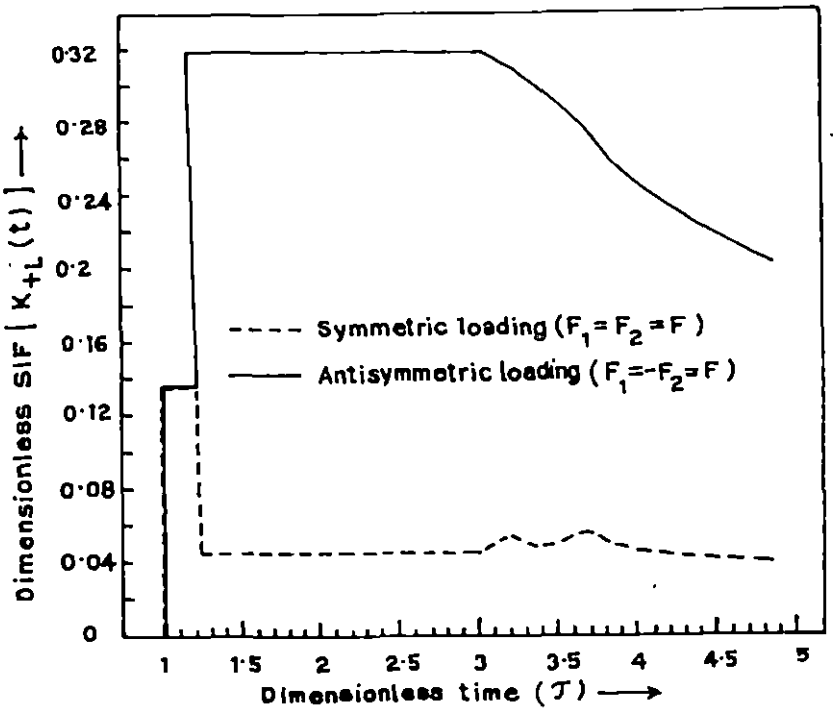

Fig.4. Stress intensity factor versus dimensionless time for Type-II material pair.

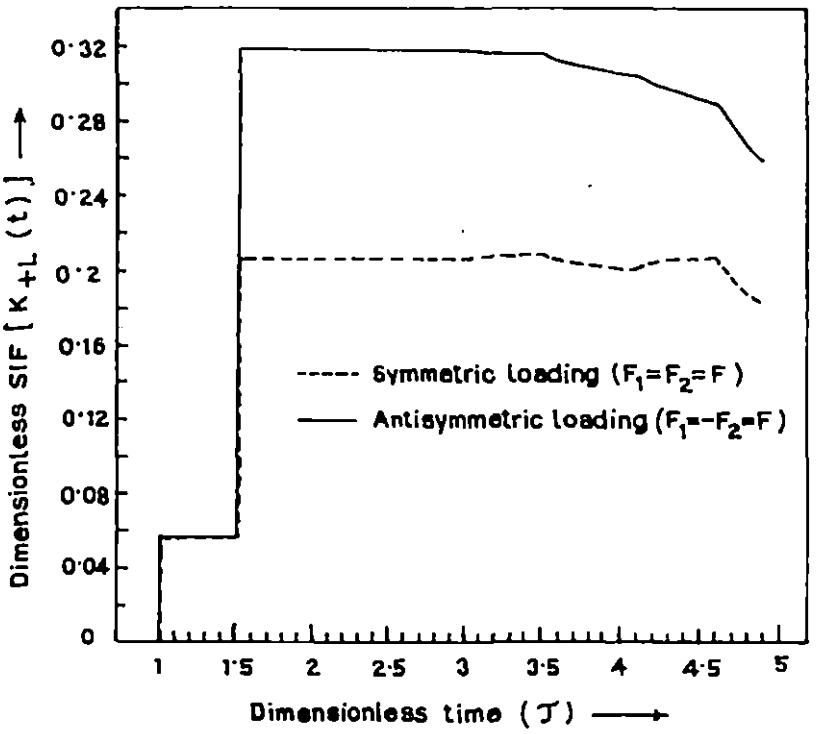

Fig.5. Stress intensity factor versus dimensionless time for Type-III material pair.

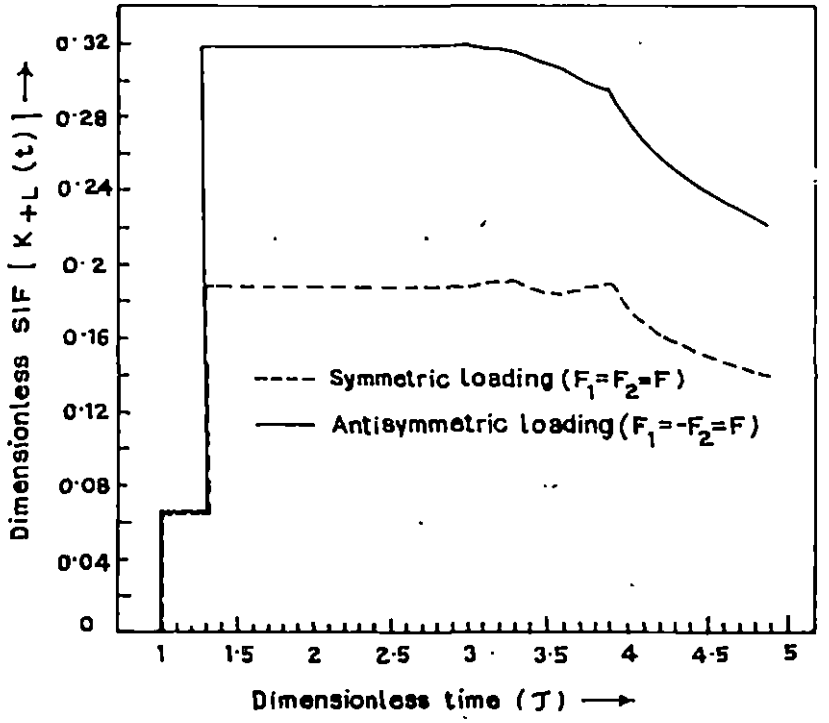

Fig.6. Stress intensity factor versus dimensionless time for Type-IV material pair.

It is interesting to note that after the arrival of the first scattered wave from the opposite edge of the crack, the stress intensity factor gradually decreases in the case of antisymmetric loading.

However in the case of symmetric loading stress intensity factor at first increases when the wave moving from the source along the upper face of the crack surface reaches the crack tip but as soon as the wave from the source moving along the lower face of the crack reaches the crack tip, suddenly it decreases for Type I and Type II material pairs and increases for Type III and Type IV material pairs until the scattered wave from the opposite crack tip arrives when the stress intensity factor shows tendency of increasing but with slow oscillations.

Appendix A

From equation (40) we obtain

$$R^1(\zeta) = \frac{(\mu_1+\mu_2)\sqrt{(\zeta^2+k_2^2)}}{\mu_1\sqrt{(\zeta^2+k_1^2)}+\mu_2\sqrt{(\zeta^2+k_2^2)}} \tag{A.1}$$

$$R^1(\zeta) = R_+^1(\zeta)R_-^1(\zeta) = \frac{1}{\frac{m}{1+m}+\frac{1}{1+m}\sqrt{\frac{\zeta^2+k_1^2}{\zeta^2+k_2^2}}},$$

where

$$m = \frac{\mu_2}{\mu_1}.$$

Taking logarithm on both sides, one obtains

$$\log R^1(\zeta) = \log R_+^1(\zeta) + \log R_-^1(\zeta) = -\log\left[\frac{m}{1+m} + \frac{1}{1+m}\sqrt{\frac{\zeta^2+k_1^2}{\zeta^2+k_2^2}}\right].$$

So

$$\log R_+^1(\zeta) = \frac{1}{2\pi i}\int_{-ic-\infty}^{-ic+\infty}\frac{\log R^1(z)}{z-\zeta}\,dz.$$

Replacing z by -z and using $R^1(-z) = R^1(z)$

$$\log R_+^1(\zeta) = -\frac{1}{2\pi i}\int_{ic-\infty}^{ic+\infty}\frac{\log R^1(z)}{z+\zeta}\,dz = \frac{1}{2\pi i}\int_{ic-\infty}^{ic+\infty}\frac{\log\left[\frac{m}{1+m}\left\{1+\frac{1}{m}\sqrt{\frac{z^2+k_1^2}{z^2+k_2^2}}\right\}\right]}{z+\zeta}\,dz$$

$$= \frac{1}{2\pi i}\int_{ic-\infty}^{ic+\infty}\frac{\log\left[1+\frac{1}{m}\sqrt{\frac{z^2+k_1^2}{z^2+k_2^2}}\right]}{z+\zeta}\,dz$$

$$= \frac{1}{2\pi i}\int_{k_1}^{k_2}\frac{\log\left[1+i\sqrt{\frac{u^2-k_1^2}{m^2(k_2^2-u^2)}}\right]}{u-i\zeta}\,du - \frac{1}{2\pi i}\int_{k_1}^{k_2}\frac{\log\left[1-i\sqrt{\frac{u^2-k_1^2}{m^2(k_2^2-u^2)}}\right]}{u-i\zeta}\,du$$

which yields,

$$R_+^1(\zeta) = \exp\left[\frac{1}{\pi}\int_{k_1}^{k_2}\frac{\tan^{-1}\left[(z^2-k_1^2)/\{m^2(k_2^2-z^2)\}\right]^{1/2}}{(z-i\zeta)}dz\right]. \qquad (A.2)$$

Similarly,

$$R_{-}^{1}(\zeta) = \exp\left[\frac{1}{\pi}\int_{k_1}^{k_2}\frac{\tan^{-1}\left[(z^2-k_1^2)/\{m^2(k_2^2-z^2)\}\right]^{1/2}}{(z+i\zeta)}dz\right]. \quad (A.3)$$

Similarly, it can be shown that

$$R_{\pm}^{2}(\zeta) = \exp\left[-\frac{1}{\pi}\int_{k_1}^{k_2}\frac{\tan^{-1}\left[m^2(k_2^2-z^2)/(z^2-k_1^2)\right]^{1/2}}{(z\mp i\zeta)}dz\right] \quad (A.4)$$

where $R^2(\zeta)$ is given by equation (43).

Using equation (40) or equation (41) it can be shown that

$$K_{\pm}(\zeta) = \left(\frac{\mu_1\mu_2}{\mu_1+\mu_2}\right)^{1/2}(\zeta\pm ik_1)^{1/2}R_{\pm}^{1}(\zeta) \quad (A.5)$$

$$= \left(\frac{\mu_1\mu_2}{\mu_1+\mu_2}\right)^{1/2}(\zeta\pm ik_2)^{1/2}R_{\pm}^{2}(\zeta). \quad (A.6)$$

From either equation (A.5) or equation (A.6) it can be easily shown that

$$K_{-}(-\zeta) = -iK_{+}(\zeta).$$

----x----

[3]INTERACTION OF HORIZONTALLY POLARISED SH-WAVE WITH A GRIFFITH CRACK MOVING ALONG THE BIMATERIAL INTERFACE

1. INTRODUCTION

Scattering of elastic waves by a stationary or moving crack of finite width at the interface of two dissimilar elastic materials is important in view of its application in seismology as well as in fracture mechanics. The diffraction of Love waves by a stationary crack of finite width at the interface was investigated by Neerhoff [1979]. Kuo [1984] carried out analytical and numerical studies of transient response of an interfacial crack between two dissimilar orthotropic half spaces. Srivastava et al [1980] also derived the low frequency solution of the interaction of SH-wave by a Griffith crack at the interface of two bonded dissimilar elastic media.

In the case of cracks of finite size, moving with uniform velocity, loads, for mathematical simplicity, are usually assumed to be independent of time. However, in practice, structures are often required to sustain oscillating loads where the dynamic disturbances propagate through the elastic medium in the form of stress waves. The problem of diffraction of a plane harmonic polarized shear wave by a half-plane crack extended under antiplane strain was first studied by Jahanshahi [1967]. Later Sih and Loeber [1970] and Chen and Sih [1975] also considered the problem of scattering of plane harmonic wave by a running crack of finite length. Recently the high frequency solution of the problem of diffraction of the horizontally polarizes shear wave by a finite crack moving on a bimaterial interface has been investigated by Pal and Ghosh [1993] using Wiener-Hopf technique.

---

[3] **In press, Indian Journal of Pure and Applied Mathematics, 2000.**

In the present paper, we have investigated the low frequency solution of the scattering of plane SH-wave by a finite crack moving on bimaterial interface with uniform velocity. Using moving co-ordinate system and Fourier transform technique, the elastodynamic problem has been reduced to two pairs of dual integral equations. Following Sih and Loeber [1969], the solution is then obtained in terms of a pair of coupled Fredholm integral equations. Finally the singular nature of the stress near about the crack tip has been determined. The numerical values of dynamic stress intensity factor versus demensionless wave number have been depicted by means of graphs for various parameters of material properties, crack speed and the angle of incidence.

2. FORMULATION OF THE PROBLEM AND ITS SOLUTION

Let a plane crack of finite length 2a located at the interface of two bonded dissimilar semi-infinite elastic media be moving with a constant velocity V due to the incidence of plane harmonic SH-wave

$$W_1^{(i)} = W_0 \exp\left[-i\left\{\Lambda_1(X\cos\theta_1 + Y\sin\theta_1) + \Omega T\right\}\right] \tag{2.1}$$

where W_0 is the wave amplitude, Λ_1 wave number, $\Omega(=\Lambda_1 C_1)$ circular frequency, $(\Pi/2 - \theta_1)$ angle of incidence and C_1 is the shear wave velocity in the upper medium denoted by (1).

The crack lies in XZ plane with Z axis directed parallel to the edge of the crack with respect to the rectangular co-ordinate system (X,Y,Z) as shown in Fig.1.

We assume that the displacement and the stress due to scattered fields are

$$W_j = W_j(X,Y)\, e^{-i\Omega T} \tag{2.2}$$

and

$$(\tau_{XZ})_j = \mu_j \frac{\partial W_j}{\partial X} \quad \text{and} \quad (\tau_{YZ})_j = \mu_j \frac{\partial W_j}{\partial Y} \tag{2.3}$$

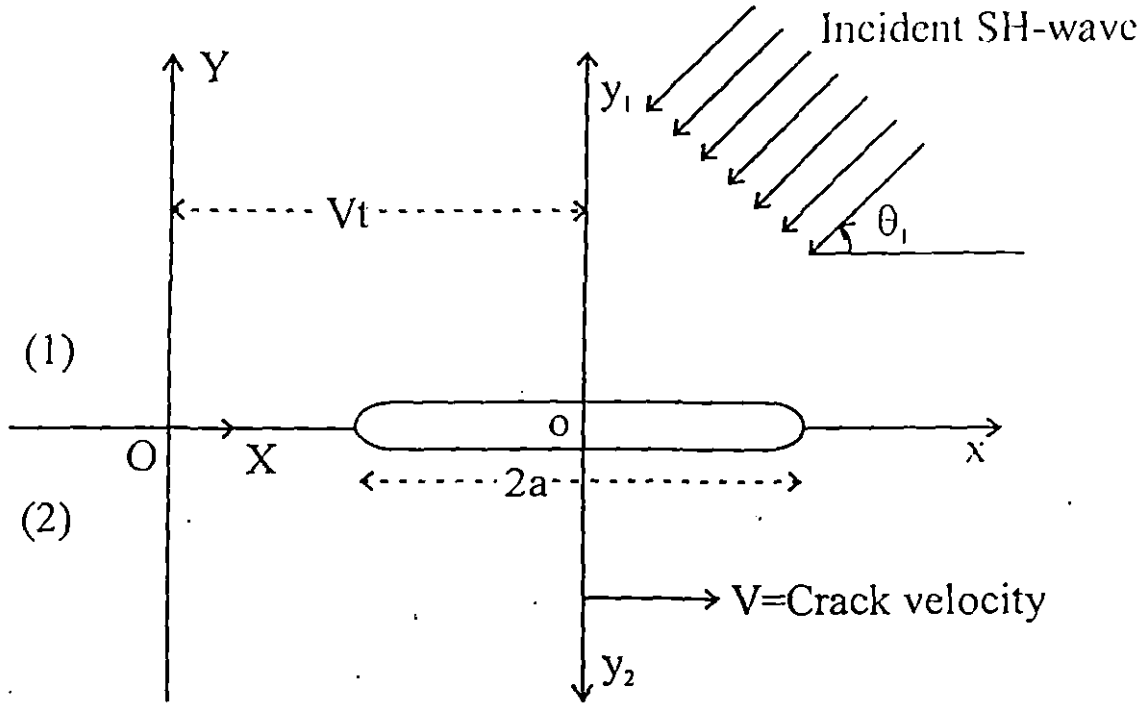

Fig.1. Moving interface crack.

where the subscripts j=1,2 refer to the upper and lower half plane respectively and T denotes time.

The equations of SH wave motion in either elastic half spaces are given by

$$\frac{\partial^2 W_j}{\partial X^2} + \frac{\partial^2 W_j}{\partial Y^2} = \frac{1}{C_j^2}\frac{\partial^2 W_j}{\partial T^2}; \qquad (j=1,2) \tag{2.4}$$

where $C_j = \sqrt{\frac{\mu_j}{\rho_j}}$ is the shear wave velocity and μ_j, ρ_j are co-efficient of rigidity and material density respectively. Without any loss of generality we further assume that $C_1 > C_2$.

Due to the incident wave given in equation (2.1), the reflected and transmitted wave in the absence of the crack may be written as

$$W_1^{(R)} = A\exp\left[-i\left\{\Lambda_1(X\cos\theta_1 - Y\sin\theta_1) + \Omega T\right\}\right]$$

and

$$W_2^{(T)} = B\exp\left[-i\left\{\Lambda_2(X\cos\theta_2 + Y\sin\theta_2) + \Omega T\right\}\right] \tag{2.5}$$

where

$$A = \frac{\mu_1\Lambda_1\sin\theta_1 - \mu_2\Lambda_2\sin\theta_2}{\mu_1\Lambda_1\sin\theta_1 + \mu_2\Lambda_2\sin\theta_2}W_0, \qquad B = \frac{2\mu_1\Lambda_1\sin\theta_1}{\mu_1\Lambda_1\sin\theta_1 + \mu_2\Lambda_2\sin\theta_2}W_0 \tag{2.6}$$

with $\Lambda_1\cos\theta_1 = \Lambda_2\cos\theta_2$.

A, B are the reflected and transmitted wave amplitudes, Λ_j wave number, $\Omega(=\Lambda_j C_j)$ the circular frequency and $(\pi/2 - \theta_1)$ and $(\pi/2 - \theta_2)$ the angles of incidence and refraction respectively.

A set of moving co-ordinate system (x, y_j, z, t) moving along with the crack at a constant velocity V in X-direction is introduced in accordance with

$$x = X - Vt, \quad y_j = s_j Y, \quad z = Z, \quad t = T \tag{2.7}$$

where $s_j^2 = 1 - M_j^2$ and $M_j = V/C_j$ is the Mach number.

$M_j < 1$, since the crack is assumed to travel at subsonic speed.

In terms of moving co-ordinate system (x, y_j, t) equation (2.4) becomes

$$\frac{\partial^2 W_j}{\partial x^2} + \frac{\partial^2 W_j}{\partial y_j^2} + \frac{1}{C_j^2 s_j^2}\frac{\partial}{\partial t}\left[2V\frac{\partial W_j}{\partial x} - \frac{\partial W_j}{\partial t}\right] = 0. \tag{2.8}$$

Further, referred to moving coordinate system, incident and reflected and transmitted wave given by equations (2.1) and (2.5) take the following form,

$$W_1^{(i)} = W_0 e^{-i\omega t}\exp\left[-i\Lambda_1\left(x\cos\theta_1 + \frac{y_1}{s_1}\sin\theta_1\right)\right],$$

$$W_1^{(R)} = A e^{-i\omega t}\exp\left[-i\Lambda_1\left(x\cos\theta_1 - \frac{y_1}{s_1}\sin\theta_1\right)\right]$$

and $$W_2^{(T)} = B e^{-i\omega t}\exp\left[-i\Lambda_2\left(x\cos\theta_2 + \frac{y_2}{s_2}\sin\theta_2\right)\right] \tag{2.9}$$

where $\omega = \Omega\,\alpha$ and $\alpha = (1 + M_1\cos\theta_1) = (1 + M_2\cos\theta_2)$ (2.10)

It is convenient to write the solution of the equation (2.8) in the form

$$W_j(x,y_j,t) = W_j(x,y_j)\,e^{-i\omega t} = w_j(x,y_j)\exp[\,i(\lambda_j M_j x - \omega t)\,] \tag{2.11}$$

where $\lambda_j = \frac{\Lambda_j}{s_j^2}\alpha$. (2.12)

Substitution of equation (2.11) into equation (2.8) yields the Helmhlotz equation governing w_j

$$\frac{\partial^2 w_j}{\partial x^2} + \frac{\partial^2 w_j}{\partial y_j^2} + \lambda_j^2 w_j = 0. \tag{2.13}$$

The solution of equation (2.13) can be written as

$$w_j(x,y_j) = \frac{1}{2\pi}\int_{-\infty}^{\infty} A_j(\xi)\,e^{-i\xi x - \beta_j|y_j|}\,d\xi \tag{2.14}$$

where $\beta_j = \sqrt{\xi^2 - \lambda_j^2}$. (2.15)

From equations (2.11) and (2.14) the displacement components of the diffracted field can be expressed as

$$W_j(x,y_j) = \frac{1}{2\pi}\int_{-\infty}^{\infty} B_j(\xi)\,e^{-i\xi x - \gamma_j|y_j|}\,d\xi \tag{2.16}$$

where

$$\gamma_j = \sqrt{(\xi + \lambda_j M_j)^2 - \lambda_j^2}, \qquad B_j(\xi) = A_j(\xi + \lambda_j M_j) \tag{2.17}$$

The unknown quantities $B_1(\xi)$ and $B(\xi)$ are to be determined from the following boundary conditions

$$\mu_1 s_1 \frac{\partial W_1}{\partial y_1} = \mu_2 s_2 \frac{\partial W_2}{\partial y_2} \quad \text{for all } x,\ y_j = 0$$

$$W_1 = W_2; \qquad |x| > a; \qquad Y_j = 0$$

$$\frac{\partial W_1}{\partial y_1} + \frac{\partial W_1^{(i)}}{\partial y_1} + \frac{\partial W_1^{(R)}}{\partial y_1} = 0; \quad |x| < a; \quad y_j = 0. \tag{2.18}$$

From the first boundary condition of equations (2.18) one obtains

$$\mu_1 s_1 \gamma_1 B_1(\xi) + \mu_2 s_2 \gamma_2 B_2(\xi) = 0. \tag{2.19}$$

The other two boundary conditions yield the following dual integral equations

$$\frac{1}{2\pi} \int_{-\infty}^{\infty} P_1(\xi) e^{-i\xi x} d\xi = 0; \quad |x| > a, \quad y_j = 0$$

and

$$\frac{1}{2\pi} \int_{-\infty}^{\infty} E_1(\xi) P_1(\xi) e^{-i\xi x} d\xi = -D_1 e^{-i\Lambda_1 x \cos\theta_1}; \quad |x| < a \tag{2.20}$$

where

$$P_1(\xi) = \frac{s_1 \mu_1 \gamma_1 + s_2 \mu_2 \gamma_2}{\gamma_2} B_1(\xi) \tag{2.21}$$

$$E_1(\xi) = \frac{\gamma_1 \gamma_2}{s_1 \mu_1 \gamma_1 + s_2 \mu_2 \gamma_2} \tag{2.22}$$

$$D_1 = \left(\frac{2\mu_2 \Lambda_2 \sin\theta_2}{\mu_1 \Lambda_1 \sin\theta_1 + \mu_2 \Lambda_2 \sin\theta_2} \right) \frac{i\Lambda_1 \sin\theta_1}{s_1} W_0 \tag{2.23}$$

The equation (2.20) can further be reduced to two sets of dual integral equations. They are

$$\frac{2}{\pi} \int_0^{\infty} P_{1e}(\xi) \cos(\xi x) d\xi = 0; \quad |x| > a, \quad y_j = 0;$$

$$\frac{2}{\pi} \int_0^{\infty} E_{1e}(\xi) P_{1e}(\xi) \cos(\xi x) d\xi$$

$$= -2D_1\cos(\Lambda_1 x\cos\theta_1) - \frac{2}{\pi}\int_0^\infty E_{1o}(\xi)P_{1o}(\xi)\cos(\xi x)\,d\xi; \quad |x|<a. \qquad (2.24)$$

and $$\frac{2}{\pi}\int_0^\infty P_{1o}(\xi)\sin(\xi x)\,d\xi = 0; \quad |x|>a, \quad y_j = 0;$$

$$\frac{2}{\pi}\int_0^\infty E_{1e}(\xi)P_{1o}(\xi)\sin(\xi x)\,d\xi$$

$$= -2D_1\sin(\Lambda_1 x\cos\theta_1) - \frac{2}{\pi}\int_0^\infty E_{1o}(\xi)P_{1e}(\xi)\sin(\xi x)\,d\xi; \quad |x|<a. \qquad (2.25)$$

where

$$P_1(\xi) = \frac{1}{2}\left[P_1(\xi)+P_1(-\xi)\right] + \frac{1}{2}\left[P_1(\xi)-P_1(-\xi)\right] = P_{1e}(\xi) + P_{1o}(\xi)$$

$$E_1(\xi) = \frac{1}{2}\left[E_1(\xi)+E_1(-\xi)\right] + \frac{1}{2}\left[E_1(\xi)-E_1(-\xi)\right] = E_{1e}(\xi) + E_{1o}(\xi). \qquad (2.26)$$

The problems in equation (2.24) and (2.25) are respectively even and odd in x. The solution procedure described in Sih and Loeber [1969], can be used to solve equations (2.24) and (2.25) and the result is a coupled Fredholm integral equation of the second kind. In order to solve equations (2.24) and (2.25) it is assumed that

$$P_{1e}(\xi) = \frac{\pi D_1 a^2}{K}\int_0^1 \sqrt{s}\,\Delta_1(s)\,J_0(a\xi s)\,ds \qquad (2.27)$$

$$P_{1o}(\xi) = \frac{\pi D_1 a}{K\xi}\left[\int_0^1 \sqrt{s}\,\Gamma_1(s)\,J_0(a\xi s)\,ds - i\Omega_1(1)J_0(a\xi)\right] \qquad (2.28)$$

where $$i\Omega_1(1) = \int_0^1 \sqrt{s}\,\Gamma_1(s)\,ds \qquad (2.29)$$

Substitution of equations (2.27) and (2.28) in equations (2.24) and (2.25) yields the following coupled integral equations for the determination of $\Delta_1(s)$ and $\Gamma_1(s)$

$$\Delta_1(s) - \int_0^1 \Delta_1(\eta)M_1(s,\eta)\,d\eta - \int_0^1 \Gamma_1(\eta)\left[N_1(s,\eta) - \sqrt{\eta}N_1(s,1)\right]d\eta$$

$$= \sqrt{s}J_0(\Lambda_1 as\cos\theta_1);$$

$$\Gamma_1(s) - \int_0^1 \Delta_1(\eta)\left\{L_1(s,\eta) - \frac{K'a}{K}M_1(s,\eta)\right\}d\eta +$$

$$+ \int_0^1 \Gamma_1(\eta)\left\{\frac{K'a}{K}\left[N_1(s,\eta) - \sqrt{\eta}N_1(s,1)\right] - \left[M_1(s,\eta) - \sqrt{\eta}M_1(s,1)\right]\right\}d\eta$$

$$= \sqrt{s}\left(\Lambda_1 a\cos\theta_1 - \frac{K'a}{K}\right) J_0(\Lambda_1 as\cos\theta_1); \qquad (2.30)$$

where $$K = -\frac{1}{(s_1\mu_1 + s_2\mu_2)} \qquad (2.31)$$

$$K' = -\frac{(\lambda_1 M_1 s_2\mu_2 + \lambda_2 M_2 s_1\mu_1)}{(s_1\mu_1 + s_2\mu_2)^2} \qquad (2.32)$$

$$M_1(s,\eta) = \frac{\sqrt{s\eta}}{K}\int_0^\infty \xi H_{1e}(\xi/a)J_0(\xi\eta)J_0(\xi s)d\xi \qquad (2.33)$$

$$N_1(s,\eta) = \frac{\sqrt{s\eta}}{K}\int_0^\infty \frac{a}{\xi}E_{1o}(\xi/a)J_0(\xi\eta)J_0(\xi s)d\xi \qquad (2.34)$$

$$L_1(s,\eta) = \frac{\sqrt{s\eta}}{K}\int_0^\infty a\xi H_{1o}(\xi/a)J_0(\xi\eta)J_0(\xi s)d\xi \qquad (2.35)$$

in which $H_{1e}(\xi)$ and $H_{1o}(\xi)$ are defined as

$$H_{1e}(\xi) = \frac{E_{1e}(\xi)}{\xi} + K \to O(\xi^{-2}) \quad \text{as } \xi \to \infty$$

$$H_{1o}(\xi) = E_{1o}(\xi) + K' \to O(\xi^{-2}) \quad \text{as } \xi \to \infty. \qquad (2.36)$$

3. STRESS INTENSITY FACTOR

Since the condition of the crack propagation is controlled by the stresses near the crack tips, we are mainly interested in determining the singular behaviour of the stress field near the crack tips.

With the aid of equation (2.16) and (2.21) the stress in medium 1 can be written as

$$\left(\tau_{yz}\right)_1 = \mu_1 s_1 \frac{\partial W_1}{\partial y_1} = -\frac{\mu_1 s_1}{2\pi}\int_{-\infty}^{\infty} E_1(\xi) P_1(\xi) e^{-i\xi x - \gamma_1 y_1}\, d\xi. \qquad (3.1)$$

For an examination of the singular behaviour of the stress near the crack tip (x=±a) it is sufficient to consider the domonating terms in the integrand of the integral (3.1) as $|\xi| \to \infty$.

Accordingly near the crack tip

$$\left[\left(\tau_{yz}\right)_1\right]_{\text{at crack tip}} = -\frac{s_1 \mu_1}{\pi(s_1\mu_1 + s_2\mu_2)} \times$$

$$\times \left[\int_0^{\infty} \xi e^{-\xi y_1} P_{1e} \cos(\xi x)\, d\xi - i\int_0^{\infty} \xi e^{-\xi y_1} P_{1o} \sin(\xi x)\, d\xi\right]. \qquad (3.2)$$

Further as $|x| \to \infty$

$$P_{1e}(\xi) = \frac{\pi D_1 a}{K\xi}\Delta_1(1) J_1(a\xi) + \ldots\ldots$$

$$P_{1o}(\xi) = -\frac{i\pi D_1 a}{K\xi}\Omega_1(1) J_0(a\xi) + \ldots\ldots \qquad (3.3)$$

Substituting the asymptotic expression of $P_{1e}(\xi)$ and $P_{1o}(\xi)$ as given by equation (3.3) in equation (3.2) the singular stress field around x=a, y=0 is obtained as

$$\left[\left(\tau_{yz}\right)_1\right]_{x=a,y=0} = -\frac{\mu_1 s_1 D_1\sqrt{a}}{\sqrt{2r}}\left\{\Omega_1(1) + \Delta_1(1)\right\} f(s_1) + O(1)$$

$$= \frac{\sigma_1\sqrt{a}}{\sqrt{2r}}\left[\frac{\mu_1 \sin\theta_2}{\mu_1 + \mu_2 \cot\theta_1 \tan\theta_2}\left(\Omega_1(1) + \Delta_1(1)\right)\right] f(s_1) + O(1) \qquad (3.4)$$

where

$$f^2(s_1) = \frac{\sec\phi}{2}\left[\left(1 + s_1^2\tan^2\phi\right)^{-1/2} + \left(1 + s_1^2\tan^2\phi\right)^{-1}\right] \qquad (3.5)$$

$$r = \sqrt{(x-a)^2 + y^2}, \qquad \phi = \tan^{-1}\left(\frac{y}{x-a}\right) \qquad (3.6)$$

and $\sigma_1 = -2\, i\, \mu_2\, A_2\, W_0.$ (3.7)

Dynamic stress intensity factor K_1 is defined by

$$K_1 = \sigma_1\sqrt{a}\left[\frac{\mu_1 \sin\theta_2}{\mu_1 + \mu_2 \cot\theta_1 \tan\theta_2}\left(\Omega_1(1) + \Delta_1(1)\right)\right] \qquad (3.8)$$

While studying the dynamic crack propagation the determination of stress intensity factor is important because it supplies useful information regarding the rate at which elastic and kinetic energies are released by the propagating crack.

4. NUMERICAL RESULTS AND DISCUSSIONS

Numerical results have been calculated to plot normalized stress intensity factor $|K_1/(\sigma_1\sqrt{a})|$ at the carck tip x=a, y=0 versus the normalized wave number $\Lambda_1 a$ for different values of the Mach number M_1 and the angle of incidence for the following sets of materials :

First set :

Steel : $\rho_1 = 7.6$ gm/cm^3, $\mu_1 = 8.32 \times 10^{11}$ dyne/cm^2

Aluminium : $\rho_2 = 2.7$ gm/cm^3, $\mu_2 = 2.63 \times 10^{11}$ dyne/cm^2

Second set :

Wrought iron : $\rho_1 = 7.8$ gm/cm^3, $\mu_1 = 7.7 \times 10^{11}$ dyne/cm^2

Copper : $\rho_2 = 8.96$ gm/cm^3, $\mu_2 = 4.5 \times 10^{11}$ dyne/cm^2

The numerical results have been obtained for low frequencies. The case $M_1=0$ corresponds to the stationary crack solution. It is found that by increasing the crack speed, the dimensionless stress intensity factor $|K_1/(\sigma_1\sqrt{a})|$ decreases with the normalized wave number $\Lambda_1 a$. It is interesting to note that as the velocity of the crack increases, the picks of the curves decreases in magnitude and occur at lower values of $\Lambda_1 a$ (Figs. 2 - 7). For both the pair of solids, graphs of stress intensity factor versus normalised wave number ($\Lambda_1 a$) have been plotted for the angles $\theta_1=\pi/3$, $\theta_1=\pi/4$, and as well as $\theta_1=\pi/6$. It is also found that for a given pair of materials and for a given Mach number, the peak values of the stress intensity factors decrease with the decrease in the values of θ_1.

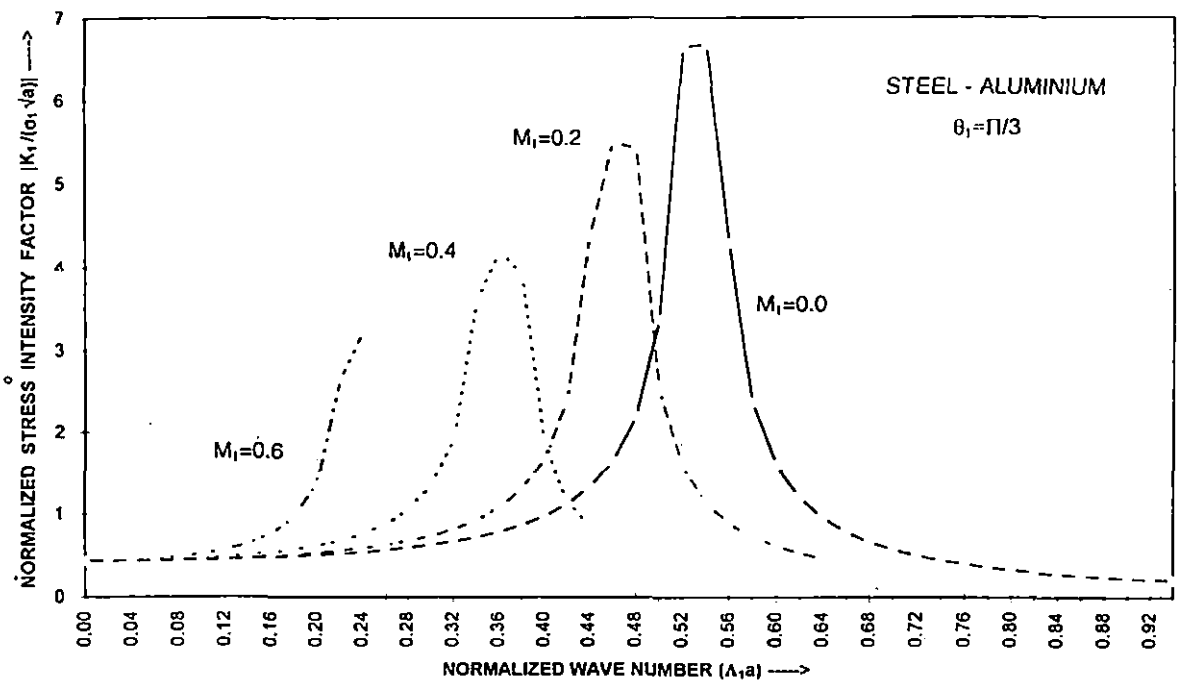

Fig.2 Stress intensity factor vs wave number.

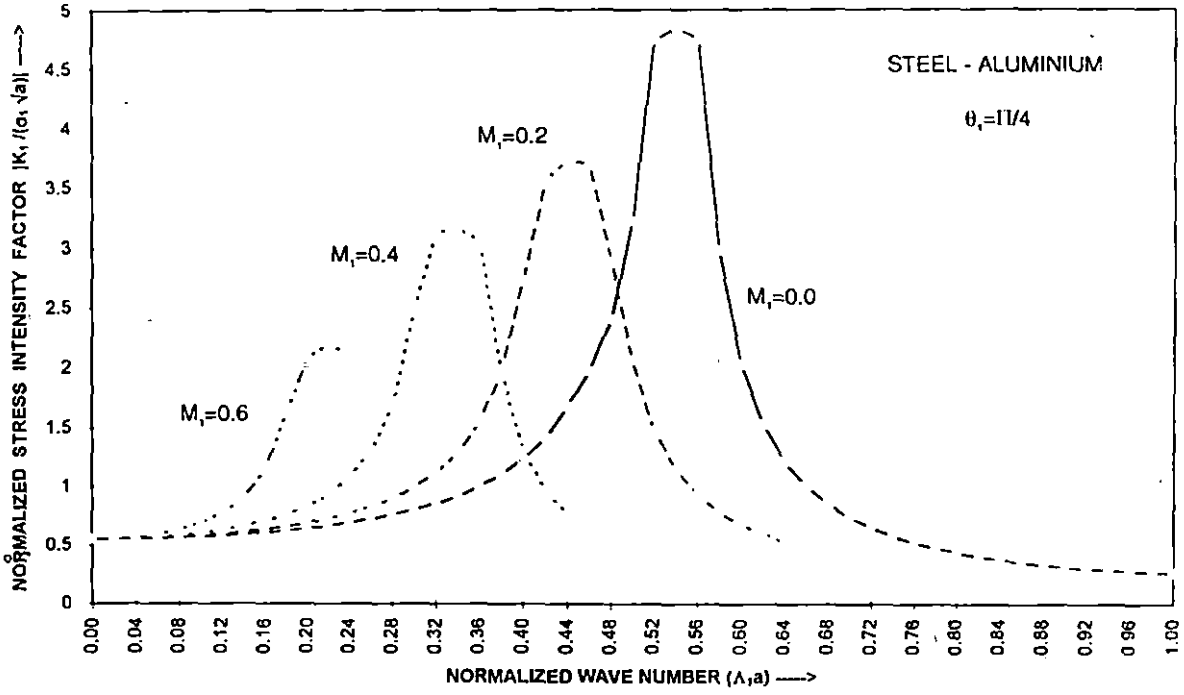

Fig.3 Stress intensity factor vs wave number.

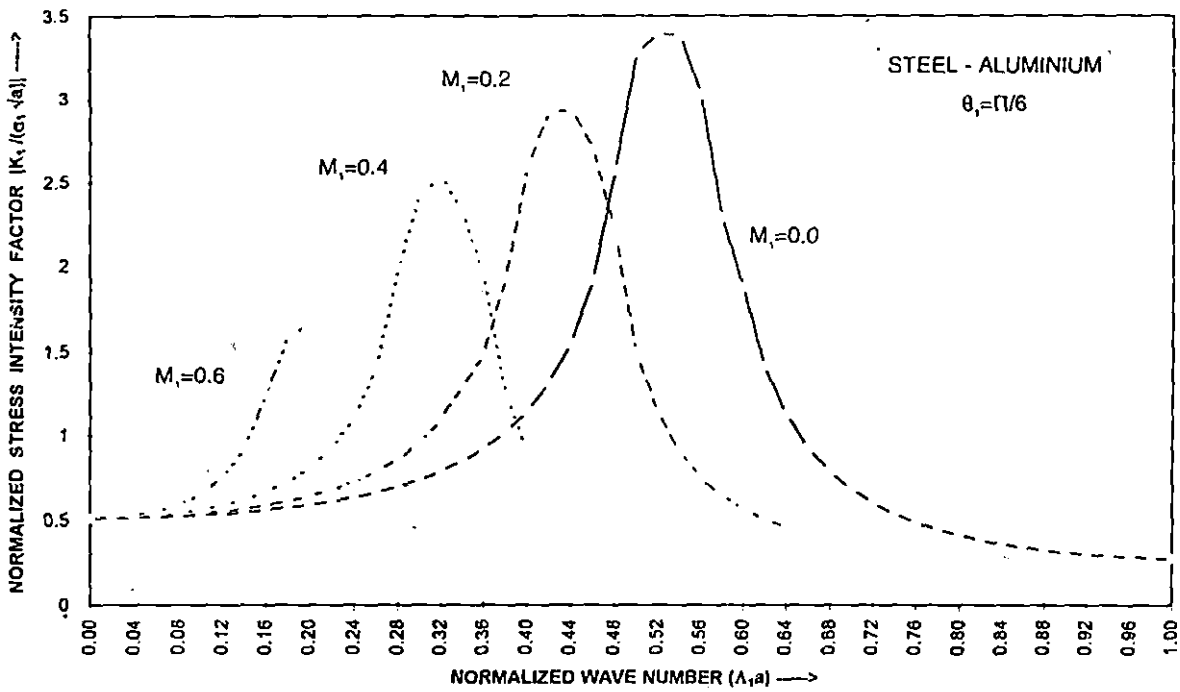

Fig.4 Stress intensity factor vs wave number.

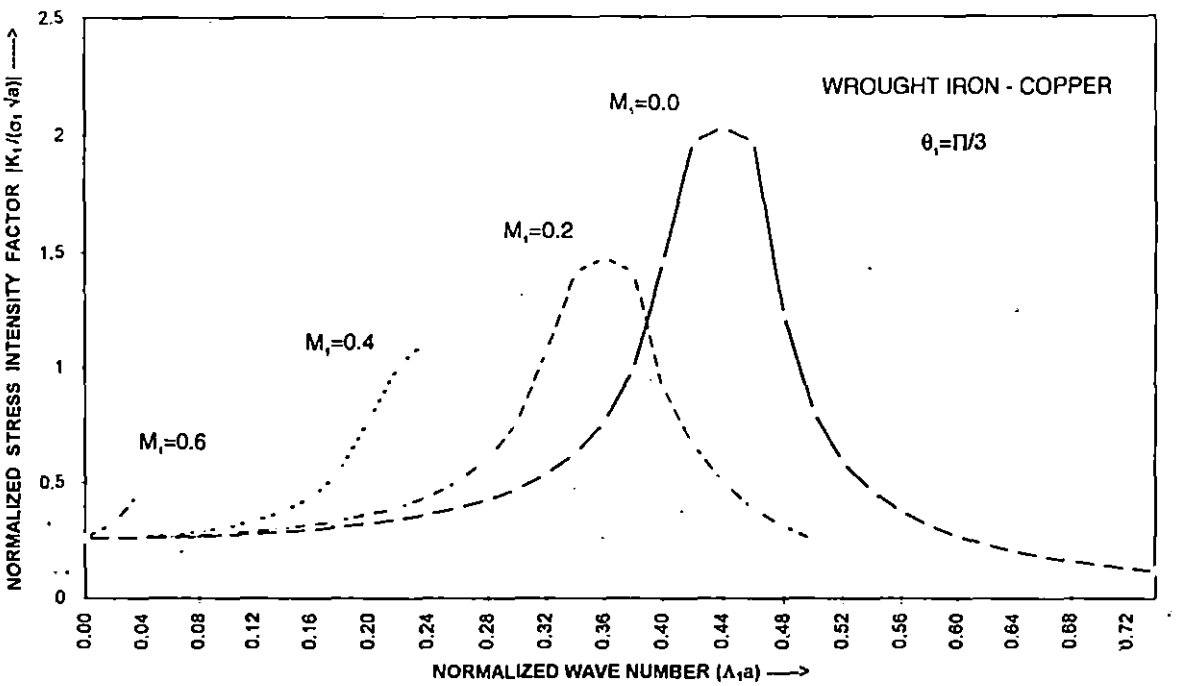

Fig.5 Stress intensity factor vs wave number.

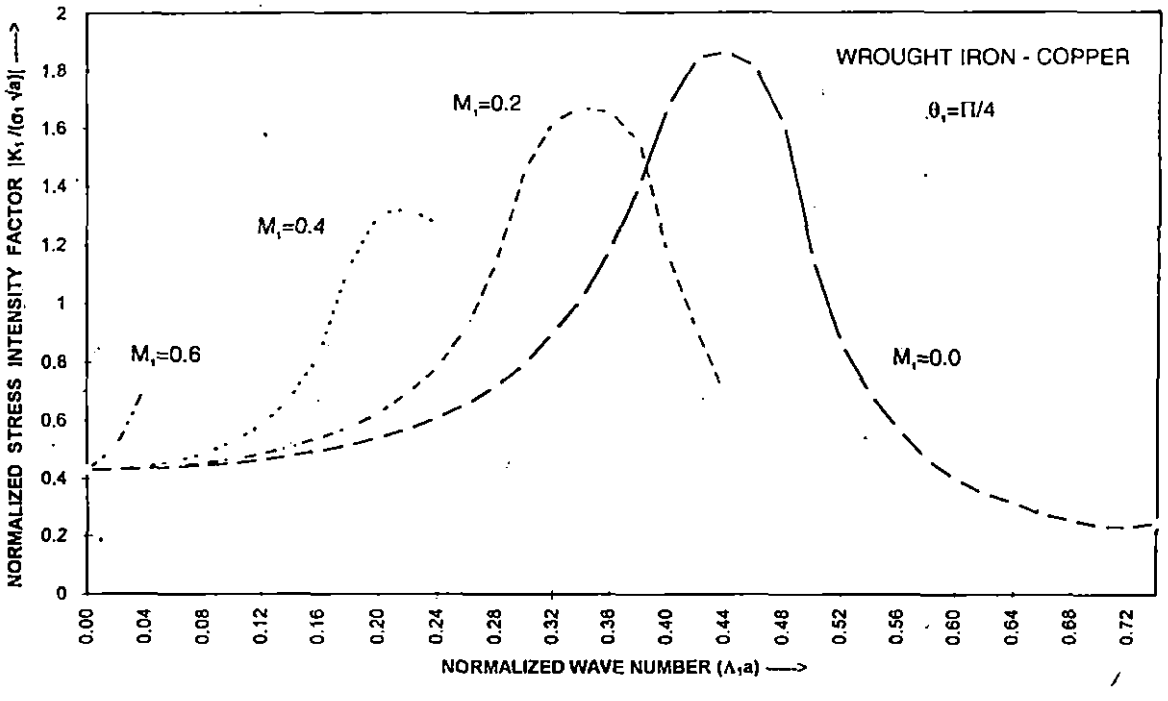

Fig.6 Stress intensity factor vs wave number.

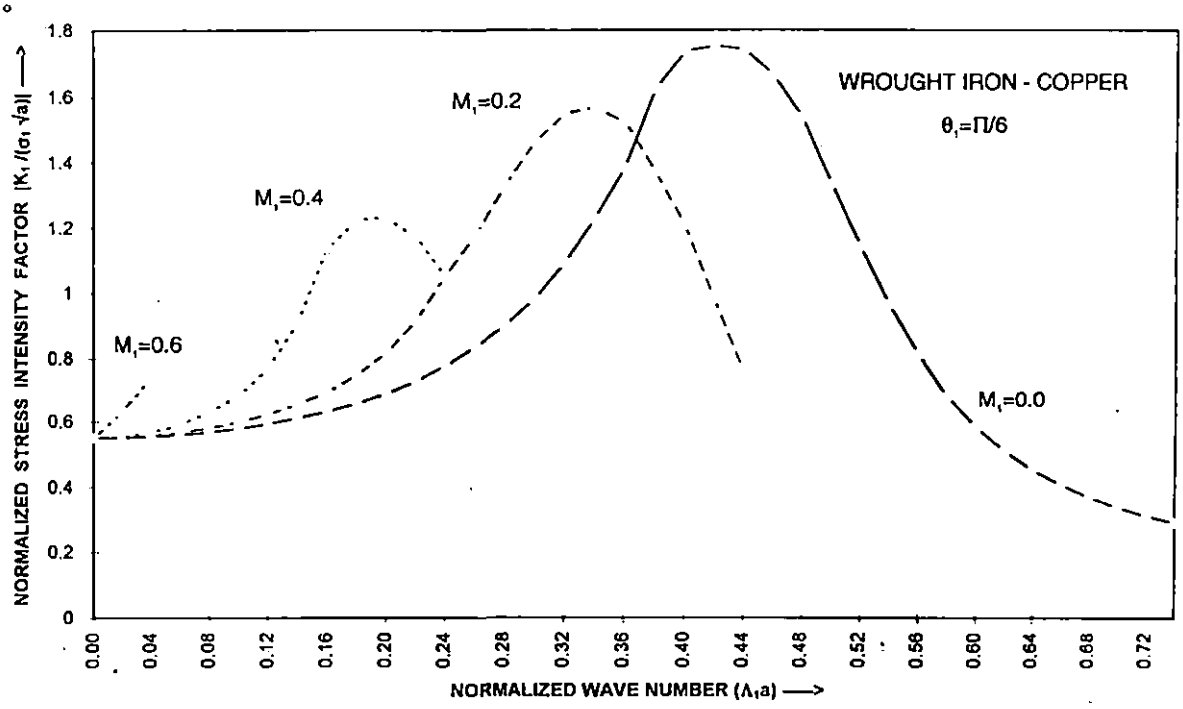

Fig.7 Stress intensity factor vs wave number.

CHAPTER - 2

INCLUSION PROBLEM

[4]SHEAR WAVE INTERACTION WITH A PAIR OF RIGID STRIPS EMBEDDED IN AN INFINITELY LONG ELASTIC STRIP

1. INTRODUCTION

In recent years great interest has been developed in studying elastic wave interaction with singularities in the form of cracks or inclusion located in an elastic medium, in view of their application in engineering fracture mechanics and geophysics. Most of the attempts have been based on the assumption that the crack or the inclusion is situated sufficiently far from the neighbouring boundaries. Mathematically, this type of problem reduces to the study of the elastic field due to the presence of cracks or inclusions in an infinite elastic medium. A detailed reference of work done on the determination of the dynamic stress field around a crack or an inclusion in an infinite elastic solid has been given by Sih [1997]. However in the presence of finite boundaries, the problem becomes complicated since they involve additional geometric parameters, describing the dimension of the solids. Papers involving a crack or a rigid strip in an infinitely long elastic strip are very few. The problem of an infinite elastic strip containing an arbitrary number of Griffith cracks of unequal size, located parallel to its surfaces and opened by an arbitrary internal pressure, has been treated by Adam [1980]. Finite crack perpendicular to the surface of the infinitely long elastic strip has been studied by Chen [1978] for impact load, and by Srivastava et al [1981] for normally incident waves. Recently Shindo et al [1986] considered the problem of impact response of a finite crack in an orthotropic strip. Itou [1980] also studied the response of a central crack in a finite strip under inplane compression impact.

---

[4] **Published in the Journal of Technical Physics, V39, 1, 31-44, 1999.**

But these solutions were limited to the problems involving a single crack or a finite rigid strip embedded in an elastic strip because of severe mathematical complexity involved in finding solutions for two or more cracks or inclusions. Recently Srivastava et al [1983] considered the problem of interaction of shear waves with two co-planar Griffith cracks situated in an infinitely long elastic strip. Tai and Li [1987] also derived the elastodynamic response of a finite strip with two co-planar cracks under impact loading. The solution of the mixed boundary value problem was expressed in terms of two Cauchy-type singular integral equations which were solved numerically, following a collocation scheme due to Erdogan and Gupta [1972]. A numerical Laplace transform inversion technique described by Miller and Guy [1966] are then used to obtain the solution.

In our paper, we have considered the diffraction of normally incident SH-wave by two co-planar finite rigid strips situated in an infinitely long isotropic elastic strip perpendicular to the lateral surface. The mixed boundary value problem gives rise to the determination of the solution of triple integral equations which finally have been reduced to the solution of a Fredholm integral equation of second kind. The equation has been solved numerically for low frequency range. Finally the elastodynamic stress intensity factors are obtained. The variations of the stress intensity factors at the tips of the rigid strips with variable frequency have been depicted by means of graphs.

2. FORMULATION OF THE PROBLEM

Consider an infinite long homogeneous isotropic elastic strip of width 2H containing two coplanar rigid strips embedded in it. Consider a rectangular Cartesian co-ordinate system (X,Y,Z) with origin at the centre of the elastic strip, such that the rigid strips occupy the region $-b \le X \le -a$; $a \le X \le b$, $|Y| < \infty$, $Z=0$. A time-harmonic antiplane shear wave is assumed to be incident normally on

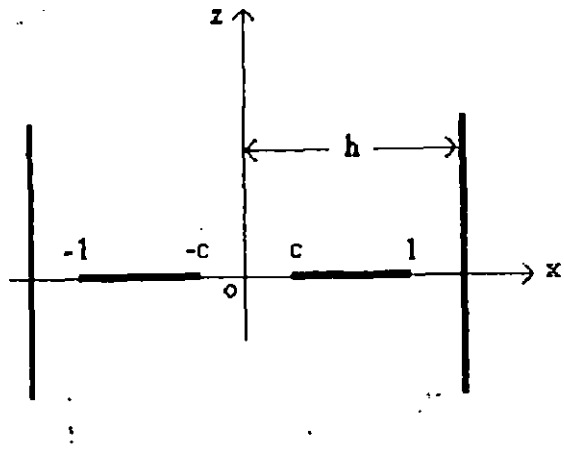

Fig.1. Geometry of the problem.

the rigid strips.

Since the non-vanishing component of displacement is only the component V, all stress components except σ_{YZ} and σ_{XY} vanish identically. Thus the problem is to find the stress distribution near the edge of strips subject to the following boundary conditions :

$$V(X,0+) = V(X,0-) = -V_0 e^{-i\omega t}; \quad a \le |X| \le b,$$

$$\sigma_{YZ}(X,0+) = \sigma_{YZ}(X,0-) = 0; \quad |X|>b, \quad |X|<a,$$

and $\sigma_{XY}(\pm h, Z) = 0.$ (2.1)

The displacement V satisfies the wave equation

$$\frac{\partial^2 V}{\partial X^2} + \frac{\partial^2 V}{\partial Y^2} = \frac{1}{C_2^2}\frac{\partial^2 V}{\partial t^2}, \tag{2.2}$$

C_2 being shear wave velocity. It is convenient to normalize all lengths with respect to b so that

$$\frac{X}{b} = x, \quad \frac{Y}{b} = y, \quad \frac{Z}{b} = z, \quad \frac{V}{b} = v, \quad \frac{V_0}{b} = v_0, \quad \frac{a}{b} = c, \quad \frac{H}{b} = h.$$

Therefore the strips are defined by $-1 \le x \le -c$, $c \le x \le 1$, $|y|<\infty$. $z=0$ (Fig.1). Supressing the time factor $e^{-i\omega t}$, the boundary conditions reduce to

$$v(x,0+) = v(x,0-) = -v_0; \quad c \le |x| \le 1,$$

$$\sigma_{yz}(x,0+) = \sigma_{yz}(x,0-) = 0; \quad |x|>1, \quad |x|<c, \tag{2.3}$$

and $\sigma_{xy}(\pm h, z) = 0.$

The scattered field v subject to the above boundary conditions should be a solution of the equation

$$\frac{\partial^2 v}{\partial x^2} + \frac{\partial^2 v}{\partial z^2} + k_2^2 v = 0 \tag{2.4}$$

where $k_2^2 = \frac{\omega^2 b^2}{c_2^2}$.

The solution of equation (2.4) can be taken as

$$v(x,z) = \int_0^\infty A(\xi) e^{-\beta|z|} \cos(\xi x)\, d\xi + \int_0^\infty B(\zeta) \cosh(\beta_1 x) \cos(\zeta z)\, d\zeta \qquad (2.5)$$

so that

$$\sigma_{yz}(x,z) = \mu\left[-\operatorname{sgn}(z) \int_0^\infty \beta A(\xi) e^{-\beta|z|} \cos(\xi x)\, d\xi - \int_0^\infty \zeta B(\zeta) \cosh(\beta_1 x) \sin(\zeta z)\, d\zeta \right], \qquad (2.6)$$

where

$$\beta = \begin{cases} \sqrt{\xi^2 - k_2^2}; & \xi > k_2, \\ -i\sqrt{k_2^2 - \xi^2}; & \xi < k_2, \end{cases} \quad \text{and} \quad \beta_1 = \begin{cases} \sqrt{\zeta^2 - k_2^2}; & \zeta > k_2, \\ -i\sqrt{k_2^2 - \zeta^2}; & \zeta < k_2, \end{cases}$$

so that

$$\beta_1 = -i\sqrt{(k_2^2 - \zeta^2)} = -i\beta_1' \quad \text{where} \quad \zeta < k_2.$$

3. DERIVATION OF INTEGRAL EQUATION

The condition of vanishing of σ_{yz} at z=0 outside the strips yields

$$\int_0^\infty \beta A(\xi) \cos(\xi x)\, d\xi = 0; \qquad |x| < c, \quad |x| > 1. \qquad (3.1)$$

Again the boundary condition $v(x,0) = -v_0$ at $c \le |x| \le 1$ gives

$$\int_0^\infty A(\xi) \cos(\xi x)\, d\xi + \int_0^\infty B(\zeta) \cosh(\beta_1 x) \cos(\zeta z)\, d\zeta = -v_0; \qquad c \le |x| \le 1. \qquad (3.2)$$

Using the boundary condition $\sigma_{xy}(\pm h, z) = 0$ one obtains

$$\int_0^\infty \beta_1 B(\zeta) \sinh(\beta_1 h) \cos(\zeta z)\, d\zeta = \int_0^\infty \xi A(\xi) e^{-\beta|z|} \sin(\xi h)\, d\xi$$

which after Fourier cosine inversion yields

$$\beta_1 B(\zeta) \sinh(\beta_1 h) = \frac{2}{\pi} \int_0^\infty \frac{\xi\beta}{\beta^2 + \zeta^2} A(\xi) \sin(\xi h)\, d\xi. \qquad (3.3)$$

Eliminating $B(\zeta)$ from equations (3.2) and (3.3) one obtains

$$\int_0^\infty A(\xi) \cos(\xi x)\, d\xi = -v_0 - \frac{2}{\pi} \int_0^\infty \frac{\cosh(\beta_1 x)}{\beta_1 \sinh(\beta_1 h)} d\zeta \int_0^\infty \frac{\xi\beta}{\beta^2 + \zeta^2} A(\xi) \sin(\xi h)\, d\xi; \qquad c \le |x| \le 1. \quad (3.4)$$

Replacing $\beta A(\xi)$ by $C(\xi)$, equations (3.1) and (3.4) become

$$\int_0^\infty C(\xi) \cos(\xi x)\, d\xi = 0; \qquad |x| < c, \quad |x| > 1 \qquad (3.5)$$

and

$$\int_0^\infty \xi^{-1}[1+H(\xi)]C(\xi)\cos(\xi x)\,d\xi = -v_0 - \frac{2}{\pi}\int_0^\infty \frac{\cosh(\beta_1 x)}{\beta_1 \sinh(\beta_1 h)}\,d\zeta \int_0^\infty \frac{\xi C(\xi)}{\beta^2+\zeta^2}\sin(\xi h)\,d\xi;\ c \le |x| \le 1, \quad (3.6)$$

where

$$H(\xi) = \left\{\frac{\xi}{\beta} - 1\right\} \to 0 \quad \text{as} \quad |\xi| \to \infty. \quad (3.7)$$

In order to solve the integral equations (3.5) and (3.6) we set

$$C(\xi) = \int_c^1 \frac{h(t^2)}{t}\{1 - \cos(\xi t)\}\,dt \quad (3.8)$$

where the unknown function $h(t^2)$ is to be determined.

Substituting $C(\xi)$ from (3.8) in equation (3.5) we note that

$$\int_0^\infty C(\xi)\cos(\xi x)\,dx = \pi \int_c^1 \frac{h(t^2)}{t}\left[\delta(x) - \frac{1}{2}\delta(x+t) - \frac{1}{2}\delta(|x-t|)\right]dt$$

so that equation (3.5) is automatically satisfied.

Again, the substitution of the value of $C(\xi)$ from (3.8) in equation (3.6) yields

$$\frac{1}{2}\int_c^1 \frac{h(t^2)}{t}\log\left|\frac{x^2-t^2}{x^2}\right|dt = -v_0 - \int_c^1 \frac{h(t^2)}{t}\,dt$$

$$\times\left[\int_{k_2}^\infty \frac{\cosh(\beta_1 x)e^{-h\beta_1}}{\beta_1 \sinh(\beta_1 h)}\{1 - \cosh(t\beta_1)\}\,d\zeta - \int_0^{k_2} \frac{\cos(\beta_1' x)\cos(\beta_1' h)}{\beta_1' \sin(\beta_1' h)}\{1 - \cos(\beta_1' t)\}\,d\zeta\right]$$

$$- \int_c^1 \frac{h(t^2)}{t}\,dt \int_0^\infty \xi^{-1}H(\xi)\cos(\xi x)\{1 - \cos(\xi t)\}\,d\xi, \qquad c \le |x| \le 1 \quad (3.9)$$

where the result

$$\int_0^\infty \frac{\cos(\xi x)\{1-\cos(\xi t)\}}{\xi}\,d\xi = \log\left|\frac{x^2-t^2}{x^2}\right|$$

has been used.

Differentiating both sides of equation (3.9) with respect to x and next multiplying by $(-2x/\pi)$, one obtains

$$\frac{2}{\pi}\int_c^1 \frac{t h(t^2)}{t^2-x^2}\,dt = \frac{2x}{\pi}\int_c^1 \frac{h(t^2)}{t}\,dt\left[\int_{k_2}^\infty \frac{\sinh(\beta_1 x)e^{-h\beta_1}}{\sinh(\beta_1 h)}\{1 - \cosh(t\beta_1)\}\,d\zeta\right.$$

$$+\int_0^{k_2}\frac{\cos(\beta_1' x)\cos(\beta_1' h)}{\sin(\beta_1' h)}\left\{1-\cos(\beta_1' t)\right\}d\zeta \;-\; \int_0^{\infty} H(\xi)\sin(\xi x)\left\{1-\cos(\xi t)\right\}d\xi\Bigg]; \quad c\le|x|\le 1. \quad (3.10)$$

It is known that using Hilbert transform technique, the solution of the integral equation (Srivastava and Lowengrue [1968])

$$\frac{2}{\pi}\int_a^b \frac{t\,h(t^2)}{t^2-y^2}dt = R(y), \quad a<y<b$$

can be obtained in the form

$$h(t^2) = -\frac{2}{\pi}\sqrt{\frac{t^2-a^2}{b^2-t^2}}\int_a^b \sqrt{\frac{b^2-y^2}{y^2-a^2}}\,\frac{yR(y)}{y^2-t^2}\,dy + \frac{D}{\sqrt{(t^2-a^2)(b^2-t^2)}} \quad (3.11)$$

with condition that R must be an even function of y so as to make integral convergent. D is an arbitrary constant.

Following (3.11), the solution of equation (3.10) is given by

$$h(u^2) + \int_c^1 \frac{h(t^2)}{t}\left\{K_1(u^2,t^2)+K_2(u^2,t^2)\right\}dt = \frac{D}{\sqrt{(u^2-c^2)(1-u^2)}} \quad (3.12)$$

where

$$K_1(u^2,t^2) = -\frac{4}{\pi^2}\sqrt{\frac{u^2-c^2}{1-u^2}}\int_c^1 \sqrt{\frac{1-x^2}{x^2-c^2}}\,\frac{x^2\,dx}{x^2-u^2}$$

$$\times\left[\int_{k_2}^{\infty}\frac{\cosh(\beta_1 x)e^{-h\beta_1}}{\sinh(\beta_1 h)}\left\{1-\cos(t\beta_1)\right\}d\zeta + \int_0^{k_2}\frac{\cos(\beta_1' x)\cos(\beta_1' h)}{\sin(\beta_1' h)}\left\{1-\cos(\beta_1' t)\right\}d\zeta\right] \quad (3.13)$$

and

$$K_2(u^2,t^2) = +\frac{4}{\pi^2}\sqrt{\frac{u^2-c^2}{1-u^2}}\int_c^1 \sqrt{\frac{1-x^2}{x^2-c^2}}\,\frac{x^2\,dx}{x^2-u^2}\int_0^{\infty} H(\xi)\sin(\xi x)\left\{1-\cos(\xi t)\right\}d\xi. \quad (3.14)$$

In order to determine the arbitrary constant D, equation (3.9) is multiplied by $\frac{x}{\sqrt{(x^2-c^2)(1-x^2)}}$ and integrated from c to 1 with respect to x, and using the result

$$\int_c^1 \frac{x\log|1-t^2/x^2|}{\sqrt{(x^2-c^2)(1-x^2)}}dx = \frac{\pi}{2}\log\left|\frac{1-c}{1+c}\right|$$

we finally obtain

$$\int_c^1 \frac{h(u^2)}{u}du = -\frac{2v_0}{\log\left|\frac{1-c}{1+c}\right|} - \frac{4}{\pi\log\left|\frac{1-c}{1+c}\right|}\int_c^1 \frac{h(t^2)}{t}dt$$

$$\times \int_c^1 \frac{x}{\sqrt{(x^2-c^2)(1-x^2)}}\left[A_1(x,t^2)+A_2(x,t^2)\right]dx \qquad (3.15)$$

where

$$A_1(x,t^2) = \int_{k_2}^{\infty} \frac{\cosh(\beta_1 x)\, e^{-h\beta_1}}{\beta_1 \sinh(\beta_1 h)}\left\{1-\cosh(t\beta_1)\right\}d\zeta$$

$$- \int_0^{k_2} \frac{\cos(\beta_1' x)\cos(\beta_1' h)}{\beta_1' \sin(\beta_1' h)}\left\{1-\cos(\beta_1' t)\right\}d\zeta, \qquad (3.16)$$

$$A_2(x,t^2) = \int_0^{\infty} \xi^{-1} H(\xi)\cos(\xi x)\{1-\cos(\xi t)\}d\zeta$$

$$= \frac{1}{2}\log\left|\frac{x^2-t^2}{x^2}\right| - \frac{\pi i}{2}H_0^{(1)}(xk_2) + \frac{\pi i}{4}H_0^{(1)}\{(x+t)k_2\} + \frac{\pi i}{4}H_0^{(1)}\{|x-t|k_2\}. \qquad (3.17)$$

Again, by substituting $h(u^2)$ from equation (3.12) in the left-hand side of equation (3.15) and simplifying, one obtains

$$D = -\frac{2v_0 c}{\pi \log\left|\frac{1-c}{1+c}\right|} - \frac{8c}{\pi^2 \log\left|\frac{1-c}{1+c}\right|}\int_c^1 \frac{h(t^2)}{t}dt$$

$$\times \int_c^1 \frac{x}{\sqrt{(x^2-c^2)(1-x^2)}}\left[A_1(x,t^2)+A_2(x,t^2)\right]dx$$

$$+ \frac{2c}{\pi}\int_c^1 \frac{h(t^2)}{t}dt \int_c^1 \frac{1}{u}\left\{K_1(u^2,t^2)+K_2(u^2,t^2)\right\}du. \qquad (3.18)$$

Eliminating D from equations (3.12) and (3.18) and simplifying on obtains

$$\sqrt{(u^2-c^2)(1-u^2)}\,h(u^2) + \int_c^1 \frac{h(t^2)}{t} + \left[K_a(u^2,t^2)+K_b(u^2,t^2)\right]dt = -\frac{4v_0 c}{\pi \log\left|\frac{1-c}{1+c}\right|} \qquad (3.19)$$

where

$$K_a(u^2,t^2) = -\frac{4}{\pi^2}(u^2-c^2)\int_c^1 \sqrt{\frac{1-x^2}{x^2-c^2}}\frac{x^2}{x^2-u^2}dx\left[\frac{\partial}{\partial x}\left\{A_1(x,t^2)+A_2(x,t^2)\right\}\right], \qquad (3.20)$$

$$K_b(u^2,t^2) = \frac{8c}{\pi^2 \log\left|\frac{1-c}{1+c}\right|} \int_c^1 \frac{x}{\sqrt{(x^2-c^2)(1-x^2)}}\left[A_1(x,t^2)+A_2(x,t^2)\right]dx, \tag{3.21}$$

$$K_c(u^2,t^2) = -\frac{4c^2}{\pi^2}\int_c^1 \sqrt{\frac{1-x^2}{x^2-c^2}}\left[\frac{\partial}{\partial x}\left\{A_1(x,t^2)+A_2(x,t^2)\right\}\right]dx. \tag{3.22}$$

Next for further simplification we put

$$\sqrt{(u^2-c^2)(1-u^2)}\; h(u^2) = H(u^2)$$

and make the substitution

$$u^2 = c^2\cos^2\phi + \sin^2\phi \quad \text{and} \quad t^2 = c^2\cos^2\theta + \sin^2\theta$$

in equation (3.19) which then reduces to the form

$$G(\phi) + \int_0^{\pi/2} \frac{G(\theta)}{c^2\cos^2\theta + \sin^2\theta}\left[K_a'(\phi,\theta) + K_b'(\phi,\theta) + K_c'(\phi,\theta)\right]d\theta$$

$$= -\frac{4v_0 c}{\pi \log\left|\frac{1-c}{1+c}\right|} \tag{3.23}$$

where

$$G(\phi) = H(c^2\cos^2\phi + \sin^2\phi), \tag{3.24}$$

$$G(\theta) = H(c^2\cos^2\theta + \sin^2\theta), \tag{3.25}$$

$$K_a'(\phi,\theta) = K_a(c^2\cos^2\phi+\sin^2\phi\,,\, c^2\cos^2\theta+\sin^2\theta), \tag{3.26}$$

$$K_b'(\phi,\theta) = K_b(c^2\cos^2\phi+\sin^2\phi\,,\, c^2\cos^2\theta+\sin^2\theta), \tag{3.27}$$

$$K_c'(\phi,\theta) = K_c(c^2\cos^2\phi+\sin^2\phi\,,\, c^2\cos^2\theta+\sin^2\theta). \tag{3.28}$$

4. STRESS INTENSITY FACTOR

From equation (2.6) for $z \to 0$, $c \le |x| < 1$, one obtains

$$\sigma_{yz}(x,0\pm) = \mp\,\mu \int_0^\infty \beta A(\xi)\cos(\xi x)\,d\xi.$$

It is useful to determine the difference of the stress components on the lower and upper

surfaces of the strips. We put

$$\Delta\sigma_{yz}(x,0) = \sigma_{yz}(x,0+) - \sigma_{yz}(x,0-);$$

then

$$\Delta\sigma_{yz}(x,0) = -2\mu \int_0^\infty C(\xi)\cos(\xi x)\,d\xi, \qquad c<|x|<1.$$

Substituting the value of $C(\xi)$ and next changing the order of integration and integrating, one obtains

$$\Delta\sigma_{yz}(x,0) = \frac{\mu\pi h(x^2)}{x}. \tag{4.1}$$

Since

$$h(x^2) = \sqrt{(x^2-c^2)(1-x^2)}\,H(x^2)$$

and $x^2 = c^2\cos^2\phi + \sin^2\phi,$

and hence equation (4.1) becomes

$$\Delta\sigma_{yz}(x,0) = \frac{\mu\pi G(\phi)}{x\sqrt{(x^2-c^2)(1-x^2)}}. \tag{4.2}$$

So the stress intensity factors N_c and N_1 at the two tips of the strip can be expressed as

$$N_c = \underset{x\to c+}{Lt}\left[\frac{\Delta\sigma_{yz}(x,0)}{\mu\pi}\sqrt{(x-c)}\right] \tag{4.3}$$

and

$$N_1 = \underset{x\to 1-}{Lt}\left[\frac{\Delta\sigma_{yz}(x,0)}{\mu\pi}\sqrt{(1-x)}\right]. \tag{4.4}$$

With the aid of equation (4.2) one obtains

$$N_c = \frac{G(0)}{c\sqrt{2c(1-c^2)}} \Rightarrow G(0) = c\sqrt{2c(1-c^2)}\,N_c \tag{4.5}$$

and

$$N_1 = \frac{G(\pi/2)}{c\sqrt{2(1-c^2)}} \Rightarrow G(\pi/2) = \sqrt{2(1-c^2)}\,N_1. \tag{4.6}$$

Making c tend to zero, the two strips merge into one and in that case

$$N_1 = \frac{1}{\sqrt{2}}G(\pi/2).$$

5. RESULTS AND DISCUSSIONS

The numerical calculations have been carried out for the determination of stress intensity factors for different values of the dimensionless frequency k_2 within the range 0.1 to 0.8. The integrals $A_1(x,t^2)$ and $A_2(x,t^2)$ given by (3.16) and (3.17), respectively, appearing in the kernel of integral equation (3.23) have been evaluated using the Gauss quadrature formula. Following Fox and Goodwin [1953], the solution of integral equation (3.23) has been obtained by converting it into a system of linear algebraic equations. Substituting these values of $[G(\phi)]$ in equations (4.3) and (4.4), the stress intensity factors N_c and N_1 at the inner and outer tips, respectively, of the rigid strips have been found to be related with $G(0)$ and $G(\pi/2)$ through the relations (4.5) and (4.6). The amplitudes $|G(0)|$ and $|G(\pi/2)|$ have been plotted against k_2 with different values of h for c=0.2, 0.4, 0.6; the values chosen for k_2 range from 0.1 to 0.8, at step of 0.05.

From the graphs it can be concluded that for fixed values of h, the stress intensity factor near the inner tip of the rigid strip decreases with the increase in the values of frequency within the range 0.1 to 0.8 (Figs. 2, 4 and 6), and for fixed values of h the stress intensity factor near the outer tip of the rigid strip at first decreases, attains a minimum and then it gradually increases with the increase in the values of frequency within the range 0.1 to 0.8 (Figs. 3, 5 and 7) for different values of c (c=0.2, 0.4 and 0.6).

It is interesting to note that for different values of k_2 within the range 0.1 to 0.8, the stress intensity factor of the inner tip of the strips, for a given value of k_2, increases with the increase in the values of h, whereas the stress intensity factor at the outer tip of strips, within the given range of values of k_2, decreases with the increase in the values of h for small values of k_2 but shows the reverse character for higher values of k_2 for any given value of the parameter c.

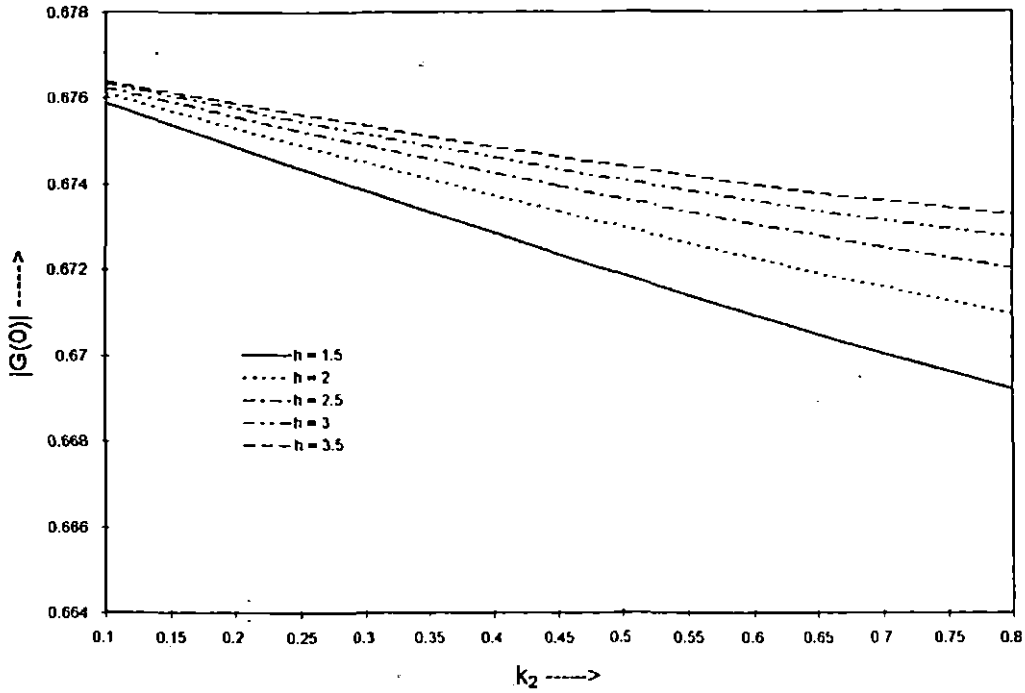

Fig.2. Amplitude of |G(0)| plotted against dimensionless frequency k_2 for c=0.2.

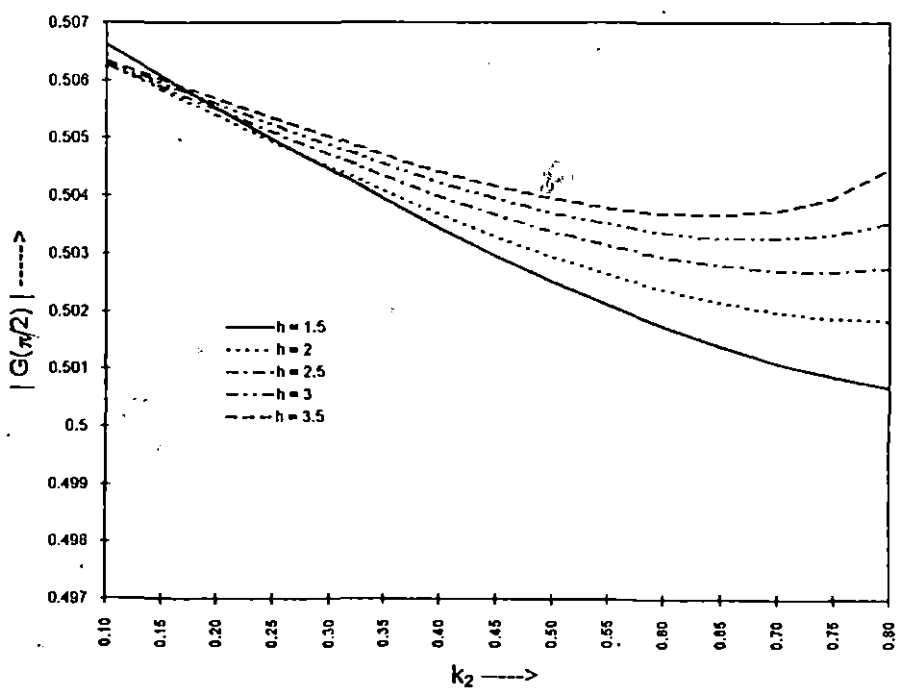

Fig.3. Amplitude of |G(π/2)| plotted against dimensionless frequency k_2 for c=0.2.

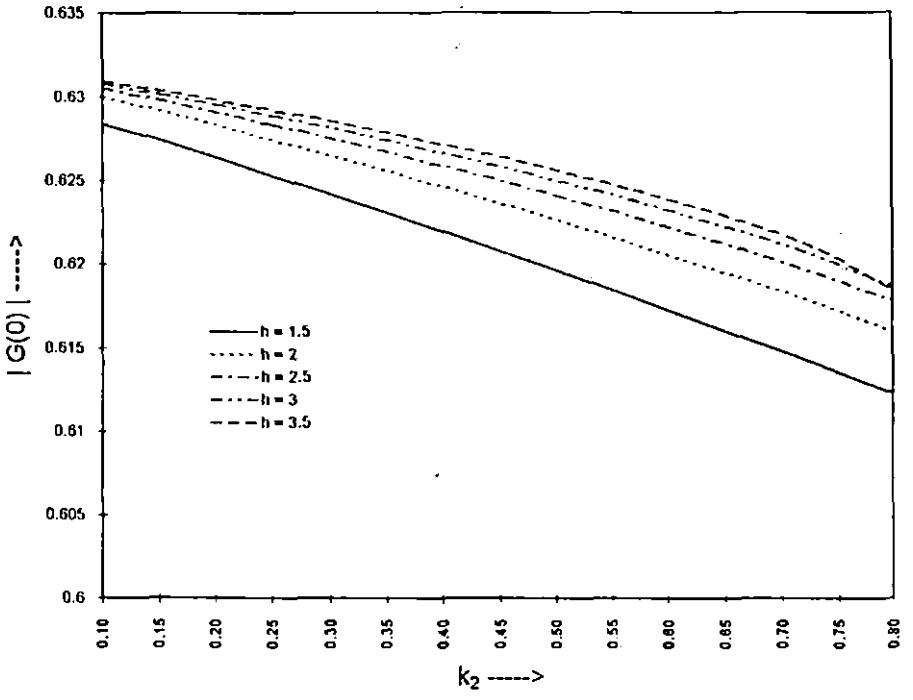
0.635
0.63
0.625
0.62
0.615
0.61
0.605
0.6
| G(0) | ----->
h = 1.5
h = 2
h = 2.5
h = 3
h = 3.5
0.10
0.15
0.20
0.25
0.30
0.35
0.40
0.45
0.50
0.55
0.60
0.65
0.70
0.75
0.80
k2 ----->
1.1
1.095
1.09
1.085
1.08
1.075
1.07
1.065
1.06
|G(π/2)| ----->
h = 1.5
h = 2
h = 2.5
h = 3
h = 3.5
0.10
0.15
0.20
0.25
0.30
0.35
0.40
0.45
0.50
0.55
0.60
0.65
0.70
0.75
0.80
K2 ----->
Fig.4. Amplitude of |G(0)| plotted against dimensionless frequency k2 for c=0.4.
Fig.5. Amplitude of |G(π/2)| plotted against dimensionless frequency k2 for c=0.4.

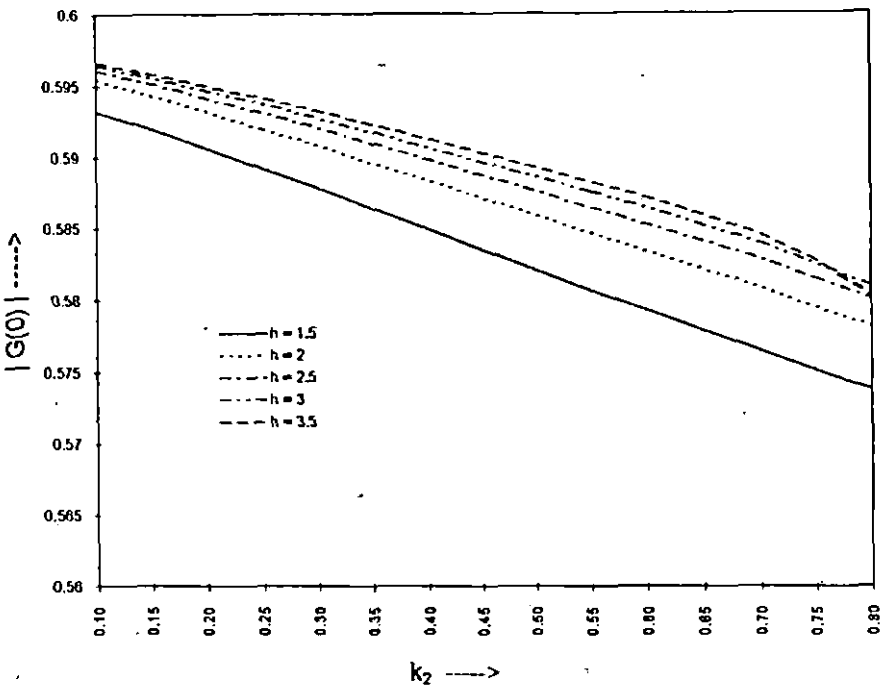

Fig.6. Amplitude of |G(0)| plotted against dimensionless frequency k_2 for c=0.6.

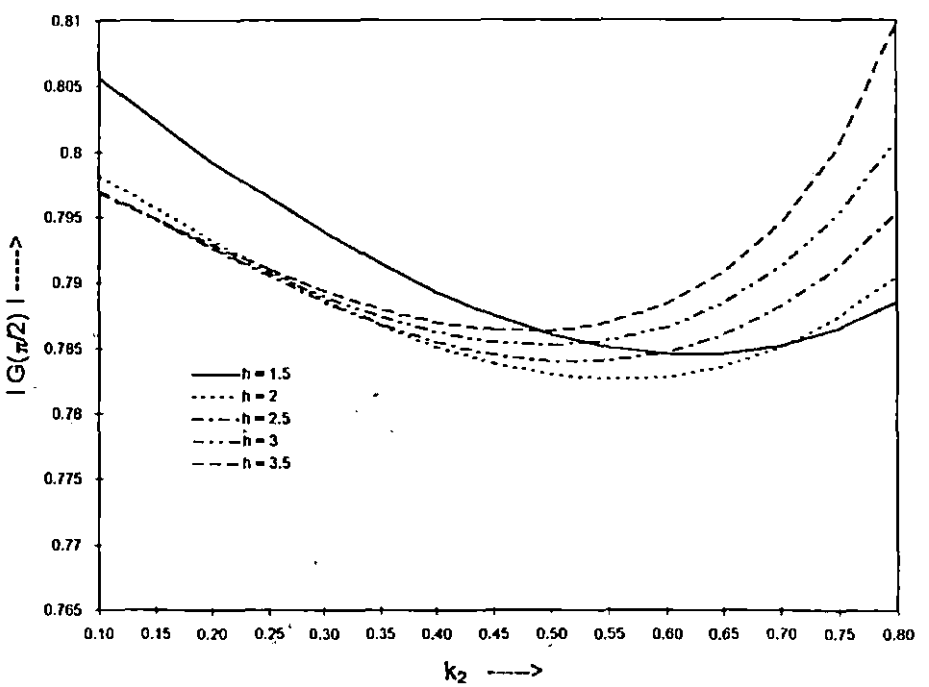

Fig.7. Amplitude of |G(π/2)| plotted against dimensionless frequency k_2 for c=0.6.

CHAPTER - 3

SCATTERING OF WAVES

[5]HIGH FREQUENCY SOLUTION OF ELASTODYNAMIC STRESS INTENSITY FACTORS DUE TO THE DIFFRACTION OF PLANE LONGITUDINAL WAVE BY AN EDGE CRACK IN A SEMI-INFINITE MEDIUM

1. INTRODUCTION

The problem of scattering of elastic waves by a surface breaking crack is of considerable importance in a variety of engineering applications. In fracture mechanics, the interest is in the determination of the stress field near the crack tip as a prerequisite to the study of crack propagation under dynamic loading.

Elastodynamic analysis of an edge crack has been done by Achenbach et al [1980] when the cracked half plane is subjected to time harmonic line load applied to its free surface. Stress intensity factors for three dimensional dynamic loading of a cracked half space has also been studied by Angel and Achenbach [1985]. Low frequency solution of the scattering of SH-wave by an inclined edge crack in a semi-infinite medium was studied by Dutta [1979] using the method of matched asymptotic expansion. The problem of anti-plane shear waves by an edge crack was studied by Stone et al [1980]. Scattering of body waves by an inclined surface breaking crack has also been studied by Zhang and Achenbach [1988] using Boundary Integral Equation method. Detailed discussion on the problems of fracture mechanics can be found in the books of Freund [1990], Brock [1986] and Cherepanov [1979].

In the present paper, the problem of the determination of the high frequency solution of

---

[5] **Communicated to The Journal of Technical Physics, 2000.**

elastodynamic stress intensity factor due to the incidence of a time harmonic plane longitudinal wave in the presence of a vertical edge crack in a semi-infinite medium has been studied. The solution of the diffraction problem is complicated by the presence of the free surface of the medium in addition to the crack surface and the associated sharp corners. The resulting boundary value problem for the cracked half-plane is decomposed into two problems for the quarter plane, which represent the symmetric and antisymmetric motions relative to the plane of the crack, respectively.

The plane longitudinal wave, when incident on the free surface of the semi-infinite medium, gives rise to reflected longitudinal and shear waves. These body waves are broken up into symmetric and antisymmetric parts with respect to the plane of the crack. In both the symmetric and antisymmetric motion, firstly, assuming the free surface of the semi-infinite medium to be absent, body waves are assumed to be incident on the semi-infinite crack. Using Wiener-Hopf technique, diffracted field arising from the tip of the crack consisting of both the body waves and Rayleigh surface wave moving along the surface of the crack are obtained. For high frequency, body waves after a few wave lengths are found to be insignificant so that important part of the diffracted field which reaches the corner of the 90^0 wedge formed by the plane free surface and the surface of the crack is Rayleigh wave. The Rayleigh wave on reaching the corner of the wedge is reflected back as Rayleigh wave, the reflection coefficient being given by Li et al [1992]. Diffracted body waves from the corner of the wedge being again insignificant after a few wave lengths may be neglected for high frequency solution. This reflected Rayleigh wave on reaching the crack tip again gives rise to diffracted Rayleigh wave which reaches the corner of the wedge and is again reflected back. This process of reflection of Rayleigh wave from the corner and subsequent diffraction from the edge of the crack tip continues. Using Wiener-Hopf technique, stress components just ahead of the crack tip

due to the incidence of body waves and all the reflected Rayleigh waves on the crack tip have been obtained. The expression for the resulting stress intensity factors have been determined. The dependence of the stress intensity factors on the frequency and on the angle of incidence has been depicted by means of graphs.

2. FORMULATION OF THE PROBLEM AND ITS SOLUTION

Let us consider a plane harmonic compressional (P-) wave of frequency ω to be incident on an edge crack of length h located at right angles to the free surface of an homogeneous isotropic semi-infinite medium. The x-axis is taken along the free surface and y-axis along the direction of the crack as shown in Fig.1.

In the absence of the crack, the free surface of the medium would give rise to the reflected plane (P) and inplane shear (SV) waves. Let the three waves be represented by the Stokes-Helmholtz potentials $e^{-i\omega t}\,\phi_I$, $e^{-i\omega t}\,\phi_R$ and $e^{-i\omega t}\,\psi_R$ respectively. Then

$$\begin{aligned}
\phi_I &= A_0 \exp\left[-ik_1(x\sin\theta_1 + y\cos\theta_1)\right] \\
\phi_R &= A_R \exp\left[-ik_1(x\sin\theta_1 - y\cos\theta_1)\right] \\
\psi_R &= B_R \exp\left[-ik_2(x\sin\theta_2 - y\cos\theta_2)\right]
\end{aligned} \tag{1}$$

where θ_1 is the angle of incidence, A_0 the amplitude of the incident wave, k_1, k_2 are the P and S wave numbers respectively related to their phase velocities c_1, c_2 through $k_1 = \omega/c_1$ and $k_2 = \omega/c_2$. The remaining quantities in (1) are given by the laws of reflection of elastic waves as

$$k_1 \sin\theta_1 = k_2 \sin\theta_2 \qquad \text{(Snell's law)}$$

$$\frac{A_R}{A_0} = \frac{(\sin 2\theta_2 \sin 2\theta_1 - k^2 \cos^2 2\theta_2)}{(\sin 2\theta_2 \sin 2\theta_1 + k^2 \cos^2 2\theta_2)}$$

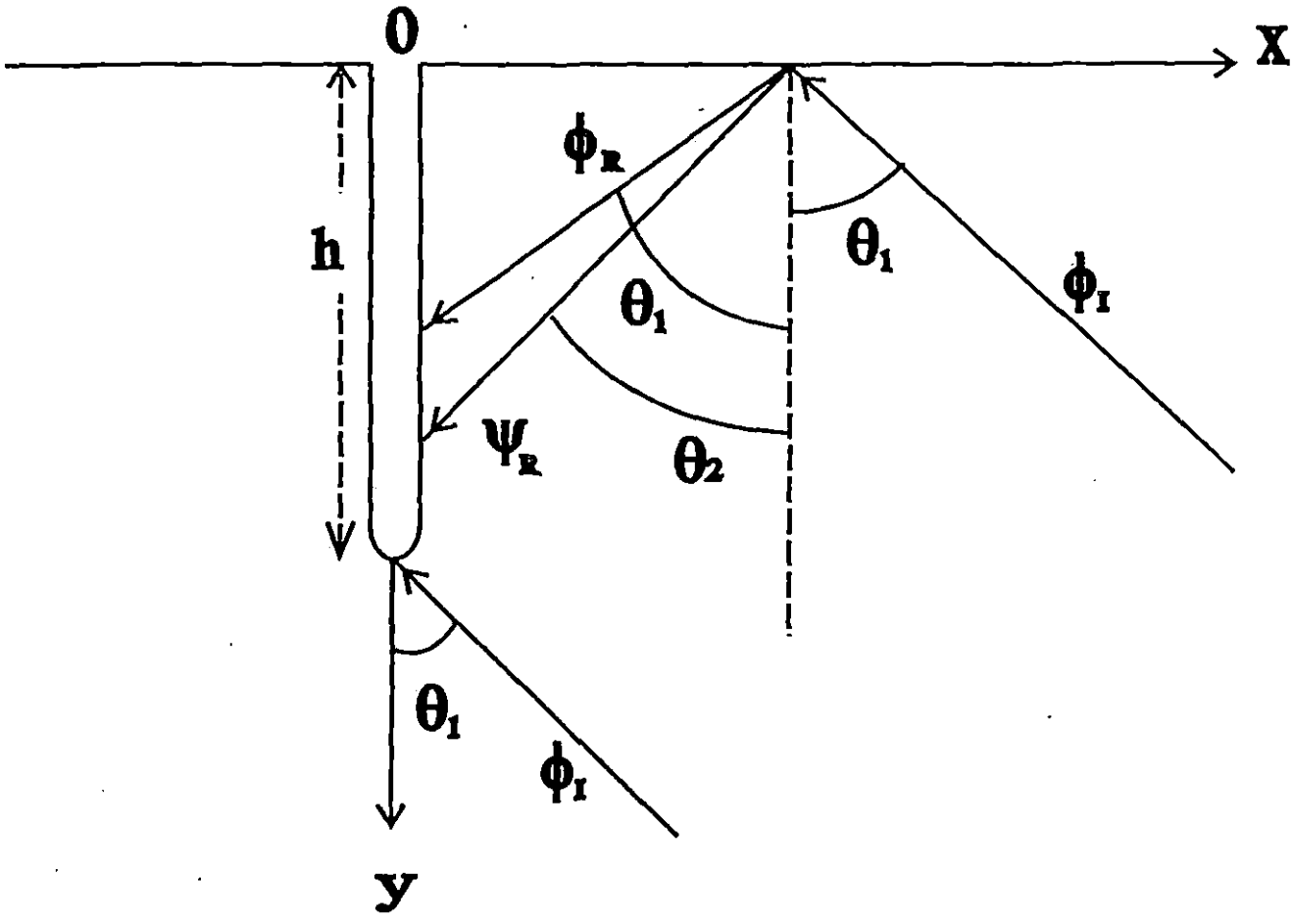

Fig.1 Geometry of the problem.

$$\frac{B_R}{A_0} = \frac{-2\cos 2\theta_2 \sin 2\theta_1}{(\sin 2\theta_2 \sin 2\theta_1 + k^2 \cos^2 2\theta_2)} \qquad (2)$$

where k^2 is the ratio of the square of longitudinal and shear wave velocities and is given by

$$k^2 = \frac{c_1^2}{c_2^2} = \frac{k_2^2}{k_1^2}.$$

We shall now determine the scattered field produced by the vertical crack when ϕ_I, ϕ_R and ψ_R are incident on it assuming for the time being that the free surface y=0 is absent.

To this end, firstly we consider the scattered field when the longitudinal wave given by

$$\phi_I = A_0 \exp\left[-ik_1(x\sin\theta_1 + y\cos\theta_1)\right]$$

is incident on a semi-infinite crack in an infinite medium. The crack is on the y-axis extending from y=-∞ to y=h. The diffrection of elastic waves by a semi-infinite crack in an infinite medium has been studied by Maue [1953], De-Hoop [1958] and also by Achenbach [1975] using Wiener-Hopf technique.

We write ϕ_I in the form $\phi_I = \phi_{Ie} + \phi_{Io}$ where

$$\phi_{Ie} = A_0 \exp(-ik_1 y\cos\theta_1)\cos(k_1 x\sin\theta_1)$$

$$\phi_{Io} = -iA_0 \exp(-ik_1 y\cos\theta_1)\sin(k_1 x\sin\theta_1). \qquad (3)$$

Clearly ϕ_{Ie} is even in x and ϕ_{Io} is odd in x.

Symmetric problem :

Now consider the interaction of the field given by ϕ_{Ie} with the semi-infinite crack. If $\phi^{(1)}$ and $\psi^{(1)}$ be the displacement potentials of the scattered field due to the incidence of ϕ_{Ie} on the semi-infinite crack, then the displacement components corresponding to the scattered field are

$$u_1^{(e)} = \frac{\partial\phi^{(1)}}{\partial x} + \frac{\partial\psi^{(1)}}{\partial y} \quad \text{and} \quad u_2^{(e)} = \frac{\partial\phi^{(1)}}{\partial y} - \frac{\partial\psi^{(1)}}{\partial x}.$$

From the geometry, it follows that in this symmetric problem $\phi^{(1)}$, $u_2^{(e)}$ and the stress components τ_{11}, τ_{22} are even functions in x while $\psi^{(1)}$, $u_1^{(e)}$ and τ_{12} are odd functions in x. Thus the

boundary conditions satisfied by the scattered field due to the incidence of ϕ_{Ie} are

$u_1^{(e)} = 0; \quad y>h, \quad x=0$ (i)

$\tau_{12} = 0; \quad -\infty<y<\infty, \quad x=0$ (ii)

$$\tau_{11} = A_0\rho\omega^2\left[1 - \frac{2c_2^2\cos^2\theta_1}{c_1^2}\right]\exp(-ik_1 y\cos\theta_1); \quad y<h, \quad x=0. \qquad \text{(iii)}$$

Introducing Fourier transform defined by

$$\bar{\phi}^{(1)}(x,\alpha) = \frac{1}{\sqrt{2\pi}}\int_{-\infty}^{\infty}\phi^{(1)}(x,y)e^{i\alpha y}\,dy \qquad (4)$$

we have

$$\bar{\phi}^{(1)} = Ae^{-\gamma_1 x} \text{ and } \quad \bar{\psi}^{(1)} = Be^{-\gamma_2 x} \quad \text{for } x\geq 0 \qquad (5)$$

where $$\gamma_j = \sqrt{\alpha^2 - k_j^2}; \quad j=1,2. \qquad (6)$$

Branches of γ_j are chosen such that $Re\gamma_1>0$ and $Re\gamma_2>0$ for $Im(-k_1)<Im(\alpha)<Im(k_1)$.

The boundary conditions (i)-(iii) now become

$$-\gamma_1 A - i\alpha B = \frac{e^{i\alpha h}}{\sqrt{2\pi}}\int_{-\infty}^{h} u_1^{(e)}(0+,y)e^{i\alpha(y-h)}dy = e^{i\alpha h}U_-(\alpha) \qquad (7)$$

$$B(\alpha^2 - k_2^2/2) - i\alpha\gamma_1 A = 0 \qquad (8)$$

and

$$2\rho c_2^2\left[(\alpha_2 - k_2^2/2)A + i\alpha\gamma_2 B\right]$$

$$= \frac{e^{i\alpha h}}{\sqrt{2\pi}}\int_{h}^{\infty}\tau_{11}(0+,y)e^{i\alpha(y-h)}dy + A_0\rho\omega^2\left(1 - \frac{2c_2^2\cos^2\theta_1}{c_1^2}\right)\times\frac{1}{\sqrt{2\pi}}\int_{-\infty}^{h}e^{iy(\alpha-k_1\cos\theta_1)}dy$$

$$= e^{i\alpha h}G_+(\alpha) + \frac{A_0\rho\omega^2}{\sqrt{2\pi}}\left(1 - \frac{2c_2^2\cos^2\theta_1}{c_1^2}\right)\frac{e^{ih(\alpha-k_1\cos\theta_1)}}{i(\alpha-k_1\cos\theta_1)}; \quad Im(\alpha)<Im(k_1\cos\theta_1) \qquad (9)$$

where

$$U_-(\alpha) = \frac{1}{\sqrt{2\pi}}\int_{-\infty}^{h}u_1^{(e)}(0+,y)e^{i\alpha(y-h)}dy$$

and $$G_+(\alpha) = \frac{1}{\sqrt{2\pi}} \int_h^\infty \tau_{11}(0+,y) e^{i\alpha(y-h)} dy. \tag{10}$$

Eliminating A and B from equation (7), (8) and (9) one obtains the Wiener-Hopf equation

$$CK_2(\alpha)U_-(\alpha) + G_+(\alpha) = \frac{Be^{-i\alpha_0 h}}{(\alpha - \alpha_0)} \tag{11}$$

where

$$\alpha_0 = k_1 \cos\theta_1; \quad C = \frac{2\rho c_2^2 (k_2^2 - k_1^2)}{k_2^2}; \quad B = -\frac{iA_0 \rho k_1^2 \left[2c_2^2 \cos^2\theta_1 - c_1^2\right]}{\sqrt{2\pi}} \tag{12}$$

and $$K_j(\alpha) = \frac{2\sqrt{(\alpha^2 - k_j^2)}}{(k_2^2 - k_1^2)} \left[\alpha^2 - \frac{(\alpha^2 - k_2^2/2)^2}{\sqrt{(\alpha^2 - k_1^2)}\sqrt{(\alpha^2 - k_2^2)}} \right] = \sqrt{(\alpha^2 - k_j^2)} R(\alpha), \quad j=1,2. \tag{13}$$

Following Chang [1971], it can be shown that

$$K_{j\pm}(\alpha) = \sqrt{(\alpha \pm k_j)}\, R_\pm(\alpha) \tag{14}$$

where

$$R_\pm(\alpha) = \frac{(\alpha \pm k_r)}{(\alpha \pm k_2)} \exp\left[\frac{1}{\pi} \int_{k_1}^{k_2} \tan^{-1}\{f(s)\} \frac{ds}{(s \pm \alpha)} \right] \tag{15}$$

with

$$f(s) = \frac{(k_2^2/2 - s^2)^2}{s^2 \sqrt{s^2 - k_1^2}\sqrt{k_2^2 - s^2}} \tag{16}$$

where $K_+(\alpha)$ and $K_-(\alpha)$ are analytic in upper and lower half of the complex α-plane and k_r is the root of Rayleigh wave equation $R(\alpha)=0$.

By the usual Wiener-Hopf argument, equation (11) subsequently yields

$$G_+(\alpha) = \frac{Be^{-i\alpha_0 h} K_{2+}(\alpha)}{(\alpha - \alpha_0)} \left[\frac{1}{K_{2+}(\alpha)} - \frac{1}{K_{2+}(\alpha_0)} \right] \tag{17}$$

$$U_-(\alpha) = \frac{Be^{-i\alpha_0 h}}{C(\alpha - \alpha_0) K_{2+}(\alpha_0) K_{2-}(\alpha)}; \quad \mathrm{Im}(\alpha) < \mathrm{Im}(\alpha_0). \tag{18}$$

In order to determine the value of τ_{11} just ahead of crack tip, we need the form of $G_+(\alpha)$ as $\alpha \to \infty$.

Using the fact that $K_{2+}(\alpha) \to \alpha^{1/2}$ as $|\alpha| \to \infty$, we obtain from equation (17)

$$G_+(\alpha) = E\alpha^{-1/2}, \text{ as } |\alpha| \to \infty, \ -\pi/2 < \arg\alpha < 3\pi/2$$

where $E = -\dfrac{Be^{-i\alpha_0 h}}{K_{2+}(\alpha_0)}$.

Taking Fourier inversion, we obtain

$$\left[\tau_{11}(0+,y)\right]_{y-h+0} = \frac{E}{\sqrt{2\pi}} \int_{-\infty+ic_1}^{\infty+ic_1} \frac{e^{-i\alpha(y-h)}}{\sqrt{\alpha}}\, d\alpha. \tag{19}$$

Here $\alpha=0$ is the branch point. We draw a cut from $\alpha=0$ along negative imaginary axis. The line of integration is deformed into a loop round the branch cut as shown in Fig.2.

So equation (19) reduces to

$$\left[\tau_{11}(0+,y)\right]_{y-h+0} = \frac{E(1-i)}{\sqrt{\pi}} \int_0^{\infty} \frac{e^{-\beta(y-h)}}{\sqrt{\beta}}\, d\beta = \frac{(i-1)Be^{-i\alpha_0 h}}{K_{2+}(\alpha_0)\sqrt{(y-h)}}. \tag{20}$$

Next, in order to determine the scattered field of displacement due to the incidence of ϕ_{Ie} on the semi-infinite crack we consider equation (18) which yields

$$u_1^{(e)}(0+,y) = \frac{Be^{-i\alpha_0 h}}{\sqrt{2\pi}CK_{2+}(\alpha_0)} \int_{-\infty+ic_1}^{\infty+ic_1} \frac{e^{-i\alpha(y-h)}}{(\alpha-\alpha_0)K_{2-}(\alpha)} d\alpha; \quad \mathrm{Im}(\alpha)<\mathrm{Im}(\alpha_0)$$

where the line of integration is in the common region of regularity of $U_-(\alpha)$ and $G_+(\alpha)$. We draw cuts through k_1 and k_2 parallel to the imaginary axis in the upper half of the complex α-plane.

Taking a semi circular contour with loops round the cuts in the upper half plane as shown in Fig.3, we get (for y<h)

$$u_1^{(e)}(0+,y) = \frac{2\pi i Be^{-i\alpha_0 y}}{\sqrt{2\pi}CK_2(\alpha_0)} + \frac{2\pi i Be^{-i\alpha_0 h}\sqrt{(k_r-k_2)}e^{-ik_r(y-h)}}{\sqrt{2\pi}C(k_r-\alpha_0)K_{2+}(\alpha_0)S(k_r)} + \\ + \text{contribution from the branch line integrals} \tag{21}$$

where

$$S(k_r) = \exp\left[\frac{1}{\pi}\int_{k_1}^{k_2} \tan^{-1}\{f(s)\}\frac{ds}{(s-k_r)}\right]. \tag{22}$$

Now consider the contribution from the branch line integral along the loop L_{k_1} round the branch point $\alpha=k_1$. This is equal to

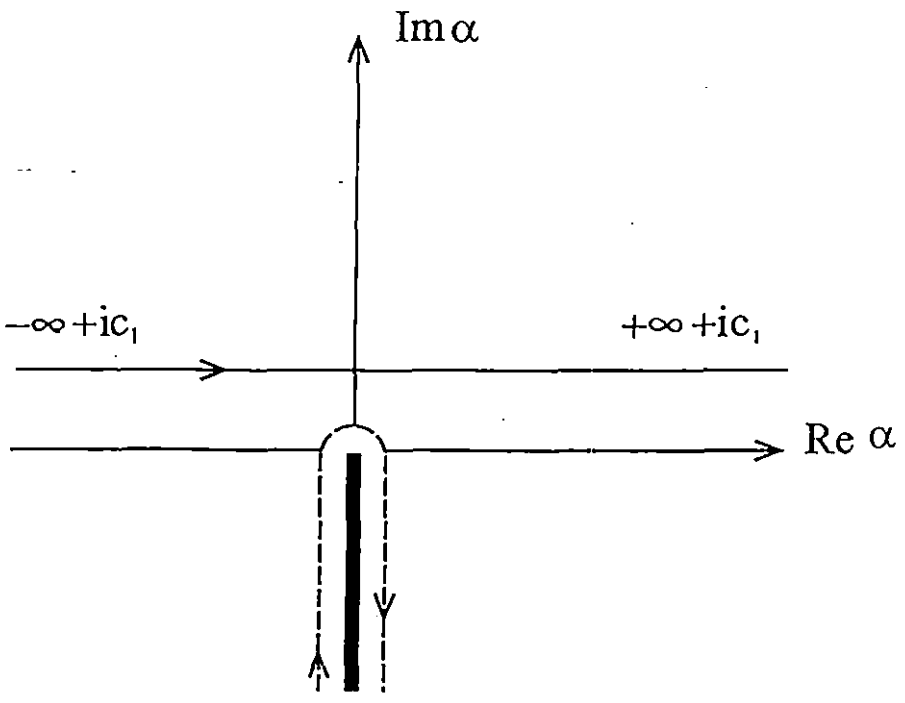

Fig.2 Path of integration.

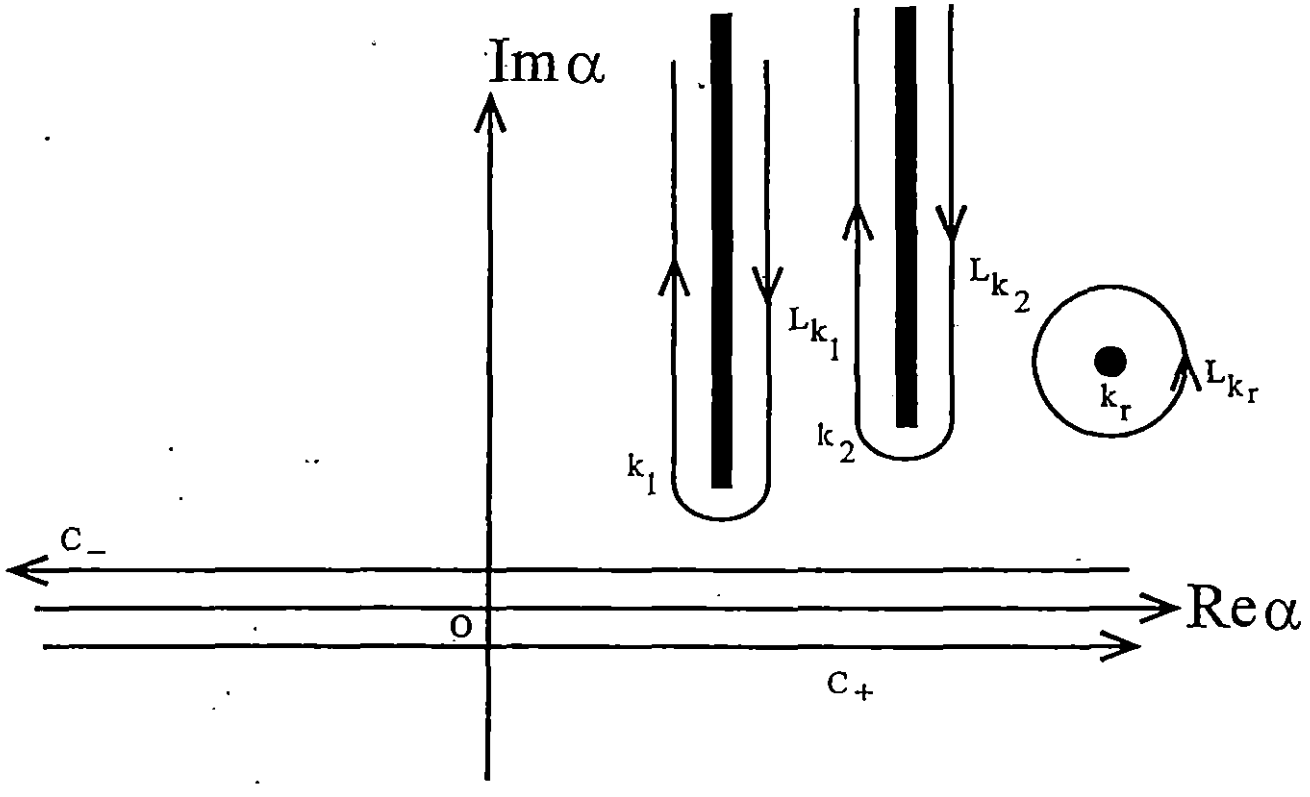

Fig.3 Region of regularity in the transformed plane.

$$\frac{Be^{-i\alpha_0 h}}{\sqrt{2\pi}CK_{2+}(\alpha_0)}\int_{L_{k_1}}\frac{e^{-i\alpha(y-h)}}{(\alpha-\alpha_0)\sqrt{(\alpha-k_2)}R_-(\alpha)}d\alpha$$

$$= \frac{Bie^{-i\alpha_0 h - ik_1(y-h)}}{\sqrt{2\pi}CK_{2+}(\alpha_0)}\int_0^\infty \frac{e^{-k_1(h-y)u}}{\sqrt{(k_2-k_1-ik_1u)}\left[u-i(1-\alpha_0/k_1)\right]R_-^{(1)}(k_1+ik_1u)}\times$$

$$\times\left[1-\frac{R_-^{(1)}(k_1+ik_1u)}{R_-^{(2)}(k_1+ik_1u)}\right]du \qquad (y<h) \qquad (24)$$

where $R_-^{(1)}(k_1+ik_1u)$ is the value of $R_-^{(1)}$ on the right hand side of the cut whereas $R_-^{(2)}(k_1+ik_1u)$ is its value on the left hand side.

If $(h-y)>0$, then for large values of $k_1(h-y)$, the main contribution to the integral (24) will be from the value of the integrand near u=0. So, for large values of $k_1(h-y)$, the integral (24) can approximately be written as

$$\frac{Bie^{-i\alpha_0 h - ik_1(y-h)}}{\sqrt{2\pi}\sqrt{(k_2-k_1)}CK_{2+}(\alpha_0)}\int_0^\infty \frac{e^{-k_1(h-y)u}}{\left[u-i(1-\alpha_0/k_1)\right]\underset{u\to 0}{Lt}\,R_-^{(1)}(k_1+ik_1u)}\times$$

$$\times \underset{u\to 0}{Lt}\left[1-\frac{R_-^{(1)}(k_1+ik_1u)}{R_-^{(2)}(k_1+ik_1u)}\right]du.$$

Now

$$R_-(k_1+ik_1u) = \frac{(k_r-k_1-ik_1u)}{(k_2-k_1-ik_1u)}\exp\left[\frac{1}{\pi}\int_{k_1}^{k_2}\tan^{-1}\{f(s)\}\frac{ds}{(s-k_1-ik_1u)}\right].$$

Integrating by parts and taking limit, we obtain

$$\underset{u\to 0}{Lt}\,R_-(k_1+ik_1u) = \frac{(k_r-k_1)e^{i\pi/4}}{C_1\sqrt{k_1(k_2-k_1)u}} \qquad (25)$$

where

$$\frac{1}{C_j} = \exp\left[-\frac{1}{\pi}\int_{k_1}^{k_2}\log(s-k_j)\frac{d}{ds}\tan^{-1}\{f(s)\}\,ds\right]; \qquad j=1,2. \qquad (26)$$

Next consider the evaluation of

$$\lim_{u\to 0}\frac{R_-^{(1)}(k_1+ik_1u)}{R_-^{(2)}(k_1+ik_1u)} = \lim_{u\to 0}\frac{R_-^{(1)}(t_2)}{R_-^{(2)}(t_1)} \qquad \text{(Say).}$$

We know

$$R_-(\alpha) = \frac{(k_r-\alpha)}{(k_2-\alpha)}\exp\left[\frac{1}{\pi}\int_{k_1}^{k_2}\tan^{-1}\{f(s)\}\frac{ds}{(s-\alpha)}\right]$$

where α is either t_1 or t_2 .

Following Chang [1971], it can be shown that $R_-(\alpha)$ can also be written as

$$R_-(\alpha) = \frac{(k_r-\alpha)}{(k_2-\alpha)}\exp\left[\frac{1}{2\pi i}\int_{L'_{k_1}+L'_{k_2}}\log\left\{1-\frac{(z^2-k_2^2/2)^2}{z^2\sqrt{z^2-k_1^2}\sqrt{z^2-k_2^2}}\right\}\frac{ds}{(s-\alpha)}\right]$$

where the paths L'_{k_1} and L'_{k_2} are shown in Fig.4.

The point t_1 and t_2 being just on opposite sides of the cut through k_1, the path L'_{k_1} is deformed so as to enclose t_2 and t_1 as shown in Fig.4.

$$\lim_{u\to 0}\frac{R_-^{(1)}(t_2)}{R_-^{(2)}(t_1)} = \exp\left[\log\left\{1-\frac{(t_2^2-k_2^2/2)^2}{t_2^2\sqrt{t_2^2-k_1^2}\sqrt{t_2^2-k_2^2}}\right\}-\log\left\{1-\frac{(t_1^2-k_2^2/2)^2}{t_1^2\sqrt{t_1^2-k_1^2}\sqrt{t_1^2-k_2^2}}\right\}\right]$$

$$= \frac{1-\sqrt{\frac{1}{u}}\dfrac{(k_1^2-k_2^2/2)^2}{(1+i)k_1^3\sqrt{k_1^2-k_2^2}}}{1+\sqrt{\frac{1}{u}}\dfrac{(k_1^2-k_2^2/2)^2}{(1+i)k_1^3\sqrt{k_1^2-k_2^2}}}$$

$$= -1+\frac{2\sqrt{u}(1-i)k_1^3\sqrt{k_2^2-k_1^2}}{(k_1^2-k_2^2/2)^2}-\ldots\ldots \qquad (27)$$

Using the results (25) and (27), the integral (24) reduces to the form

$$\frac{2BC_1e^{\pi i/4}\sqrt{k_1}e^{-i\alpha_0 h}e^{-ik_1(y-h)}}{\sqrt{2\pi}C(k_r-k_1)k_{2+}(\alpha_0)}\int_0^\infty\frac{e^{-k_1(h-y)u}\sqrt{u}}{\{u-i(1-\alpha_0/k_1)\}}du$$

$$= \frac{2BC_1e^{\pi i/4}\sqrt{k_1}e^{-i\alpha_0 h}e^{-ik_1(y-h)}}{\sqrt{2\pi}C(k_r-k_1)k_{2+}(\alpha_0)\sqrt{k_1(h-y)}}W_0\{-ik_1(h-y)(1-\cos\theta_1)\} \qquad (28)$$

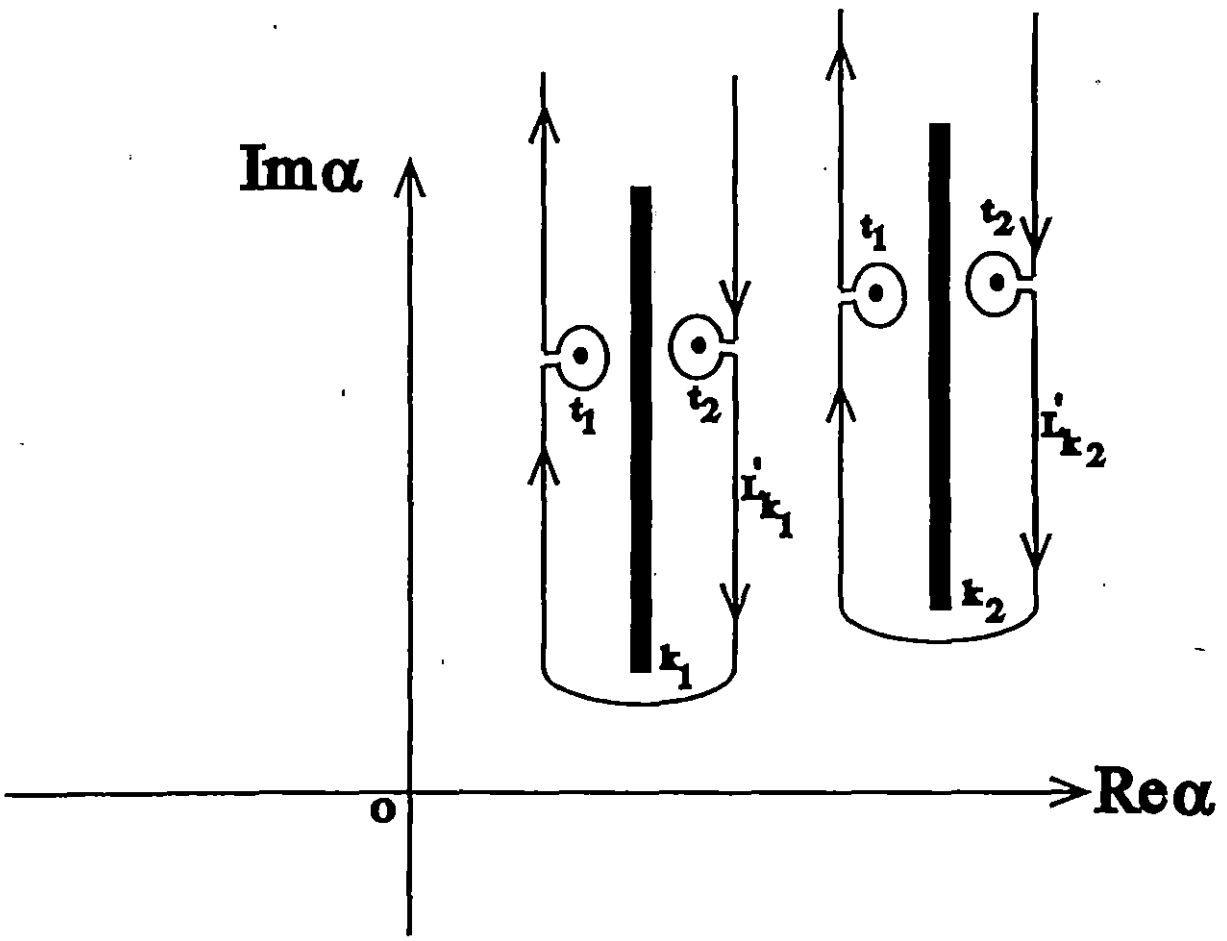

Fig.4 Deformation of the contour for the calculation of $R_{-}^{(1)}(t_2)$ and $R_{-}^{(2)}(t_1)$.

where

$$W_0(-iz) = \int_0^\infty \frac{e^{-u}\sqrt{u}}{u-iz}du = \sqrt{\pi} + 2\sqrt{\pi}ie^{-iz}\sqrt{z}\{F(\sqrt{z})\}$$

where F(y) is the Fresnel integral given by

$$F(y) = \int_y^\infty e^{iu^2}du \qquad \text{(c.f. Noble [1958]).}$$

Using the asymptotic value of

$$W_0(-iz) = \frac{\sqrt{\pi}}{-2iz} \quad \text{as} \quad |z|\to\infty$$

expression (28) becomes

$$\frac{BC_1 ie^{\pi i/4}\sqrt{k_1}e^{-i\alpha_0 h}e^{-ik_1(y-h)}}{\sqrt{2}C(k_r-k_1)k_{2+}(\alpha_0)\{k_1(h-y)\}^{3/2}(1-\cos\theta_1)} \tag{29}$$

provided $k_1(h-y)$ is large and $\cos\theta_1$ is neither equal to 1 nor nearly equal to 1.

Expression (29) is the diffracted P-wave originating from the edge of the crack due to the incidence of ϕ_{Ie}.

Next consider the contribution to $u_1^{(e)}(0+,y)$, (y<h) from the branch line integral along the loop L_{k_2} round k_2. This is equal to

$$\frac{Be^{-i\alpha_0 h}}{\sqrt{2\pi}CK_{2+}(\alpha_0)}\int_{L_{k_2}}\frac{e^{-i\alpha(y-h)}}{(\alpha-\alpha_0)\sqrt{\alpha-k_2}R_-(\alpha)}d\alpha \tag{30}$$

Using similar procedure as used while evaluating (23), it can be shown that for large value of $k_1(h-y)$, the expression (30) becomes

$$\frac{4iBC_2e^{i\pi/4}(k_2-k_1)\sqrt{k_1(k_2+k_1)}e^{-i\alpha_0 h}e^{-ik_2(y-h)}}{C(k_r-k_2)K_{2+}(\alpha_0)k_2^{3/2}\{k_1(h-y)\}^{3/2}(k_2/k_1-\cos\theta_1)}. \tag{31}$$

Therefore in the symmetric problem involving ϕ_{Ie}, the x-component of displacement $u_1^{(e)}(0+,y)$, (y<h) due to scattering by semi-infinite crack is given by

$$u_1^{(e)}(0+,y) = \frac{2\pi i B e^{-i\alpha_0 y}}{\sqrt{2\pi}\,CK_2(\alpha_0)} + \frac{2\pi i B\sqrt{k_r - k_2}\,e^{-i\alpha_0 h} e^{-ik_r(y-h)}}{\sqrt{2\pi}\,CK_{2+}(\alpha_0)(k_r-\alpha_0)\,S(k_r)} +$$

$$+ \frac{iBC_1 e^{\pi i/4}\sqrt{k_1}\,e^{-i\alpha_0 h} e^{-ik_1(y-h)}}{\sqrt{2}\,C(k_r-k_1)K_{2+}(\alpha_0)\,\{k_1(h-y)\}^{3/2}(1-\cos\theta_1)} +$$

$$+ \frac{4iBC_2 e^{i\pi/4}(k_2-k_1)\sqrt{k_1(k_2+k_1)}\,e^{-i\alpha_0 h} e^{-ik_2(y-h)}}{C(k_r-k_2)K_{2+}(\alpha_0)\,k_2^{3/2}\{k_1(h-y)\}^{3/2}(k_2/k_1-\cos\theta_1)}. \qquad (32)$$

The first term of $u_1^{(e)}(0+,y)$ in (32) arises due to the reflection of ϕ_{Ie} on the surface of the crack. The second term gives the Rayleigh wave and the last two terms are difffracted body waves due to the diffraction of ϕ_{Ie} from the edge of the crack. While evaluating body wave contribution, it has been assumed that $k_1(h-y)$ is large and that $(1 - \cos\theta_1)$ is different from zero. For $\cos\theta_1=1$, the third term of (32) giving diffracted P-wave is $O\{[k_1(h-y)]^{1/2}\}$ for large values of $[k_1(h-y)]$.

The diffracted body waves near the edge of the crack are of the same order as the Rayleigh wave terms since their joint contribution must vanish at the edge. However, at high frequencies the order of these body wave terms change to $O\{[k_1(h-y)]^{-3/2}\}$ within the distance of a few wave lengths from the edge. Therefore at distances away from the crack, the displacement on the crack surface can be approximated very well by Rayleigh wave contribution in (32) (c. f. Achenbach et al [1982])

$$u_1^{(e)}(0+,y) \approx \frac{2\pi i B e^{-i\alpha_0 y}}{\sqrt{2\pi}\,CK_2(\alpha_0)} + 2\pi i D_1 M_2 e^{-ik_r(y-h)} \qquad (33)$$

where

$$D_1 = \frac{B e^{-i\alpha_0 h}}{\sqrt{2\pi}\,CK_{2+}(\alpha_0)(k_r-\alpha_0)} \text{ and } M_j = \frac{(k_r-k_2)}{\sqrt{(k_r-k_j)}\,S(k_r)}; \quad j=1,2. \qquad (34)$$

The first term of (33) is due to the geometrical reflection of ϕ_{Ie} from the surface of the crack.

The geometrically reflected rays from the surface of the crack after striking the free surface y=0 generate reflected rays again. These reflected rays do not reach the surface of the crack and therefore do not make any new contribution to $u_1^{(e)}$ (0+,y). The second term of (33) is due to diffracted Rayleigh wave arising from the edge of the crack occuring due to the incidence of ϕ_{le} . The corresponding displacement component in the y-direction which is even in x can easily be determined and is found to be equal to

$$\frac{2\pi i D_1 M_2 (2k_r^2 - k_2^2)\, e^{-ik_r(y-h)}}{2ik_r\sqrt{(k_r^2 - k_1^2)}}. \qquad (35)$$

The Rayleigh wave with displacement components given by (35) and the second term of (33) when incident on the free surface y=0 gives rise to reflected Rayleigh wave and body waves.

The displacement on the surface of the crack arising from the reflected body waves can again be neglected as in the case of direct incidence. The reflection co-efficient of the Rayleigh waves when Rayleigh wave is incident on a wedge has been determined by Hudson and Knopoff [1964] and by Mal and Knopoff [1965] theoretically and also recently by Li, Achenbach et al [1992]. We denote the complex reflection co-efficient for a 90^0 corner by $A_r^{2\pi i\delta}$ where A_r=0.32, δ=0.106 for Poisson ratio equal to 1/4 (c. f. Li, Achenbach et al [1992]). Therefore the reflected Rayleigh wave components on the surface of the crack corresponding to the incident Rayleigh wave given by (35) and second term of (33) are

$$u_{1R}^{(e)}(0+,y) = 2\pi i D_1 M_2 A_r e^{2\pi i\delta} e^{ik_r(y+h)}$$

and

$$u_{2R}^{(e)}(0+,y) = \frac{2\pi i D_1 M_2 A_r e^{2\pi i\delta} (2k_r^2 - k_2^2) e^{ik_r(y+h)}}{2ik_r\sqrt{(k_r^2 - k_1^2)}}. \qquad (36)$$

These reflected Rayleigh waves when incident on the crack tip will again generate diffracted Rayleigh waves which can be determined by the usual Wiener-Hopf technique. While carrying out

the Wiener-Hopf procedure, it should be remembered that Rayleigh waves from the corner given by (36) which are incident on the crack tip are such that $u_{1R}^{(e)}$ is odd in x whereas $u_{2R}^{(e)}$ is even in x.

Clearly the shear stress $\tau_{12}^{(R)}$ of the first reflected Rayleigh wave given by (36) is odd in x and the stress $\tau_{11}^{(R)}(0+,y)$ for that Rayleigh wave is even in x. Since the total x-component of displacement for y>h, x=0 is zero, the scattered field due to incidence of the Rayleigh wave given by equation (36) on the crack must satisfy the boundary conditions

$$u_{1RD}(0+,y) = -2\pi i D_1 M_2 A_r e^{2\pi i\delta} e^{ik_r(y+h)}, \qquad y>h, \quad x=0 \qquad \text{(iv)}$$

$$\tau_{12}^{(1)}(0+,y) = 0; \qquad -\infty<y<\infty, \quad x=0 \qquad \text{(v)}$$

$$\tau_{11}^{(1)}(0+,y) = 0; \qquad y<h, \quad x=0. \qquad \text{(vi)}$$

where $\tau_{12}^{(1)}(0+,y)$ and $\tau_{11}^{(1)}(0+,y)$ are stresses of the scattered field due to the incidence of the Rayleigh wave given by (36) on the crack tip.

The boundary conditions yield the Wiener-Hopf equation

$$G_{1+}(\alpha) = -CK_2(\alpha)\left[U_{1-}(\alpha) + \frac{\sqrt{2\pi}\, D_1 M_2 A_r e^{2\pi i\delta} e^{2ik_r h}}{(\alpha + k_r)}\right] \qquad (37)$$

where

$$G_{1+}(\alpha) = \frac{1}{\sqrt{2\pi}} \int_h^\infty \tau_{11}^{(1)}(0+,y)\, e^{i\alpha(y-h)} dy$$

$$U_{1-}(\alpha) = \frac{1}{\sqrt{2\pi}} \int_{-\infty}^h U_{1RD}(0+,y)\, e^{i\alpha(y-h)} dy. \qquad (38)$$

By the usual Wiener-Hopf argument, equation (37) subsequently yields

$$\frac{G_{1+}(\alpha)}{K_{2+}(\alpha)} = -\frac{C\sqrt{2\pi} D_1 M_2 |A_r| e^{2\pi i\delta} e^{2ik_r h}}{(\alpha + k_r)} K_{2-}(-k_r); \qquad \mathrm{Im}(\alpha) > -\mathrm{Im}(k_r) \qquad (39)$$

$$U_{1-}(\alpha) = -\frac{\sqrt{2\pi} D_1 M_2 |A_r| e^{2\pi i\delta} e^{2ik_r h}}{(\alpha + k_r) K_{2-}(\alpha)} \left[K_{2-}(\alpha) - K_{2-}(-k_r)\right]. \qquad (40)$$

In order to determine the value of $\tau_{11}^{(1)}(0+,y)$ just ahead of the crack tip, we need the form

$G_{1+}(\alpha)$ as $\alpha \to \infty$. Using the fact $K_{2+}(\alpha) \to \alpha^{1/2}$ as $|\alpha| \to \infty$, we obtain from equation (39)

$$G_{1+}(\alpha) = -\frac{C\sqrt{2\pi}D_1 M_2 |A_r| e^{2\pi i\delta} e^{2ik_r h}}{\sqrt{\alpha}} K_{2-}(-k_r); \qquad \text{as } |\alpha| \to \infty.$$

Fourier inversion gives

$$\tau_{11}^{(1)}(0+,y) = -\frac{B e^{-i\alpha_0 h} M_2 |A_r| e^{2\pi i\delta} e^{2ik_r h} K_{2-}(-k_r)(1-i)}{(k_r-\alpha_0)K_{2+}(\alpha_0)\sqrt{(y-h)}} \tag{41}$$

just ahead of the crack tip.

Assuming the Rayleigh waves given by equation (36) to be incident on the semi-infinite crack extending from y= -∞ to y=h on the y-axis in an infinite medium, the x-component of the displacement on the cracked surface due to the diffracted Rayleigh wave from the crack tip is obtained by taking the Fourier inversion of equation (40) and considering only the contribution to the integral from the Rayleigh pole $\alpha=k_r$ in the upper half of the complex α-plane for y<h, the Rayleigh wave part of the diffracted wave is given by

$$u_{1RD}(0+,y) = 2\pi i |A_r| e^{2\pi i\delta} D_1 M_2 \left[\frac{M_2 K_{2-}(-k_r) e^{2ik_r h}}{2k_r}\right] e^{-ik_r(y-h)}.$$

This waves on reflection from the corner (x=0, y=0) again gives rise to Rayleigh waves with displacement on the crack surface

$$u_{1RDR}(0+,y) = 2\pi i |A_r|^2 e^{4\pi i\delta} D_1 M_2 \left[\frac{M_2 K_{2-}(-k_r) e^{2ik_r h}}{2k_r}\right] e^{ik_r(y+h)} \tag{42}$$

and the corresponding stress $\tau_{11}^{(11)}$ due to the incidence of the Rayleigh wave given by equation (42) just ahead of the crack tip is

$$\tau_{11}^{(11)}(0+,y) = -\frac{B e^{-i\alpha_0 h} M_2 |A_r| e^{2\pi i\delta} e^{2ik_r h} K_{2-}(-k_r)}{(k_r-\alpha_0)K_{2+}(\alpha_0)} \left[\frac{|A_r| e^{2\pi i\delta} e^{2ik_r h} M_2 K_{2-}(-k_r)}{2k_r}\right] \frac{(1-i)}{\sqrt{(y-h)}}. \tag{43}$$

In presence of the free surface at y=0 Rayleigh wave which originates at the crack tip and moves along the surface of the crack is reflected back to the crack tip which again gives rise to the Rayleigh wave that is subsequently reflected from the free surface. This process continues again and again. Considering the contribution to τ_{11} at the crack tip due to the incidence of all Rayleigh waves

which are reflected from the free surface and summing up and adding with (20), the total stress just ahead of the crack tip due to the incidence of ϕ_{Ie} is obtained as

$$\left[\tau_{11}(0+,y)\right]_{y\to h+0} = -\frac{Be^{-i\alpha_0 h}}{K_{2+}(\alpha_0)}\left[1+\frac{N_2}{(k_r-\alpha_0)}\right]\frac{(1-i)}{\sqrt{(y-h)}} \tag{44}$$

where

$$N_j = \frac{|A_r|e^{2\pi i\delta}M_j e^{2ik_r h}K_{j-}(-k_r)}{\left[1-(-1)^j\dfrac{|A_r|e^{2\pi i\delta}M_j e^{2ik_r h}K_{j-}(-k_r)}{2k_r}\right]}. \tag{45}$$

Next suppose that $\phi_{Io} = -iA_0\exp(-ik_1 y\cos\theta_1)\sin(k_1 x\sin\theta_1)$ is incident on the semi-infinite crack given by $-\infty<y<h$, $x=0$ in an infinite medium.

Antisymmetric problem :

From geometry, it follows that in the antisymmetric problem involving ϕ_{Io}, the scattered field given by $\phi^{(2)}$, $u_2^{(2)}$, $\tau_{11}^{(2)}$, $\tau_{22}^{(2)}$ will be odd functions of x whereas $\psi^{(2)}$, $u_1^{(2)}$, $\tau_{12}^{(2)}$ Will be even functions of x.

So the conditions to be satisfied are

$$u_2^{(2)} = 0; \quad y>h, \quad x=0 \tag{vii}$$

$$\tau_{11}^{(2)} = 0; \quad -\infty<y<\infty, \quad x=0 \tag{viii}$$

$$\tau_{12}^{(2)} = \rho c_2^2 k_1^2 A_0 \sin 2\theta_1 e^{-i\alpha_0 y}; \quad y<h, \quad x=0. \tag{ix}$$

Using these conditions we obtain the Wiener-Hopf equation

$$H_+(\alpha) + CK_1(\alpha)V_-(\alpha) = \frac{Pe^{-i\alpha_0 h}}{(\alpha-\alpha_0)} \tag{46}$$

where

$$P = \frac{iA_0\mu k_1^2\sin 2\theta_1}{\sqrt{2\pi}} \tag{47}$$

$$H_+(\alpha) = \frac{1}{\sqrt{2\pi}}\int_h^\infty \tau_{12}^{(2)}(0+,y)\,e^{i\alpha(y-h)}\,dy$$

and

$$V_-(\alpha) = \frac{1}{\sqrt{2\pi}} \int_{-\infty}^{h} u_2^{(2)}(0+,y)\, e^{i\alpha(y-h)}\, dy. \tag{48}$$

Using the usual Wiener-Hopf argument, equation (46) subsequently yields

$$\frac{H_+(\alpha)}{K_{1+}(\alpha)} = \frac{Pe^{-i\alpha_0 h}}{(\alpha-\alpha_0)}\left[\frac{1}{K_{1+}(\alpha)} - \frac{1}{K_{1+}(\alpha_0)}\right] \tag{49}$$

and

$$V_-(\alpha) = \frac{Pe^{-i\alpha_0 h}}{CK_{1+}(\alpha_0)K_{1-}(\alpha)(\alpha-\alpha_0)}. \tag{50}$$

From (49) we can derive the shear stress just ahead of the crack tip due to the incidence of ϕ_{Io} as

$$\tau_{12}^{(2)}(0+,y) = -\frac{Pe^{-i\alpha_0 h}}{K_{1+}(\alpha_0)}\frac{(1-i)}{\sqrt{(y-h)}} \qquad |\alpha| \to \infty. \tag{51}$$

Taking Fourier inversion of (50) we obtain (neglecting the diffracted body waves)

$$u_2^{(2)}(0+,y) = \frac{2\pi i Pe^{-i\alpha_0 y}}{\sqrt{2\pi}CK_1(\alpha_0)} + 2\pi i D_2 M_1 e^{-ik_r(y-h)} \tag{52}$$

where

$$D_2 = \frac{Pe^{-i\alpha_0 h}}{\sqrt{2\pi}CK_{1+}(\alpha_0)(k_r-\alpha_0)}. \tag{53}$$

The first term of (52) is due to the geometrical reflection of ϕ_{Io} from the surface of the crack and the second term is due to diffracted Rayleigh wave arising from the crack tip. Taking account of the shear stress contribution due to successive reflection and diffraction of the Rayleigh wave given by the second term of (52) from the corner of the wedge and the edge of the crack respectively and summing up, we obtain finally the shear stress just ahead of the crack tip due to the incidence of ϕ_{Io} as

$$\left[\tau_{12}(\phi_{Io})\right]_{y-h+0} = -\frac{Pe^{-i\alpha_0 h}}{K_{1+}(\alpha_0)}\left[1 - \frac{N_1}{(k_r-\alpha_0)}\right]\frac{(1-i)}{\sqrt{(y-h)}}. \tag{54}$$

Following the same procedure, the stresses just ahead of the crack tip due to the incidence of $\phi_R=\phi_{Re}+\phi_{Ro}$ are given by

$$\left[\tau_{11}(\phi_{Re})\right]_{y\to h+0} = -\frac{B_1 e^{i\alpha_0 h}}{K_{2+}(-\alpha_0)}\left[1+\frac{N_2}{(k_r+\alpha_0)}\right]\frac{(1-i)}{\sqrt{(y-h)}} \tag{55}$$

where

$$B_1 = -\frac{iA_R\mu k_1^2(2\cos^2\theta_1 - c_1^2/c_2^2)}{\sqrt{2\pi}} \tag{56}$$

and

$$\left[\tau_{12}(\phi_{Ro})\right]_{y\to h+0} = -\frac{P_1 e^{i\alpha_0 h}}{K_{1+}(-\alpha_0)}\left[1-\frac{N_1}{(k_r+\alpha_0)}\right]\frac{(1-i)}{\sqrt{(y-h)}} \tag{57}$$

where

$$P_1 = -\frac{iA_R\mu k_1^2\sin 2\theta_1}{\sqrt{2\pi}}. \tag{58}$$

Similarly the stresses just ahead of the crack tip due to the incidence of $\psi_R=\psi_{Ro}+\psi_{Re}$ are given by

$$\left[\tau_{11}(\psi_{Ro})\right]_{y\to h+0} = -\frac{B_2 e^{i\beta_0 h}}{K_{2+}(-\beta_0)}\left[1+\frac{N_2}{(k_r+\beta_0)}\right]\frac{(1-i)}{\sqrt{(y-h)}} \tag{59}$$

where

$$B_2 = -\frac{iB_R\mu k_1^2(c_1^2/c_2^2)\sin 2\theta_2}{\sqrt{2\pi}}; \qquad \beta_0 = k_2\cos\theta_2 \tag{60}$$

and

$$\left[\tau_{12}(\psi_{Re})\right]_{y\to h+0} = -\frac{P_2 e^{i\beta_0 h}}{K_{1+}(-\beta_0)}\left[1-\frac{N_1}{(k_r+\beta_0)}\right]\frac{(1-i)}{\sqrt{(y-h)}} \tag{61}$$

where

$$P_2 = \frac{iB_R\mu k_1^2(c_1^2/c_2^2)\cos 2\theta_2}{\sqrt{2\pi}}. \tag{62}$$

Therefore considering the contribution from ϕ_I, ϕ_R and ψ_R together, the resultant stress components just ahead of the crack tip are given by

$$\left[\tau_{11}(0+,y)\right]_{y\to h+0} = -\left[\frac{Be^{-i\alpha_0 h}}{K_{2+}(\alpha_0)}\left\{1+\frac{N_2}{(k_r-\alpha_0)}\right\} + \right.$$

$$\left. + \frac{B_1 e^{i\alpha_0 h}}{K_{2+}(-\alpha_0)}\left\{1+\frac{N_2}{(k_r+\alpha_0)}\right\} + \frac{B_2 e^{i\beta_0 h}}{K_{2+}(-\beta_0)}\left\{1+\frac{N_2}{(k_r+\beta_0)}\right\}\right]\frac{(1-i)}{\sqrt{(y-h)}} \tag{63}$$

and

$$\left[\tau_{12}(0+,y)\right]_{y\to h+0} = -\left[\frac{Pe^{-i\alpha_0 h}}{K_{1+}(\alpha_0)}\left\{1-\frac{N_1}{(k_r-\alpha_0)}\right\}+\right.$$

$$\left.+\frac{P_1 e^{i\alpha_0 h}}{K_{1+}(-\alpha_0)}\left\{1-\frac{N_1}{(k_r+\alpha_0)}\right\}+\frac{P_2 e^{i\beta_0 h}}{K_{1+}(-\beta_0)}\left\{1-\frac{N_1}{(k_r+\beta_0)}\right\}\right]\frac{(1-i)}{\sqrt{(y-h)}}. \qquad (64)$$

3. STRESS INTENSITY FACTOR

The singular parts of the stress components τ_{11} and τ_{12} just ahead of the crack tip may be expressed in the form

$$\tau_{11} = \frac{K_I}{\sqrt{y/h-1}} \quad \text{and} \quad \tau_{12} = \frac{K_{II}}{\sqrt{y/h-1}}$$

and the corresponding stress intensity factors at the crack tip are defined by

$$S_1 = \left|\frac{\sqrt{2\pi}\,K_I}{(1-i)A_0\mu k_1^2}\right| \qquad (65) \qquad \text{and} \qquad S_2 = \left|\frac{\sqrt{2\pi}\,K_{II}}{(1-i)A_0\mu k_1^2}\right| \qquad (66)$$

4. NUMERICAL RESULTS AND DISCUSSION

The absolute values of the complex dynamic stress intensity factors S_1 and S_2 as defined by equations (65) and (66) have been plotted against the dimensionless wave number k_1h for different values of the angle of incidence $\theta_1=30^0$, 40^0, and 50^0. Numerical results have been computed for Poisson ratio $\gamma=1/4$ so that $\frac{c_1}{c_2}=\sqrt{3}$ and $\frac{c_1}{c_R}=\frac{\sqrt{3}}{0.9194}$. In the figure, values of k_1h have been taken to vary from $k_1h=1$ to 30.

Both stress intensity factors show a tendency to decrease, though oscillatory for increasing k_1h. The general oscillatory feature for the curves in Fig.5 and Fig.6 is due to the effect of interaction between the incident plane waves and Rayleigh waves which originate at the crack tip and are reflected back and forth between the crack tip and the corner of the free surface. In both the figures Fig.5 and Fig.6, S_1 and S_2 show distinct peaks, which indicate constructive interference phenomena.

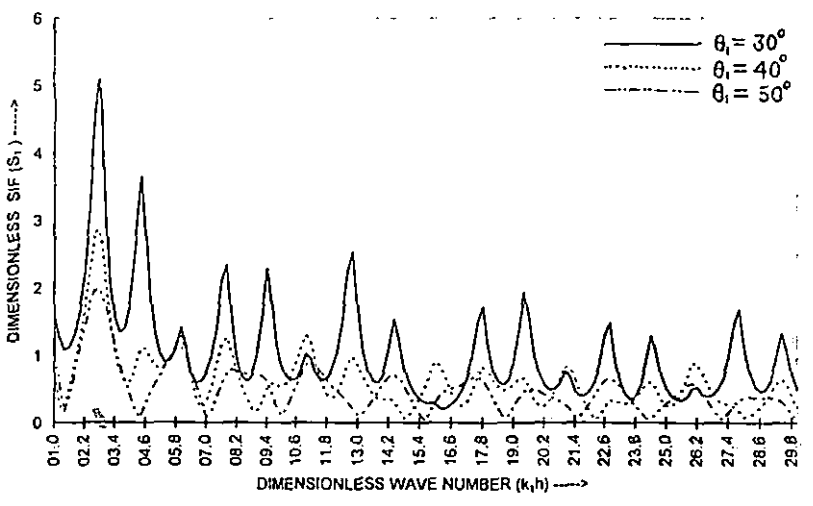

Fig.5 Stress intensity factor S_1 versus dimensionless wave number k_1h for $\theta_1=30^0$, 40^0, and 50^0.

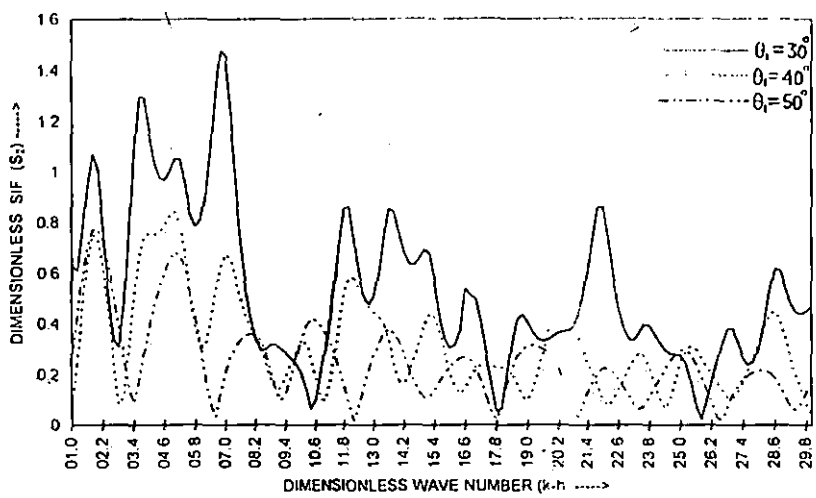

Fig.6 Stress intensity factor S_2 versus dimensionless wave number k_1h for $\theta_1=30^0$, 40^0, and 50^0.

CHAPTER - 4

ELASTODYNAMIC GREEN'S FUNCTION

[6]ELASTODYNAMIC GREEN'S FUNCTION FOR TIME-HARMONIC RING SOURCE IN AN INFINITE ANISOTROPIC MEDIUM

1. INTRODUCTION

The study of the scattering of the elastic waves by cracks or inclusions in an elastic medium is of considerable importance in view of its application in the quantitative nondestructive evaluation of materials. When there are only axially symmetric scatterers like circular cracks or inclusions, the incidence of torsional waves results in torsional waves only where as the incidence of logitudinal waves gives rise longitudinal wave consisting of axial and radial components of the displacement which are coupled. The torsional wave modes are useful in detecting longitudinal flaws in cylindrical materials and longitudinal wave modes are useful for detecting transverse flaws and corrosion defects.

Keeping this fact in view different investigators studied diffraction of elastic waves by cirdular cracks and inclusions in different times. Work of Kundu and Bostrom [1991], Kundu [1990], Krenk and Schmidt [1982], Schmidt and Krenk [1982] may be mentioned in this connection.

While studing elastodynamic scattering due to axisymmetric scatter, calculation can be greatly simplified if an elastodynamic Green's function for ring source is available and used.

In our paper the elastodynamic Green's function for a torsional ring source as well as for a axial and a radial ring source in a transversely isotropic solid has been obtained. The axis of material

---

[6] **Communicated to the journal ARCHIVES OF MECHANICS, 2000.**

symmetric and the axis of the ring source have been assumed to coincide. The Green's functions are derived using Fourier and Hankel transforms in the integral form. Using stationary phase method, the far field displacement has been derived and depicted by means of graphs in the case of Graphite-epoxy composite. Recently, the elastodynamic Green's function for a circular ring source in homogeneous isotropic elastic medium has been derived by Lu [1998, 1999].

2. RING SOURCE OF FORCE IN RADIAL DIRECTION

Consider a cylindrical polar co-ordinate system r, θ, z with the cetre of the ring source on the z-axis so that the ring source of radius $r=r'$ is located at $z=z'$. The time dependence of all the field quantities, assumed to be of the form exp(-iwt), will be suppressed in the subsequent development.

The material is assumed to be a unidirectionally fiber-reinforced composite solid whose fiber diameter is small compared to the wave length so that one can consider the material as a transversely isotropic solid. The fiber direction is parallel to the z-axis.

Since the problem is axisymmetric for radial ring source of force, so the only non-vanishing displacement components are $u_{rr}(r,z)$ and $u_{zr}(r,z)$ where the first subscript denotes the direction of the displacement and the second one the direction of the ring source of force. The equations of motion for the probleme are

$$c_1\left(\frac{\partial^2 u_{rr}}{\partial r^2}+\frac{1}{r}\frac{\partial u_{rr}}{\partial r}-\frac{u_{rr}}{r^2}\right)+c_3\frac{\partial^2 u_{zr}}{\partial r\partial z}+c_5\left(\frac{\partial^2 u_{zr}}{\partial r\partial z}+\frac{\partial^2 u_{rr}}{\partial z^2}\right)+\rho\omega^2 u_{rr}=-\frac{\delta(r-r')\,\delta(z-z')}{r} \tag{2.1}$$

and

$$(c_3 + c_5)\left(\frac{\partial^2 u_{rr}}{\partial r \partial z} + \frac{1}{r}\frac{\partial u_{rr}}{\partial r} \right) + c_5\left(\frac{\partial^2 u_{zr}}{\partial r^2} + \frac{1}{r}\frac{\partial u_{zr}}{\partial r} \right) + c_4 \frac{\partial^2 u_{zr}}{\partial z^2} + \rho\omega^2 u_{zr} = 0 \qquad (2.2)$$

where ρ is the material density and the term $\frac{\delta(r-r')\,\delta(z-z')}{r}$ represent the radial ring source of force.

We apply the Fourier transform to the axial co-ordinate, z, and the Hankel transform to the radial co-ordinate, r. The Fourier transform is defined as

$$U^*(r,\eta;r',z') = \int_{-\infty}^{\infty} U(r,z;r',z')\, e^{-i\eta z}\, dz \qquad (2.3a)$$

$$U(r,z;r',z') = \frac{1}{2\pi}\int_{-\infty}^{\infty} U^*(r,\eta;r',z')\, e^{i\eta z}\, d\eta \qquad (2.3b)$$

while the Hankel transform is defined as

$$\bar{U}^*_{rr}(\xi,\eta;r',z') = \int_0^{\infty} U^*_{rr}(r,\eta;r',z')\, J_1(\xi r)\, r\, dr \qquad (2.4a)$$

$$U^*_{rr}(r,\eta;r',z') = \int_0^{\infty} \bar{U}^*_{rr}(\xi,\eta;r',z')\, J_1(\xi r)\, \xi\, d\xi \qquad (2.4b)$$

$$\bar{U}^*_{zr}(\xi,\eta;r',z') = \int_0^{\infty} U^*_{zr}(r,\eta;r',z')\, J_0(\xi r)\, r\, dr \qquad (2.5a)$$

$$U^*_{zr}(r,\eta;r',z') = \int_0^{\infty} \bar{U}^*_{zr}(\xi,\eta;r',z')\, J_0(\xi r)\, \xi\, d\xi \qquad (2.5b)$$

where η and ξ are transform parameters and $J_0(z)$ and $J_1(z)$ are the Bessel functions of the first kind of order zero and one respectively.

Using Fourier transform with respect to z to equations (2.1) and (2.2) one obtains,

$$c_1\left(\frac{\partial^2 u^*_{rr}}{\partial r^2} + \frac{1}{r}\frac{\partial u^*_{rr}}{\partial r} - \frac{u^*_{rr}}{r^2} \right) + i\eta(c_3 + c_5)\frac{\partial u^*_{zr}}{\partial r} - c_5\eta^2 u^*_{rr} + \rho\omega^2 u^*_{rr} = -\frac{\delta(r-r')\, e^{-i\eta z'}}{r} \qquad (2.6a)$$

$$i\eta(c_3+c_5)\left(\frac{\partial u_{rr}^*}{\partial r}+\frac{u_{rr}^*}{r}\right)+c_5\frac{1}{r}\left[\frac{\partial}{\partial r}\left(r\frac{\partial u_{zr}^*}{\partial r}\right)\right]-c_4\eta^2u_{zr}^*+\rho\omega^2u_{zr}^*=0 \qquad (2.6b)$$

Use of equation (2.5b) and (2.5a) to equations (2.6a) and (2.6b) respectively yield

$$(\rho\omega^2-c_1\xi^2-c_5\eta^2)\bar{u}_{rr}^*-i\xi\eta(c_3+c_5)\bar{u}_{zr}^*=-J_1(\xi r')e^{-i\eta z'} \qquad (2.7a)$$

and

$$i\xi\eta(c_3+c_5)\bar{u}_{rr}^*+(\rho\omega^2-c_5\xi^2-c_4\eta^2)\bar{u}_{zr}^*=0. \qquad (2.7b)$$

Solving equations (2.7a) and (2.7b) one obtains

$$\bar{u}_{rr}^*=-\frac{(\rho\omega^2-c_4\eta^2-c_5\xi^2)}{c_4c_5(\eta^2-\eta_1^2)(\eta^2-\eta_2^2)}J_1(\xi r')e^{-i\eta z'} \qquad (2.8a)$$

$$\bar{u}_{zr}^*=\frac{i\xi\eta(c_3+c_5)}{c_4c_5(\eta^2-\eta_1^2)(\eta^2-\eta_2^2)}J_1(\xi r')e^{-i\eta z'} \qquad (2.8b)$$

where

$$\eta_j^2=\frac{1}{2c_4c_5}\left\{b_2-b_1\xi^2+(-1)^j(B_1\xi^4+B_2\xi^2+B_3)^{1/2}\right\} \qquad (2.9a)$$

η_1^2 and η_2^2 are the roots of the quadratic equation in η^2 given by

$$c_4c_5\eta^4+\left\{(c_1c_4-c_3^2-2c_3c_5)\xi^2-\rho\omega^2(c_4+c_5)\right\}\eta^2+\left\{c_1c_5\xi^4-\rho\omega^2(c_1+c_5)\xi^2+\rho^2\omega^4\right\}=0 \qquad (2.9b)$$

and
$$b_1=c_1c_4-c_3^2-2c_3c_5$$
$$b_2=\rho\omega^2(c_4+c_5)$$
$$B_1=b_1^2-4c_1c_4c_5^2 \qquad (2.10)$$
$$B_2=4\rho\omega^2c_4c_5(c_1+c_5)-2b_1b_2$$
$$B_3=\rho^2\omega^4(c_4-c_5)^2.$$

From equation (2.9a) it can be shown that η_j (j=1,2) is equal to zero at $\xi=k_j$ where

$$k_1=\omega\sqrt{\rho/c_1}\,, \qquad k_2=\omega\sqrt{\rho/c_5} \qquad (2.11)$$

For $\xi < k_j$; η_j^2 is positive and η_j is taken to be a positive real number whereas for $\xi > k_j$; η_j^2 is negative and η_j is taken to be a positive imaginary number.

Now we apply equation (2.3b) to equations (2.8a) and (2.8b) to obtain

$$\bar{u}_{rr}(\xi,z,;r',z') = \frac{i}{2c_4c_5}\left[-\frac{(\rho\omega^2-c_5\xi^2-c_4\eta_1^2)}{\eta_1(\eta_1^2-\eta_2^2)}e^{i\eta_1|z-z'|}+\frac{(\rho\omega^2-c_5\xi^2-c_4\eta_2^2)}{\eta_2(\eta_1^2-\eta_2^2)}e^{i\eta_2|z-z'|}\right]J_1(\xi r') \tag{2.12a}$$

and

$$\bar{u}_{zr}(\xi,z,;r',z') = -\frac{\mathrm{sgn}(z-z')(c_3+c_5)}{2c_4c_5(\eta_1^2-\eta_2^2)}\left[e^{i\eta_1|z-z'|}-e^{i\eta_2|z-z'|}\right]\xi J_1(\xi r'). \tag{2.12b}$$

Taking Hankel inversion one obtains

$$u_{rr}(r,z;r',z') = \frac{i}{2c_4c_5}\sum_{j=1}^{2}(-1)^j\int_0^\infty \sqrt{\xi}F_j(\xi)e^{i\eta_j|z-z'|}J_1(\xi r)\,d\xi \tag{2.13a}$$

where

$$F_j(\xi) = \frac{\sqrt{\xi}(\rho\omega^2-c_5\xi^2-c_4\eta_j^2)}{\eta_j(\eta_1^2-\eta_2^2)}J_1(\xi r') \tag{2.13b}$$

and

$$u_{zr}(r,z;r',z') = \frac{\mathrm{sgn}(z-z')(c_3+c_5)}{2c_4c_5}\sum_{j=1}^{2}(-1)^j\int_0^\infty \sqrt{\xi}\,E(\xi)e^{i\eta_j|z-z'|}J_0(\xi r)\,d\xi \tag{2.14a}$$

where

$$E(\xi) = \frac{\xi^{3/2}J_1(\xi r')}{\eta_1^2-\eta_2^2}. \tag{2.14b}$$

3. FAR FIELD CALCULATION FOR RING SOURCE OF FORCE IN RADIAL DIRECTION

In the near field (small z and r), the integrals in equation (2.13a) and in equation (2.14a) can be evaluated numerically. However, in the far field, the numerical evaluation of these integrals is awkward because of the rapid oscillation introduced in the integral by the Bessel functions and trigonometric functions.

Assume the ring source to be situated at z=0-plane so that $z'=0$. Next for large ξr, taking the first term in the asymptotic expansion of the Bessel function

$$J_m(\xi r) \approx \frac{1}{\sqrt{2\pi\xi r}}\left[e^{i\xi r-i(2m+1)\pi/4}+e^{-i\xi r+i(2m+1)\pi/4}\right]. \tag{3.1}$$

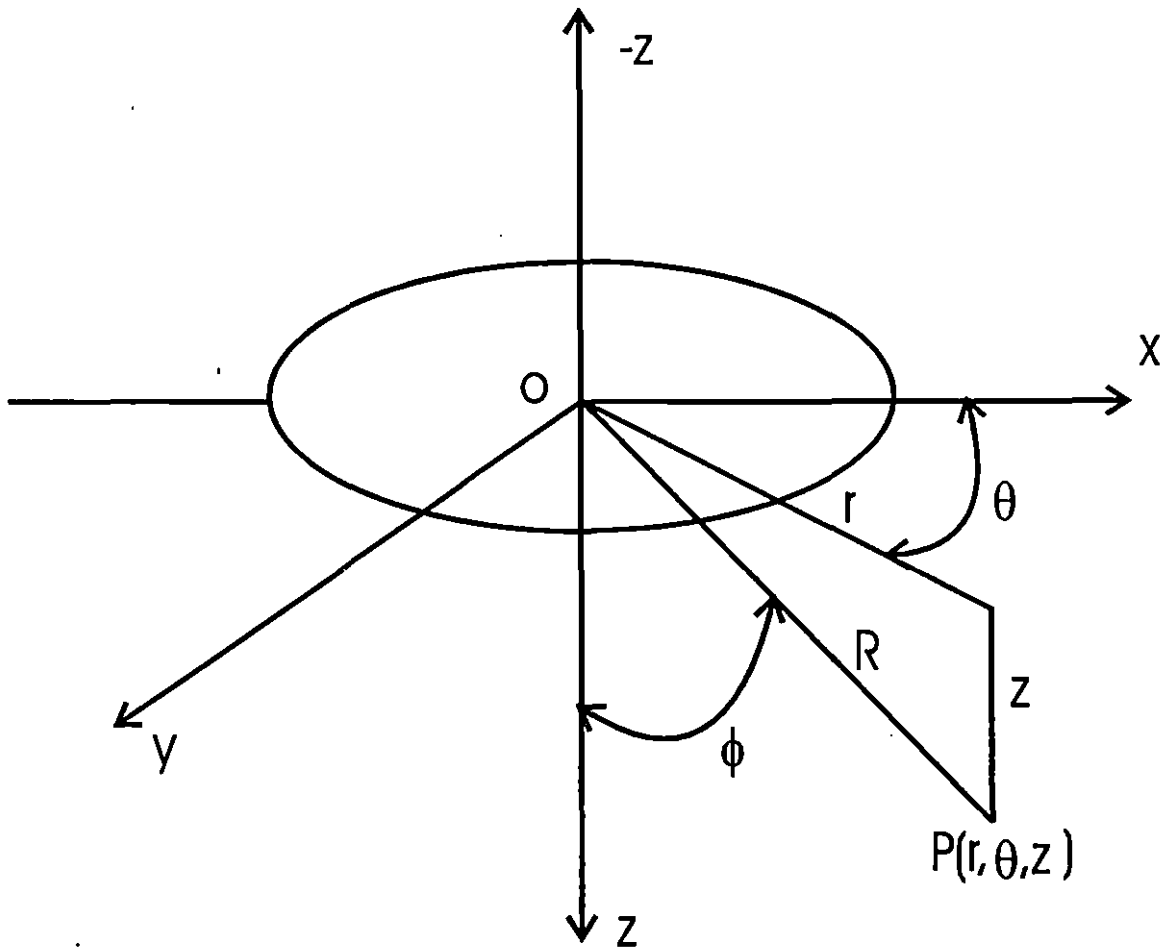

Fig.1. Schematic diagram of the problem geometry.

Displacement components given by equation (2.13a) and equation (2.14a) become,

$$u_{rr}(r,z;r',0) = \frac{i}{2c_4c_5\sqrt{2\pi r}}\sum_{j=1}^{2}(-1)^j\int_0^\infty F_j(\xi)\left[e^{-3\pi i/4}e^{i\eta_j|z|+i\xi r} + e^{3\pi i/4}e^{i\eta_j|z|-i\xi r}\right]d\xi \quad (3.2)$$

$$u_{zr}(r,z;r',0) = \frac{\mathrm{sgn}(z)(c_3+c_5)}{2c_4c_5\sqrt{2\pi r}}\left[\sum_{j=1}^{2}(-1)^j\left\{e^{-i\pi/4}\int_0^\infty E(\xi)e^{i\eta_j|z|+i\xi r}d\xi + e^{i\pi/4}\int_0^\infty E(\xi)e^{i\eta_j|z|-i\xi r}\right\}\right] \quad (3.3)$$

So, oscillations in the integrand are introduced by the factors of the form $\exp(i\eta_j|z| \pm i\xi r)$. This type of oscillatory integrals can be evaluated by the method of stationary phase [1950] for large distance away from the source.

For this purpose, we substitute

$$|z| = R\cos\phi \quad \text{and} \quad r = R\sin\phi \quad (3.4)$$

where R is large; then

$$e^{i\eta_j|z|\pm i\xi r} = e^{iR(\eta_j\cos\phi \pm \xi\sin\phi)} = e^{iR\psi_j(\xi)} \text{ or } e^{iR\chi_j(\xi)} \quad (3.5)$$

where $\psi_j(\xi) = \eta_j\cos\phi + \xi\sin\phi$, $\chi_j(\xi) = \eta_j\cos\phi - \xi\sin\phi$. (3.6)

With the help of equation (3.5), equation (3.2) and equation (3.3) can be expressed as

$$u_{rr}(r,z;r',0) = \frac{1}{2c_4c_5\sqrt{2\pi R\sin\phi}}\sum_{j=1}^{2}(-1)^j\left[e^{-i\pi/4}\int_0^\infty F_j(\xi)e^{iR\psi_j(\xi)}d\xi - e^{i\pi/4}\int_0^\infty F_j(\xi)e^{iR\chi_j(\xi)}d\xi\right] \quad (3.7)$$

and

$$u_{zr}(r,z;r',0) = \frac{\mathrm{sgn}(z)(c_3+c_5)}{2c_4c_5\sqrt{2\pi R\sin\phi}}\sum_{j=1}^{2}(-1)^j\left[e^{-i\pi/4}\int_0^\infty E(\xi)e^{iR\psi_j(\xi)}d\xi + e^{i\pi/4}\int_0^\infty E(\xi)e^{iR\chi_j(\xi)}d\xi\right]. \quad (3.8)$$

The statonary points are given by $\psi_j'(\xi) = 0$ and $\chi_j'(\xi) = 0$ which yield,

$$\frac{2b_1\xi - (-1)^j(2B_1\xi^3 + B_2\xi)/B(\xi)}{[b_2 - b_1\xi^2 + (-1)^jB(\xi)]^{1/2}} = \pm\sqrt{8c_4c_5}\tan\phi \quad (3.9)$$

where $B(\xi) = [B_1\xi^4 + B_2\xi^2 + B_3]^{1/2}$ (3.10)

and positive sign in the equation (3.9) on right hand side corresponds to $\psi_j'(\xi) = 0$ whereas negative sign corresponds to $\chi_j'(\xi) = 0$.

For an anisotropic material the roots of equation (3.9) can be solved numerically. We know that for Graphite-epoxy composite, c_1=13.92 Gpa, c_2=6.92 Gpa, c_3=6.44 Gpa, c_4=160.73 Gpa, c_5=7.07 Gpa, ρ=1578 kg/m^3, [1991]. For this type of material, it can be shown that the equation $\chi_j'(\xi) = 0$ does not give any positive root of ξ. $\psi_1'(\xi) = 0$ gives only one positive root whereas $\psi_2'(\xi) = 0$ gives three positive roots for some values of ϕ and a single positive root for other values of ϕ. These roots are denoted by ξ_{01} and ξ_{02}^m respectively. For multiple values of ξ_{02} , the superscript m takes the values 1, 2, 3. The values of ξ_{01} and ξ_{02}^m for different values of ϕ are given in the following table :

Table-1. Roots of the equations $\psi_1'(\xi) = 0$ and $\psi_2'(\xi) = 0$.

ϕ	ξ_{01}	ξ_{02}^1	ξ_{02}^2	ξ_{02}^3
10°	0.5079	0.0971	0	0
15°	0.5845	0.1460	0	0
20°	0.6200	0.1952	0	0
25°	0.6402	0.2448	0	0
30°	0.6537	0.2948	0.8194	0.9172
35°	0.6636	0.3452	0.7995	0.9459
40°	0.6714	0.3958	0.7873	0.9626
45°	0.6779	0.4463	0.7780	0.9738
50°	0.6835	0.4964	0.7702	0.9815
55°	0.6885	0.5454	0.7630	0.9871
60°	0.6931	0.5927	0.7558	0.9913
65°	0.6974	0.6377	0.7478	0.9943
70°	0.7015	0.6815	0.7363	0.9965
75°	0.7054	0	0	0.9981

For far field computation we can neglect all the terms containing $e^{-i\xi r}$ in equation (3.7) and also in equation (3.8) because $\chi_j'(\xi) = 0$ does not give any positive root. Using the stationary-phase method the far field components of displacement are thus given by

$$u_{rr}(r,z;r',0) = \frac{e^{-i\pi/4}}{2c_4c_5R\sqrt{\sin\phi}}\left[\sum_{m=1}^{M}\frac{F_2(\xi_{02}^m)}{\sqrt{|\psi_2''(\xi_{02}^m)|}}\exp\left\{iR\psi_2(\xi_{02}^m)+\frac{i\pi}{4}\operatorname{sgn}\psi_2''(\xi_{02}^m)\right\}\right.$$

$$\left. - \frac{F_1(\xi_{01})}{\sqrt{|\psi_1''(\xi_{01})|}}\exp\left\{iR\psi_1(\xi_{01})+\frac{i\pi}{4}\operatorname{sgn}\psi_1''(\xi_{01})\right\}\right] \tag{3.11}$$

and

$$u_{zr}(r,z;r',0) = \frac{\operatorname{sgn}z(c_3+c_5)e^{-i\pi/4}}{2c_4c_5R\sqrt{\sin\phi}}\left[\sum_{m=1}^{M}\frac{E(\xi_{02}^m)}{\sqrt{|\psi_2''(\xi_{02}^m)|}}\exp\left\{iR\psi_2(\xi_{02}^m)+\frac{i\pi}{4}\operatorname{sgn}\psi_2''(\xi_{02}^m)\right\}\right.$$

$$\left. - \frac{E(\xi_{01})}{\sqrt{|\psi_1''(\xi_{01})|}}\exp\left\{iR\psi_1(\xi_{01})+\frac{i\pi}{4}\operatorname{sgn}\psi_1''(\xi_{01})\right\}\right] \tag{3.12}$$

where

$$\psi_1'(\xi_{01}) = 0 \quad \text{and} \quad \psi_2'(\xi_{02}^m) = 0 \tag{3.13}$$

and M is the number of roots of the equation $\psi_2'(\xi) = 0$ and

$$\psi_j''(\xi) = -\frac{\cos\phi}{\sqrt{8c_4c_5}}\left[\left\{2b_1-(-1)^jB^{-3}(\xi)(2B_1^2\xi^6+3B_1B_2\xi^4+6B_1B_3\xi^2+B_2B_3)\right\}\right.$$

$$\times\left\{b_2-b_1\xi^2+(-1)^jB(\xi)\right\}+\frac{1}{2}\left\{2b_1\xi-(-1)^jB^{-1}(\xi)(2B_1\xi^3+B_2\xi)\right\}^2\Big]$$

$$\times\left\{b_2-b_1\xi^2+(-1)^jB(\xi)\right\}^{-3/2} \tag{3.14}$$

where b_1, b_2, B_1, B_2, B_3, $B(\xi)$ have been defined previously.

4. RING SOURCE OF FORCE IN AXIAL DIRECTION

For an axial ring source of force, the equations of motion become

$$c_1\left(\frac{\partial^2 u_{rz}}{\partial r^2}+\frac{1}{r}\frac{\partial u_{rz}}{\partial r}-\frac{u_{rz}}{r^2}\right)+c_3\frac{\partial^2 u_{zz}}{\partial r\partial z}+c_5\left(\frac{\partial^2 u_{zz}}{\partial r\partial z}+\frac{\partial^2 u_{rz}}{\partial z^2}\right)+\rho\omega^2 u_{rz}=0 \qquad (4.1)$$

and

$$(c_3+c_5)\left(\frac{\partial^2 u_{rz}}{\partial r\partial z}+\frac{1}{r}\frac{\partial u_{rz}}{\partial z}\right)+c_5\left(\frac{\partial^2 u_{zz}}{\partial r^2}+\frac{1}{r}\frac{\partial u_{zz}}{\partial r}\right)+c_4\frac{\partial^2 u_{zz}}{\partial z^2}+\rho\omega^2 u_{zz}=-\frac{\delta(r-r')\delta(z-z')}{r}. \qquad (4.2)$$

Using the similar procedure which has been applied previously, we obtain,

$$\bar{u}^*_{rz}(\xi,\eta;r',z')=-\frac{i\xi\eta(c_3+c_5)J_0(\xi r')e^{-i\eta z'}}{c_4c_5(\eta^2-\eta_1^2)(\eta^2-\eta_2^2)} \qquad (4.3)$$

$$\bar{u}^*_{zz}(\xi,\eta;r',z')=-\frac{(\rho\omega^2-c_1\xi^2-c_5\eta^2)J_0(\xi r')e^{-i\eta z'}}{c_4c_5(\eta^2-\eta_1^2)(\eta^2-\eta_2^2)}. \qquad (4.4)$$

Taking Fourier inversion and Hankel inversion we obtain finally,

$$u_{rz}(r,z;r',0)=\frac{\mathrm{sgn}(z)(c_3+c_5)}{2c_4c_5}\left[\sum_{j=1}^{2}\frac{(-1)^{j+1}}{\sqrt{2\pi r}}\left\{e^{-3\pi i/4}\int_0^\infty H(\xi)\,e^{i\eta_j|z|+i\xi r}d\xi + e^{3\pi i/4}\int_0^\infty H(\xi)e^{i\eta_j|z|-i\xi r}d\xi\right\}\right] \qquad (4.5)$$

where

$$H(\xi)=\frac{\xi^{3/2}J_0(\xi r')}{(\eta_1^2-\eta_2^2)} \qquad (4.6)$$

$$u_{zz}(r,z;r',0)=\frac{i}{2c_4c_5\sqrt{2\pi r}}\int_0^\infty\sum_{j=1}^{2}(-1)^j\,N_j(\xi)\left[e^{-\pi i/4}e^{i\eta_j|z|+i\xi r}+e^{\pi i/4}e^{i\eta_j|z|-i\xi r}\right]d\xi \qquad (4.7)$$

where

$$N_j(\xi)=\frac{\sqrt{\xi}\,(\rho\omega^2-c_1\xi^2-c_5\eta_j^2)}{\eta_j(\eta_1^2-\eta_2^2)}J_0(\xi r'). \qquad (4.8)$$

Using the method of stationary phase for evaluation of the integrals arising in equation (4.5) and (4.6) for large distance away from the ring source we have

$$u_{rz}(r,z;r',0) = \frac{\operatorname{sgn} z(c_3+c_5)e^{-3\pi i/4}}{2c_4c_5R\sqrt{\sin\phi}}\left[\frac{H(\xi_{01})}{\sqrt{|\psi_1''(\xi_{01})|}}\exp\left\{iR\psi_1(\xi_{01})+\frac{i\pi}{4}\operatorname{sgn}\psi_1''(\xi_{01})\right\}\right.$$

$$\left.-\sum_{m=1}^{M}\frac{H(\xi_{02}^m)}{\sqrt{|\psi_2''(\xi_{02}^m)|}}\exp\left\{iR\psi_2(\xi_{02}^m)+\frac{i\pi}{4}\operatorname{sgn}\psi_2''(\xi_{02}^m)\right\}\right] \qquad (4.9)$$

and

$$u_{zz}(r,z;r',0) = \frac{e^{i\pi/4}}{2c_4c_5R\sqrt{\sin\phi}}\left[\sum_{m=1}^{M}\frac{N_2(\xi_{02}^m)}{\sqrt{|\psi_2''(\xi_{02}^m)|}}\exp\left\{iR\psi_2(\xi_{02}^m)+\frac{i\pi}{4}\operatorname{sgn}\psi_2''(\xi_{02}^m)\right\}\right.$$

$$\left.-\frac{N_1(\xi_{01})}{\sqrt{|\psi_1''(\xi_{01})|}}\exp\left\{iR\psi_1(\xi_{01})+\frac{i\pi}{4}\operatorname{sgn}\psi_1''(\xi_{01})\right\}\right]. \qquad (4.10)$$

5. NUMERICAL RESULTS FOR RADIAL AND AXIAL RING SOURCE

Numerical results for normalized displacement components $|2c_4Ru_{rr}|$, $|2c_4Ru_{zr}|$ for radial ring source and $|2c_4Ru_{rz}|$, $|2c_4Ru_{zz}|$ for axial ring source at large distace away from the source for different values of k_2r' (=2,8) have been plotted graphically for different values of R/r' (=20, 40, 60) in the graphite-epoxy composite for which the material properties have been presented in the earlier section. Variation of normalized displacement components for different values of ϕ varying from 10° to 75° where $\phi = \tan^{-1}\frac{r}{|z|}$ has been depicted by means of graphs (Figs.2-9). It is interesting to naote that for smaller angles less than 25° and for angles greater than 70°, the variation of the normalized displacement components with values of R/r' is not prominent.

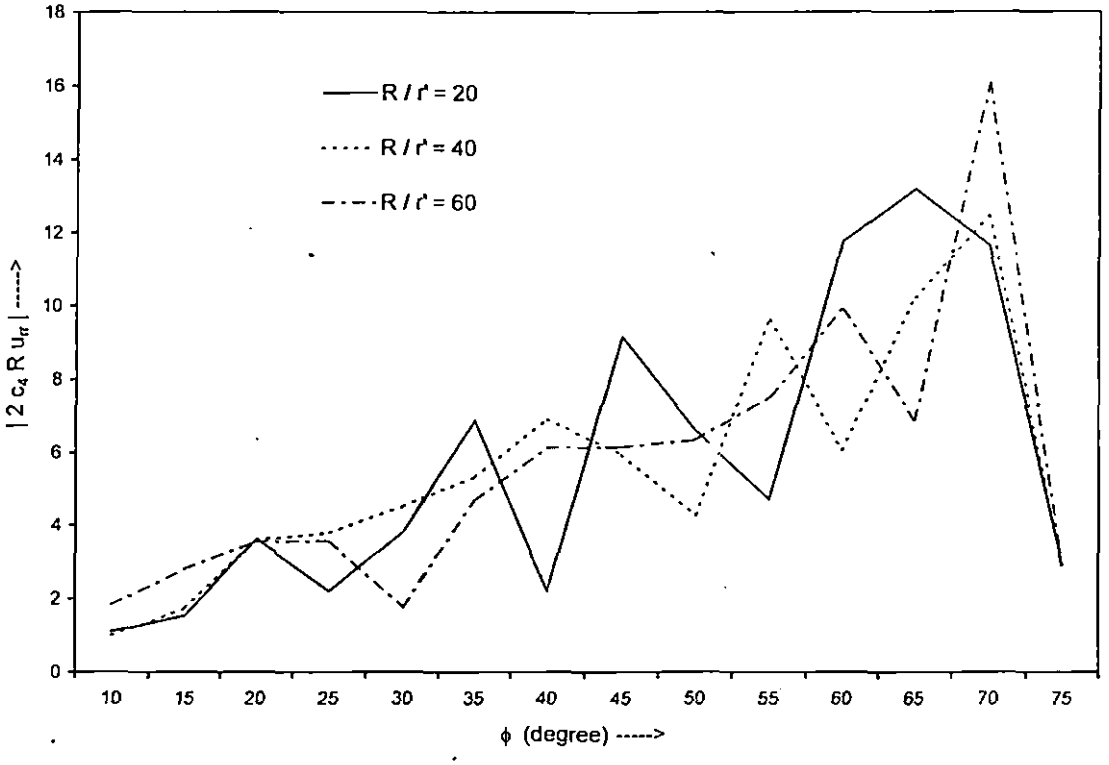

Fig.2. Normalized radial displacement due to radial ring source in graphite-epoxy composite (for $k_2 r' = 2$).

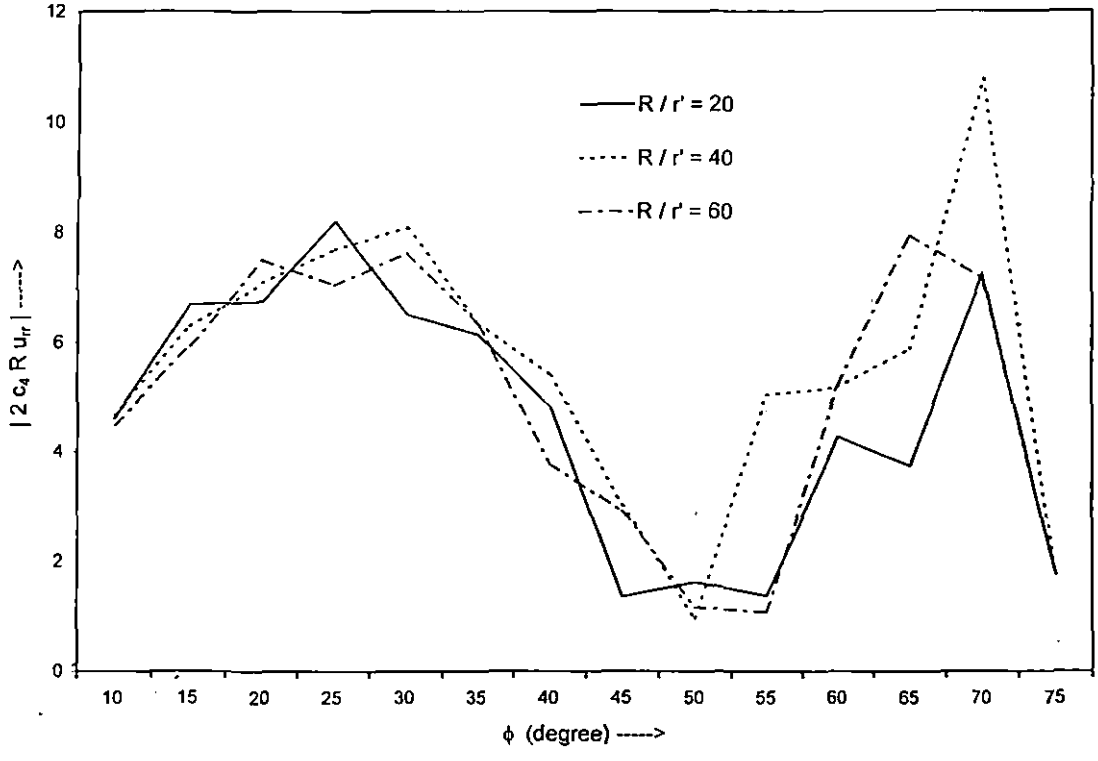

Fig.3. Normalized radial displacement due to radial ring source in graphite-epoxy composite (for $k_2 r' = 8$).

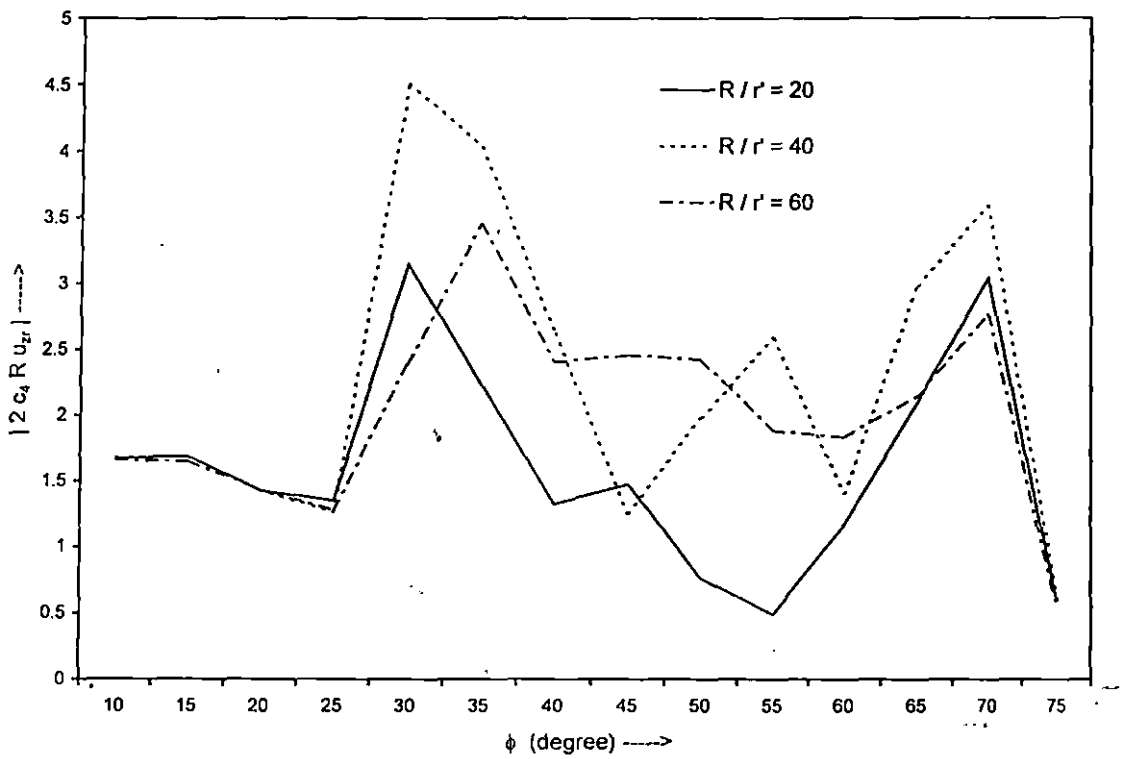

Fig.4. Normalized axial displacement due to radial ring source in graphite-epoxy composite (for $k_2 r' = 2$).

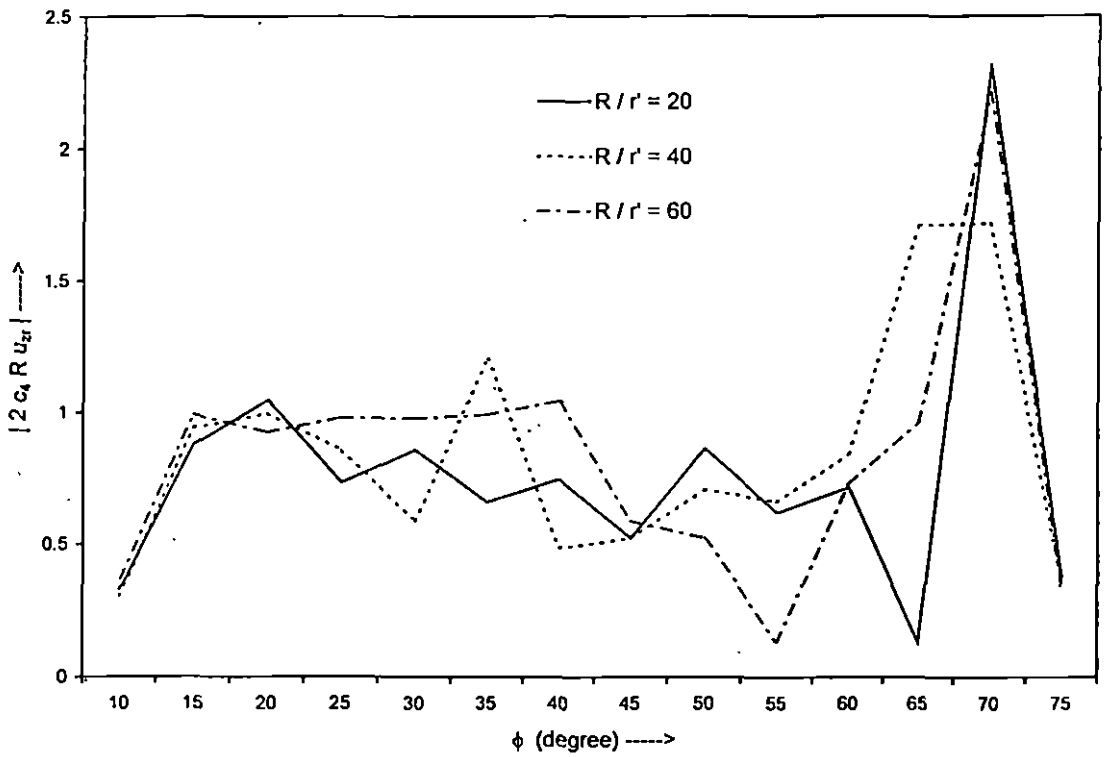

Fig.5. Normalized axial displacement due to radial ring source in graphite-epoxy composite (for $k_2 r' = 8$).

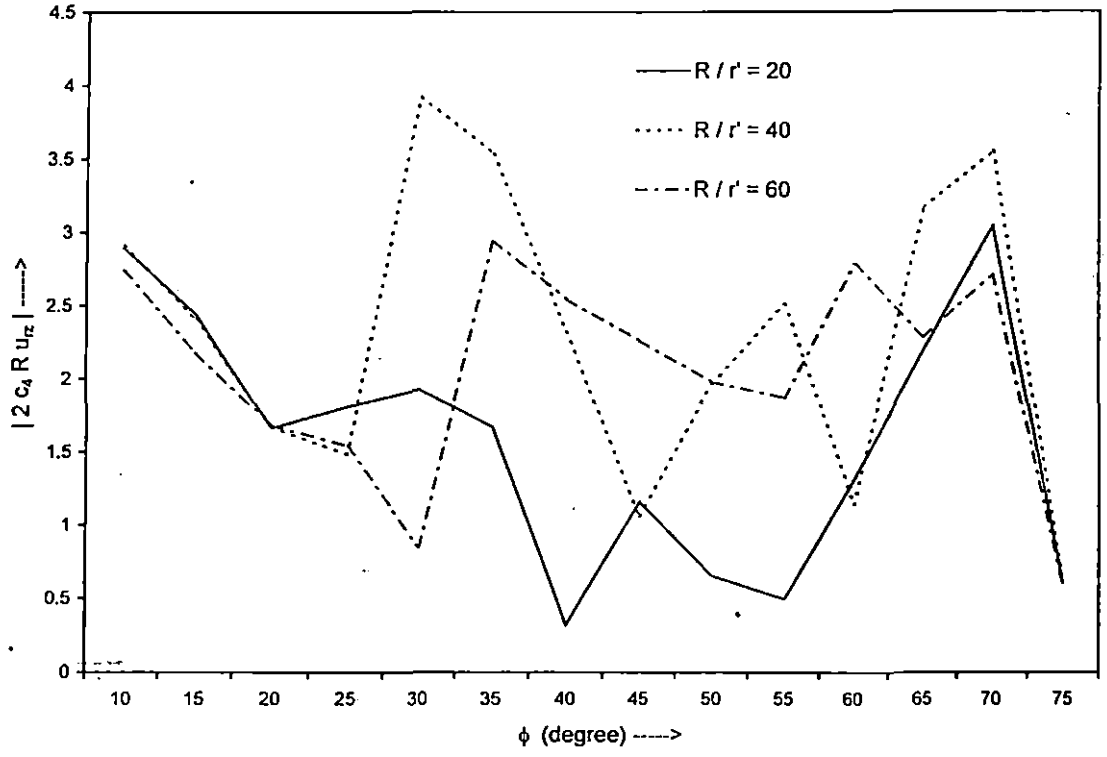

Fig.6. Normalized radial displacement due to axial ring source in graphite-epoxy composite (for $k_2 r' = 2$).

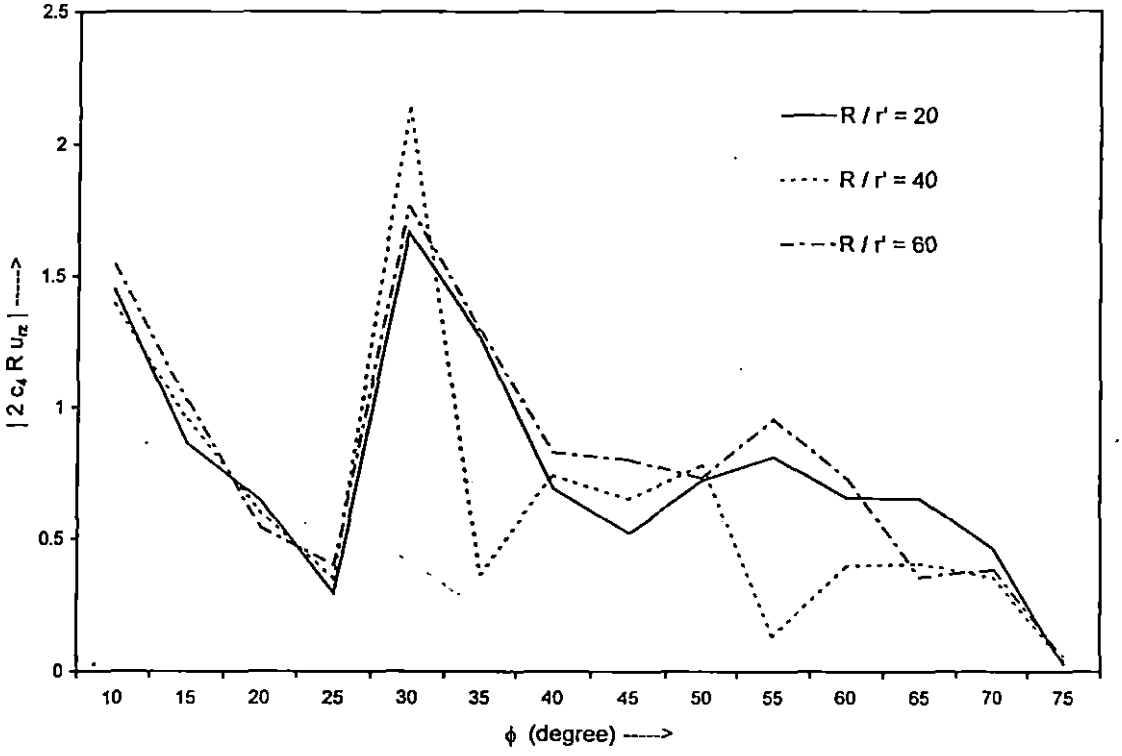

Fig.7. Normalized radial displacement due to axial ring source in graphite-epoxy composite (for $k_2 r' = 8$).

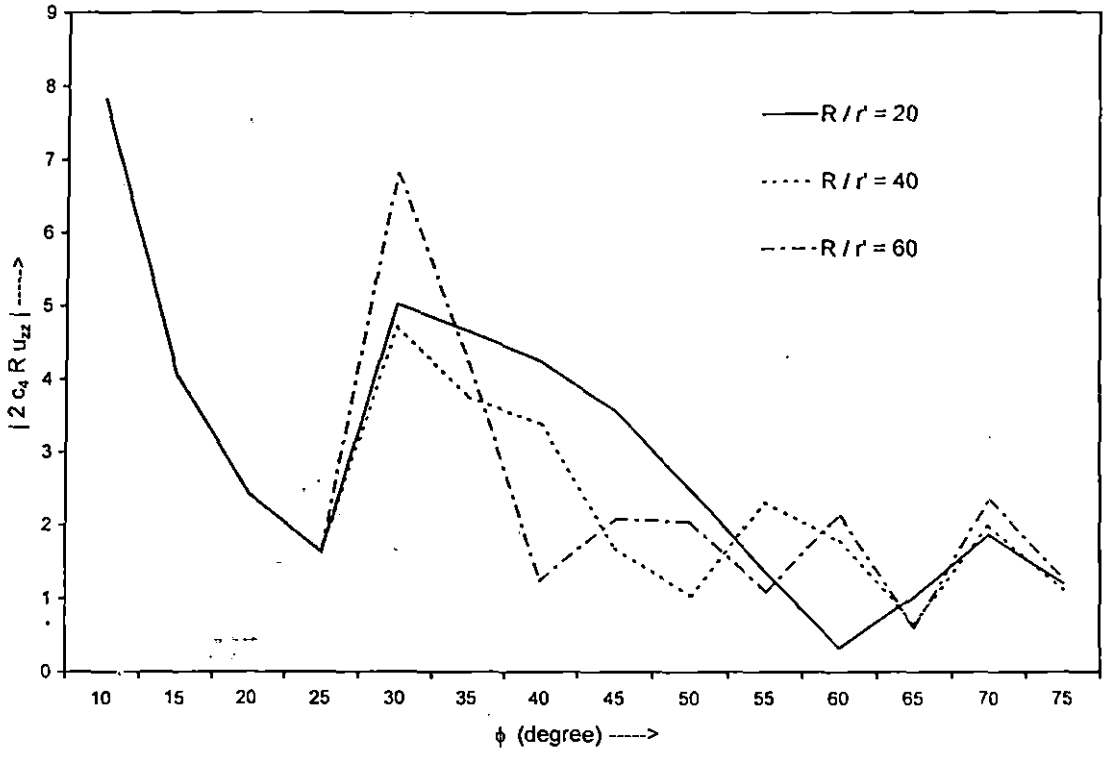

Fig.8. Normalized axial displacement due to axial ring source in graphite-epoxy composite (for $k_2 r' = 2$).

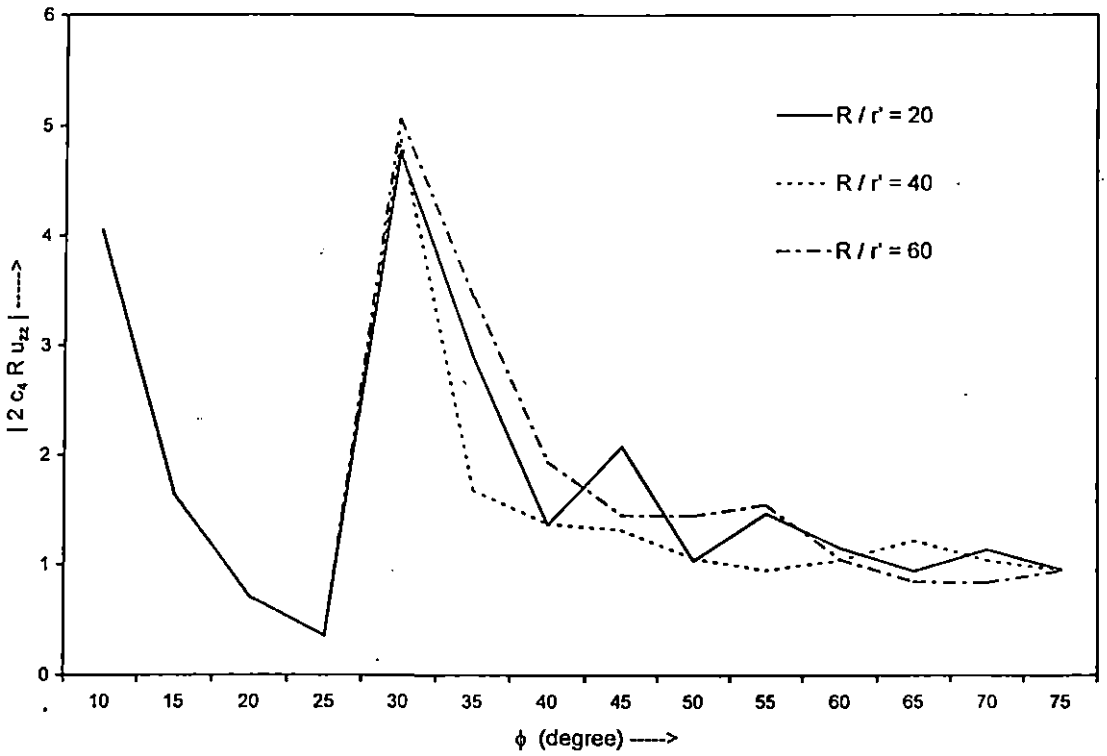

Fig.9. Normalized axial displacement due to axial ring source in graphite-epoxy composite (for $k_2 r' = 8$).

6. TORSIONAL RING SOURCE OF FORCE

For torsional ring source of force , the equation of motion for Green's function $u_\theta(r,z;r',z')$, can be written as

$$G\left(\frac{\partial^2 u_\theta}{\partial r^2}+\frac{1}{r}\frac{\partial u_\theta}{\partial r}-\frac{u_\theta}{r^2}\right)+\mu\frac{\partial^2 u_\theta}{\partial z^2}+\rho\omega^2 u_\theta=-\frac{\delta(r-r')\,\delta(z-z')}{r} \tag{6.1}$$

where u_θ is the tangential component of displacement and μ and G are shear moduli in the θz and $r\theta$ directions respectively. $\frac{\delta(r-r')\,\delta(z-z')}{r}$ represents the torsional ring source, ρ is the material density. The time dependence of all the field quantities, assumed to be of the form exp(-iwt), will be suppressed in the subsequent development.

We use the Fourier transform for the axial co-ordinate, z, and the Hankel transform for the radial co-ordinate, r. The Fourier transform is defined as

$$U_\theta^*(r,\eta;r',z')=\int_{-\infty}^{\infty}U_\theta(r,z;r',z')\,e^{-i\eta z}\,dz \tag{6.2a}$$

$$U_\theta(r,z;r',z')=\frac{1}{2\pi}\int_{-\infty}^{\infty}U_\theta^*(r,\eta;r',z')\,e^{i\eta z}\,d\eta \tag{6.2b}$$

The Hankel transform is defined as

$$\bar{U}_\theta^*(\xi,\eta;r',z')=\int_0^{\infty}U_\theta^*(r,\eta;r',z')\,J_1(\xi r)\,r\,dr \tag{6.3a}$$

$$U_\theta^*(r,\eta;r',z')=\int_0^{\infty}\bar{U}_\theta^*(\xi,\eta;r',z')\,J_1(\xi r)\,\xi\,d\xi \tag{6.3b}$$

where η and ξ are transform parameters.

Applying Fourier and Hankel transform equation (6.1) becomes

$$\bar{U}_\theta^*(\xi,\eta;r',z')=\frac{J_1(\xi r')\,e^{-i\eta z'}}{G[a^2\eta^2+\xi^2-k^2]} \tag{6.4}$$

where

$$\frac{\mu}{G} = a^2 \quad \text{and} \quad \frac{\rho\omega^2}{G} = k^2 . \tag{6.5}$$

Substituting equation (6.4) into equation (6.3b) and then taking Fourier inversion one obtains, using residue theorem

$$U_\theta(r,z;r',z') = \frac{1}{2\mu}\int_0^\infty \frac{e^{-\beta|z-z'|}}{\beta} J_1(\xi r') J_1(\xi r)\xi d\xi \tag{6.6}$$

where

$$\beta = \frac{1}{a}(\xi^2 - k^2)^{1/2} \qquad \text{for } \xi > k \tag{6.7a}$$

$$= -i\frac{1}{a}(k^2 - \xi^2)^{1/2} \qquad \text{for } \xi < k \tag{6.7b}$$

$$= -i\beta_1 \qquad \text{(say)}.$$

7. FAR-FIELD CALCULATIONS AND NUMERICAL RESULTS FOR TORSIONAL RING SOURCE

The integral arising in (6.6) can be evaluated numerically in the near field (small z, and r). However in the far-field the numerical evaluation of this integral is not possible because of the rapid oscillation introduced in the integrand by the Bessel function. For large ξr

$$J_1(\xi r) \approx \frac{1}{\sqrt{2\pi\xi r}}\left[e^{i\xi r - 3\pi i/4} + e^{-i\xi r + 3\pi i/4}\right]. \tag{7.1}$$

Substituting equation (7.1) into equation (6.6), one obtains

$$U_\theta(r,z;r',z') = \frac{e^{-\pi i/4}}{2\mu\sqrt{2\pi r}}\int_0^\infty L(\xi) e^{i\beta_1|z| + i\xi r} d\xi$$

$$- \frac{e^{\pi i/4}}{2\mu\sqrt{2\pi r}}\int_0^\infty L(\xi) e^{i\beta_1|z| - i\xi r} d\xi \tag{7.2}$$

where

$$L(\xi) = \frac{\sqrt{\xi}\, J_1(\xi r')}{\beta_1} . \tag{7.3}$$

So oscillations in the integrand are introduced by the factors of the form $\exp(i\beta_1|z| \pm i\xi r)$. This type of oscillatary integrals can be easily evaluated by the method of stationary phase [1950].

For this purpose we substitute $|z| = R\cos\phi$ and $r = R\sin\phi$ where R, the distance from the centre of the ring source, is taken to be large.

So, $$e^{i\beta_1|z|\pm i\xi r} = e^{iR(\beta_1\cos\phi \pm \xi\sin\phi)} = e^{iRf_1(\xi)} \quad \text{or} \quad e^{iRf_2(\xi)} \tag{7.4}$$

where $$f_j(\xi) = \beta_1\cos\phi - (-1)^j \xi\sin\phi, \quad j=1,2. \tag{7.5}$$

The stationary points can be obtained from $f_1'(\xi) = 0$ and $f_2'(\xi) = 0$. Thus one gets the stationary points ξ_0, where

$$\xi_0 = \pm \frac{k(\sqrt{\mu/G}\tan\phi)}{\sqrt{1+(\mu/G)\tan^2\phi}}. \tag{7.6}$$

If one defines

$$\tan\alpha = \sqrt{\mu/G}\tan\phi \tag{7.7}$$

then equation (7.6) simplifies to

$$\xi_0 = \pm k\sin\alpha. \tag{7.8}$$

One needs to consider only the positive value of ξ_0 since the negative value is not within the limit of the integral, hence

$$u_\theta(r,z;r',0) = \frac{e^{-i\pi/4}}{2\mu R\sqrt{\sin\phi}} \frac{L(\xi_0)}{\sqrt{|f_1''(\xi_0)|}} \exp\left\{iRf_1(\xi_0) + \frac{i\pi}{4}\operatorname{sgn} f_1''(\xi_0)\right\} \tag{7.9}$$

where

$$f_1''(\xi_0) = -\sqrt{\frac{G}{\mu}}\frac{1}{k}\left(1+\frac{\mu}{G}\tan^2\phi\right)^{3/2}\cos\phi. \tag{7.10}$$

Numerical results for normalized displacement $|\mu R u_\theta|$ for torsional ring source at large distances away from the source have been depicted by means of graph for graphite-epoxy composite

material. For this type of material shear modulus μ=7.07 Gpa and shear modulus G=3.50 Gpa whereas density ρ=1578 Kg/m^3. For different values of $k_2 r'$(=5, 20), normalized displacement has been plotted against ϕ where $\phi = \tan^{-1}\frac{r}{|z|}$, shown in Fig.10. It is found that as the frequency increases the displacement becomes stronger near ϕ=0 and diminishes for larger values of ϕ.

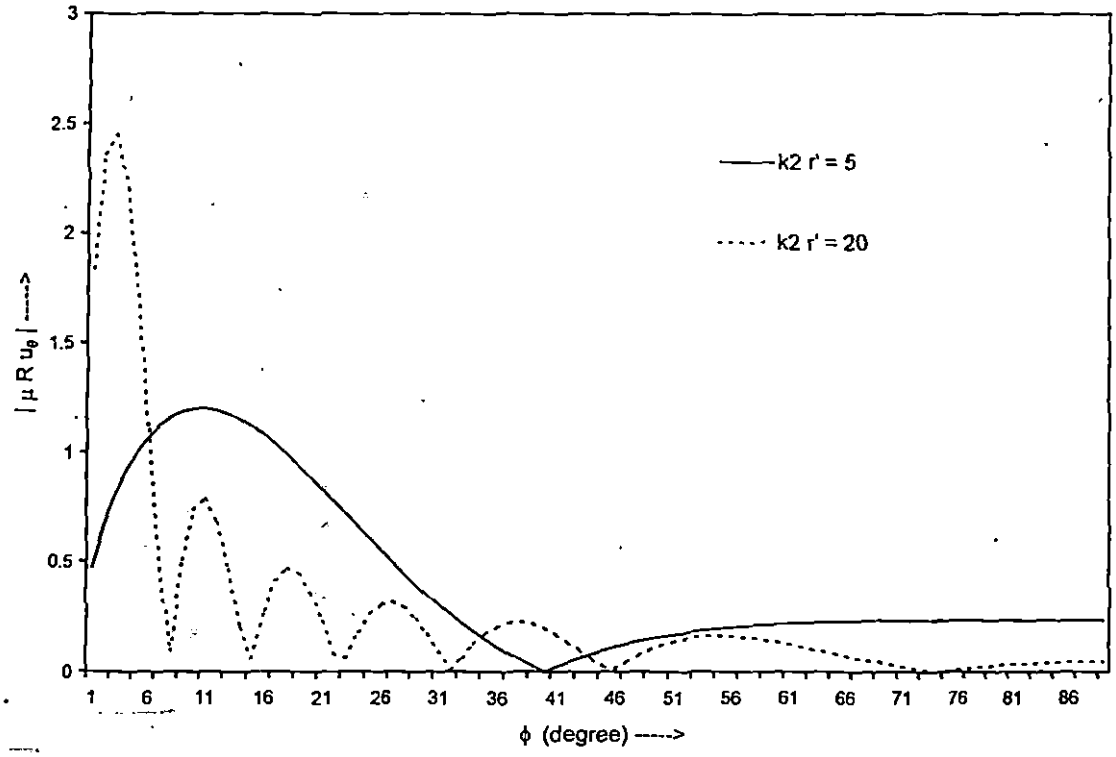

Fig.10. Normalized displacement due to torsional ring source in graphite-epoxy composite.

B I B L I O G R A P G Y

B I B L I O G R A P G Y

1. ACHENBACH, J. D. [1970] :

   Brittle and ductile extension of a finite crack by a horizontally polarized shear wave., Int. J. Engng. Sci., V8, p947.

2. ACHENBACH, J. D. [1972] :

   Dynamic effects in brittle fracture, Mechanics Today., V1, ed. S. Nemat-Nasser, Pergamon Press, New York.

3. ACHENBACH, J. D. [1973] :

   Wave propagation in elastic solids, North-Hollands, Amsterdam.

4. ACHENBACH, J. D. [1975] :

   Wave propagation in elastic solids., North-Holland Publishing Company, Amsterdam -Oxford, American Elsevier Publishing Company, INC., New York.

5. ACHENBACH, J. D. and BAZANT, Z. P. [1975] :

   Elstodynamic near-tip stress and displacement fields for rapidly propagating cracks in orthotropic materials, J. Appl. Mech., V42, p183.

6. ACHENBACH, J. D. [1976] :

   Wave propagation, elastodynamic stress intensity factors and fracture, Theoratical and Applied Mechanics, ed. W. T. Koiter, Proc. 14th IUTAM Congress, North Holland Publishing Co., Amsterdam.

7. ACHENBACH, J. D., ANGEL, Y. C. and LIN, W. [1984] :

Scattering from surface-breaking and near surface-crack. In wave propagation in homogeneous medium and ultrasonic nondestrutive evaluation, G. C. Johnson (ed) 93-109, New York : American Society of Mechanical Engineers, AMD V62.

8. ACHENBACH, J. D., Goutesen, A. K. and McMaken, H. [1982] :

Ray methods for wave in elastic solids with applications to scattering by cracks, Pitman, Boston.

9. ACHENBACH, J. D. and Kuo, M. K. [1986] :

Effect of transverse isotropy on strong ground motion due to strike slip faulting. In Earthquake Source Mechanics, American Geophysical Union, Washington (Edited by S. Das et al) pp111-120.

10. ACHENBACH, J. D., Keer, L. K. and Mendelson, D. A. [1980] :

Elastodynamic analysis of an edge crack. Journal of Appl. Mech., V47, pp551-556.

11. ACHENBACH, J. D., Lin, W. and Keer, L. M. [1983] :

Surface wave due to scattering by a near-surface parallel crack., IEEE Trans. Sonics and Ultrasonics SU-30, pp270-276.

12. ADAMS, G. G. [1980] :

Crack interaction in an infinite elastic strip, Int. J. Engng. Sci., V18, p455.

13. AKI, K. and RICHARDS, P. G. [1980] :

Quantitative seismology; theory and methods, Volume I & II, W. H. Freeman and Company., San Francisco.

14. ANG, D. D. [1958] :

Disertation, California Institute of Technology.

15. ANG, D. and KNOPOFF, L. [1964] :

Diffraction of scalar elastic waves by a finite crack, Proceedings of National Academy of Science., V51, p593.

16. ANGEL, Y. C. and ACHENBACH, J. D. [1985] :

Stress intensity factors for 3-D dynamic loading of a cracked half-space., Journal of Elasticity., V15, pp89-102.

17. ARWIN, K. and ERDOGAN, F. [1971] :

Penny-shaped crack in an elastic layer bonded to dissimilar half-spaces., Int. J. Engng. Sci., V9, p213.

18. ASVESTAS, J. S. and KLEINMAN, R. E. [1970] :

Low frequency scattering by spheriods and discs., I, II and III., J. Inst. Maths. Applics., V6, p42, 57 and 157.

19. ATKINSON, C. and ESHEBLY, J. D. [1968] :

The flow of energy into the tip of a moving crack., Int. J. Frac. Mech., V4, p3.

20. BAKER, B. R. [1962] :

Dynamic stress created by a moving crack., J. Appl. Mech., V24, p449.

21. BOSTROM, A. [1987] :

Elastic wave scattering from an interface crack : Antiplane strain., J. Appl. Mech., V54, p503.

22. BROCK, L. M. and ACHENBACH, J. D. [1973a] :

Dynamic and quasi-static extension of an interface flaw, Developments in Mechanics., Proc. 13th Midwestern Mechanics Conference, V7, p595.

23. BROCK, L. M. and ACHENBACH, J. D. [1973b] :

Extension of an interface flaw under the influence of transient waves., Int. J. Solids Structures, V9, p53.

24. BROCK, L. M. and ACHENBACH, J. D. [1974] :

Rapid tearing along an interface, Z. Angew, Math. Phys., V25, p331.

25. BROCK, L. M. [1975] :

Interface flaw extension under in-plane loadings., Proc. 12th Annual Meeting Soc. Engng. Sci..

26. BUCHWALD, V. T. [1961] :

Rayleigh waves in transversely isotropic medium., Q. J. Mech. Appl. Math., V14, pp293-317.

27. BULLEN, K. E. [1963] :

An introduction to the theory of seismology, University Press, Cambridge.

28. BURRIDGE, R. [1976] :

An influence function for the intensity factor in tensile fracture., Int. J. Engng. Sci., V14, p725.

29. CAGNIARD, L. [1962] :

Reflection and refraction of progressive waves, translated and revised by E. A. Flinn and C. H. Dix, McGraw-Hill Book Co., New York.

30. CAMPRIN, S. [1981] :

A review of wave motion in anisotropic and cracked elastic media; Wave Motion, V3, pp343-392.

31. CARRIER, G. F. [1946] :

The propagation of waves in orthotropic media., Quart. Appl. Maths., V4, p160.

32. CHANG, SHIH-JUNG. [1971] :

Diffraction of plane dilatational waves by a finite crack., Quart. J. Mech. Appl. Math., V24, pp423-443.

33. CHAPLYGIN, S. A. [1950] :

Pressure of a rigid die on an elastic foundation, Collected works., p317 (in Russian).

34. CHEN, E. P. and SIH, G. C. [1975] :

Scattering of plane wave by a propagating crack., J. Appl. Mech., V42, p705.

35. CHEN, E. P. [1978] :

Sudden appearence of a crack in a stretched finite strip., J. Appl. Mech., V45, p277.

36. CRAGGS, J. W. [1960] :

On the propagation of a crack in an elastic - brittle material., J. Mech. Phys. Solids., V8, p66.

37. DAS, A. N. and GHOSH, M. L. [1992] :

Four coplanar Griffith cracks in an infinite elastic medium., Engng. Frac. Mech., V43, pp941-955.

38. DATTA, S. K. [1974] :

Diffraction of SH-waves by an elliptic elastic cylinder., Int. J. Solids Structures., V10, p123.

39. DATTA, S. K. [1979] :

Diffraction of SH-waves by an edge crack., Journal of Appl. Mechanics., V46, pp101-106.

40. DE-HOOP [1958] :

Representation theorems for the displacement in an elastic solid and their application to elastodynamic diffraction theory.

41. DESARKAR, P. K. [1985a] :

The problem of a hot punch in a micropolar elastic solid, Indian J. Pure Appl. Math., V16, p1181.

42. DESARKAR, P. K. [1985b] :

The problem of a circular punch on a micropolar elastic solid., Int. J. Engng. Sci., V23, p599.

43. DHAWAN, G. K. [1973] :

Axisymmetric distribution of thermal stress in a thick plate containing a penny-shaped crack., Indian J. Pure Appl. Math., V4, p205.

44. EMBLEY, G. T. and SIH, G. C. [1971] :

Response of a penny-shaped crack to impact waves., Proceedings of the 12th Midwestern Mech. Conf., V6, p473.

45. ERDOGAN, F. and GUPTA, G. D. [1972] :

On the numerical solution of singular integral equations., Q. Appl. Maths., V29, p525.

46. ERINGEN, A. C. and SUHUBI, E. S. [1975] :

Elastodynamics, Vol. II., Linear theory, Academic Press, New York.

47. ERGUVEN, M. E. [1987] :

The elastic torsion problem for a non-homogeneous and transversely isotropic half-spaces., Acta Mechanica., V37, p151.

48. EWING, W. M., JARDETZKY, W. S. and PRESS, F. [1957] :

Elastic wave in layered media., McGraw Hill Book Co., New York.

49. FOX, L. and GOODWIN, E. T. [1953] :

The numerical solution of non singular linear integral equations., Phil. Trans., Vol. A245, p501.

50. FREUND, L. B. [1973] :

Crack propagation in an elastic solid subjected to general loading-III, stress wave loading., J. Mech. Phys. Solids., V21, p47.

51. FREUND, L. B. [1975] :

Dynamic crack propagation, The Mathematics of Fracture, ed. F. Erdogan, ASME AMD, V19, American Society of Mechanical Engineers, New York.

52. FREUND, L. B. [1976] :

The analysis of elastodynamic crack tip stress fields, Mechanics Today, ed. S. Nemat-Nasser, V11, Pergamon Press, New York.

53. FREUND, L. B. [1990] :

Dynamic Fracture Mechanics, Cambridge University Press.

54. GLADWELL, G. M. L. [1980] :

Contact problems in the classical theory of elasticity, Sfjthoff and Noordhoff, Netherlands.

55. GLAGOLEV, N. I. [1942] :

Elastic stresses along the bottom of a dam, Akademiia nauk, USSER, V34, p181.

56. GOL'DSHTEIN, R. V. [1966] :

On the steady motion of a crack along a straight line boundary between two joined materials., Inzh. Zh. M.T.T., V5, p93.

57. GOL'DSHTEIN, R. V. [1967] :

On surface waves in joined elastic meterials and their relation to crack propagation along the junction, Appl. Maths. Mech., V31, p496.

58. GREEN, A. E. [1949] :

On Boussinesque problem and penny-shaped cracks, Proc. Camb. Phil. Soc., V45, p251.

59. HUDSON, J. A. and KNOPOFF, L. [1964] :

Transmission and reflection of surface waves at a corner, 2. Rayleigh waves (theoretical)., J. Geophys Res., V69, pp281-290.

60. IRWIN, G. R. [1957] :

Analysis of stresses and strains near a crack travelling a plate., J. Appl. Mech., (Trans. ASME), V24, p361.

61. ITOU, S. [1978] :

Dynamic stress concentration around two coplanar Griffith cracks in an infinite elastic medium., J. Appl. Mech., V4, p803.

62. ITOU, S. [1980] :

Transient response of a finite crack in a finite strip with stress free edges strip (Trans ASME), J. Applied Mechanics., V47, p801.

63. ITOU, S. [1980a] :

Transient analysis of stress waves around two coplanar Griffith cracks under impact load., Engng. Frac. Mech., V13, p349.

64. ITOU, S. [1980b] :

Diffraction of antiplane shear wave by two coplanar Griffith cracks in an infinite elastic medium., Int. J. Solid Structures., V16, p1147.

65. JAHANSHAHI, A. [1967] :

A diffraction problem and crack propagation., J. Appl. Mech., V34, p100.

66. JEFFREYS, H. and JEFFREYS, B. S. [1950] :

Methods of Mathematical Physics (Cambridge University Press, Cambridge), 2nd ed., pp505-507.

67. KANNINEN, M. F. [1974] :

A dynamic analysis of unstable crack propagation and arrest in the DCB test specimen., Int. J. Frac., V10, p415.

68. KARIM, M. R. and KUNDU, T. [1988] :

Transient surface response of layered isotropic and anisotropic half-spaces with interface cracks : SH case, International Journal of Fracture, V37, pp245-262.

69. KARP, S. N. and KARAL, F. C. Jr. [1962] :

The elastic field behaviour in the neighbourhood of a crack of arbitrary angle., Com. P. Appl. Math., V.XV, p413.

70. KASSIR, M. K. and TSE, S. [1983] :

Moving Griffith crack in an orthotropic material., Int. J. Engng. Sci., V21, p315.

71. KASSIR, M. K. and BANDYOPADHYAY, K. K. [1983] :

Impact response of a cracked orthotropic medium, J. Appl. Mech., V50, p630.

72. KELLER, J. B. [1958] :

A geometrical theory of diffraction in calculas of vibrations and its applications, V.VIII, McGraw Hill Publishing Co., New York.

73. KOSTROV, B. V. [1964] :

The axisymmetric problem of propagation of a tensile crack, Appl. Math. Mech., V28, p793.

74. KOSTROV, B. V. [1966] :

Unsteady crack propagation for longitudinal shear cracks, Appl. Math. Mech., V30, p1042.

75. KOSTROV, B. V. [1975] :

Crack propagation at variable velocity, Int. J. Frac., V11, p47.

76. KRENK, S. and SCHIMIDT, H. [1982] :

Elastic wave scattering by a circular crack, Phil. Trans. Roy. Soc. (London), V.A308, p167.

77. KUNDU, T. [1987] :

The transient response of two cracks at the interface of a layered half-space, Int. J. Engng. Sci., V25, pp1427-1439.

78. KUNDU, T. [1988] :

International Journal of Solids and Structures, V24, pp27-39.

79. KUNDU, T. and BOSTROM, A. [1991] :

Axisymmetric scattering of a plane longitudinal wave by a circular crack in a transversely isotropic solid, J. Appl. Mech., V58, p595.

80. KUNDU, T. and BOSTROM, A. [1991] :

Axisymmetric scattering of a plane longitudinal wave by a circular crack in a transversely isotropic solid, Journal of Appled Mechanics, V58, pp694-702.

81. KUNDU, T. [1990] :

Scattering of torsional waves by a circular crack in a transversely isotropic solid, J. Acous. Soc. Am., vol.88(4), pp1975-1990.

82. KUO, A. Y. [1982] :

Dynamic analysis of interfacial cracks in composite laminates, Ph.D. Dissertation, Department of Theoretical and Applied Mechanics, University of Illinois at Urbana Champaign.

83. KUO, A. Y. [1984] :

Transient stress intensity factors of an interfacial crack between two dissimilar anisotropic half-spaces, Journal of Applied Mechanics, V51, pp71-76.

84. KUO, M. K. [1992] :

Transient stress intensity factors for a cracked plane strip under antiplane point forces, Int. Journal of Engineering Science, V30, pp199-211.

85. KUO, M. K. and CHENG, S. H. [1991] :

Elastodynamic responses due to antiplane point impact loadings on the faces of an interface crack along dissimilar anisotropic materials, Int. J. Solids and Structures, V28, pp751-768.

86. LI, Z. L., ACHENBACH, J. D., KOMSKY, I. and LEE, Y. C. [1992] :

Reflection and transmission of obliquely incident surface waves by an edge of a quarter space : Theory and experiment., Journal of Appl. Mech., V59, pp348-355.

87. LOEBER, J. F. and SIH, G. C. [1968] :

Diffraction of antiplane shear waves by a finite crack, J. Acou. Soc. America, V44, p90.

88. LU, Y. [1998] :

The elastodynamic Green's function for a torsional ring source, Transactions of the ASME, vol.65, pp566-568.

89. LU, Y. [1999] :

The full-space elastodynamic Green's functions for time-harmonic radial and axial ring source in a homogeneous isotropic medium, Journal of Applied Mechanics, vol.66, pp638-645.

90. MA, C. C. [1989] :

Analysis of dissimilar anisotropic wedges subject to antiplane shear deformation, Int. J. Solids and Structures, V25, pp1295-1309.

91. MAL, A. K. [1968] :

Diffraction of elastic waves by a penny-shaped crack, Qr. Appl. Math., V26, p231.

92. MAL, A. K. [1970a] :

Interaction of elastic waves with a penny shaped crack, Int. J. Engng. Sci., V8, p381.

93. MAL, A. K. [1970b] :

Interaction of elastic waves with a Griffith crack, Int. J. Engng. Sci., V8, p763.

94. MAL, A. K. [1972] :

A note on the low frequency diffraction of elastic waves by a Griffith crack, Int. J. Engng. Sci., V10, p609.

95. MAL, A. K. and KNOPOFF, L. [1968] :

Transmission of Rayleigh waves past a step chang in elevation, Bull. Scis. Soc. Amer., V55, pp319-334.

96. MALMEISTER, A. K., TAMUZH, V. P. and TETERS, G. A. [1972] :

Resistance of rigid polymeric materials, second edition, zinatne, Riga (in Russian).

97. MANDAL, S. C. and GHOSH, M. L. [1992a] :

Diffraction of anti-plane shear wave by a pair of parallel rigid strips at the interface of two bonded dissimilar elastic media, J. Maths. Phys. Sci., V26, p105.

98. MANDAL, S. C. and GHOSH, M. L. [1992b] :

Forced vertical vibration of two rigid strips on a semi-infinite elastic solid, J. Sound Vibration, V156(1), p169.

99. MARKENSCOFF, X. and NI, L. [1984] :

The transient motion of a screw dislocation in an anisotropic medium, Journal of Elasticity, V14, pp93-95.

100. MANOLIS, G. D. and BESKOS, D. E. [1988] :

Boundary Element Methods in Elastodynamics, (UNWIN HYMAN), LONDON.

101. MATCZYNSKI, M. [1973] :

Quasi-static problem of a crack in an elastic strip to antiplane state of strain, Arch. Mech. Stosow., V25, p851.

102. MAU, A. W. [1953] :

Die beugung elastischer wellen an der halbebene, Z Angew Math., V33, pp1-10.

103. MAU, A. W. [1954] :

Die entspannuangswelle bei plot-zlichen einschnitt eines gespannten elastischen korpers, ZAMM, V34, p1.

104. MCMAKEN, H. [1984] :

A uniform theory of diffraction for elastic solids, J. Acoust. Soc. Am., V75, pp1352-1359.

105. MILLER, M. K. and GUY, W. T. [1966] :

Numerical inversion of the Laplace transform by use of Jacobi polynomials, J. Numer. Anal., V3, p624.

106. MOSSAKOVSKII, V. I. [1958] :

Pressure of a circular die (punch) on an elastic half-space, whose modulus of elasticity is an exponential function of depth, J. Appl. Math. Mech., V22, p168.

107. MUSHKELISHVILLI, N. I. [1953] :

Singular integral equations (Ch.13) English Translation, Noordhoff.

108. MUSHKELISHVILLI, N. I. [1963] :

Some basic problems of the mathematical theory of elasticity, Noordhoff Ltd., Groningen.

109. NAYFEN, A. H. [1995] :

Wave propagation in layered anisotropic media with applications to composite, Elesevier.

110. NEERHOFF, F. L. [1979] :

Diffraction of Love waves by a stress-free crack of finite width in the plane interface of a layered composite, Appl. Sci. Res., V35, p237.

111. NIWA and HIROSE [1986] :

Application of the BEM to elastodynamics in a three dimensional half-space. In recent applications in computational mechanics, D. L. Karabalis (ed)., 1-15, New York, American Society of Civil Engineers.

112. NOBLE, B. [1958] :

Methods based on the Wiener-Hopf technique, New York, Pergamon Press, p48.

113. NOBLE, E. B. [1963] :

The solution of Bessel function dual integral equations by a multiplying-factor method., Proc. Camb. Philos., V59, p351.

114. OLESIAK, Z. and SNEDDON, I. N. [1959] :

The distribution of thermal stresses in an infinite elastic solid containing a penny-shaped crack., Arch. Rat. Mech. Anal., V4, p238.

115. OROWAN, E. [1948] :

Fracture and strength of solids, Reports on progress in Physics, V12, p185.

116. PAL, S. C. and GHOSH, M. L. [1990] :

High frequency scattering of antiplane shear waves by an interface crack., Indian J. Pure Appl. Math., V21, pp1107-1124.

117. PAL, S. C. and GHOSH, M. L. [1993] :

High frequency scattering of plane horizontal shear waves by a Griffith crack propagating along the bimaterial interface., Engng. Fracture Mech., V45, pp105-118.

118. PALAIYA, R. M. and MAJUMDER, P. [1981] :

Interaction of anti-plane shear waves by rigid strips lying at the interface of two bonded dissimilar elastic half-spaces, ZAMM, V16, p120.

119. PAUL, H. S. and SRIDHARAN, K. [1980a] :

The penny-shaped crack problem in Micropolar Elasticity, Int. J. Engng. Sci., V18, p651.

120. PAUL, H. S. and SRIDHARAN, K. [1980b] :

The penny-shaped crack problem in Micropolar Elasticity, Int. J. Engng. Sci., V18, p1431.

121. PILANT ,WALTER L.[1979] :

Elastic waves in the earth , Elsevier Scientific Publishing Co. Amsterdam-Oxford, New York.

122. PIPES, R. B. and PAGANO, N. J. [1970] :

Interlaminar stresses in laminates under uniform axial extension , J. of composite Materials, V4, pp538-548.

123. ROBERTSON, I. A. [1967] :

Diffraction of a plane longitudinal wave by a penny-shaped crack , Proc.Camb. Phil. Soc., V63, p229.

124. ROY, A. [1982a] :

Diffraction of elastic waves by an elliptical crack, Comunicaciones Tecnicas del II MAS-UNAM, Serie Naranja, No. 299.

125. ROY, A. [1982b] :

Low frequency scalar diffraction by hard elliptic disc , Comunicaciones Tecnicas del II MAS-UNAM, Serie Naranja, No. 301.

126. ROY, A. : [1982c]

Scattering of plane elastic waves by an elliptical crack, Comunicaciones Tecnicas del II MAS-UNAM, Serie Naranja, No. 307.

127. ROY, A. and SABINA, F. J. [1982] :

Low frequency acoustic diffraction by a soft disc, J. Accoust. Soc., V73, p1494.

128. SACK, R. A. [1946] :

Extension of Griffith's theory of rupture to three dimensions, Proc. Phy. Sco., V58, p729.

129. SARKAR, J., MANDAL, S. C. and GHOSH, M. L. [1994a] :

Interaction of elastic waves with two co-planar Griffith cracks in an orthotropic medium, Engng. Frac. Mech., V49, pp411-425.

130. SATO, R. [1961] :

J. Phys. Earth., V9, p19.

131. SCHMIDT, H. and KRENK, S. [1982] :

Asymmetric vibrations of a circular elastic plate on an elastic half- space, Int. J. Solids Structures, vol.18, No.2, pp91-105.

132. SENIOR, T. B. A. [1971] :

Low frequency scattering by a finite cone, Appl. Sci. Res., V23, p459.

133. SHINDO, Y. [1981] :

Normal compression waves scattering at a flat annular crack in an infinite elastic solid, Quart. Appl. Math., V.XXIX, p305.

134. SHINDO, Y., NOZAKI, H. and HIGAKI, H. [1986] :

Impact response of a finite crack in an orthotropic strip, Acta Mechanica, V62, p87.

135. SIH, G. C. [1977] :

Elastodynamic crack problems in mechanics and fracture, V4, Noordhoff Leyden.

136. SIH, G. C. and LOEBER, J. F. [1968] :

Torsional vibration of an elastic solid containing a penny-shaped crack, J. Accous. Soc. A., V44, p1237.

137. SIH, G. C. and LOEBER, J. F. [1969] :

Wave propagation in an elastic solid with a line of discontinuity or finite crack, Quart. Appl. Math., V27, p193.

138. SIH, G. C. and LOEBER, J. F. [1970] :

Interaction of horizontal shear waves with a running crack, J. Appl. Mech., V37, p324.

139. SIH, G. C. [1972] :

Proceedings of an International Conference on Dynamic crack propagation, Noordhoff International Publishing, Netherlands.

140. SIH, G. C., EMBLEY, G. T. and RAVERA, R. S. [1972] :

Impact response of a plane crack in extension, Int. J. Solids Structures, V8, p977.

141. SIH, G. C. and CHEN, E. P. [1980] :

Normal and shear impact of layered composite with a crack dynamic stress intensification, J. Appl. Mech., V47, p351.

142. SINGH, B. M. and DHALIWAL, R. S. [1984] :

Closed form solutions of dynamic punch problems by integral transform method, ZAMM, V64, p31.

143. SLEEMAN, B. D. [1967] :

The low frequency scalar diffraction by an elliptic disc, Proc. Camb. Phil. Soc., V63, p1273.

144. SNEDDON, I. N. and LOWENGRUB, M. [1969] :

Crack problems in the theory of elasticity, Wiley, New York.

145. SPENCE, D. A. [1968] :

Self similar solutions to adhesive contact problems with incremental loading, Proc. Roy. Soc. Ser., V305, p55.

146. SPENCE, D. A. [1975] :

The Hertz contact problem with finite function, Journal of Elasticity, V5, p297.

147. SRIVASTAVA, K. N. and LOWENGRUB, M. [1968] :

Finite Hilbert transform technique for triple integral equations with trigonometric kernals, Proc. Roy. Soc. Edinb., p309.

148. SRIVASTAVA, K. N., PALAIYA, R. M. and KARAULIA, D. S. [1980a] :

Interaction of anti-plane shear waves by a Griffith crack at the interface of two bonded dissimilar elastic half-spaces, Int. J. Frac., V4, p349.

149. SRIVASTAVA, K. N., PALAIYA, R. M. and KARAULIA, D. S. [1980b] :

Interaction of torsional wave by a penny shaped crack at the interface of two bonded dissimilar elastic solids, Z. Angew. Math. Mech., V59, p731.

150. SRIVASTAVA, K. N., PALAIYA, R. M. and KARAULIA, D. S. [1983] :

Interaction of shear waves with two coplanar Griffith cracks situated in an infinitely long elastic strip, Int. J. of Fracture, V23, pp3-14.

151. SRIVASTAVA, K. N., GUPTA, O. P. and PALAIYA, R. M. [1981] :

Interaction of elastic waves with a Griffith crack situated in an infinitely long strip, ZAMM, V61, p583.

152. TAI, W. H. and LI, K. R. [1987] :

Elastodynamic response of a finite strip with two coplanar cracks under impact load, Engng. Fracture Mechanics, V27, p379.

153. TAIT, R. J. and MOODIE, T. B. [1981] :

Complex variable methods and closed form solutions to dynamic crack and punch problems in the classical theory of elasticity, Int. J. Engng. Sci., V19, p221.

154. TAKEI, M., SHINDO, Y. and ATSUMI, A. [1982] :

Diffraction of transient horizontal shear waves by a finite crack at the interface of two bonded dissimilar elastic solids, Engng. Frac. Mech., V16, p799.

155. THAU, S. A. and LU, T. H. [1970] :

Diffraction of transient horizontal shear waves by a finite crack and a finite rigid ribbon, Int. J. Engineering Science, V8, pp857-874.

156. THAU, S. A. and LU, T. H. [1971] :

Transient stress intensity factors for a crack in an elastic solid caused by a dilatational wave, Int. J. Solids Structures, V7, p731.

157. TRANTER, C. J. [1968] :

Bessel functions with some physical applications, The English University Press Ltd., London.

158. TRICOMI, F. G. [1951] :

On the finite Hilbert transformation, Quart. J. Math., V2, p199.

159. UEDA, S., SHINDO, Y. and ATSUMI, A. [1983] :

Torsional impact response of a penny shaped crack lying on a bimaterial interface, Engng. Frac. Mech., V18, p1059.

160. UFLIAND, I. A. S. [1956] :

The contact problem of the theory of elasticity for a die, circular in its plane in the presence of adhesion, Prinkl. Math. Mech., V20, p578.

161. VAN DER HIJDEN, J. H. M. T. and NEERHOFF, F. L. [1984a] :

Scattering of elastic waves by a plane crack of finite width, J. Appl. Mech., V51, pp646-651.

162. VAN DER HIJDEN, J. H. M. T. and NEERHOFF, F. L. [1984b] :

Diffraction of elastic waves by a sub-surface crack (in plane motion), J. Acoust. Soc. Am., V75, pp1694-1704.

163. VISWANATHAN, K. and SHARMA, J. P. [1978] :

On the Matched Asymptotic solution of the diffraction of a plane elastic wave by a semi-infinite rigid boundary of finite width, Proc. IUTAM Symposium on modern problems in elastic wave propagation, Eds. J. Miklowitz and J. D. Achenbach (Wiley, New York).

164. VISWANATHAN, K., SHARMA, J. P. and DATTA, S. K. [1982] :

On the Matched Asymptotic solution to the diffraction of a plane elastic waves by a semi-infinite boundary of finite width, Wave Motion, V4, p1.

165. WICKHAM, G. R. [1980] :

Short wave radiation from a rigid strip in smooth contact with a semi-infinite elastic solid, Quart. J. Mech. & Appl. Maths., V33, pp409-433.

166. WILLIAMS, M. L. [1957] :

On the stress distribution at the base of a stationary crack, J. Appl. Mech., V24, p109.

167. WILLIAMS, M. L. [1961] :

The bending stress distribution at the base of a stationary crack, J. Appl. Mech., V28, p78.

168. WILLIS, J. R. [1967] :

A comparision of the fracture criteria of Griffith and Barenblatt, J. Mech. Phys. Solids, V15, p151.

169. YOFFE, E. H. [1951] :

The moving Griffith crack, Philosophical Magazine, V42, p739.

170. ZHANG, CH. and ACHENBACH, J. D. [1988] :

Scattering of body waves by an inclined surface-breaking crack, Ultrasonics, V26, pp132-138.

-----x-----

Eur. J. Mech. A/Solids 18 (1999) 1013–1026

High frequency scattering due to a pair of time-harmonic antiplane forces on the faces of a finite interface crack between dissimilar anisotropic materials

Ramkrishna Pramanik [a], Subhas Chandra Pal [b], Mohan Lal Ghosh [a]

[a] *Department of Mathematics, University of North Bengal, Dist. Darjeeling, 734430, West Bengal, India*
[b] *Computer Centre, University of North Bengal, Dist. Darjeeling, 734430, West Bengal, India*

(Received 28 September 1998; revised 5 March 1999)

Abstract – The high-frequency elastodynamic problem involving the excitation of an interface crack of finite width lying between two dissimilar anisotropic elastic half-planes has been analyzed. The crack surface is excited by a pair of time-harmonic antiplane line sources situated at the middle of the cracked surface. The problem has first been reduced to one with the interface crack lying between two dissimilar isotropic elastic half-planes by a transformation of relevant co-ordinates and parameters. The problem has then been formulated as an extended Wiener–Hopf equation (cf. Noble, 1958) and the asymptotic solution for high-frequency has been derived. The expression for the stress intensity factor at the crack tips has been derived and the numerical results for different pairs of materials have been presented graphically. © 1999 Éditions scientifiques et médicales Elsevier SAS

crack in anisotropic media / high frequency scattering / Wiener–Hopf technique

1. Introduction

The extensive use of composite materials in modern technology has created interest among the scientists for carrying on considerable research work in the modeling, testing and analysis of laminated media. The laminated composites which behave as anisotropic material may be weakened by interface flaws which can lead to serious degradation in load carrying capacity.

Neerhoff (1979), therefore, studied the diffraction of Love waves by a crack of finite width at the interface of a layered half-space. Kuo (1992) carried out numerical and analytical studies of transient response of an interfacial crack between two dissimilar orthotropic half-spaces. Kuo and Cheng (1991) studied the elastodynamic responses due to antiplane point impact loading on the faces of a semi-infinite crack lying at the interface of two dissimilar anisotropic elastic materials. The problem of diffraction of normally incident antiplane shear wave by a crack of finite width situated at the interface of two bonded dissimilar isotropic elastic half-spaces has been studied by Pal and Ghosh (1990).

In the present paper we are interested in finding the high-frequency solution of the diffraction of elastic waves by a Griffith crack of finite width excited by a pair of time-harmonic concentrated antiplane line loads situated at the centres of the cracked surfaces. The materials are assumed to possess certain material symmetry and the crack plane is assumed to coincide with one of the planes of material symmetry, so that the inplane and the antiplane motion are not coupled.

The high-frequency solution of the diffraction of elastic waves by a crack of finite size is interesting in view of the fact that the transient solution close to the wave front can be represented by an integral of the high-frequency component of the solution. The analysis of the paper is first based on the observation of several researchers, e.g., Achenbach and Kuo (1986), Ma and Hou (1989), Markenscoff and Ni (1984) that antiplane shear deformation in an anisotropic solid can be deduced from the corresponding deformations of an isotropic

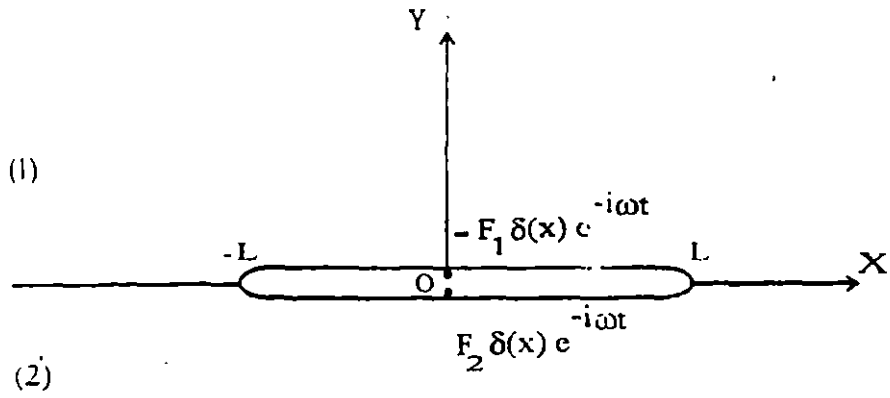

Figure 1. Geometry of the problem.

solid by a transformation of relevant co-ordinates and parameters. Based on this observation, analysis of the interface crack by line loads between two bonded dissimilar anisotropic elastic solids can first be converted to that of a crack between two dissimilar isotropic elastic materials. Later, following the method of Chang (1971), the problem has been formulated as an extended Wiener–Hopf equation. The Wiener–Hopf equation in brief can be found in the book of Achenbach (1973). The asymptotic solutions for high-frequencies or for wave lengths short compared to the width of the crack have been derived. Expression for the dynamic stress intensity factor near the crack tips has been obtained and the results have been illustrated for different pairs of materials.

2. Formulation of the problem

Let (X, Y, Z) be rectangular Cartesian co-ordinates. The X-axis is taken along the interface, Y-axis vertically upwards into the medium and Z-axis is perpendicular to the plane of the paper. Let an open crack of finite width $2L$ be located at the interface of two bonded dissimilar anisotropic semi-infinite elastic solids lying parallel to X-axis. The anisotropic half-planes are characterized by the elastic moduli $(C_{ik})_j$; $(i, k = 4, 5)$ and mass density $\bar{\rho}_j$. The subscript j $(j = 1, 2)$ corresponds to the upper and lower semi-infinite media respectively.

A pair of concentrated time-harmonic antiplane shear forces in the Z-direction of magnitudes F_1 and F_2 act on the crack faces $Y = 0+$ and $Y = 0-$ respectively at $X = 0$ as shown in *figure 1*. Thus the crack boundary conditions are

$$\sigma_{YZ}(X, Y, t) = \begin{cases} -F_1\delta(X)\,e^{-i\omega t}; & |X| < L,\ Y = 0+, \\ F_2\delta(X)\,e^{-i\omega t}; & |X| < L,\ Y = 0-, \end{cases} \tag{1}$$

$$\sigma_{YZ}^{(1)}(X, Y, t) = \sigma_{YZ}^{(2)}(X, Y, t) \quad \text{at } Y = 0,\ |X| > L \tag{2}$$

and

$$W_1(X, Y, t) = W_2(X, Y, t) \quad \text{at } Y = 0,\ |X| > L, \tag{3}$$

where ω is the circular frequency. Two dimensional antiplane wave motions of homogeneous anisotropic linearly elastic solids are governed by

$$(C_{55})_j \frac{\partial^2 W_j}{\partial X^2} + 2(C_{45})_j \frac{\partial^2 W_j}{\partial X \partial Y} + (C_{44})_j \frac{\partial^2 W_j}{\partial Y^2} = \bar{\rho}_j \frac{\partial^2 W_j}{\partial t^2} \quad (j = 1, 2), \tag{4}$$

where $W_j(X, Y, t)$ are the out-of-plane displacements.

The XY-plane has been assumed to coincide with one of the planes of material symmetry such that inplane and anti-plane motions are not coupled.

The relevant stress components are

$$\sigma_{XZ}^{(j)} = (C_{55})_j \frac{\partial W_j}{\partial X} + (C_{45})_j \frac{\partial W_j}{\partial Y}, \tag{5}$$

$$\sigma_{YZ}^{(j)} = (C_{45})_j \frac{\partial W_j}{\partial X} + (C_{44})_j \frac{\partial W_j}{\partial Y}. \tag{6}$$

Following Achenbach and Kuo (1986) and Kuo and Cheng (1991) we introduce a co-ordinate transformation

$$\left.\begin{aligned} x &= X - \frac{(C_{45})_j}{(C_{44})_j} Y, \\ y &= \frac{\mu_j}{(C_{44})_j} Y, \\ z &= Z, \end{aligned}\right\} \quad (j = 1, 2) \tag{7}$$

where

$$\mu_j = \left[(C_{44})_j (C_{55})_j - (C_{45})_j^2\right]^{1/2} \quad (j = 1, 2). \tag{8}$$

Equation (7) and the chain rule of differentiation reduced (4) to the standard wave equation

$$\frac{\partial^2 W_j}{\partial x^2} + \frac{\partial^2 W_j}{\partial y^2} = s_j^2 \frac{\partial^2 W_j}{\partial t^2}, \tag{9}$$

where

$$s_j^2 = \frac{\rho_j}{\mu_j} \quad \text{and} \quad \rho_j = \frac{\bar{\rho}_j (C_{44})_j}{\mu_j}, \tag{10}$$

s_j is the slowness of shear waves. Without loss of generality we assume that

$$s_1 < s_2. \tag{11}$$

Assume

$$W_j(x, y, t) = w_j(x, y)\, e^{-i\omega t}, \quad j = 1, 2, \tag{12}$$

so that $w_j(x, y)$ satisfy the following Helmholtz equations

$$\nabla^2 w_j(x, y) + k_j^2 w_j(x, y) = 0, \quad j = 1, 2, \tag{13}$$

with

$$\nabla^2 = \frac{\partial^2}{\partial x^2} + \frac{\partial^2}{\partial y^2} \quad \text{and} \quad k_j = \omega s_j, \ j = 1, 2.$$

It follows from Eq. (11) that $k_2 > k_1$.

It is easily verified from (4), (5) and (6) that the relevant displacement and the stress component in a physical anisotropic solid are related to those in the corresponding isotropic solid by

$$W_j(X, Y, t) = W_j(x, y, t), \tag{14}$$

$$\sigma_{XZ}^{(j)}(X, Y, t) = \frac{\mu_j}{(C_{44})_j}\sigma_{xz}^{(j)}(x, y, t) + \frac{(C_{45})_j}{(C_{44})_j}\sigma_{yz}^{(j)}(x, y, t), \tag{15}$$

$$\sigma_{YZ}^{(j)}(X, Y, t) = \sigma_{yz}^{(j)}(x, y, t). \tag{16}$$

Further writing

$$\sigma_{yz}^{(j)}(x, y, t) = \tau_{yz}^{(j)}(x, y)\,e^{-i\omega t}, \quad j = 1, 2, \tag{17}$$

under the changed co-ordinate system the boundary conditions (1), (2) and (3) reduce to

$$\tau_{yz}^{(1)}(x, y) = \mu_1\frac{\partial w_1}{\partial y} = -F_1\delta(x); \quad |x| < L,\ y = 0+, \tag{18}$$

$$\tau_{yz}^{(2)}(x, y) = \mu_2\frac{\partial w_2}{\partial y} = F_2\delta(x); \quad |x| < L,\ y = 0- \tag{19}$$

and

$$\mu_1\frac{\partial w_1}{\partial y} = \mu_2\frac{\partial w_2}{\partial y}, \quad |x| > L,\ y = 0, \tag{20}$$

$$w_1(x, 0+) = w_2(x, 0-), \quad |x| > L. \tag{21}$$

To obtain the solutions to the wave equations (13), introduce the Fourier transform defined by

$$\bar{w}(\alpha, y) = \frac{1}{\sqrt{2\pi}}\int_{-\infty}^{\infty} w(x, y)\,e^{i\alpha x}\,dx. \tag{22}$$

The transformed wave equations are

$$\frac{d^2\bar{w}_1}{dy^2} - (\alpha^2 - k_1^2)\bar{w}_1(\alpha, y) = 0, \quad y \geqslant 0, \tag{23}$$

$$\frac{d^2\bar{w}_2}{dy^2} - (\alpha^2 - k_2^2)\bar{w}_2(\alpha, y) = 0, \quad y \leqslant 0. \tag{24}$$

The solutions of (23) and (24) which are bounded as $y \to \infty$ are

$$\bar{w}_1(\alpha, y) = A_1(\alpha)\,e^{-\gamma_1 y}; \quad y \geqslant 0, \tag{25}$$

$$\bar{w}_2(\alpha, y) = A_2(\alpha)\,e^{\gamma_2 y}; \quad y < 0, \tag{26}$$

where

$$\gamma_j = \begin{cases} (\alpha^2 - k_j^2)^{1/2}; & |\alpha| > k_j, \\ -i(k_j^2 - \alpha^2)^{1/2}; & |\alpha| < k_j. \end{cases} \tag{27}$$

Introduce, for a complex α

$$G_+(\alpha)=\frac{1}{\sqrt{2\pi}}\int_L^\infty \tau_{yz}^{(1)}(x,0)\,e^{i\alpha(x-L)}\,dx, \tag{28}$$

$$G_-(\alpha)=\frac{1}{\sqrt{2\pi}}\int_{-\infty}^{-L} \tau_{yz}^{(1)}(x,0)\,e^{i\alpha(x+L)}\,dx, \tag{29}$$

$$G_j(\alpha)=\frac{1}{\sqrt{2\pi}}\int_{-L}^{L} \tau_{yz}^{(j)}(x,0)\,e^{i\alpha x}\,dx. \tag{30}$$

The transformed stress at the interface $y=0$ can therefore be written as

$$\bar{\tau}_{yz}^{(j)}(\alpha,0)=G_+(\alpha)\,e^{i\alpha L}+G_-(\alpha)\,e^{-i\alpha L}+G_j(\alpha). \tag{31}$$

Using the boundary conditions (18) and (19), we get

$$G_j(\alpha)=(-1)^j\frac{F_j}{\sqrt{2\pi}}\quad (j=1,2). \tag{32}$$

Now

$$\bar{\tau}_{yz}^{(1)}(\alpha,0+)=\mu_1\frac{\partial\bar{w}_1(\alpha,0+)}{\partial y}=-\mu_1\gamma_1A_1(\alpha), \tag{33}$$

$$\bar{\tau}_{yz}^{(2)}(\alpha,0-)=\mu_2\frac{\partial\bar{w}_2(\alpha,0-)}{\partial y}=\mu_2\gamma_2A_2(\alpha). \tag{34}$$

Using (33) and (34), Eq. (31) can be written in the form

$$(-1)^j\mu_j\gamma_jA_j(\alpha)=G_+(\alpha)\,e^{i\alpha L}+G_-(\alpha)\,e^{-i\alpha L}+(-1)^j\frac{F_j}{\sqrt{2\pi}}.$$

Therefore,

$$A_j(\alpha)=\frac{(-1)^j}{\mu_j\gamma_j}\left[G_+(\alpha)\,e^{i\alpha L}+G_-(\alpha)\,e^{-i\alpha L}+(-1)^j\frac{F_j}{\sqrt{2\pi}}\right]. \tag{35}$$

Now

$$\bar{w}_1(\alpha,0+)-\bar{w}_2(\alpha,0-)=\frac{1}{\sqrt{2\pi}}\int_{-L}^{L}\{w_1(x,0+)-w_2(x,0-)\}\,e^{i\alpha x}\,dx=B(\alpha),\quad \text{say}$$

which is the measure of the displacement discontinuity across the crack surface. Therefore

$$B(\alpha)=A_1(\alpha)-A_2(\alpha). \tag{36}$$

Substituting the values of $A_j(\alpha)$ from (35) in Eq. (36) one finds an extended Wiener–Hopf equation namely

$$G_+(\alpha)\,e^{i\alpha L}+G_-(\alpha)\,e^{-i\alpha L}+B(\alpha)K(\alpha)=\frac{K(\alpha)}{\sqrt{2\pi}}\left\{\frac{F_1}{\mu_1\gamma_1}-\frac{F_2}{\mu_2\gamma_2}\right\}, \tag{37}$$

where

$$K(\alpha)=\frac{\mu_1\mu_2\gamma_1\gamma_2}{\mu_1\gamma_1+\mu_2\gamma_2}=\frac{\mu_1\mu_2(\alpha^2-k_1^2)^{1/2}}{\mu_1+\mu_2}R(\alpha) \tag{38}$$

and

$$R(\alpha)=\frac{(\mu_1+\mu_2)(\alpha^2-k_2^2)^{1/2}}{\mu_1(\alpha^2-k_1^2)^{1/2}+\mu_2(\alpha^2-k_2^2)^{1/2}}. \tag{39}$$

In order to obtain the high-frequency solution of the Wiener–Hopf equation given by (37) one assumes that the branch points $\alpha=k_1$ and $\alpha=k_2$ of $K(\alpha)$ possess a small imaginary part. Therefore k_1 and k_2 are replaced by k_1+ik_1' and k_2+ik_2' respectively where k_1' and k_2' are infinitesimally small positive quantities which would ultimately be made to tend to zero.

Now $K(\alpha)=K_+(\alpha)K_-(\alpha)$ where $K_+(\alpha)$ is analytic in the upper half-plane $\mathrm{Im}\,\alpha > -k_2'$ whereas $K_-(\alpha)$ is analytic in the lower half-plane $\mathrm{Im}\,\alpha < k_2'$ are given by (cf. Pal and Ghosh, 1990; Wickham, 1980)

$$K_\pm(\alpha)=\left(\frac{\mu_2(\alpha\pm k_1)}{1+m}\right)^{1/2}\exp\left[\frac{1}{\pi}\int_1^\gamma \frac{\tan^{-1}\left\{\frac{(t^2-1)^{1/2}}{m(\gamma^2-t^2)^{1/2}}\right\}}{t\pm\frac{\alpha}{k_1}}\,\mathrm{d}t\right],$$

where $m=\frac{\mu_2}{\mu_1}$ and $\gamma=\frac{k_2}{k_1}$.

Since $\tau_{yz}(x,0)$ decreases exponentially as $x\to\pm\infty$, $G_+(\alpha)$ and $G_-(\alpha)$ have the common region of regularity as $K_+(\alpha)$ and $K_-(\alpha)$. It may be noted that $B(\alpha)$ is analytic in the whole of α-plane.

Now (37) can easily be expressed as two integral equations relating $G_+(\alpha)$, $G_-(\alpha)$ and $B(\alpha)$ as follows:

$$\begin{aligned}
&\frac{G_\pm(\alpha)}{K_\pm(\alpha)}+\frac{1}{2\pi i}\int_{C_\pm}\frac{G_\mp(s)\,\mathrm{e}^{\mp 2isL}}{(s-\alpha)K_\pm(s)}\,\mathrm{d}s\\
&\quad-\frac{1}{2\pi i}\int_{C_\pm}\frac{\mathrm{e}^{\mp isL}K_\mp(s)}{\sqrt{2\pi}(s-\alpha)}\left\{\frac{F_1}{\mu_1\gamma_1(s)}-\frac{F_2}{\mu_2\gamma_2(s)}\right\}\mathrm{d}s\\
&=-B(\alpha)K_\mp(\alpha)\,\mathrm{e}^{\mp i\alpha L}-\frac{1}{2\pi i}\int_{C_\mp}\frac{G_\mp(s)\,\mathrm{e}^{\mp 2isL}}{(s-\alpha)K_\pm(s)}\,\mathrm{d}s\\
&\quad+\frac{1}{2\pi i}\int_{C_\mp}\frac{\mathrm{e}^{\mp isL}K_\mp(s)}{\sqrt{2\pi}(s-\alpha)}\left\{\frac{F_1}{\mu_1\gamma_1(s)}-\frac{F_2}{\mu_2\gamma_2(s)}\right\}\mathrm{d}s,
\end{aligned} \tag{40}$$

where C_+ and C_- are the straight contours situated within the common region of regularity of $G_+(s)$, $G_-(s)$, $K_+(s)$ and $K_-(s)$ as shown in *figure 2*.

In the first equation of (40) (i.e. the equation involving upper subscripts), the left-hand side is analytic in the upperhalf plane whereas the right-hand side is analytic in the lowerhalf plane and both of them are equal in the

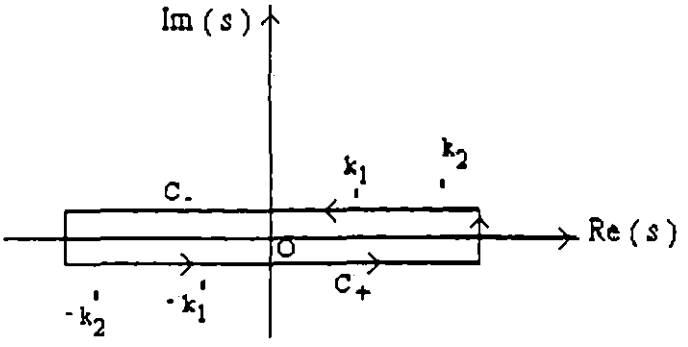

Figure 2. Path of integration in the complex s-plane.

common region of analyticity of these two functions. So by analytic continuation, both sides of the equation are analytic in the whole of the s-plane. Now, since

$$\tau_{yz} = O(|x \mp L|^{-1/2}) \quad \text{as } x \to \pm L$$

so

$$G_+(\alpha) = O(\alpha^{-1/2}) \quad \text{as } |\alpha| \to \infty,\ \operatorname{Im}\alpha > 0$$

and also

$$K_\pm(\alpha) = O(\alpha^{1/2}) \quad \text{as } |\alpha| \to \infty,\ \operatorname{Im}\alpha \gtrless 0.$$

So it follows that

$$\frac{G_+(\alpha)}{K_+(\alpha)} = O(\alpha^{-1}) \quad \text{as } |\alpha| \to \infty,\ \operatorname{Im}\alpha > 0.$$

Presumably one has $w_1(x, 0+) - w_2(x, 0-) = O(|x \mp L|^{1/2})$ as $x \to \pm L$.

Then it follows by standard Abelian asymptotics (cf. Noble, 1958; p. 36) that

$$B(\alpha) = e^{i\alpha L} O(\alpha^{-3/2}) + e^{-i\alpha L} O(\alpha^{-3/2}) \quad \text{as } |\alpha| \to \infty.$$

Consequently one has

$$B(\alpha) K_-(\alpha) e^{-i\alpha L} = O(\alpha^{-1}) \quad \text{as } |\alpha| \to \infty,\ \operatorname{Im}\alpha < 0.$$

Thus both sides of the first equation of (40) are $O(\alpha^{-1})$ as $|\alpha| \to \infty$ in the respective half-planes.

Therefore by Liouville's Theorem, both sides of the first equation of (40) are equal to zero. The second equation of (40) (i.e. the equation involving lower subscripts) can be treated similarly. Therefore from (40) one obtains the system of integral equations given by

$$\frac{G_\pm(\alpha)}{K_\pm(\alpha)} + \frac{1}{2\pi i}\int_{C_\pm} \frac{G_\mp(s)\, e^{\mp 2isL}}{(s-\alpha)K_\pm(s)}\, ds - \frac{1}{2\pi i}\int_{C_\pm} \frac{e^{\mp isL} K_\mp(s)}{\sqrt{2\pi}(s-\alpha)} \left\{ \frac{F_1}{\mu_1\gamma_1(s)} - \frac{F_2}{\mu_2\gamma_2(s)} \right\} ds = 0. \tag{41}$$

Since $\tau_{yz}^{(1)}(x, 0)$ is an even function of x, so from (28) and (29) it can be shown that $G_+(-\alpha) = G_-(\alpha)$ and that $K_+(-\alpha) = iK_-(\alpha)$ (cf. Pal and Ghosh, 1990). Using these results and replacing α by $-\alpha$ and s by $-s$ in the first equation of (41) it can easily be shown that both the equations in (41) are identical. So $G_+(\alpha)$ and $G_-(\alpha)$ are to be determined from any one of the integral equations in (41).

3. High frequency solution of the integral equation

To solve the second integral equation of (41) in the case when the normalized wave number $k_1 L \gg 1$, the integration along the path C_- in (41) is replaced by the integration along the contours L_{k_1} and L_{k_2} around the branch cuts through the branch points k_1 and k_2 of the function $K_-(s)$ as shown in *figure 3*. Thus the second equation in (41) takes the form

$$G_-(\alpha) = -\frac{K_-(\alpha)}{2\pi i}\int_{L_{k_1}+L_{k_2}} \frac{G_+(s)\, e^{2isL}}{(s-\alpha)K_-(s)}\, ds + \frac{K_-(\alpha)}{2\pi i}\int_{L_{k_1}+L_{k_2}} \frac{e^{isL} K_+(s)}{\sqrt{2\pi}(s-\alpha)} \left\{ \frac{F_1}{\mu_1\gamma_1(s)} - \frac{F_2}{\mu_2\gamma_2(s)} \right\} ds. \tag{42}$$

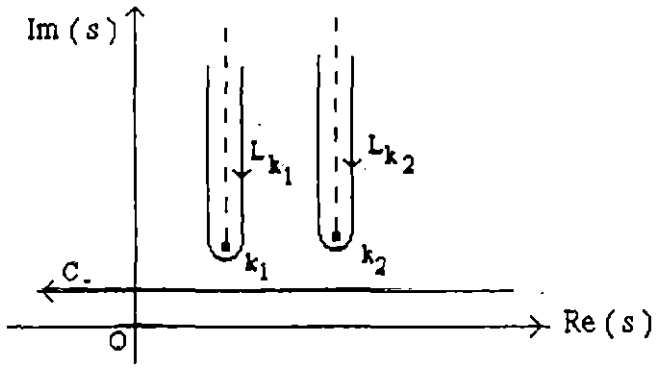

Figure 3. Paths of integration C_-, L_{k_1}, L_{k_2}.

For $k_1 L \gg 1$, it can be shown that

$$\int_{L_{k_j}} \frac{G_+(s)\,e^{2isL}}{(s-\alpha)K_-(s)}\,ds \approx -\frac{1}{\mu_j}\sqrt{\frac{\pi}{k_j L}}\,\frac{G_+(k_j)K_+(k_j)}{(k_j-\alpha)}\,e^{i\pi/4}\,e^{2ik_jL}, \quad j=1,2, \tag{43}$$

and

$$\int_{L_{k_1}+L_{k_2}} \frac{K_+(s)}{\sqrt{2\pi}(s-\alpha)}\left\{\frac{F_1}{\mu_1(s^2-k_1^2)^{1/2}}-\frac{F_2}{\mu_2(s^2-k_2^2)^{1/2}}\right\}e^{isL}\,ds \approx \sum_{j=1}^{2}(-1)^j\frac{F_j}{\mu_j}\frac{K_+(k_j)}{(k_j-\alpha)}\frac{e^{i(k_jL+\pi/4)}}{(k_jL)^{1/2}}. \tag{44}$$

Using the results of (43) and (44) and also the relations $G_+(-\alpha)=G_-(\alpha)$ and $K_-(\alpha)=-iK_+(-\alpha)$ one obtains from (42)

$$F_+(-\alpha)+\sum_{j=1}^{2}\frac{A(k_j)\,e^{2ik_jL}}{\mu_j(k_j-\alpha)(k_jL)^{1/2}}F_+(k_j)=-C(-\alpha), \tag{45}$$

where

$$F_+(\xi)=\frac{G_+(\xi)}{K_-(-\xi)}=\frac{G_-(-\xi)}{K_-(-\xi)}, \tag{46}$$

$$A(\xi)=\frac{[K_+(\xi)]^2\,e^{i\pi/4}}{2\sqrt{\pi}}, \tag{47}$$

$$C(\xi)=\frac{1}{2\pi i}\sum_{j=1}^{2}(-1)^{j+1}\frac{F_j}{\mu_j}\frac{K_+(k_j)}{(k_j+\xi)}\frac{e^{i(k_jL+\pi/4)}}{(k_jL)^{1/2}}. \tag{48}$$

Substituting $\alpha=-k_1$ and $\alpha=-k_2$ in (45) one obtains respectively the equations

$$[1+M_1(k_1)\,e^{2ik_1L}]F_+(k_1)+\frac{\mu_1}{\mu_2}M_1(k_2)\,e^{2ik_2L}F_+(k_2)=-C(k_1) \tag{49}$$

and

$$\frac{\mu_2}{\mu_1}M_2(k_1)\,e^{2ik_1L}F_+(k_1)+[1+M_2(k_2)\,e^{2ik_2L}]F_+(k_2)=-C(k_2), \tag{50}$$

where

$$M_j(\xi) = \frac{A(\xi)}{\mu_j(k_j+\xi)\sqrt{\xi L}}. \tag{51}$$

Now solution of (49) and (50) gives

$$F_+(k_m) = \left[\frac{\mu_m}{\mu_n} M_m(k_n) C(k_n)\, e^{2ik_nL} - C(k_m)\{1 + M_n(k_n)\, e^{2ik_nL}\}\right] P(k_1, k_2)$$
$$(\text{for } m = 1,\ n = 2 \text{ and for } m = 2,\ n = 1), \tag{52}$$

where

$$P(k_1, k_2) = \left[1 + M_1(k_1)\, e^{2ik_1L} + M_2(k_2)\, e^{2ik_2L} + \left(\frac{k_1 - k_2}{k_1 + k_2}\right)^2 M_1(k_1) M_2(k_2)\, e^{2i(k_1+k_2)L}\right]^{-1}. \tag{53}$$

For high-frequency, expanding $P(k_1, k_2)$ up to $O(k_jL)^{-1}$ and neglecting the terms involving $(k_jL)^{-2}$ and the higher order terms in $F_+(k_1)$ and $F_+(k_2)$ in (52) respectively, one obtains from Eqs (45) and (46)

$$G_-(\alpha) = \frac{K_-(\alpha)}{2\pi i} \sum_{j=1}^{2} (-1)^j L(k_j) F_j \left\{\frac{1}{(k_j - \alpha)\mu_j} - \sum_{m=1}^{2} \frac{M_j(k_m)}{\mu_m(k_m - \alpha)} e^{2ik_mL} + \sum_{m=1}^{2}\sum_{n=1}^{2} \frac{M_j(k_m) M_m(k_n)}{\mu_n(k_n - \alpha)} e^{2i(k_m+k_n)L}\right\}, \tag{54}$$

where

$$L(\xi) = \frac{K_+(\xi)\, e^{i(\xi L + \pi/4)}}{\sqrt{\xi L}}. \tag{55}$$

Replacing α by $-\alpha$ and using the relation $K_-(-\alpha) = -iK_+(\alpha)$ and $G_-(-\alpha) = G_+(\alpha)$ one obtains,

$$G_+(\alpha) = -\frac{K_+(\alpha)}{2\pi} \sum_{j=1}^{2} (-1)^j L(k_j) F_j \left\{\frac{1}{(k_j + \alpha)\mu_j} - \sum_{m=1}^{2} \frac{M_j(k_m)}{\mu_m(k_m + \alpha)} e^{2ik_mL} + \sum_{m=1}^{2}\sum_{n=1}^{2} \frac{M_j(k_m) M_m(k_n)}{\mu_n(k_n + \alpha)} e^{2i(k_m+k_n)L}\right\}. \tag{56}$$

4. Stress intensity factor near the crack tips

For $\alpha \to +\infty$ along the real axis,

$$K_\pm(\alpha) \sim \alpha^{1/2} \sqrt{\frac{\mu_1\mu_2}{\mu_1 + \mu_2}}. \tag{57}$$

From (53) and (56) one obtains,

$$G_+(\alpha) \sim S\alpha^{-1/2} \quad \text{and} \quad G_-(\alpha) \sim -iS\alpha^{-1/2}, \tag{58}$$

where

$$S = -\frac{1}{2\pi}\sqrt{\frac{\mu_1\mu_2}{\mu_1+\mu_2}}\sum_{j=1}^{2}(-1)^j L(k_j)F_j\left\{\frac{1}{\mu_j} - \sum_{m=1}^{2}\frac{1}{\mu_m}M_j(k_m)\,e^{2ik_mL} + \sum_{m=1}^{2}\sum_{n=1}^{2}\frac{1}{\mu_n}M_j(k_m)M_m(k_n)\,e^{2i(k_m+k_n)L}\right\}. \tag{59}$$

Using (57) and (58), Eq. (37) yields

$$B(\alpha) = \frac{S}{\alpha\sqrt{\alpha}}\{i\,e^{-i\alpha L} - e^{i\alpha L}\}\left(\frac{\mu_1+\mu_2}{\mu_1\mu_2}\right) + \frac{1}{\sqrt{2\pi}}\left\{\frac{F_1}{\mu_1} - \frac{F_2}{\mu_2}\right\}\frac{1}{\alpha}. \tag{60}$$

From Eqs (18), (19) and (20) one obtains,

$$\tau_{yz}^{(1)}(x,0+) - \tau_{yz}^{(2)}(x,0-) = -(F_1+F_2)\delta(x).$$

Taking Fourier transformation on both sides, we obtain

$$\bar{\tau}_{yz}^{(1)}(\alpha,0+) - \bar{\tau}_{yz}^{(2)}(\alpha,0-) = -\frac{(F_1+F_2)}{\sqrt{2\pi}}$$

or

$$\mu_1\gamma_1A_1(\alpha) + \mu_2\gamma_2A_2(\alpha) = \frac{(F_1+F_2)}{\sqrt{2\pi}}. \tag{61}$$

From Eqs (60), (61) and (36) one obtains when $\alpha \to +\infty$ along the real axis,

$$A_j(\alpha) = \frac{(-1)^{j+1}S}{\mu_j\alpha\sqrt{\alpha}}[i\,e^{-i\alpha L} - e^{i\alpha L}] + \frac{1}{\sqrt{2\pi}}\frac{1}{\alpha}\frac{F_j}{\mu_j}; \quad j = 1,2. \tag{62}$$

Now

$$\tau_{yz}^{(j)}(x,y) = \mu_j\frac{\partial w_j(x,y)}{\partial y} = \mu_j\frac{\partial}{\partial y}\left[\frac{1}{\sqrt{2\pi}}\int_{-\infty}^{\infty}A_j(\alpha)\,e^{-\gamma_j|y|-i\alpha x}\,d\alpha\right]$$
$$= (-1)^j\frac{\mu_j}{\sqrt{2\pi}}\int_0^{\infty}\gamma_jA_j(\alpha)\,e^{-\gamma_j|y|}[e^{-i\alpha x} + e^{i\alpha x}]\,d\alpha \tag{63}$$

as by Eq. (35) $A_j(\alpha)$ is an even function of α.

Substituting the values of $A_j(\alpha)$ as $|\alpha| \to \infty$ we can write the stress in the vicinity of the crack tip as

$$\tau_{yz}^{(j)}(x,y) \approx \frac{S}{\sqrt{2\pi}}\int_0^{\infty}\frac{e^{-\alpha|y|}}{\sqrt{\alpha}}[e^{i\alpha(x+L)} - i\,e^{i\alpha(x-L)} - i\,e^{-i\alpha(x+L)} + e^{-i\alpha(x-L)}]\,d\alpha$$
$$+ (-1)^j\frac{F_j}{\pi}\int_0^{\infty}e^{-\alpha|y|}\cos\alpha x\,d\alpha$$
$$= \frac{S(1-i)}{\sqrt{2\pi}}\int_0^{\infty}\frac{e^{-\alpha|y|}}{\sqrt{\alpha}}[\cos\alpha(x+L) - \sin\alpha(x+L) + \cos\alpha(x-L) + \sin\alpha(x-L)]\,d\alpha$$
$$+ (-1)^j\frac{F_j}{\pi}\int_0^{\infty}e^{-\alpha|y|}\cos\alpha x\,d\alpha$$
$$= S(1-i)\left[\frac{1}{\sqrt{r_1}}\cos\frac{\theta_1}{2} + \frac{1}{\sqrt{r_2}}\cos\frac{\theta_2}{2}\right] + (-1)^j\frac{F_j}{\pi}\frac{|y|}{x^2+y^2}, \tag{64}$$

where

$$(x-L)+iy=r_1 e^{i\theta_1}, \qquad -(x+L)+iy=r_2 e^{i\theta_2}, \qquad \pi \leqslant \theta_{1,2} \leqslant \pi. \tag{65}$$

It is to be noted that the final term in Eq. (64) which can be reduced to $-\frac{F_j}{\pi}\frac{y}{x^2+y^2}$ describes the behaviour of the stress near the source. Therefore at the interface ($y=0$) we obtain

$$\tau_{yz} \approx \frac{S(1-i)}{\sqrt{x-L}} \quad \text{as } x \to L+0, \tag{66}$$

$$\tau_{yz} \approx \frac{S(1-i)}{\sqrt{-(x+L)}} \quad \text{as } x \to -L-0. \tag{67}$$

Now the dimensionless stress intensity factor is defined by,

$$K=\left|\frac{S(1-i)}{F_1\sqrt{k_1}}\right|, \tag{68}$$

where S is given by (59).

5. Results and discussions

Since from Eqs (7) and (16) we note that for $Y=0$, $x=X$ and $y=0$ and that $\sigma_{YZ}^{(j)}(X,0,t)=\sigma_{yz}^{(j)}(x,0,t)$, therefore, the elastodynamic mode-III stress intensity factor of the interface crack in an anisotropic bimaterials is the same as that of an interface crack of the corresponding isotropic bimaterial given by (68).

Numerical calculations have been carried out for both the cases of antisymmetric ($F_1=-F_2=F$) and symmetric ($F_1=F_2=F$) antiplane loadings. For numerical evaluation of the stress intensity factors, the three material pairs (Nayfen, 1995), given in *table 1*, have been considered.

The absolute values of the complex stress intensity factors defined by (68) have been plotted against k_1L in *figures 4–6*, for symmetric as well as for antisymmetric loadings for values of dimensionless frequency k_1L varying from 1.01 to 10.

It is interesting to note that in the case of symmetric loading, the stress intensity factor first increases with increasing k_1L, attains a maximum and then with further increase of k_1L, decreases gradually with oscillatory

Table I. Engineering elastic constants of different materials.

Medium Name	$\hat{\rho}$ (kg m^{-3})	C_{44} (GPa)	C_{55} (GPa)	C_{45} (GPa)
Type of material pair: I				
1. Carbon-epoxy	1.57×10^3	3.98	6.4	0
2. Graphite-epoxy	1.60×10^3	6.55	2.6	0
Type of material pair: II				
1. Isotropic Chromium	7.20×10^3	115.2	115.2	0
2. Isotropic Steel	7.90×10^3	81.91	81.91	0
Type of material pair: III				
1. Graphite	1.79×10^3	5.52	28.3	0
2. Carbon-epoxy	1.57×10^3	3.98	6.4	0

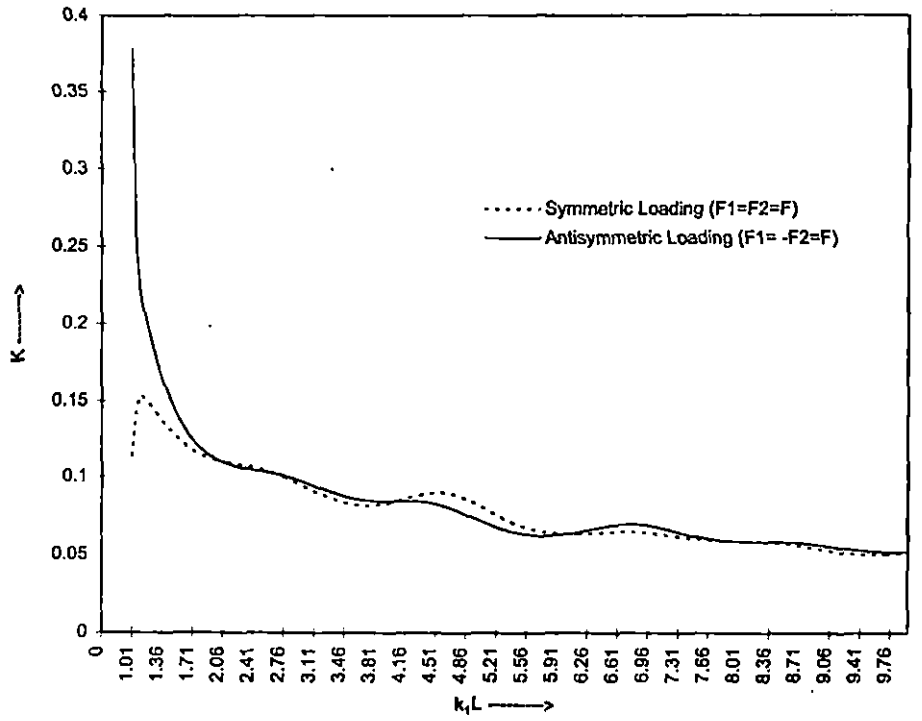

Figure 4. Stress intensity factor K versus dimensionless frequency $k_1 L$ for Type-I material pair.

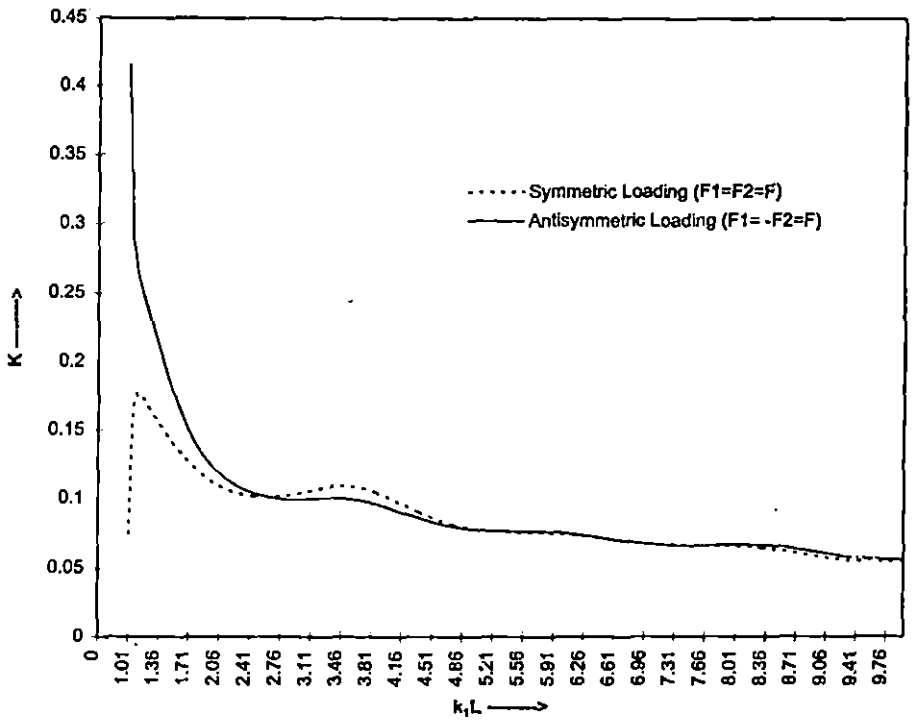

Figure 5. Stress intensity factor K versus dimensionless frequency $k_1 L$ for Type-II material pair.

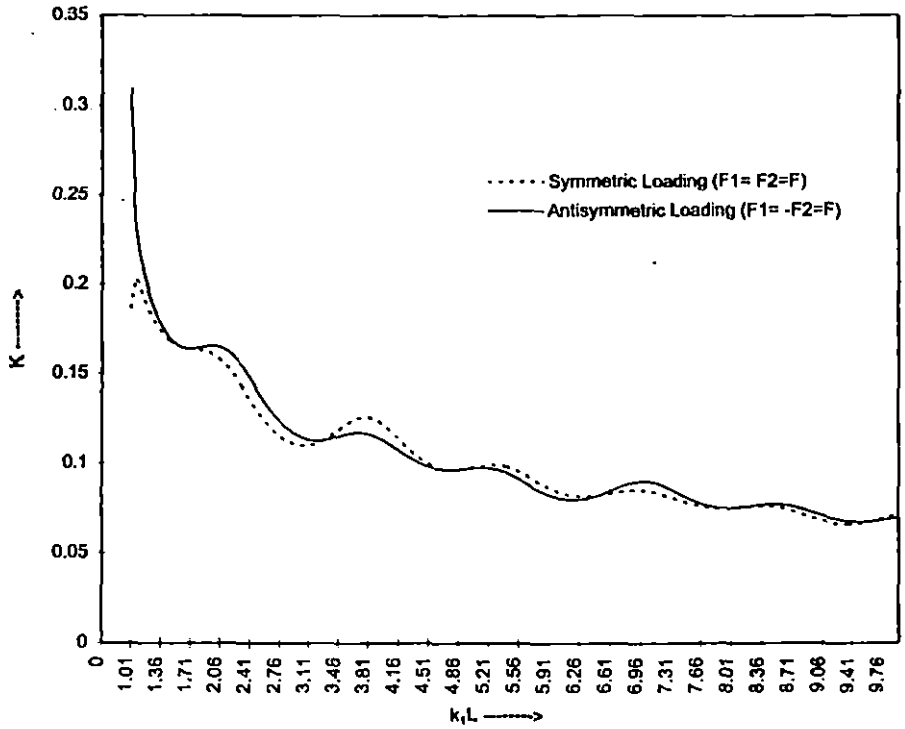

Figure 6. Stress intensity factor K versus dimensionless frequency $k_1 L$ for Type-III material pair.

behavior. On the other hand in the case of antisymmetric loading, stress intensity factor at first decreases sharply but with the increase of $k_1 L$, it shows almost the same behaviours as the case for symmetric loading. The general oscillatory feature for the curves in *figures 4–6* are due to the effect of interaction between the waves generated by the two tips of the crack.

Acknowledgement

We take the opportunity of thanking the referee for suggesting some improvement of the paper.

References

Achenbach J.D., 1973. Wave Propagation in Elastic Solids. North-Holland, Amsterdam.

Achenbach J.D., Kuo M.K., 1986. Effect of transverse isotropy on strong ground motion due to strike slip faulting. In: Das S. et al. (Eds). Earthquake Source Mechanics, American Geophysical Union, Washington, pp. 111–120.

Chang S.J., 1971. Diffraction of plane dilatational waves by a finite crack. Quart. J. Mech. Appl. Math. 24, 423–443.

Kuo M.K., 1992. Transient stress intensity factors for a cracked plane strip under antiplane point forces. Int. J. Engrg. Sci. 30, 199–211.

Kuo M.K., Cheng S.H., 1991. Elastodynamic responses due to antiplane point impact loadings on the faces of an interface crack along dissimilar anisotropic materials. Int. J. Solids Structures 28, 751–768.

Ma C.C., Hou B.L., 1989. Analysis of dissimilar anisotropic wedges subjected to antiplane shear deformation. Int. J. Solids Structures 25, 1295–1309.

Markenscoff X., Ni L., 1984. The transient motion of a screw dislocation in an anisotropic medium. J. Elasticity 14, 93–95.

Nayfen A.H., 1995. Wave Propagation in Layered Anisotropic Media with Applications to Composites. Elsevier.

Neerhoff F.L., 1979. Diffraction of Love waves by a stress free crack of finite width in the plane interface of a layered composite. Appl. Sci. Res. 35, 265–315.

Noble B., 1958. Methods based on the Wiener–Hopf technique (Sec. 5.5). Pergamon Press, New York.

Pal S.C., Ghosh M.L., 1990. High-frequency scattering of antiplane shear waves by an interface crack. Indian J. Pure Appl. Math. 21, 1107–1124.

Wickham G.R., 1980. Short wave radiation from a rigid strip in smooth contact with a semi-infinite elastic solid. Quart. J. Mech. Appl. Math. 33, 409–433.

PERGAMON International Journal of Engineering Science 36 (1998) 1197–1213

International Journal of Engineering Science

Transient response due to a pair of antiplane point impact loading on the faces of a finite griffith crack at the bimaterial interface of anisotropic solids

R.K. Pramanik[a], S.C. Pal[b,*], M.L. Ghosh[a]

[a]*Department of Mathematics, University of North Bengal, Dist. Darjeeling, West Bengal 734430, India*
[b]*Computer Centre, University of North Bengal, Dist. Darjeeling, West Bengal 734430, India*

Received 10 February 1997; accepted 29 October 1997

Abstract

The transient elastodynamic problem involving the scattering of elastic waves by a Griffith crack of finite width lying at the interface of two dissimilar anisotropic half planes has been analysed. The crack faces are subjected to a pair of suddenly applied antiplane line loads situated at the middle of the cracked surface. The problem has first been reduced to one with the interface crack of finite width lying between two dissimilar isotropic elastic half planes by a transformation of relevant coordinates and parameters. Spatial and time transforms are then applied to the governing differential equations and boundary conditions which yield generalized Wiener–Hopf type equations. The integral equations arising are solved by the standard iteration technique. Physically each successive order of iteration corresponds to successive scattered or rescattered wave from one crack tip to the other. Finally, expressions for the resulting mode III stress intensity factors are determined as a function of time for both symmetric and antisymmetric loadings. Each crack tip stress intensity factor has been plotted versus time for four pairs of different types of materials.

1. Introduction

The problem of a crack in an elastic material under the action of impulsive loading has been a subject of considerable interest recently. Sih et al. [1] have considered the problem for an infinite isotropic material and Kassir and Bandyopadhyay [2] studied infinite orthotropic

* Corresponding author. Tel.: +91-0353-450-440; fax: +91-0353-450-546.

0020-7225/98/$19.00
PII: S0020-7225(98)00019-6

material. Stephen and Hwel [3] also investigated the problem of diffraction of transient SH-waves by a crack of finite width and a rigid ribbon, also of finite width.

However in present years the extensive use of composite materials in the modern technology has created interest among scientists for carrying on considerable research work in the modeling, testing and analysis of laminated media. The laminated composites which behave as anisotropic material may be weakened by interface flaws which lead to serious degradation in load carrying capacity.

Kuo [4] carried out numerical and analytical studies of transient response of an interfacial semi-infinite crack between two dissimilar orthotropic half spaces. The problem of diffraction of transient horizontal shear waves by a finite crack located at the interface of two bonded dissimilar elastic half spaces has been treated by Takei et al. [5].

Neerhoff [6] studied the diffraction of Love waves by a crack of finite width at the interface of a layered half space. Kuo and Cheng [7] considered the elastodynamic response due to antiplane point impact loadings on the faces of an interface semi-infinite crack along dissimilar anisotropic materials.

In our present paper, we are interested in the antiplane transient elastodynamic responses and stress intensity factors of a Griffith crack of finite width lying along the interface of two dissimilar anisotropic elastic materials. The crack is subjected to a pair of suddenly applied antiplane concentrated line loading situated at the middle of the cracked surface. The materials are assumed to possess certain material symmetry and the crack plane is assumed to coincide with one of the planes of material symmetry, so that the inplane and the antiplane motion are not coupled.

The analysis of the paper is first based on the observation of several researches, e.g. Markenscoff and Ni [8], Achenbach and Kuo [9], that antiplane shear deformation in an anisotropic solid can be deduced from the corresponding deformations of an isotropic solid by a transformation of relevant co-ordinates and parameters. Based on this observation, analysis of the interface crack by transient line loads between two bonded dissimilar anisotropic elastic materials has first been converted to the corresponding problem between two dissimilar isotropic elastic solids. Later following Thau and Lu [3], spatial and time transforms are applied to the governing differential equations and generalized Wiener–Hopf type equations are obtained. The integral equation arising are solved by the standard iteration procedure. Physically, each successive order of iteration corresponds to successive scattered or rescattered wave from one crack tip to other.

Finally results are presented for the stress intensity factor near the crack tips. Each crack tip stress intensity factor is plotted versus time for a pair of different type of anisotropic materials.

2. Formulation of the problem

Consider antiplane deformation of a Griffith crack of finite width $2L$ lying between dissimilar anisotropic half planes which are characterized by the elastic moduli $(c_{ik})_j$; $i, k = 4, 5$ and mass densities $\hat{\rho}_j$. The subscripts j ($j = 1, 2$) refers to the upper and lower media respectively. Let (X, Y, Z) be Cartesian co-ordinates. The X-axis is taken along the interface,

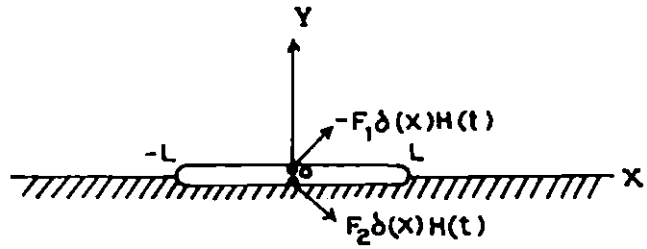

Fig. 1. Geometry of the problem.

Y-axis vertically upwards into the medium and Z-axis is perpendicular to the plane of the paper (Fig. 1).

For time $t < 0$, the elastic solids are at rest. For time $t \geq 0$, a pair of concentrated antiplane shear forces in the Z-direction of magnitudes F_1 and F_2 act on the crack faces $Y = 0+$ and $Y = 0-$ respectively at $X = 0$. Thus the crack face boundary conditions are

$$\hat{\sigma}_{YZ}(X, Y, t) = \begin{cases} -F_1\delta(X)H(t); |X| < L, Y = 0+ \\ F_2\delta(X)H(t); |X| < L, Y = 0- \end{cases}, \tag{1}$$

where $H(\,)$ and $\delta(\,)$ are the Heaviside step and Dirac delta functions respectively. Ahead of the crack tips, the interface boundary conditions which corresponds to the continuity of the displacement and traction along the welded part of the interface along $|X| > L$, $Y = 0$ are

$$\hat{\sigma}^{(1)}_{YZ}(X, 0, t) = \hat{\sigma}^{(2)}_{YZ}(X, 0, t) \tag{2}$$

$$\hat{W}_1(X, 0, t) = \hat{W}_2(X, 0, t). \tag{3}$$

Two dimensional antiplane wave motions of homogeneous anisotropic linearly elastic solids are governed by [10]

$$(C_{55})_j \frac{\partial^2 \hat{W}_j}{\partial X^2} + 2(C_{45})_j \frac{\partial^2 \hat{W}_j}{\partial X \partial Y} + (C_{44})_j \frac{\partial^2 \hat{W}_j}{\partial Y^2} = \hat{\rho}_j \frac{\partial^2 \hat{W}_j}{\partial t^2}; \quad (j = 1, 2), \tag{4}$$

where $\hat{W}_j(X, Y, t)$ is the out-of-plane displacement.

The crack plane has been assumed to coincide with one of the plane of material symmetry such that inplane and outplane motions are not coupled.

The relevant stress components are

$$\hat{\sigma}^{(j)}_{XZ}(X, Y, t) = (C_{55})_j \frac{\partial \hat{W}_j}{\partial X} + (C_{45})_j \frac{\partial \hat{W}_j}{\partial Y} \tag{5}$$

$$\hat{\sigma}^{(j)}_{YZ}(X, Y, t) = (C_{45})_j \frac{\partial \hat{W}_j}{\partial X} + (C_{44})_j \frac{\partial \hat{W}_j}{\partial Y}. \tag{6}$$

Following Achenbach and Kuo [9] and Ma [11], we introduce a co-ordinate transformation which has also been used by Kuo and Cheng [7]

$$\left.\begin{aligned} x &= X - \frac{(C_{45})_j}{(C_{44})_j} Y \\ y &= \frac{\mu_j}{(C_{44})_j} Y \\ z &= Z \end{aligned}\right\} (j = 1, 2), \tag{7}$$

where

$$\mu_j = [(C_{44})_j (C_{55})_j - (C_{45})_j^2]^{1/2}, \quad (j = 1, 2). \tag{8}$$

Transformation given by Eq. (7) reduce Eq. (4) to the standard wave equation

$$\frac{\partial^2 \hat{W}_j}{\partial x^2} + \frac{\partial^2 \hat{W}_j}{\partial y^2} = s_j^2 \frac{\partial^2 \hat{W}_j}{\partial t^2}, \tag{9}$$

where

$$s_j^2 = \frac{\rho_j}{\mu_j} \text{ and } \rho_j = \frac{\hat{\rho}_j (C_{44})_j}{\mu_j} \tag{10}$$

s_j is the slowness of shear waves. Without any loss of generality we assume that

$$s_1 < s_2 \tag{11}$$

It is easily verified from Eqs. (4)–(6) that the relevant displacement and the stress component in the physical anisotropic solid are related to those in the corresponding isotropic solid by

$$\hat{W}_j(X, Y, t) = w_j(x, y, t), \tag{12}$$

$$\hat{\sigma}_{XZ}^{(j)}(X, Y, t) = \frac{\mu_j}{(C_{44})_j} \sigma_{xz}^{(j)}(x, y, t) + \frac{(C_{45})_j}{(C_{44})_j} \sigma_{yz}^{(j)}(x, y, t), \tag{13}$$

$$\hat{\sigma}_{YZ}^{(j)}(X, Y, t) = \sigma_{yz}^{(j)}(x, y, t). \tag{14}$$

From Eqs. (9) and (12), the antiplane wave motions of the corresponding isotropic bimaterial in the transformed co-ordinate are governed by the standard wave equation

$$\frac{\partial^2 w_j}{\partial x^2} + \frac{\partial^2 w_j}{\partial y^2} = s_j^2 \frac{\partial^2 w_j}{\partial t^2}; \quad (j = 1, 2) \tag{15}$$

and the relevant stress component is

$$\sigma_{yz}^{(j)}(x, y, t) = \mu_j \frac{\partial w_j}{\partial y}. \tag{16}$$

Under the changed co-ordinate system the boundary conditions Eqs. (1)–(3) reduce to

$$\sigma_{yz}(x, y, t) = \begin{cases} -F_1\delta(x)H(t); |x|<L, y = 0+ \\ F_2\delta(x)H(t); |x|<L, y = 0- \end{cases} \tag{17}$$

$$\sigma_{yz}^{(1)}(x, y, t) = \sigma_{yz}^{(2)}(x, y, t); \quad |x| > L, \quad y = 0, \tag{18}$$

$$w_1(x, y, t) = w_2(x, y, t); \quad |x| > L, \quad y = 0. \tag{19}$$

Hence

$$\mu_1 \frac{\partial w_1}{\partial y} = -F_1\delta(x)H(t); \quad |x|<L, \quad y = 0+ \tag{20}$$

$$\mu_2 \frac{\partial w_2}{\partial y} = F_2\delta(x)H(t); \quad |x|<L, \quad y = 0- \tag{21}$$

and

$$\mu_1 \frac{\partial w_1}{\partial y} = \mu_2 \frac{\partial w_2}{\partial y}; \quad |x| > L, \quad y = 0 \tag{22}$$

$$w_1(x, 0, t) = w_2(x, 0, t); \quad |x| > L, \quad y = 0. \tag{23}$$

We begin the analysis by introducing unknown functions w_j and $\partial w_j/\partial y$ along the x-axis over the intervals where the functions are not specified by Eqs. (22) and (23).

Assume that

$$w_j(x, 0, t) = g_j(x, 0, t); \quad -L<x<L \tag{24}$$

and

$$\mu_j \frac{\partial w_j}{\partial y} = \begin{cases} \phi(x + L, t); y = 0x + L<0 \\ \phi(x - L, t); y = 0x - L > 0. \end{cases} \tag{25}$$

Now we introduce Laplace and Fourier transforms defined as

$$F(x, y, p) = \int_0^\infty f(x, y, t)e^{-pt}dt, \qquad \bar{F}(\zeta, y, p) = \int_{-\infty}^\infty F(x, y, p)e^{-i\zeta x}dx \tag{26}$$

so that their inverse transforms are

$$f(x, y, t) = \frac{1}{2\pi i}\int_{BR} F(x, y, p)e^{pt}dp, \qquad F(x, y, p) = \frac{1}{2\pi}\int_{-\infty}^{\infty} \bar{F}(\zeta, y, p)e^{i\zeta x}d\zeta. \tag{27}$$

Taking Laplace transform with respect to t of both sides of Eq. (24) (for $|x| < L$)

$$W_j(x, 0, p) = \int_0^{\infty} w_j(x, 0, t)e^{-pt}dt = \int_0^{\infty} g_j(x, 0, t)e^{-pt}dt = G_j(x, 0, p); \quad |x|<L. \tag{28}$$

Next taking Laplace and Fourier transform on wave Eq. (15) one obtains

$$\frac{\partial^2 \bar{w}_1}{\partial y^2} - (\zeta^2 + k_1^2)\bar{w}_1 = 0; \quad (y > 0), \tag{29}$$

$$\frac{\partial^2 \bar{w}_2}{\partial y^2} - (\zeta^2 + k_2^2)\bar{w}_2 = 0; \quad (y<0), \tag{30}$$

where

$$k_j^2 = s_j^2 p^2; \quad (j = 1, 2). \tag{31}$$

The solutions of the Eqs. (29) and (30) which are bounded as $|y| \to \infty$ are

$$\bar{w}_1(\zeta, y, p) = A_1(\zeta)e^{-\gamma_1 y}; \quad y > 0, \tag{32}$$

$$\bar{w}_2(\zeta, y, p) = A_2(\zeta)e^{\gamma_2 y}; \quad y<0, \tag{33}$$

where

$$\gamma_j = (\zeta^2 + k_j^2)^{1/2}; \quad (j = 1, 2). \tag{34}$$

The transformed stress at the interface $y = 0$ can be written as

$$\mu_j \frac{\partial \bar{W}_j(\zeta, 0, p)}{\partial y} = e^{i\zeta L}\bar{\Phi}_+(\zeta, p) + \frac{1}{p}\epsilon_j F_j + e^{-i\zeta L}\bar{\Phi}_-(\zeta, p), \qquad [j = 1, 2, \epsilon_j = (-1)^j], \tag{35}$$

where

$$\bar{\Phi}_+(\zeta, p) = \int_{-\infty}^{-L} e^{-i\zeta x}\left[\int_0^{\infty} \phi(x + L, t)e^{-pt}dt\right]dx$$

and

$$\bar{\Phi}_-(\zeta, p) = \int_{L}^{\infty} e^{-i\zeta x}\left[\int_0^{\infty} \phi(x - L, t)e^{-pt}dt\right]dx.$$

$\bar{\Phi}_+$ and $\bar{\Phi}_-$ are analytic in the complex half plane $\mathrm{Im}(\zeta) > -k_1$ and $\mathrm{Im}(\zeta) < k_1$ respectively. So from Eqs. (32) and (33) one obtains

$$\mu_1 \frac{\partial \bar{W}_1(\zeta, 0, p)}{\partial y} = -\mu_1 \gamma_1 A_1(\zeta), \qquad \mu_2 \frac{\partial \bar{W}_2(\zeta, 0, p)}{\partial y} = \mu_2 \gamma_2 A_2(\zeta) \tag{36}$$

Eq. (35) with aid of Eq. (36) yields

$$(-1)^j \mu_j \gamma_j A_j(\zeta) = e^{i\zeta L}\bar{\Phi}_+(\zeta, p) + e^{-i\zeta L}\bar{\Phi}_-(\zeta, p) + (-1)^j \frac{F_j}{p}; \quad (j = 1, 2). \tag{37}$$

Taking aid of Eqs. (19), (28), (32), and (33) one obtains

$$\bar{W}_1(\zeta, 0, p) - \bar{W}_2(\zeta, 0, p) = \int_{-\infty}^{\infty} [W_1(x, 0, p) - W_2(x, 0, p)] e^{-i\zeta x} dx$$

$$= \int_{-L}^{L} [G_1(x, 0, p) - G_2(x, 0, p)] e^{-i\zeta x} dx = B(\zeta) \text{ (say)}$$

so that

$$A_1(\zeta) - A_2(\zeta) = B(\zeta). \tag{38}$$

By the help of Eqs. (37) and (38) one finds an extended Wiener–Hopf equation namely

$$K(\zeta)B(\zeta) = -\bar{\Phi}_+(\zeta, p)e^{i\zeta L} + \bar{\Phi}_-(\zeta, p)e^{-i\zeta L} + \frac{K(\zeta)}{p}\left[\frac{F_1}{\mu_1 \gamma_1} - \frac{F_2}{\mu_2 \gamma_2}\right], \tag{39}$$

where

$$K(\zeta) = \frac{\mu_1 \mu_2 \gamma_1 \gamma_2}{\mu_1 \gamma_1 + \mu_2 \gamma_2} = \frac{\mu_1 \mu_2 (\zeta^2 + k_1^2)^{1/2}}{\mu_1 + \mu_2} R^1(\zeta), \tag{40}$$

$$= \frac{\mu_1 \mu_2 (\zeta^2 + k_2^2)^{1/2}}{(\mu_1 + \mu_2)} R^2(\zeta) \tag{41}$$

so that

$$R^1(\zeta) = \frac{(\mu_1 + \mu_2)(\zeta^2 + k_2^2)^{1/2}}{\mu_1(\zeta^2 + k_1^2)^{1/2} + \mu_2(\zeta^2 + k_2^2)^{1/2}}, \tag{42}$$

$$R^2(\zeta) = \frac{(\mu_1 + \mu_2)(\zeta^2 + k_1^2)^{1/2}}{\mu_1(\zeta^2 + k_1^2)^{1/2} + \mu_2(\zeta^2 + k_2^2)^{1/2}}. \tag{43}$$

The solution of Eq. (39) along with two transform inversions completes the problem. Here we shall concentrate on finding and then inverting $\bar{\Phi}_+$ and $\bar{\Phi}_-$ since $\phi(x + L, t)$ and $\phi(x - L, t)$ from Eq. (25) are equal to the shear stresses directly ahead of the crack tips. Hence they are required for the determination of dynamic stress intensity factors at the crack tips.

In order to solve Eq. (39), the function $K(\zeta)$ is at first made single valued by drawing branch cuts along the η-axis (recall $\zeta = \xi + i\eta$) from $\eta = k_1$ to ∞ and from $\eta = -k_1$ to $-\infty$. It is then broken up into the product of two functions which are analytic in the overlapping regions $\mathrm{Im}(\zeta) > -k_1$ and $\mathrm{Im}(\zeta) < k_1$ so that

$$K(\zeta) = K_+(\zeta)K_-(\zeta). \tag{44}$$

Next we divide Eq. (39) by $K_+(\zeta)$ and change ζ to ζ' in it and redivide it by $2\pi i e^{i\zeta' L}(\zeta' - \zeta)$ which yields

$$\frac{e^{-i\zeta' L}K_-(\zeta')B(\zeta')}{2\pi i(\zeta' - \zeta)} = -\frac{\bar{\Phi}_+(\zeta')}{2\pi i K_+(\zeta')(\zeta' - \zeta)} + \frac{\bar{\Phi}_-(\zeta')e^{-2i\zeta' L}}{2\pi i K_+(\zeta')(\zeta' - \zeta)} + \frac{K_-(\zeta')e^{-i\zeta' L}}{2\pi i(\zeta' - \zeta)p} \times \left[\frac{F_1}{\mu_1(\zeta'^2 + k_1^2)^{1/2}} - \frac{F_2}{\mu_2(\zeta'^2 + k_2^2)^{1/2}}\right] \tag{45}$$

Now with $\zeta' = \xi' + i\eta'$, take a line L_1 in the ζ'-plane lying in the strip $-k_1 < \eta' < k_1$; choose ζ to be a point lying above L_1 (i.e. $\eta > \eta'$) and integrate Eq. (45) along L_1 from $-\infty < \xi' < \infty$

$$\int_{L_1} \frac{e^{-i\zeta' L}K_-(\zeta')B(\zeta')}{2\pi i(\zeta' - \zeta)}d\zeta' = -\int_{L_1} \frac{\bar{\Phi}_+(\zeta')}{2\pi i K_+(\zeta')(\zeta' - \zeta)}d\zeta' + \int_{L_1} \frac{\bar{\Phi}_-(\zeta')e^{-2i\zeta' L}}{2\pi i K_+(\zeta')(\zeta' - \zeta)}d\zeta' + \int_{L_1} \frac{K_-(\zeta')e^{-i\zeta' L}}{2\pi i(\zeta' - \zeta)p}\left[\frac{F_1}{\mu_1(\zeta'^2 + k_1^2)^{1/2}} - \frac{F_2}{\mu_2(\zeta'^2 + k_2^2)^{1/2}}\right]d\zeta'. \tag{46}$$

Since $B(\zeta')$ is analytic in the entire plane and $K_-(\zeta')e^{-i\zeta' L}$ is analytic in the lower half plane, so considering semicircular contour in the lower half plane the first integral is found to be equal to zero.

Again while evaluating the second integral, a semicircular contour in the upper half plane is considered. Consequently the second integral is found to yield the value $\bar{\Phi}_+(\zeta)/K_+(\zeta)$.

Next for the last two integrals the integration path is deformed to the path round the branch cut through the branch points $\zeta = -ik_1$ and $-ik_2$ as shown in Fig. 2 so that finally Eq. (46) takes the form

$$\bar{\Phi}_+(\zeta) = \frac{iK_+(\zeta)}{\pi\mu_1}\int_0^\infty \frac{\bar{\Phi}_-[-ik_1(1+\lambda)]K_-[-ik_1(1+\lambda)]e^{-2Lk_1(1+\lambda)}}{[ik_1(1+\lambda)+\zeta][\lambda(\lambda+2)]^{1/2}}d\lambda + \frac{iK_+(\zeta)}{\pi\mu_2}\int_0^\infty \frac{\bar{\Phi}_-[-ik_2(1+\lambda)]K_-[-ik_2(1+\lambda)]e^{-2Lk_2(1+\lambda)}}{[ik_2(1+\lambda)+\zeta][\lambda(\lambda+2)]^{1/2}}d\lambda + \frac{iF_1K_+(\zeta)}{\pi\mu_1 p}\int_0^\infty \frac{K_-[-ik_1(1+\lambda)]e^{-Lk_1(1+\lambda)}}{[ik_1(1+\lambda)+\zeta][\lambda(\lambda+2)]^{1/2}}d\lambda - \frac{iF_2K_+(\zeta)}{\pi\mu_2 p}\int_0^\infty \frac{K_-[-ik_2(1+\lambda)]e^{-Lk_2(1+\lambda)}}{[ik_2(i+\lambda)+\zeta][\lambda(\lambda+2)]^{1/2}}d\lambda. \tag{47}$$

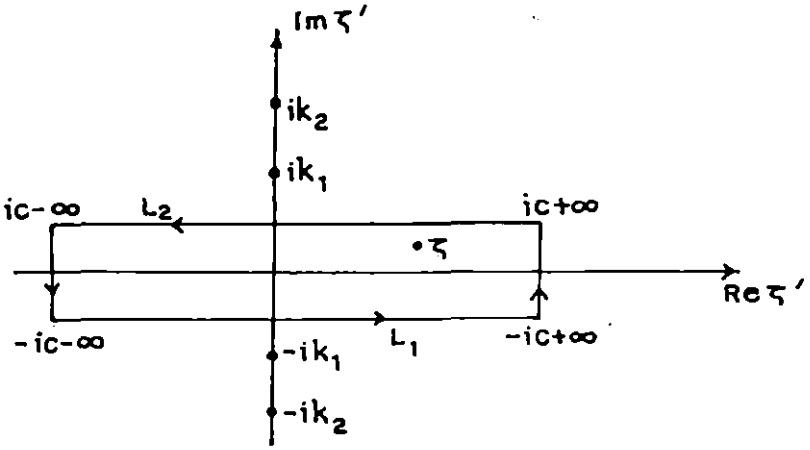

Fig. 2. Path of integration.

Similarly we can derive an equation for $\bar{\Phi}_-(\zeta)$ by dividing Eq. (39) by $2\pi i e^{-2\zeta' L} K_-(\zeta')(\zeta' - \zeta)$ after first changing ζ to ζ' and then choosing a line of integration L_2 in the strip $-k_1 < \eta' < k_1$. The point ζ is taken below L_2 and the result analogous to Eq. (47), then becomes;

$$\begin{aligned}\bar{\Phi}_-(\zeta) = {} & \frac{iK_-(\zeta)}{\pi\mu_1}\int_0^\infty \frac{\bar{\Phi}_+[ik_1(1+\lambda)]K_+[ik_1(1+\lambda)]e^{-2Lk_1(1+\lambda)}}{[ik_1(1+\lambda)-\zeta][\lambda(\lambda+2)]^{1/2}}d\lambda \\ & + \frac{iK_-(\zeta)}{\pi\mu_2}\int_0^\infty \frac{\bar{\Phi}_+[ik_2(1+\lambda)]K_+[ik_2(1+\lambda)]e^{-2Lk_2(1+\lambda)}}{[ik_2(1+\lambda)-\zeta][\lambda(\lambda+2)]^{1/2}}d\lambda \\ & - \frac{iF_1K_-(\zeta)}{\pi\mu_1 p}\int_0^\infty \frac{K_+[ik_1(1+\lambda)]e^{-Lk_1(1+\lambda)}}{[ik_1(1+\lambda)-\zeta][\lambda(\lambda+2)]^{1/2}}d\lambda \\ & + \frac{iF_2K_-(\zeta)}{\pi\mu_2 p}\int_0^\infty \frac{K_+[ik_2(1+\lambda)]e^{-Lk_2(1+\lambda)}}{[ik_2(1+\lambda)-\zeta][\lambda(\lambda+2)]^{1/2}}d\lambda. \end{aligned} \tag{48}$$

The integral equations have been solved by the standard iteration method and it may be noted that each successive order of iteration is a solution of the problem for successively increasing units of time starting from $t = 0$. Since each unit of time here corresponds exactly to the time required for an SH-wave to traverse the crack width, we can interpret physically each order of iteration in terms of the successive scatterings of waves from one crack to other and back again. Now we consider the zeroth order solutions of Eqs. (47) and (48) as

$$\begin{aligned}\bar{\Phi}_+^{(0)}(\zeta) = {} & \frac{iF_1K_+(\zeta)e^{-Lk_1}}{\pi\mu_1 p}\int_0^\infty \frac{K_-[-ik_1(1+\lambda)]e^{-Lk_1\lambda}}{[ik_1(1+\lambda)+\zeta][\lambda(\lambda+2)]^{1/2}}d\lambda \\ & - \frac{iF_2K_+(\zeta)e^{-Lk_2}}{\pi\mu_2 p}\int_0^\infty \frac{K_-[ik_2(1+\lambda)]e^{-Lk_2\lambda}}{[ik_2(1+\lambda)+\zeta][\lambda(\lambda+2)]^{1/2}}d\lambda \end{aligned} \tag{49}$$

and

$$\bar{\Phi}_{-}^{(0)}(\zeta) = -\frac{iF_1K_-(\zeta)e^{-Lk_1}}{\pi\mu_1 p}\int_0^\infty \frac{K_+[ik_1(1+\lambda)]e^{-Lk_1\lambda}}{[ik_1(1+\lambda)-\zeta][\lambda(\lambda+2)]^{1/2}}d\lambda$$
$$+\frac{iF_2K_-(\zeta)e^{-Lk_2}}{\pi\mu_2 p}\int_0^\infty \frac{K_+[ik_2(1+\lambda)]e^{-Lk_2\lambda}}{[ik_2(1+\lambda)-\zeta][\lambda(\lambda+2)]^{1/2}}d\lambda. \tag{50}$$

Due to the presence of exponentially decaying terms in the integrands the main contribution to the integrals would be from small values of λ. So approximately evaluating the integrals we obtain finally

$$\bar{\Phi}_{+}^{(0)}(\zeta) = \frac{F_1K_+(\zeta)K_+(ik_1)e^{-Lk_1}}{\mu_1 p(\zeta+ik_1)(2\pi Lk_1)^{1/2}} - \frac{F_2K_+(\zeta)K_+(ik_2)e^{-Lk_2}}{\mu_2 p(\zeta+ik_2)(2\pi Lk_2)^{1/2}}, \tag{51a}$$

$$\bar{\Phi}_{-}^{(0)}(\zeta) = \frac{iF_1K_-(\zeta)K_+(ik_1)e^{-Lk_1}}{\mu_1 p(\zeta-ik_1)(2\pi Lk_1)^{1/2}} - \frac{iF_2K_-(\zeta)K_+(ik_2)e^{-Lk_2}}{\mu_2 p(\zeta-ik_2)(2\pi Lk_2)^{1/2}}. \tag{51b}$$

The expressions for $\bar{\Phi}_{+}^{(0)}(\zeta)$ and $\bar{\Phi}_{-}^{(0)}(\zeta)$ may be recognised as the solutions corresponding to the separate problems of diffraction of semi-infinite cracks $y = 0$, $x > -L$ and $y = 0$, $x < L$ respectively because until the scattered wave emanating from a given crack tip reaches the opposite crack tip, the semi-infinite crack solution must apply.

The waves originating from concentrated line sources at $x = 0$, $y = 0+$ and $x = 0$, $y = 0-$ arrive at the crack edges at $t = s_1L$ and $t = s_2L$ respectively.

The waves arriving at one edge at time $t = s_1L$ and $t = s_2L$ respectively through the upper and lower media reach the opposite edge at times $t = 3s_1L$, $s_2L + 2s_1L$ through the upper medium and at time $t = s_1L + 2s_2L$, $3s_2L$ through the lower medium. So the first order solution $\bar{\Phi}_{+}^{(1)}(\zeta)$ and $\bar{\Phi}_{-}^{(1)}(\zeta)$ which we obtain by substituting Eqs. (51a)–(b) into the integral Eqs. (47) and (48) gives the effect of these waves and it is valid until $t = 5s_1L$ when the second scattered wave from the opposite edge first arrives. So the first order iteration becomes

$$\bar{\Phi}_{+}^{(1)}(\zeta) = \sum_{r=1}^{2}\frac{K_+(\zeta)\bar{\Phi}_{-}^{(0)}(-ik_r)K_+(ik_r)e^{-2Lk_r}}{2\mu_r(\zeta+ik_r)(\pi Lk_r)^{1/2}} - \sum_{r=1}^{2}\frac{(-1)^rF_rK_+(\zeta)K_+(ik_r)e^{-Lk_r}}{\mu_r p(\zeta+ik_r)(2\pi Lk_r)^{1/2}} \tag{52a}$$

and

$$\bar{\Phi}_{-}^{(1)}(\zeta) = -i\sum_{r=1}^{2}\frac{K_-(\zeta)\bar{\Phi}_{+}^{(0)}(ik_r)K_+(ik_r)e^{-2Lk_r}}{2\mu_r(\zeta-ik_r)(\pi Lk_r)^{1/2}} - i\sum_{r=1}^{2}\frac{(-1)^rF_rK_-(\zeta)K_+(ik_r)e^{-Lk_r}}{\mu_r p(\zeta-ik_r)(2\pi Lk_r)^{1/2}}. \tag{52b}$$

For stress intensity factor since we are interested in the singular part of the stress near the crack tips, so making $|\zeta| \to \infty$ and noting that $R_{+}^{1,2}(\zeta)$ tends to unity as $|\zeta| \to \infty$ we obtain

$$\bar{\Phi}_{+}^{(1)}(\zeta) = \left(\frac{\mu_1\mu_2}{\mu_1+\mu_2}\right)^{1/2}\left[\sum_{r=1}^{2}\frac{\bar{\Phi}_{-}^{(0)}(-ik_r)K_+(ik_r)e^{-2Lk_r}}{2\mu_r(\zeta+ik_r)^{1/2}(\pi Lk_r)^{1/2}} - \sum_{r=1}^{2}\frac{(-1)^rF_rK_+(ik_r)e^{-Lk_r}}{\mu_r p(\zeta+ik_r)^{1/2}(2\pi Lk_r)^{1/2}}\right] \tag{53a}$$

and

$$\bar{\Phi}_{-}^{(1)}(\zeta)=\left(\frac{\mu_1\mu_2}{\mu_1+\mu_2}\right)^{1/2}\mathrm{i}\left[-\sum_{r=1}^{2}\frac{\bar{\Phi}_{+}^{(0)}(\mathrm{i}k_r)K_{+}(ik_r)\mathrm{e}^{-2Lk_r}}{2\mu_r(\zeta-\mathrm{i}k_r)^{1/2}(\pi Lk_r)^{1/2}}-\sum_{r=1}^{2}\frac{(-1)^r F_r K_{+}(\mathrm{i}k_r)\mathrm{e}^{-Lk_r}}{\mu_r p(\zeta-\mathrm{i}k_r)^{1/2}(2\pi Lk_r)^{1/2}}\right]. \tag{53b}$$

Taking inverse Fourier transform we obtain,

$$\begin{aligned}\Phi_{\pm}(x\pm L)=\pm\left(\frac{\mu_1\mu_2}{\mu_1+\mu_2}\right)^2\frac{1}{2\pi(L|x\pm L|)^{1/2}}\Bigg[&-\frac{F_1}{\mu_1^2}\frac{[R_{+}^{1}(ik_1)]^3}{(\pi s_1 L)^{1/2}}\frac{\mathrm{e}^{s_1 p(\pm x-2L)}}{p^{3/2}}\\&+\frac{F_2}{\mu_1\mu_2}\frac{R_{+}^{1}(ik_1)R_{+}^{1}(ik_2)R_{+}^{2}(ik_1)}{(\pi s_2 L)^{1/2}}\frac{\mathrm{e}^{p(\pm s_1 x-s_1 L-s_2 L)}}{p^{3/2}}\\&-\frac{F_1}{\mu_1\mu_2}\frac{R_{+}^{2}(ik_2)R_{+}^{2}(ik_1)R_{+}^{1}(ik_2)}{(\pi s_1 L)^{1/2}}\frac{\mathrm{e}^{p(\pm s_2 x-s_1 L-s_2 L)}}{p^{3/2}}\\&+\frac{F_2}{\mu_2^2}\frac{[R_{+}^{2}(ik_2)]^3}{(\pi s_2 L)^{1/2}}\frac{\mathrm{e}^{s_2 p(\pm x-2L)}}{p^{3/2}}\Bigg]\pm\frac{1}{\pi}\left(\frac{\mu_1\mu_2}{\mu_1+\mu_2}\right)\frac{1}{(L|x\pm L|)^{1/2}}\\&\times\sum_{r=1}^{2}\frac{(-1)^{r+1}F_r R_{+}^{1}(ik_r)\mathrm{e}^{\pm s_r x p}}{\mu_r p}\ \text{as}\ x\longrightarrow\mp(L+0).\end{aligned} \tag{54}$$

Next from Eq. (54) the normalized stress intensity factors $K_{\pm L}(t)$ where subscripts $-L$, $+L$ refer to the corresponding values at the crack tips at $x=-L$ and $x=L$ respectively have been derived.

Noting that $R_{+}^{1,2}(ik_1)$ and $R_{+}^{1,2}(ik_2)$ are independent of p and using shifting theorem, the inverse Laplace transform finally gives the normalised dynamic stress intensity factors as

$$\begin{aligned}|K_{\mp L}(t)|=\left|\frac{1}{F_1}Lt_{x\to\mp L}\frac{\phi(x\pm L)}{(L|x\pm L|)^{1/2}}\right|=\Bigg|&-\frac{1}{\pi(1+m)}\left[mR_{+}^{1}(ik_1)H(\tau-1)-\frac{F_2}{F_1}R_{+}^{2}(ik_2)H(\tau-\gamma)\right]\\&+\frac{1}{\pi^2(1+m)^2}\Bigg[m^2[R_{+}^{1}(ik_1)]^3\sqrt{\tau-3}\,H(\tau-3)\\&-\frac{F_2}{F_1}mR_{+}^{1}(ik_1)R_{+}^{1}(ik_2)R_{+}^{2}(ik_1)\sqrt{\frac{\tau}{\gamma}-\frac{2}{\gamma}-1}\,H(\tau-2-\gamma)\\&+mR_{+}^{2}(ik_2)R_{+}^{2}(ik_1)R_{+}^{1}(ik_2)\sqrt{\tau-2\gamma-1}\,H(\tau-2\gamma-1)\\&-\frac{F_2}{F_1}[R_{+}^{2}(ik_2)]^3\sqrt{\frac{\tau}{\gamma}-3}H(\tau-3\gamma)\Bigg]\Bigg|,\quad 1<\tau<5,\end{aligned} \tag{55}$$

where

$$m = \frac{\mu_2}{\mu_1}, \quad \gamma = \frac{s_2}{s_1} \text{ and } \tau = \frac{t}{s_1 L}$$

It may be noted that stress intensity factors at the both edges $|K_{+L}(t)|$ and $|K_{-L}(t)|$ are the same which is also obvious from the symmetry of the problem.

3. Results and discussions

From Eqs. (7) and (14) it is to be noted that for $Y = 0$, $x = X$ and $\gamma = 0$ and that $\hat{\sigma}^{(j)}_{YZ}(X, 0, t) = \sigma^{j}_{yz}(x, 0, t)$.

Therefore, elastodynamic mode III stress intensity factors at the crack tips of the interface crack in an anisotropic bimaterial are the same as that of the interface crack of the corresponding isotropic bimaterial given by Eq. (55).

While carrying out numerical calculations both the cases of symmetric ($F_1 = F_2 = F$) and antisymmetric ($F_1 = -F_2 = F$) loading have been treated. For numerical evaluation of stress intensity factors at the tips of the cracks of finite width situated at the interface, the four material pairs [12], given in Table 1, have been considered.

The absolute value of the stress intensity factors defined by Eq. (55) has been plotted against $\tau(= t/(s_1 L))$ for different material pairs in Figs. 3–6 for both the symmetric and antisymmetric loading for values of τ varying from 1.0 to 5.0.

It is to be noted that in the case of antisymmetric loading, stress intensity factor increases in two steps, the first step corresponds to the first arrival of the wave at the crack tip moving along the upper face of the crack from the source and the second jump occurring because of the arrival of the wave at the crack tip due to wave moving along the lower face of the crack.

Table 1
Engineering elastic constants of different materials

Medium Name	$\hat{\rho}$ (kg m^{-3})	C_{44} (GPa)	C_{55} (GPa)	C_{45} (GPa)
Type of material pair II				
(1) Carbon-epoxy	1.57×10^3	3.98	6.4	0
(2) Graphite-epoxy	1.6×10^3	6.55	2.6	0
Type of material pair II				
(1) Isotropic chromium	7.2×10^3	115.2	115.2	0
(2) Isotropic steel	7.9×10^3	81.91	81.91	0
Type of material pair III				
(1) Isotropic aluminium	2.7×10^3	26.45	26.45	0
(2) Carbon-epoxy	1.57×10^3	3.98	6.4	0
Type of material pair IV				
(1) Copper coated stainless steel	8×10^3	91	135	0
(2) Isotropic aluminium	2.7×10^3	26.45	26.45	0

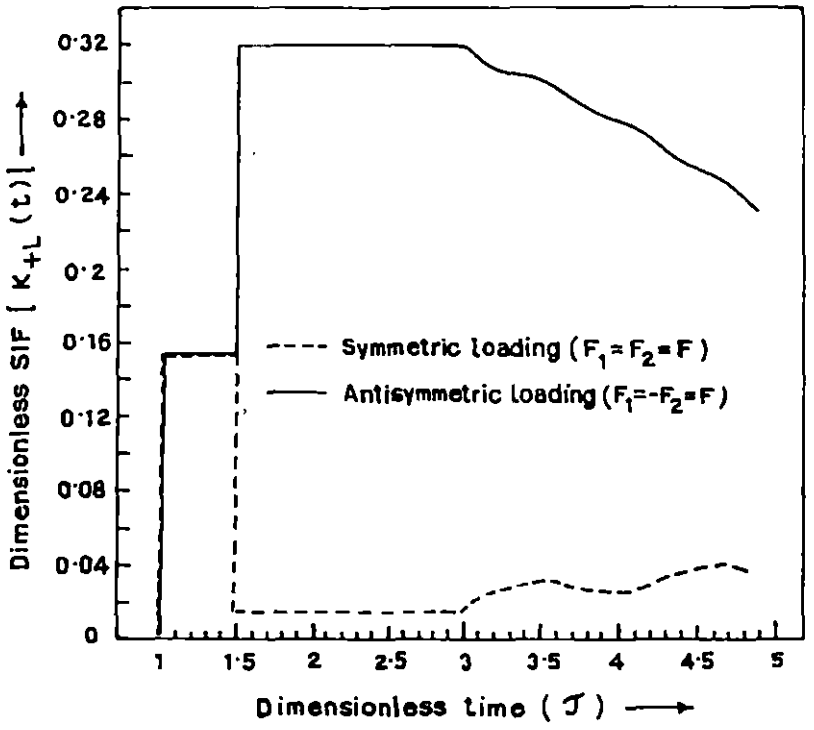

Fig. 3. Stress intensity factor versus dimensionless time for type I material pair.

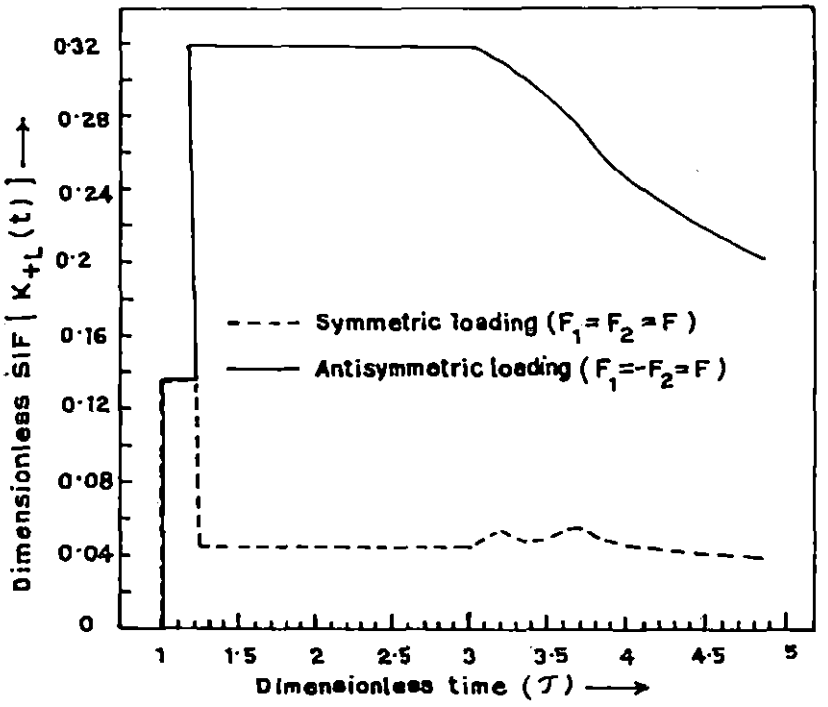

Fig. 4. Stress intensity factor versus dimensionless time for type II material pair.

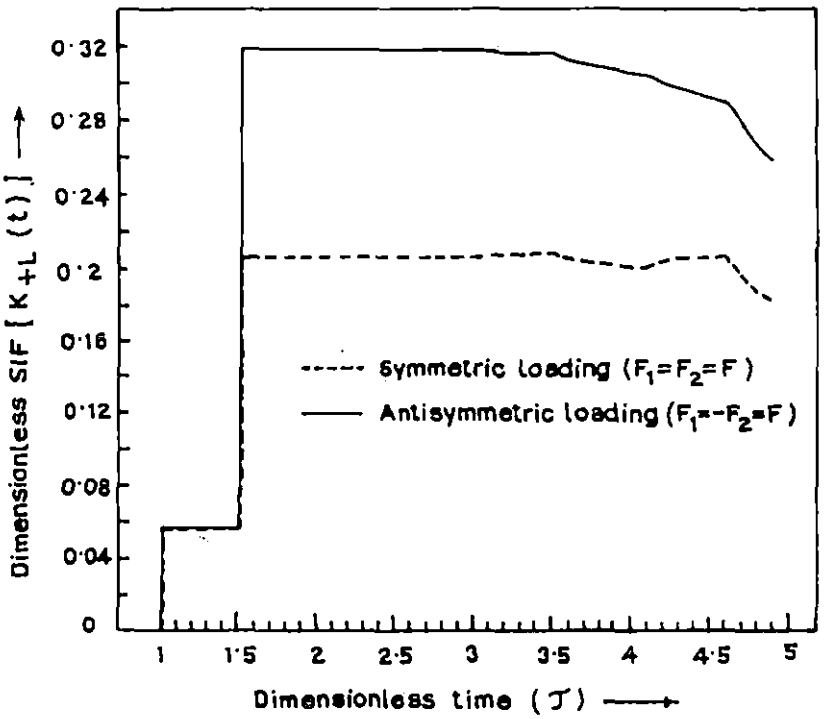

Fig. 5. Stress intensity factor versus dimensionless time for type III material pair.

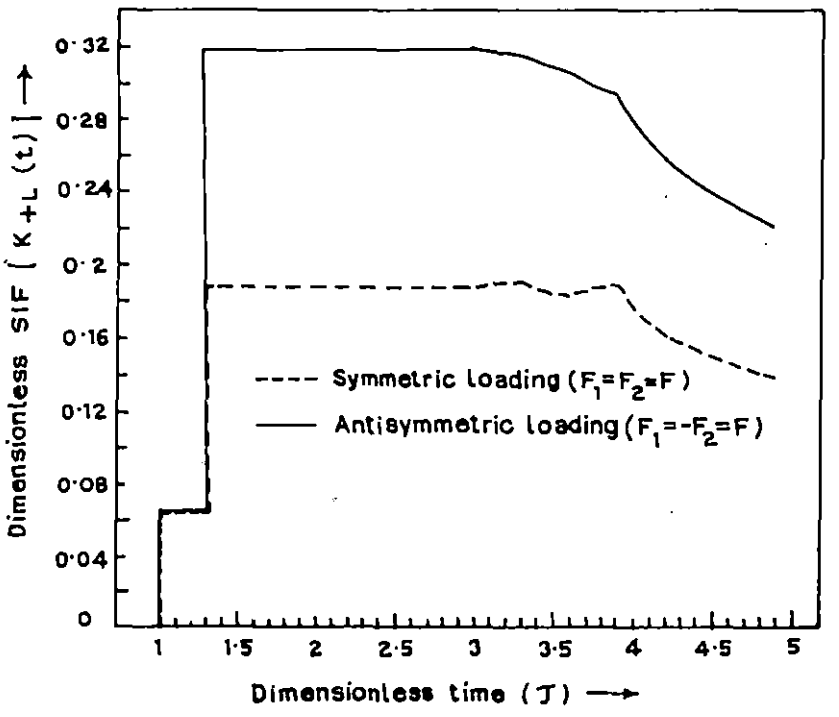

Fig. 6. Stress intensity factor versus dimensionless time for type IV material pair.

It is interesting to note that after the arrival of the first scattered wave from the opposite edge of the crack, the stress intensity factor gradually decreases in the case of antisymmetric loading.

However in the case of symmetric loading stress intensity factor at first increases when the wave moving from the source along the upper face of the crack surface reaches the crack tip but as soon as the wave from the source moving along the lower face of the crack reaches the crack tip, suddenly it decreases for type I and Type II material pairs and increases for type III and type IV material pairs until the scattered wave from the opposite crack tip arrives when the stress intensity factor shows tendency of increasing but with slow oscillations.

Acknowledgements

We take the opportunity of thanking the referee for suggesting some improvement of the paper.

Appendix A

From Eq. (40) we obtain

$$R^1(\zeta) = \frac{(\mu_1 + \mu_2)(\zeta^2 + k_2^2)^{1/2}}{\mu_1(\zeta^2 + k_1^2)^{1/2} + \mu_2(\zeta^2 + k_2^2)^{1/2}} \tag{A.1}$$

$$R^1(\zeta) = R_+^1(\zeta)R_-^1(\zeta) = \frac{1}{m/(1+m) + (1/(1+m))((\zeta^2 + k_1^2)/(\zeta^2 + k_2^2))^{1/2}},$$

where

$$m = \frac{\mu_2}{\mu_1}$$

Taking logarithm on both sides, one obtains

$$\log R^1(\zeta) = \log R_+^1(\zeta) + \log R_-^1(\zeta) = -\log\left[\frac{m}{1+m} + \frac{1}{1+m}\left(\frac{\zeta^2 + k_1^2}{\zeta^2 + k_2^2}\right)^{1/2}\right].$$

So

$$\log R_+^1(\zeta) = \frac{1}{2\pi i}\int_{-ic-\infty}^{-ic+\infty} \frac{\log R^1(z)}{z - \zeta} dz.$$

Replacing z by $-z$ and using $R^1(-z) = R^1(z)$

$$\log R^1_+(\zeta) = -\frac{1}{2\pi i}\int_{ic-\infty}^{ic+\infty}\frac{\log R^1(z)}{z+\zeta}dz = \frac{1}{2\pi i}\int_{ic-\infty}^{ic+\infty}\frac{\log\left[\dfrac{m}{1+m}\left\{1+\dfrac{1}{m}\left(\dfrac{z^2+k_1^2}{z^2+k_2^2}\right)^{1/2}\right\}\right]}{(z+\zeta)}dz$$

$$= \frac{1}{2\pi i}\int_{ic-\infty}^{ic+\infty}\frac{\log\left[1+\dfrac{1}{m}\left(\dfrac{z^2+k_1^2}{z^2+k_2^2}\right)^{1/2}\right]}{(z+\zeta)}dz = \frac{1}{2\pi i}\int_{k_1}^{k_2}\frac{\log\left[1+i\left(\dfrac{u^2-k_1^2}{m^2(k_2^2-u^2)}\right)^{1/2}\right]}{(u-i\zeta)}du -$$

$$-\frac{1}{2\pi i}\int_{k_1}^{k_2}\frac{\log\left[1-i\left(\dfrac{u^2-k_1^2}{m^2(k_2^2-u^2)}\right)^{1/2}\right]}{(u-i\zeta)}du$$

which yields,

$$R^1_+(\zeta) = \exp\left[\frac{1}{\pi}\int_{k_1}^{k_2}\frac{\tan^{-1}[(z^2-k_1^2)/m^2(k_2^2-z^2)]^{1/2}}{(z-i\zeta)}dz\right]. \tag{A.2}$$

Similarly,

$$R^1_-(\zeta) = \exp\left[\frac{1}{\pi}\int_{k_1}^{k_2}\frac{\tan^{-1}[(z^2-k_1^2)/m^2(k_2^2-z^2)]^{1/2}}{z+i\zeta}dz\right]. \tag{A.3}$$

Similarly, it can be shown that

$$R^2_\pm(\zeta) = \exp\left[-\frac{1}{\pi}\int_{k_1}^{k_2}\frac{\tan^{-1}[m^2(k_2^2-z^2)/(z^2-k_1^2)]^{1/2}}{z\mp i\zeta}dz\right]. \tag{A.4}$$

where $R^2(\zeta)$ is given by Eq. (43).

Using Eq. (40) or Eq. (41) it can be shown that

$$K_\pm(\zeta) = \left(\frac{\mu_1\mu_2}{\mu_1+\mu_2}\right)^{1/2}(\zeta\pm ik_1)^{1/2}R^1_\pm(\zeta) \tag{A.5}$$

$$= \left(\frac{\mu_1\mu_2}{\mu_1+\mu_2}\right)^{1/2}(\zeta\pm ik_2)^{1/2}R^2_\pm(\zeta) \tag{A.6}$$

From either Eq. (A.5) or Eq. (A.6) it can be easily shown that

$$K_-(-\zeta) = -iK_+(\zeta).$$

References

[1] Sih GC, Embley GT, Ravera RS. Int J Solids Struct 1972;8:977.
[2] Kassir MK, Bandyopadhyay KK. ASME J Appl Mech 1983;50:630.
[3] Stephen TA, Hwel LT. Int J Eng Sci 1970;8:857.
[4] Kuo AY. J Appl Mech 1984;51:71.
[5] Takei M, Shindo Y, Atsumi A. Eng Fract Mech 1982;16(6):799.
[6] Neerhoff FL. Appl Sci Res 1979;35:265.
[7] Kuo MK, Cheng SH. Int J Solids Struct 1991;28(6):751.
[8] Markenscoff X, Ni L. J Elast 1984;14:93.
[9] Achenbach JD and Kuo MK. Effect of tranverses isotropy on strong ground motion due to strike slip faulting. In: Das S et al., editors. Earthquake Source Mechanics, Washington: American Geophysical Union. 111–120.
[10] Camprin S. Wave Motion 1981;3:343.
[11] Ma CC. Int J Solids Struct 1989;25(11):1295.
[12] Nayfeh AH. Wave Propagation in Layered Anisotropic Media with Applications to Composites. North Holland, 1995.

Journal of Technical Physics, J. Tech. Phys., 39, 1, 31–44, 1999.
Polish Academy of Sciences, Institute of Fundamental Technological Research, Warszawa.
Military University of Technology, Warszawa.

SHEAR WAVE INTERACTION WITH A PAIR OF RIGID STRIPS EMBEDDED IN AN INFINITELY LONG ELASTIC STRIP

R.K. PRAMANIK [1], S.C. PAL [2] and M.L. GHOSH [1]

[1] DEPARTMENT OF MATHEMATICS UNIVERSITY OF NORTH BENGAL
DIST. DARJEELING, WEST BENGAL – 734430, INDIA

[2] COMPUTER CENTRE UNIVERSITY OF NORTH BENGAL
DIST. DARJEELING, WEST BENGAL – 734430, INDIA

In this paper, the problem of diffraction of normally incident SH wave by two co-planar finite rigid strips placed symmetrically in an infinitely long isotropic elastic strip perpendicular to the lateral surface of the elastic strip has been treated. The mixed boundary value problem gives rise to the determination of the solution of triple integral equations which finally have been reduced to the solution of a Fredholm integral equation of second kind. The equation has been solved numerically for low frequency range. Finally the elastodynamic stress intensity factors are obtained. The variations of the stress intensity factors at the tips of the rigid strips with frequency have been depicted by means of graphs.

1. Introduction

In recent years great interest has been developed in studying elastic wave interaction with singularities in the form of cracks or inclusion located in an elastic medium, in view of their application in engineering fracture mechanics and geophysics. Most of the attempts have been based on the assumption that the crack or the inclusion is situated sufficiently far from the neighbouring boundaries. Mathematically, this type of problem reduces to the study of the elastic field due to the presence of cracks or inclusions in an infinite elastic medium. A detailed reference of work done on the determination of the dynamic stress field around a crack or an inclusion in an infinite elastic solid has been given by SIH [1]. However in the presence of finite boundaries, the problem becomes complicated since they involve additional geometric parameters, describing the dimension of the solids. Papers involving a crack or a rigid strip in an infinitely long elastic strip are very few. The problem of an infinite elastic strip containing an arbitrary number of Griffith cracks of unequal size, located parallel to its surfaces and opened by an arbitrary internal pressure, has been treated by ADAM [2]. Finite crack perpendicular to the surface of the infinitely long elastic strip has been studied by CHEN [3] for impact load, and by SRIVASTAVA *et al.* [4] for normally incident waves. Recently SHINDO *et al.* [5]

considered the problem of impact response of a finite crack in an orthtropic strip. ITOU [6] also studied the response of a central crack in a finite strip under inplane compression impact.

But these solutions were limited to the problems involving a single crack or a finite rigid strip embedded in an elastic strip because of severe mathematical complexity involved in finding solutions for two or more cracks or inclusions. Recently SRIVASTAVA *et al.* [7] considered the problem of interaction of shear waves with two co-planar Griffith cracks situated in an infinitely long elastic strip. TAI and LI [8] also derived the elastodynamic response of a finite strip with two co-planar cracks under impact loading. The solution of the mixed boundary value problem was expressed in terms of two Cauchy-type singular integral equations which were solved numerically, following a collocation scheme due to ERDOGAN and GUPTA [9]. A numerical Laplace transform inversion technique described by MILLER and GUY [10] are then used to obtain the solution.

In our paper, we have considered the diffraction of normally incident SH wave by two co-planar finite rigid strips situated in an infinitely long isotropic elastic strip perpendicular to the lateral surface. The mixed boundary value problem gives rise to the determination of the solution of triple integral equations which finally have been reduced to the solution of a Fredholm integral equation of second kind. The equation has been solved numerically for low frequency range. Finally the elastodynamic stress intensity factors are obtained. The variations of the stress intensity factors at the tips of the rigid strips with variable frequency have been depicted by means of graphs.

2. Formulation of the Problem

Consider an infinitely long homogeneous isotropic elastic strip of width 2H containing two coplanar rigid strips embedded in it. Consider a rectangular Cartesian coordinate system (X, Y, Z) with origin at the centre of the elastic strip, such that the rigid strips occupy the region $-b \leqslant X \leqslant -a$; $a \leqslant X \leqslant b$, $|Y| < \infty$, $Z = 0$. A time-harmonic antiplane shear wave is assumed to be incident normally on the rigid strips.

Since the non-vanishing component of displacement is only the component V, all stress components except σ_{YZ} and σ_{XY} vanish identically. Thus the problem is to find the stress distribution near the edges of strips subject to the following boundary conditions:

$$V(X,0+) = V(X,0-) = -V_0 e^{-i\omega t}; \qquad a \leqslant |X| \leqslant b,$$

$$\sigma_{YZ}(X,0+) = \sigma_{YZ}(X,0-) = 0; \qquad |X| > b, \qquad |X| < a, \tag{2.1}$$

and

$$\sigma_{XY}(\pm h, Z) = 0.$$

The displacement V satisfies the wave equation

$$\frac{\partial^2 V}{\partial X^2} + \frac{\partial^2 V}{\partial Y^2} = \frac{1}{C_2^2}\frac{\partial^2 V}{\partial t^2}, \tag{2.2}$$

C_2 being shear wave velocity. It is convenient to normalize all lengths with respect to b so that

$$\frac{X}{b} = x, \quad \frac{Y}{b} = y, \quad \frac{Z}{b} = z, \quad \frac{V}{b} = v, \quad \frac{V_0}{b} = v_0, \quad \frac{a}{b} = c, \quad \frac{H}{b} = h.$$

Therefore the strips are defined by $-1 \leqslant x \leqslant -c$, $c \leqslant x \leqslant 1$, $|y| < \infty$, $z = 0$ (Fig. 1). Suppressing the time factor $e^{-i\omega t}$, the boundary conditions reduce to

$$\begin{aligned} v(x,0+) &= v(x,0-) = -v_0; \qquad c \leqslant |x| \leqslant 1, \\ \sigma_{yz}(x,0+) &= \sigma_{yz}(x,0-) = 0; \qquad |x| > 1, \qquad |x| < c, \end{aligned} \tag{2.3}$$

and $\sigma_{xy}(\pm h, z) = 0$.

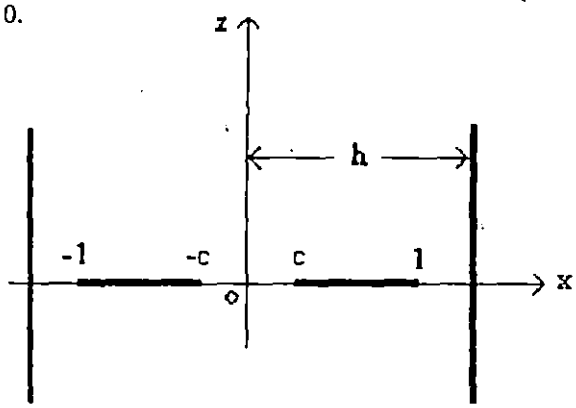

FIG. 1. Geometry of the problem.

The scattered field v subject to the above boundary conditions should be a solution of the equation

$$\frac{\partial^2 v}{\partial x^2} + \frac{\partial^2 v}{\partial z^2} + k_2^2 v = 0 \tag{2.4}$$

where $k_2^2 = \dfrac{\omega^2 b^2}{c_2^2}$.

The solution of Eq. (2.4) can be taken as

$$v(x,z) = \int_0^\infty A(\xi) e^{-\beta|z|} \cos(\xi x)\, d\xi + \int_0^\infty B(\zeta) \cosh(\beta_1 x) \cos(\zeta z)\, d\zeta \tag{2.5}$$

so that

$$\sigma_{yz}(x,z) = \mu \left[-\operatorname{sgn}(z) \int_0^\infty \beta A(\xi) e^{-\beta|z|} \cos(\xi x)\, d\xi - \int_0^\infty \zeta B(\zeta) \cosh(\beta_1 x) \sin(\zeta z)\, d\zeta \right], \tag{2.6}$$

where

$$\beta = \begin{cases} (\xi^2 - k_2^2)^{1/2}; & \xi > k_2, \\ -i(k_2^2 - \xi^2)^{1/2}; & \xi < k_2, \end{cases}$$

and

$$\beta_1 = \begin{cases} (\zeta^2 - k_2^2)^{1/2}; & \zeta > k_2, \\ -i(k_2^2 - \zeta^2)^{1/2}; & \zeta < k_2, \end{cases}$$

so that $\beta_1 = -i(k_2^2 - \zeta^2)^{1/2} = -i\beta_1'$ where $\zeta < k_2$.

3. Derivation of Integral Equation

The condition of vanishing of σ_{yz} at $z = 0$ outside the strips yields

$$\int_0^\infty \beta A(\xi)\cos(\xi x)d\xi = 0; \qquad |x| < c, \qquad |x| > 1. \tag{3.1}$$

Again the boundary condition $v(x,0) = -v_0$ at $c \leqslant |x| \leqslant 1$ gives

$$\int_0^\infty A(\xi)\cos(\xi x)d\xi + \int_0^\infty B(\zeta)\cosh(\beta_1 x)d\zeta = -v_0; \qquad c \leqslant |x| \leqslant 1. \tag{3.2}$$

Using the boundary condition $\sigma_{xy}(\pm h, z) = 0$ one obtains

$$\int_0^\infty \beta_1 B(\zeta)\sinh(\beta_1 h)\cos(\zeta z)d\zeta = \int_0^\infty \xi A(\xi)e^{-\beta|z|}\sin(\xi h)d\xi$$

which after Fourier cosine inversion yields

$$\beta_1 B(\zeta)\sinh(\beta_1 h) = \frac{2}{\pi}\int_0^\infty \frac{\xi\beta}{\beta^2 + \zeta^2}A(\xi)\sin(\xi h)d\xi. \tag{3.3}$$

Eliminating $B(\zeta)$) from equations (3.2) and (3.3) one obtains

$$\int_0^\infty A(\xi)\cos(\xi x)d\xi = -v_0 - \frac{2}{\pi}\int_0^\infty \frac{\cosh(\beta_1 x)}{\beta_1 \sinh(\beta_1 h)}d\zeta \times \int_0^\infty \frac{\xi\beta}{\beta^2 + \zeta^2}A(\xi)\sin(\xi h)d\xi; \qquad c \leqslant |x| \leqslant 1. \tag{3.4}$$

Replacing $\beta A(\xi)$ by $C(\xi)$, Eqs. (3.1) and (3.4) become

$$\int_0^\infty C(\xi)\cos(\xi x)d\xi = 0; \qquad |x| < c; \quad |x| > 1 \tag{3.5}$$

and

$$\int_0^\infty \xi^{-1}\,[1+H(\xi)]\,C(\xi)\cos(\xi x)d\xi = -v_0 - \frac{2}{\pi}\int_0^\infty \frac{\cosh(\beta_1 x)}{\beta_1\sinh(\beta_1 h)}d\zeta \times \int_0^\infty \frac{\xi C(\xi)}{\beta^2+\zeta^2}\sin(\xi h)d\xi; \qquad c\leqslant|x|\leqslant 1, \tag{3.6}$$

where

$$H(\xi) = \left\{\frac{\xi}{\beta}-1\right\} \to 0 \quad \text{as} \quad |\xi|\to\infty. \tag{3.7}$$

In order to solve the integral Eqs. (3.5) and (3.6) we set

$$C(\xi) = \int_c^1 \frac{h(t^2)}{t}\{1-\cos(\xi t)\}\,dt \tag{3.8}$$

where the unknown function $h(t^2)$ is to be determined.

Substituting $C(\xi)$ from (3.8) in equation (3.5) we note that

$$\int_0^\infty C(\xi)\cos(\xi x)dx = \pi\int_c^1 \frac{h(t^2)}{t}\left[\delta(x)-\frac{1}{2}\delta(x+t)-\frac{1}{2}\delta(|x-t|)\right]dt$$

so that Eq. (3.5) is automatically satisfied.

Again, the substitution of the value of $C(\xi)$ from (3.8) in equation (3.6) yields

$$\frac{1}{2}\int_c^1 \frac{h(t^2)}{t}\log\left|\frac{x^2-t^2}{x^2}\right|dt = -v_0 - \int_c^1 \frac{h(t^2)}{t}dt \times\left[\int_{k_2}^\infty \frac{\cosh(\beta_1 x)e^{-h\beta_1}}{\beta_1\sinh(\beta_1 h)}\{1-\cosh(t\beta_1)\}\,d\zeta - \int_0^{k_2}\frac{\cos(\beta_1' x)\cos(\beta_1' h)}{\beta_1'\sin(\beta_1' h)}\{1-\cos(\beta_1' t)\}\,d\zeta\right] - \int_c^1 \frac{h(t^2)}{t}dt\int_0^\infty \xi^{-1}H(\xi)\cos(\xi x)\{1-\cos(\xi t)\}\,d\xi, \qquad c\leqslant|x|\leqslant 1 \tag{3.9}$$

where the result

$$\int_0^\infty \frac{\cos(\xi x)\{1-\cos(\xi t)\}}{\xi}d\xi = \log\left|\frac{x^2-t^2}{x^2}\right|$$

has been used.

Differentiating both sides of Eq. (3.9) with respect to x and next multiplying by $(-2x/\pi)$, one obtains

$$(3.10)\qquad \frac{2}{\pi}\int_c^1 \frac{th(t^2)}{(t^2-x^2)}dt = \frac{2x}{\pi}\int_c^1 \frac{h(t^2)}{t}dt\left[\int_{k_2}^{\infty}\frac{\sinh(\beta_1 x)e^{-h\beta_1}}{\sinh(\beta_1 h)}\{1-\cosh(t\beta_1)\}\,d\zeta\right.$$

$$+\int_0^{k_2}\frac{\sin(\beta_1' x)\cos(\beta_1' h)}{\sin(\beta_1' h)}\{1-\cos(\beta_1' t)\}\,d\zeta$$

$$\left.-\int_0^{\infty}H(\xi)\sin(\xi x)\{1-\cos(\xi t)\}\,d\xi\right];\qquad c\leqslant|x|\leqslant 1.$$

It is known that using Hilbert transform technique, the solution of the integral equation (SRIVASTAVA and LOWENGRUB [11])

$$\frac{2}{\pi}\int_a^b \frac{th(t^2)}{(t^2-y^2)}dt = R(y),\qquad a<y<b$$

can be obtained in the form

$$(3.11)\qquad h(t^2) = -\frac{2}{\pi}\left(\frac{t^2-a^2}{b^2-t^2}\right)^{1/2}\int_a^b\left(\frac{b^2-y^2}{y^2-a^2}\right)^{1/2}\frac{yR(y)}{y^2-t^2}dy$$

$$+\frac{D}{(t^2-a^2)^{1/2}(b^2-t^2)^{1/2}}$$

with condition that R must be an even function of y so as to make integral convergent. D is an arbitrary constant.

Following (3.11), the solution of Eq. (3.10) is given by

$$(3.12)\qquad h(u^2)+\int_c^1\frac{h(t^2)}{t}\left\{K_1(u^2,t^2)+K_2(u^2,t^2)\right\}dt = \frac{D}{(u^2-c^2)^{1/2}(1-u^2)^{1/2}}$$

where

$$(3.13)\qquad K_1(u^2,t^2) = -\frac{4}{\pi^2}\left(\frac{u^2-c^2}{1-u^2}\right)^{1/2}\int_c^1\left(\frac{1-x^2}{x^2-c^2}\right)^{1/2}\frac{x^2dx}{x^2-u^2}$$

$$\times\left[\int_{k_2}^{\infty}\frac{\sinh(\beta_1 x)e^{-h\beta_1}}{\sinh(\beta_1 h)}\{1-\cos(t\beta_1)\}\,d\zeta+\int_0^{k_2}\frac{\sin(\beta_1' x)\cos(\beta_1' h)}{\sin(\beta_1' h)}\{1-\cos(\beta_1' t)\}\,d\zeta\right]$$

and

$$K_2(u^2,t^2) = +\frac{4}{\pi^2}\left(\frac{u^2-c^2}{1-u^2}\right)^{1/2}\int_c^1\left(\frac{1-x^2}{x^2-c^2}\right)^{1/2}\frac{x^2dx}{x^2-u^2} \times \int_0^\infty H(\xi)\sin(\xi x)\{1-\cos(\xi t)\}\,d\xi. \tag{3.14}$$

In order to determine the arbitrary constant D, Eq. (3.9) is multiplied by $\frac{x}{(x^2-c^2)^{1/2}(1-x^2)^{1/2}}$ and integrated from c to 1 with respect to x, and using the result

$$\int_c^1 \frac{x\log|1-t^2/x^2|}{(x^2-c^2)^{1/2}(1-x^2)^{1/2}}dx = \frac{\pi}{2}\log\left|\frac{1-c}{1+c}\right|$$

we finally obtain

$$\int_c^1\frac{h(u^2)}{u}du = -\frac{2v_0}{\log\left|\frac{1-c}{1+c}\right|} - \frac{4}{\pi\log\left|\frac{1-c}{1+c}\right|}\int_c^1\frac{h(t^2)}{t}dt \times \int_c^1\frac{x}{(x^2-c^2)^{1/2}(1-x^2)^{1/2}}\left[A_1(x,t^2)+A_2(x,t^2)\right]dx \tag{3.15}$$

where

$$A_1(x,t^2) = \int_{k_2}^\infty \frac{\cos h(\beta_1 x)e^{-h\beta_1}}{\beta_1\sinh(\beta_1 h)}\{1-\cosh(t\beta_1)\}\,d\zeta - \int_0^{k_2}\frac{\cos(\beta_1' x)\cos(\beta_1' h)}{\beta_1'\sin(\beta_1' h)}\{1-\cos(\beta_1' t)\}\,d\zeta, \tag{3.16}$$

$$A_2(x,t^2) = \int_0^\infty \xi^{-1}H(\xi)\cos(\xi x)\{1-\cos(\xi t)\}\,d\xi = \frac{1}{2}\log\left|\frac{x^2-t^2}{x^2}\right| - \frac{\pi i}{2}H_0^{(1)}(xk_2) + \frac{\pi i}{4}H_0^{(1)}\{(x+t)k_2\} + \frac{\pi i}{4}H_0^{(1)}\{|x-t|k_2\}. \tag{3.17}$$

Again, by substituting $h(u^2)$ from Eq. (3.12) in the left-hand side of equation (3.15) and simplifying, one obtains

$$D = -\frac{4v_0 c}{\pi \log\left|\frac{1-c}{1+c}\right|} - \frac{8c}{\pi^2 \log\left|\frac{1-c}{1+c}\right|}\int_c^1 \frac{h(t^2)}{t}dt \times \int_c^1 \frac{x}{(x^2-c^2)^{1/2}(1-x^2)^{1/2}}\left[A_1(x,t^2)+A_2(x,t^2)\right]dx + \frac{2c}{\pi}\int_c^1 \frac{h(t^2)}{t}dt \int_c^1 \frac{1}{u}\left\{K_1(u^2,t^2)+K_2(u^2,t^2)\right\}du. \tag{3.18}$$

Eliminating D from Eqs. (3.12) and (3.18) and simplifying one obtains

$$\left[(u^2-c^2)(1-u^2)\right]^{1/2} h(u^2) + \int_c^1 \frac{h(t^2)}{t} + \left[K_a(u^2,t^2)+K_b(u^2,t^2)+K_c(u^2,t^2)\right]dt = -\frac{4v_0 c}{\pi \log\left|\frac{1-c}{1+c}\right|} \tag{3.19}$$

where

$$K_a(u^2,t^2) = -\frac{4}{\pi^2}(u^2-c^2)\int_c^1 \left(\frac{1-x^2}{x^2-c^2}\right)^{1/2} \frac{x^2}{x^2-u^2}dx \times \left[\frac{\partial}{\partial x}\left\{A_1(x,t^2)+A_2(x,t^2)\right\}\right], \tag{3.20}$$

$$K_b(u^2,t^2) = \frac{8c}{\pi^2 \log\left|\frac{1-c}{1+c}\right|}\int_c^1 \frac{x\,dx}{(x^2-c^2)^{1/2}(1-x^2)^{1/2}} \times \left\{A_1(x,t^2)+A_2(x,t^2)\right\}, \tag{3.21}$$

$$K_c(u^2,t^2) = -\frac{4c^2}{\pi^2}\int_c^1 \left(\frac{1-x^2}{x^2-c^2}\right)^{1/2} \times \left[\frac{\partial}{\partial x}\left\{A_1(x,t^2)+A_2(x,t^2)\right\}\right]dx. \tag{3.22}$$

Next for further simplification we put

$$\left[(u^2 - c^2)(1 - u^2)\right]^{1/2} h(u^2) = H(u^2)$$

and make the substitution

$$u^2 = c^2 \cos^2 \phi + \sin^2 \phi \qquad \text{and} \qquad t^2 = c^2 \cos^2 \theta + \sin^2 \theta$$

in Eq. (3.19) which then reduces to the form

$$G(\phi) + \int_0^{\pi/2} \frac{G(\theta)}{c^2 \cos^2 \theta + \sin^2 \theta} \left[K_a'(\phi, \theta) + K_b'(\phi, \theta) + K_c'(\phi, \theta)\right] d\theta = -\frac{4v_0 c}{\pi \log \left|\frac{1-c}{1+c}\right|} \tag{3.23}$$

where

$$G(\phi) = H(c^2 \cos^2 \phi + \sin^2 \phi), \tag{3.24}$$

$$G(\theta) = H(c^2 \cos^2 \theta + \sin^2 \theta), \tag{3.25}$$

$$K_a'(\phi, \theta) = K_a(c^2 \cos^2 \phi + \sin^2 \phi, c^2 \cos^2 \theta + \sin^2 \theta), \tag{3.26}$$

$$K_b'(\phi, \theta) = K_b(c^2 \cos^2 \phi + \sin^2 \phi, c^2 \cos^2 \theta + \sin^2 \theta), \tag{3.27}$$

$$K_c'(\phi, \theta) = K_c(c^2 \cos^2 \phi + \sin^2 \phi, c^2 \cos^2 \theta + \sin^2 \theta). \tag{3.28}$$

4. Stress Intensity Factor

From equation (2.6) for $z \to 0$, $c \leqslant |x| < 1$, one obtains

$$\sigma_{yz}(x, 0\pm) = \mp\mu \int_0^\infty \beta A(\xi) \cos(\xi x) d\xi.$$

It is useful to determine the difference of the stress components on the lower and upper surfaces of the strips. We put

$$\Delta\sigma_{yz}(x, 0) = \sigma_{yz}(x, 0+) - \sigma_{yz}(x, 0-);$$

then

$$\Delta\sigma_{yz}(x, 0) = -2\mu \int_0^\infty C(\xi) \cos(\xi x) d\xi, \qquad c < |x| < 1.$$

Substituting the value of $C(\xi)$ and next changing the order of integration and integrating, one obtains

$$\Delta\sigma_{yz}(x,0) = \frac{\mu\pi h(x^2)}{x}. \tag{4.1}$$

Since

$$h(x^2) = \left[(x^2-c^2)(1-x^2)\right]^{-1/2} H(x^2)$$

and

$$x^2 = c^2\cos^2\phi + \sin^2\phi,$$

and hence Eq. (4.1) becomes

$$\Delta\sigma_{yz}(x,0) = \frac{\mu\pi G(\phi)}{x\left[(x^2-c^2)(1-x^2)\right]^{1/2}}. \tag{4.2}$$

So the stress intensity factors N_c and N_1 at the two tips of the strip can be expressed as

$$N_c = \underset{x\to c+}{Lt}\left[\frac{\Delta\sigma_{yz}(x,0)}{\mu\pi}(x-c)^{1/2}\right] \tag{4.3}$$

and

$$N_1 = \underset{x\to 1-}{Lt}\left[\frac{\Delta\sigma_{yz}(x,0)}{\mu\pi}(1-x)^{1/2}\right]. \tag{4.4}$$

With the aid of Eq. (4.2) one obtains

$$N_c = \frac{G(0)}{c\sqrt{2c(1-c^2)}} \Rightarrow G(0) = c\sqrt{2c(1-c^2)}N_c \tag{4.5}$$

and

$$N_1 = \frac{G(\pi/2)}{\sqrt{2(1-c^2)}} \Rightarrow G(\pi/2) = \sqrt{2(1-c^2)}N_1. \tag{4.6}$$

Making c tend to zero, the two strips merge into one and in that case

$$N_1 = \frac{1}{\sqrt{2}}G(\pi/2).$$

5. Results and Discussions

The numerical calculations have been carried out for the determination of stress intensity factors for different values of the dimensionless frequency k_2 within the range 0.1 to 0.8. The integrals $A_1(x,t^2)$ and $A_2(x,t^2)$ given by (3.16) and (3.17), respectively, appearing in the kernel of integral Eq. (3.23) have been evaluated using the Gauss quadrature formula. Following Fox and Goodwin [12], the solution of integral equation (3.23) has been obtained by converting it into a system of linear algebraic equations. Substituting these values of $[G(\phi)]$ in equations (4.3) and (4.4), the stress intensity factors N_c and N_1 at the inner and outer tips, respectively, of the rigid strips have been found to be related with $G(0)$ and $G(\pi/2)$ through the relations (4.5) and (4.6). The

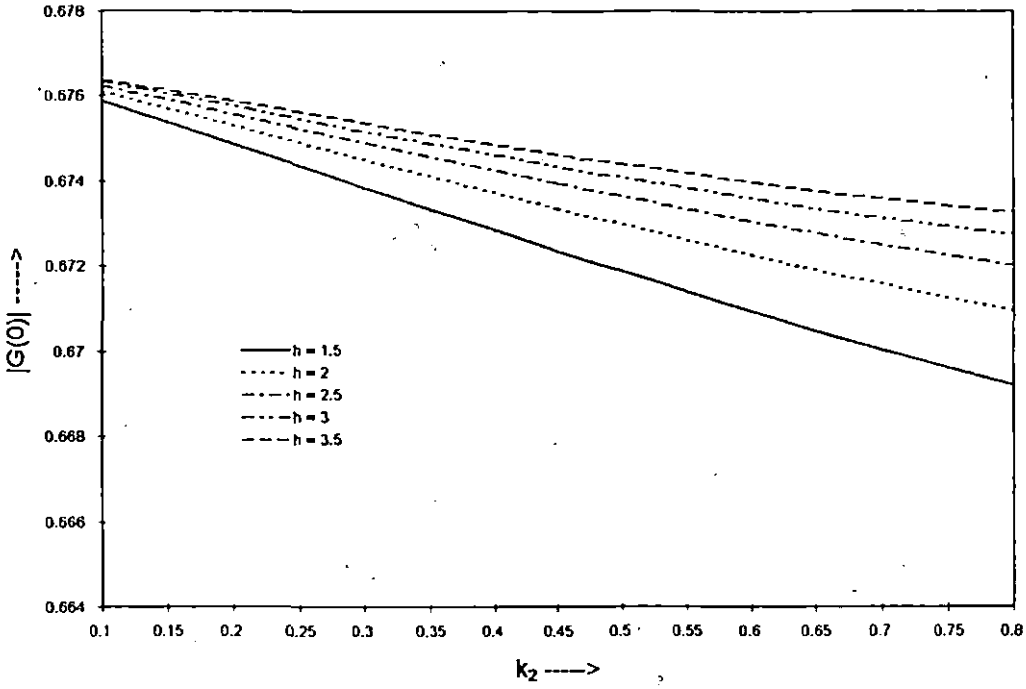

FIG. 2. Amplitude of $|G(0)|$ plotted against dimensionless frequency k_2 for $c = 0.2$.

FIG. 3. Amplitude of $|G(\pi/2)|$ plotted against dimensionless frequency k_2 for $c = 0.2$.

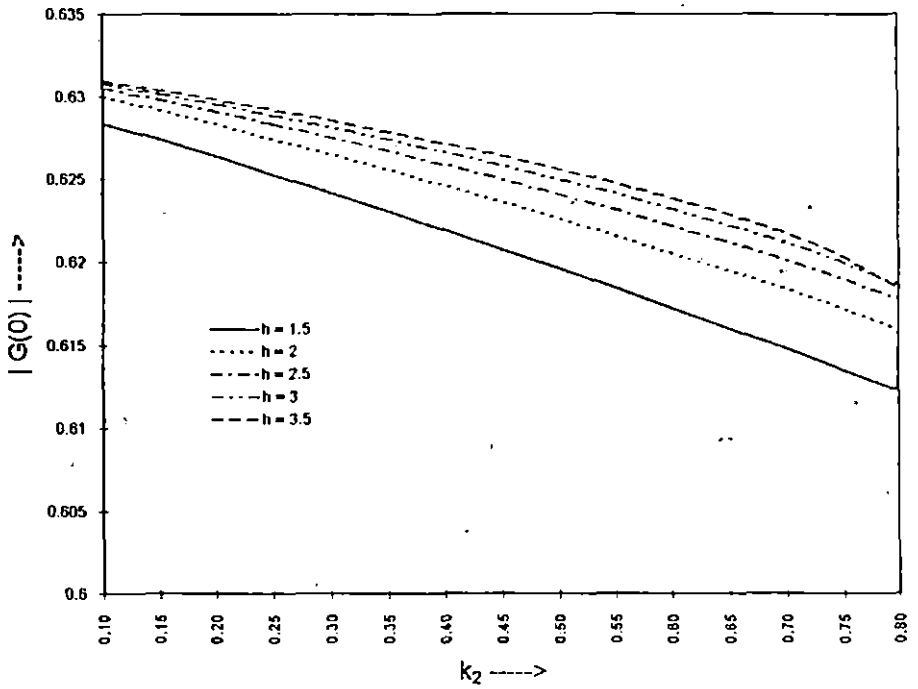

FIG. 4. Amplitude of $|G(0)|$ plotted against dimensionless frequency k_2 for $c = 0.4$.

FIG. 5. Amplitude of $|G(\pi/2)|$ plotted against dimensionless frequency k_2 for $c = 0.4$.

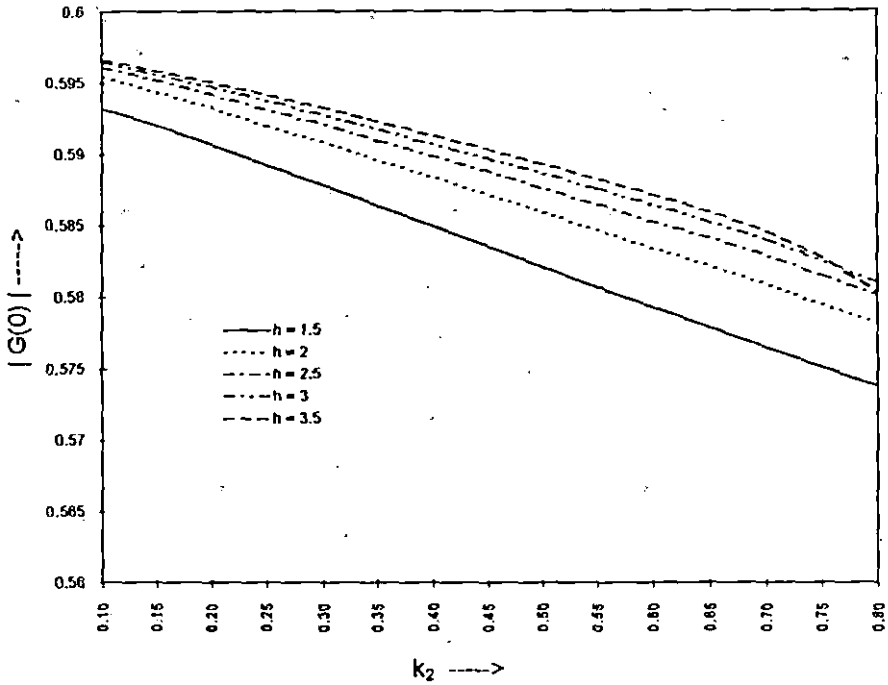

FIG. 6. Amplitude of $|G(0)|$ plotted against dimensionless frequency k_2 for $c = 0.6$.

FIG. 7. Amplitude of $|G(\pi/2)|$ plotted against dimensionless frequency k_2 for $c = 0.6$.

amplitudes $|G(0)|$ and $|G(\pi/2)|$ have been plotted against k_2 with different values of h for c = 0.2, 0.4, 0.6; the values chosen for k_2 range from 0.1 to 0.8, at step of 0.05.

From the graphs it can be concluded that for fixed values of h, the stress intensity factor near the inner tip of the rigid strip decreases with the increase in the values of frequency within the range 0.1 to 0.8 (Figs. 2, 4 and 6), and for fixed values of h the stress intensity factor near the outer tip of the rigid strip at first decreases, attains a minimum and then it gradually increases with the increase in the values of frequency within the range 0.1 to 0.8 (Figs. 3, 5 and 7) for different values of c ($c = 0.2$, 0.4 and 0.6).

It is interesting to note that for different values of k_2 within the range 0.1 to 0.8, the stress intensity factor of the inner tip of the strips, for a given value of k_2, increases with the increase in the values of h, whereas the stress intensity factor at the outer tip of the strips, within the given range of values of k_2, decreases with the increase in the values of h for small values of k_2 but shows the reverse character for higher values of k_2 for any given value of the parameter c.

References

1. G. C. Sih, *Elastodynamic crack problems in mechanics and fracture*, Vol. 4, Noordhoff Leyden, 1997.
2. G. G. Adam, *Crack interaction in an infinite elastic strip*, Int. J. Engng. Sci., 18, p. 455, 1980.
3. E. P. Chen, *Sudden appearance of a crack in a stretched finite strip*, Journal Appl. Mechanic., 45, p. 277, 1978.
4. K. N. Srivastava O. P. Gupta and R. M. Palaiya, *Interaction of elastic waves with a Griffith crack situated in an infinitely long elastic strip*, ZAMM 61, p. 583, 1981.
5. Y. Shindo, H. Nozaki and H. Higaki, *Impact response of a finite crack in an orthotropic strip*, Acta Mechanica, 62, p. 87, 1986
6. S. Itou, *Transient response of a finite crack in a finite strip with stress-free edges strip*, Trans. ASME, J. Appl. Mech., 47, p. 801, 1980.
7. K. N. Srivastava, R. M. Palaiya and D. S. Karaulia, *Interaction of shear waves with two coplanar Griffith cracks situated in an infinitely long elastic strip*, Int. J. of Fracture., 23, p. 3–14, 1983.
8. W. H. Tai and K. R. Li, *Elastodynamic response of a finite strip with two co-planar cracks under impact load*, Engng. Fracture Mechanics., 27, p. 379, 1987.
9. F. Erdogan and G. D. Gupta, *On the numerical solution of singular integral equations*, Q. Appl. Maths., 29, p. 525, 1972.
10. M. K. Miller and W. T. Guy, *Numerical inversion of the Laplace transform by use of Jacobi polynomials*, J. Numer. Anal., 3, p. 624, 1966.
11. K. N. Srivastava and M. Lowengrub, *Finite Hilbert transform technique for triple integral equations with trigonometrical kernals*, Int. J. Engng. Sci., 6, p. 359, 1968.
12. I. Fox and E. T. Goodwin, *The numerical solution of nonsingular linear integral equations*, Philosophical Transactions of the Royal Society, A-245, p. 501, 1953.

Received February 20, 1998.